



UNIVERSITAT^{DE}
BARCELONA

Effects of dam decommissioning on carbon cycling in reservoirs. Case study of the Enobieta Reservoir, N Iberian Peninsula

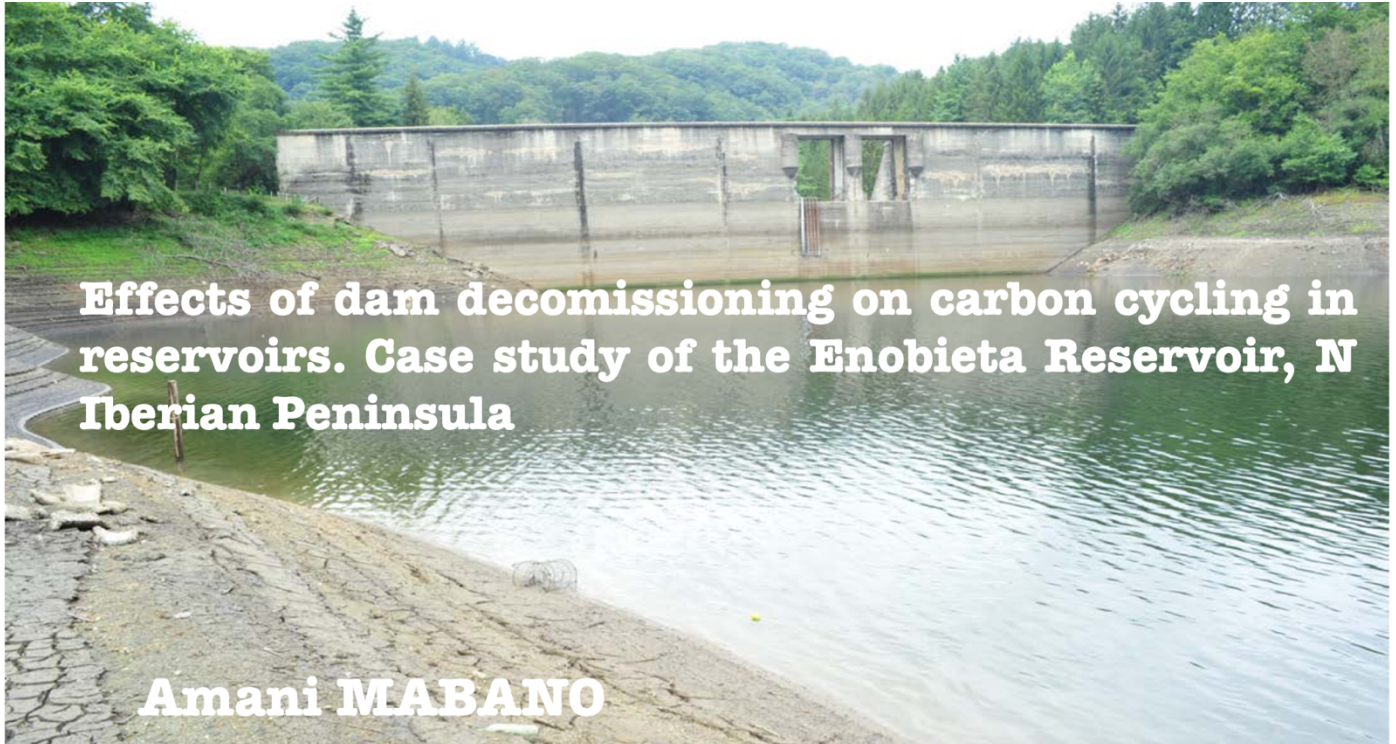
Amani Mabano



Aquesta tesi doctoral està subjecta a la llicència **Reconeixement 4.0. Espanya de Creative Commons.**

Esta tesis doctoral está sujeta a la licencia **Reconocimiento 4.0. España de Creative Commons.**

This doctoral thesis is licensed under the **Creative Commons Attribution 4.0. Spain License.**



Effects of dam decommissioning on carbon cycling in reservoirs. Case study of the Enobieta Reservoir, N Iberian Peninsula

Amani MABANO



UNIVERSITAT DE
BARCELONA

Departament de Biologia Evolutiva, Ecologia i Ciències Ambientals
Programa de Dctora Ecologia, Ciències Ambientals i Fisiologia Vegetal

**Effects of dam decommissioning on carbon cycling in reservoirs.
Case study of the Enobieta Reservoir, N Iberian Peninsula**

Memòria presentada per Amani MABANO per optar al grau de Doctor per la
Universitat de Barcelona

Amani MABANO
Barcelona, September 2023

A handwritten signature in blue ink, appearing to read 'Amani Mabano'.

Approval of thesis supervisors:

Dr. Biel Obrador Sala (tutor of the thesis)
Associate Professor
University of Barcelona

Dr. Daniel von Schiller
Assistant Professor
University of Barcelona

Table of Contents

<i>Acknowledgement</i>	1
<i>1. General introduction</i>	3
1.1. Freshwater: a valuable, scarce resource.....	5
1.2. A dammed world	6
1.3. Carbon cycling in reservoirs	8
1.3.1. Global relevance of carbon cycling in inland waters.....	9
1.3.2. Processes of C cycling in inland waters	11
1.3.3. Carbon biogeochemical processes in reservoirs	14
1.3.4. Effects of water level fluctuations on CO ₂ and CH ₄ emissions in reservoirs ..	18
1.4. Dam decommissioning: a new global challenge	19
1.4.1. Dam ageing and dam decommissioning as an unavoidable action	19
1.4.2. Resistance to DD.....	20
1.4.3. Environmental effects of DD	21
1.4.4. Potential effect of DD on C cycling in reservoirs	22
<i>2. Objectives and hypotheses of the study</i>	25
<i>Supervisor's report</i>	29
<i>3. The drawdown phase of dam decommissioning is a hot moment of gaseous carbon emissions from a temperate reservoir</i>	33
3.1. Abstract.....	35
3.2. Introduction.....	37
3.3. Materials and Methods	39
3.3.1. Study site	39
3.3.2. Sampling design	39
3.3.3. Determination of CO ₂ fluxes.....	40
3.3.4. Determination of CH ₄ fluxes	42
3.4. Results.....	45
3.4.1. Spatial extent of the environments and areal CO ₂ and CH ₄ fluxes	45
3.4.2. Ecosystem CO ₂ and CH ₄ fluxes	47
3. 5. Discussion.....	48
3.5.1. The drawdown phase of DD increased CO ₂ and CH ₄ fluxes from the reservoir	49
3.5.2. Conclusion: implication of DD for the carbon footprint of the reservoir and future perspectives	51
3.6. Acknowledgements.....	51
<i>4. Exposed sediments in a temperate-climate reservoir under dam decommissioning contain large stocks of highly bioreactive organic matter</i>	53
4.1. Abstract.....	55
4.2. Introduction.....	57
4.3. Materials and Methods	59
4.3.1. Study site	59

4.3.2. Sampling strategy and treatment of sediment samples	60
4.3.3. Sediment texture	60
4.3.4. Content of bulk sediment OM and sediment WEOM	60
4.3.5. Reactivity of bulk sediment OM and sediment WEOM.....	59
4.3.6. Meteorological and vegetation data	63
4.3.7. Statistical analyses.....	64
4.4. Results.....	64
4.4.1. Sediment texture	64
4.4.2. Content of bulk sediment OM and sediment WEOM	64
4.4.3. Reactivity of bulk sediment OM and WEOM.....	66
4.4.4. Meteorological and vegetation data	68
4.5. Discussion.....	68
4.6. Conclusion	72
4.7. Acknowledgements.....	72
<i>5. Vegetation growth partially offsets carbon dioxide emissions from exposed sediments: a study in a decommissioned reservoir.....</i>	<i>73</i>
5.1. Abstract.....	75
5.2. Introduction.....	77
5.3. Materials and Methods	79
5.3.1. Study site	79
5.3.2. Sampling design	79
5.3.3. Vegetation sampling.....	80
5.3.4. Instantaneous CO ₂ fluxes.....	80
5.3.5. Upscaling C fluxes to the ecosystem level.....	82
5.3.6. Statistical analysis	83
5.4. Results.....	84
5.4.1. Vegetation dynamics	84
5.4.2. Carbon fluxes	85
5.5. Discussion.....	88
5.6. Conclusion	90
5.7. Acknowledgements.....	91
<i>6. General discussion.....</i>	<i>93</i>
6.1. Dam decommissioning: mitigation of C emissions from reservoirs	95
6.2. Counteracting reservoir sedimentation: a move to relatively sustainable reservoirs.....	103
6.3. Terrestrialization: a potential positive long-term effect of DD.....	105
6.4. Study limitations and future research agenda.....	107
<i>7. General conclusions.....</i>	<i>111</i>
<i>8. References.....</i>	<i>115</i>
<i>9. Appendices.....</i>	<i>143</i>

9. 1. Supplemental information Chapter 3.....	143
9. 2. Supplemental information Chapter 4.....	147
9. 3. Supplemental information Chapter 5.....	173
9.4. Published article: Amani et al. (2022) Inland Waters.....	177
9.5. Published article: Amani et al. (2024) Limnetica.....	189

Acknowledgement

I would like to express my heartfelt gratitude to the following individuals and organizations for their unwavering support and contributions to my doctoral journey:

My supervisors: Dr. Biel Obrador and Daniel von Schiller

I am profoundly grateful to my supervisors, Biel and Dani, for their exceptional guidance, mentorship, and patience throughout my doctoral research. Their expertise, encouragement, and dedication were instrumental in shaping the direction of my work and my growth as a researcher.

My Committee Members: Dr. Muñoz Gracia Maria Isabel, Matthias Koschorreck, and Bernal Berenguer Susana

I extend my appreciation to my dissertation committee members, Isabel, Matthias, and Susana, for their valuable insights, constructive feedback, and commitment to enhancing the quality of my research. Their diverse perspectives enriched my work and broadened my horizons.

Family and Friends

To my family and friends, who provided unwavering support, understanding, and encouragement during the ups and downs of this journey – your belief in me kept me motivated and determined to persevere.

Agencia de Gestión de Ayudas Universitarias y de Investigación (AGAUR)

I am thankful for the financial support provided by AGAUR, which enabled me to carry out my research and complete my doctoral studies successfully.

University of Barcelona

I acknowledge the University of Barcelona for providing an enriching academic environment and the necessary resources for my research endeavors.



1. General introduction

1.1. Freshwater: a valuable, scarce resource

Freshwater is an essential resource for all life, supporting agriculture, ecosystems, and human societies. Early human civilizations emerged in river valleys and floodplains because they were sustained by ecosystem services (i.e., benefits that people obtain from ecosystems; MEA (2005)) provided by freshwater ecosystems (Wang & He, 2022). Freshwater ecosystems provide water for consumptive use (e.g., for agriculture, drinking, domestic, and industrial use) and non-consumptive use (e.g., hydroelectricity and transport), aquatic organisms for food and medicines and other cultural, regulatory, and supporting services, which have long been recognized (Ferreira et al., 2023). As the human population has grown and the power of technology has expanded, human demand and degradation of freshwater resources have increased drastically (Vitousek et al., 1997; Wetzel, 2001). Deleterious human activities on freshwater ecosystems threaten water security for humans and freshwater biodiversity (Vörösmarty et al., 2010). Since the second half of the 20th century, the need for adequate quality and quantity of freshwater to sustain human well-being has emerged as a significant global concern (Wetzel, 2001).

Rich countries have massively invested in water technology, whereas less wealthy countries remain vulnerable to two types of freshwater scarcity: economic and physical water scarcity. The economic water scarcity means that regions have enough water but lack the infrastructure to access and use it efficiently (Juniper, 2019). Sub-Saharan Africa and parts of Central America face severe economic water scarcity (Juniper, 2019). Physical water scarcity affects regions, such as North Africa, the Arabian Peninsula, large areas of central and southern Asia, northern China, and the southwest of the US, that do not naturally have enough water (Juniper, 2019). Water scarcity is exacerbated by climate change and the uneven distribution of water resources and people between regions (Pekel et al., 2016). Thus, readily usable freshwater is a scarce resource that threatens food and water security with more than two billion people living in heavily water-stressed regions globally (Oki & Kanae, 2006).

The ongoing escalation in water extraction by humans and climate change intensifies water scarcity. For instance, Kazakhstan and Uzbekistan lost much of the eastern part of the southern Aral Sea mainly due to the diversion and unregulated water withdrawal from the Amu and Syr rivers since 1960 (Micklin, 2007, 2016; Pekel et al., 2016). The increases in physical water shortages may lead to the use of non-renewable or fossil water. For instance, 75% of the water used in Saudi Arabia is groundwater (Vörösmarty et al., 2010). Groundwater is globally being withdrawn 3.5 times faster than aquifers can replenish water sustainably (Gleeson et al., 2012). The depletion of groundwater may cause severe compound effects because it is, for instance, critical to agriculture (Gleeson et al., 2012; Vörösmarty et al., 2010). Agricultural water scarcity is expected to increase in more than 80% of the world's croplands by 2050 due to global warming (Liu et al., 2022). As water is a catalyst for human development and well-being, water shortages are confronted with various actions. However, human actions to counteract water scarcity, rather than being true

corrective or prophylactic measures, have been therapeutic adaptations and adjustments, such as dam construction.

1.2. A dammed world

According to the online Cambridge dictionary, a dam is *a wall built across a river that stops the river's flow and collects the water, especially to make a reservoir (i.e., an artificial lake) that provides water for an area* (<http://dictionary.cambridge.org/dictionary/english/dam>). Dam construction dates to ~2000 before the common era in the Egyptian Empire (Thornton et al., 1990). Dams exist in different designs and types, depending on numerous context-specific factors, such as reservoir storage capacity and intended function. Dams can be divided into five key categories, in the descending order of their numbers: earth or embankment (65% of all dams), gravity (14%), rockfill (13%), arch (4%), and buttress dams (Duda & Bellmore, 2022; ICOLD WRD, 2022). Dams can also be categorized based on the surface area of their reservoirs as small dams ($\leq 10 \text{ km}^2$), medium dams ($> 10\text{--}100 \text{ km}^2$), or large dams ($> 100 \text{ km}^2$) (Soued et al., 2022). In addition, a dam is considered large if it has a height of $\geq 15 \text{ m}$ from the lowest foundation to the crest, or if it is 5–15 m high with a storage capacity of $\geq 3,000,000 \text{ m}^3$ (ICOLD WRD, 2022).

Globally, there are ~16.7 million small and 58,700 large dams (Lehner et al., 2011; Perera et al., 2021). The global surface area of water impounded by dams is 507,102–1,500,000 km^2 , with large dams covering 77%, small dams 13%, and medium dams 10% of this area (Lehner et al., 2011; St. Louis et al., 2000). The global water volume stored in dams is 8,069 km^3 , where large dams hold 57%, small dams 28%, and medium dams 15% of this water (Lehner et al., 2011). The global water volume stored in reservoirs corresponds to ~10% of the water in all natural freshwater lakes on Earth and ~17% of the global river discharge into the ocean, 40,000 $\text{km}^3 \text{ yr}^{-1}$ (Hanasaki et al., 2006). Many large dams are in the northern hemisphere (Fig.1.1), with China (23,841) and the US (9,263) possessing ~50% of global large dams (Perera et al., 2021). Spain (1,064), Iran (594), Australia (567), and Zimbabwe (256) have the highest number of large dams on their respective continents (Perera et al., 2021). Despite their large number (Couto & Olden, 2018; Downing et al., 2006), small dams have received lower attention than large dams in the literature (Lehner et al., 2011).

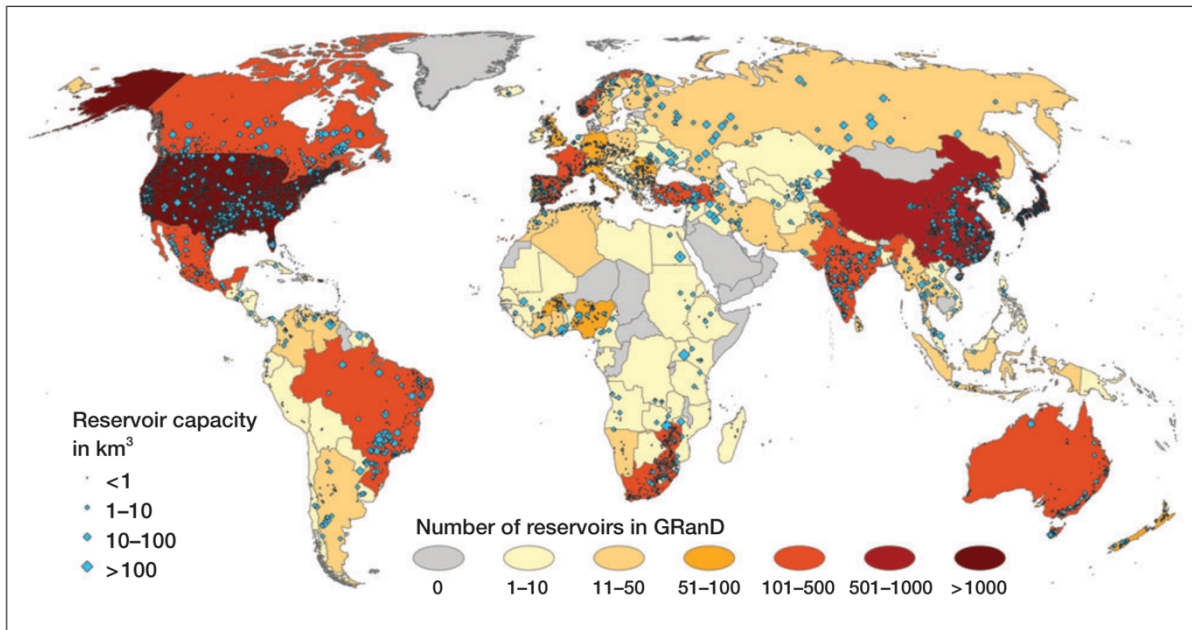


Figure 1.1 Global distribution (by country) of large reservoirs. Source: Lehner et al. (2011)

The first wave of dam construction, the period spanning 1950–1990, was characterized by a surge in the construction of large dams and a rapid expansion of dam construction in many parts of the world (Soued et al., 2022). For instance, the global surface area of dams increased from 10,000 km² in 1915 to 51,000 km² in 1950 and 285,000 km² in 1990 (Soued et al., 2022). The global surface area covered by dams in 1990 was already 75% of the predicted global surface area of dams in 2040 (Soued et al., 2022). Dams in temperate zones covered 74% of the global surface area of dams in 1915 (Soued et al., 2022). However, reservoirs in boreal, subtropical, and tropical regions covered, respectively, 26%, 14%, and 16% of the global surface area of dams in 1990 (Soued et al., 2022). The construction of large dams peaked in the 1960s/70s in Asia, North America, and Western Europe, and in the 1980s in Africa (Perera et al., 2021).

The growing demand for hydroelectricity and irrigation is driving the second wave of dam construction, the period 2010–2040. The rate of dam construction decreased between 1990 and 2009 (Soued et al., 2022) due to many factors (Grigg, 2019). However, it resurged in 2010 and will continue until 2040 (Soued et al., 2022). About 83% of sites suitable for the construction of hydroelectric dams are still available, and approximately one billion people are without electricity, especially in developing countries (Gernaat et al., 2017; Zarfl et al., 2015). Thus, 3,700 more hydroelectric dams, each with a generating capacity ≥ 1 MW, will be built and completed by 2030 in Africa, Balkan Peninsula, South America, and Southeast Asia (Zarfl et al., 2015). In addition, for every built large hydroelectric dam, 11 small hydroelectric dams are built (Couto & Olden, 2018). This construction will double the number of large hydroelectric dams by 2030–2040 and increase global hydroelectricity to $\sim 1,700$ GW, an increase of 73% (Zarfl et al., 2015). Furthermore, since the world population is expected to reach 10 billion people by 2050, more food will be needed (UN Water, 2019). About 100% of this food will be needed in developing countries and produced mainly on

irrigated land, which will require 11% more water, often provided by reservoirs (Lehner et al., 2011).

Humans have built dams for thousands of years because they serve several functions. The main functions of dams are, in the descending order of their numbers: irrigation, hydroelectricity, water supply, flood control, and recreation, but it must be noted that one dam can serve single or multiple purposes (ICOLD WRD, 2022). Controlling floods, securing water supply, and harnessing hydroelectricity bring numerous benefits to people, including expanded spatial and temporal capacity for food production. For instance, large dams contribute 12–16% of global food production and hydroelectricity provides ~19% of world electricity, which is ~72% of global renewable energy (Gernaat et al., 2017; Lehner et al., 2011). All hydroelectric dams produce 2.3 trillion kWh, which is 24% of global electricity and ~90% of renewable electricity (ICOLD WRD, 2022). Reservoirs annually generate 256 billion US dollars through hydroelectricity, irrigation, industrial and domestic water supply, flood protection, fishing, and recreation (Hogeboom et al., 2018). Most of the economic value of reservoirs is derived from hydroelectricity, irrigation, and residential and industrial water supply (Hogeboom et al., 2018). Furthermore, irrigated land covers 18% of the world's arable land (277,000,000 ha), produces ~30–40% of global food, and employs ~30% of people in rural areas worldwide (ICOLD WRD, 2022). Dams have played a crucial role in human development and well-being, but they are also associated with significant harmful impacts for human societies and the environment.

Dam construction adversely affects people through displacement or resettlement, social disruption, threats to water and food security, and an increased incidence of communicable diseases (ICOLD WRD, 2022; Lehner et al., 2011). For instance, the construction of five large dams in China displaced ~2,000,000 people recently (ICOLD WRD, 2022). Dams reduce sediment delivery to highly productive river deltas and floodplains, which is a threat to food security for people who depend on these ecosystems for food production (Richter et al., 2010; Syvitski et al., 2009; Tockner et al., 2008). Dams increase water retention and water loss through evaporation in reservoirs (Hogeboom et al., 2018; Lehner et al., 2011). Furthermore, the construction of the Aswan High Dam in Egypt in 1965, for instance, increased the incidences of schistosomiasis from 47% to 80% (Stiling, 2002). Dam construction also affects biodiversity by altering water quality and connectivity between ecosystems and allowing the invasion of alien species (Bednarek, 2001; Vörösmarty et al., 2003; Winton et al., 2019). For instance, ~50% of large rivers in the world have lost their hydromorphological and ecological connectivity, a figure that may increase to 93% considering planned projects of dam construction (Grill et al., 2015; Habel et al., 2020; Zarfl et al., 2015). The alteration of fluvial connectivity due to dam construction can also influence biogeochemical cycling in inland waters, as discussed in the following section.

1.3. Carbon cycling in reservoirs

1.3.1. Global relevance of carbon cycling in inland waters

The lateral flux of carbon (C) along the terrestrial-to-aquatic continuum is an integral component of the global C cycle. The global C cycle is the flux of C atoms in and between C reservoirs, such as inland waters (Grace, 2013). Inland waters include lentic (i.e., non-flowing or standing waters: lakes, ponds, reservoirs, and wetlands) and lotic (i.e., flowing or running waters: rivers and streams) ecosystems. Global C budgets recognize the role of inland waters in the global C cycle because the amounts of terrestrial C they receive, emit to the atmosphere as CO₂ and CH₄, bury in their sediments, and transfer to the sea are globally relevant (Cole et al., 2007; Tranvik et al., 2009). For instance, these fluxes are comparable to the net terrestrial C sink, 2.6 Pg C yr⁻¹, the average atmospheric C increase, 4 Pg C yr⁻¹, and the marine C sink, 2.3 Pg C yr⁻¹ (IPCC, 2013) (Fig.1.2).

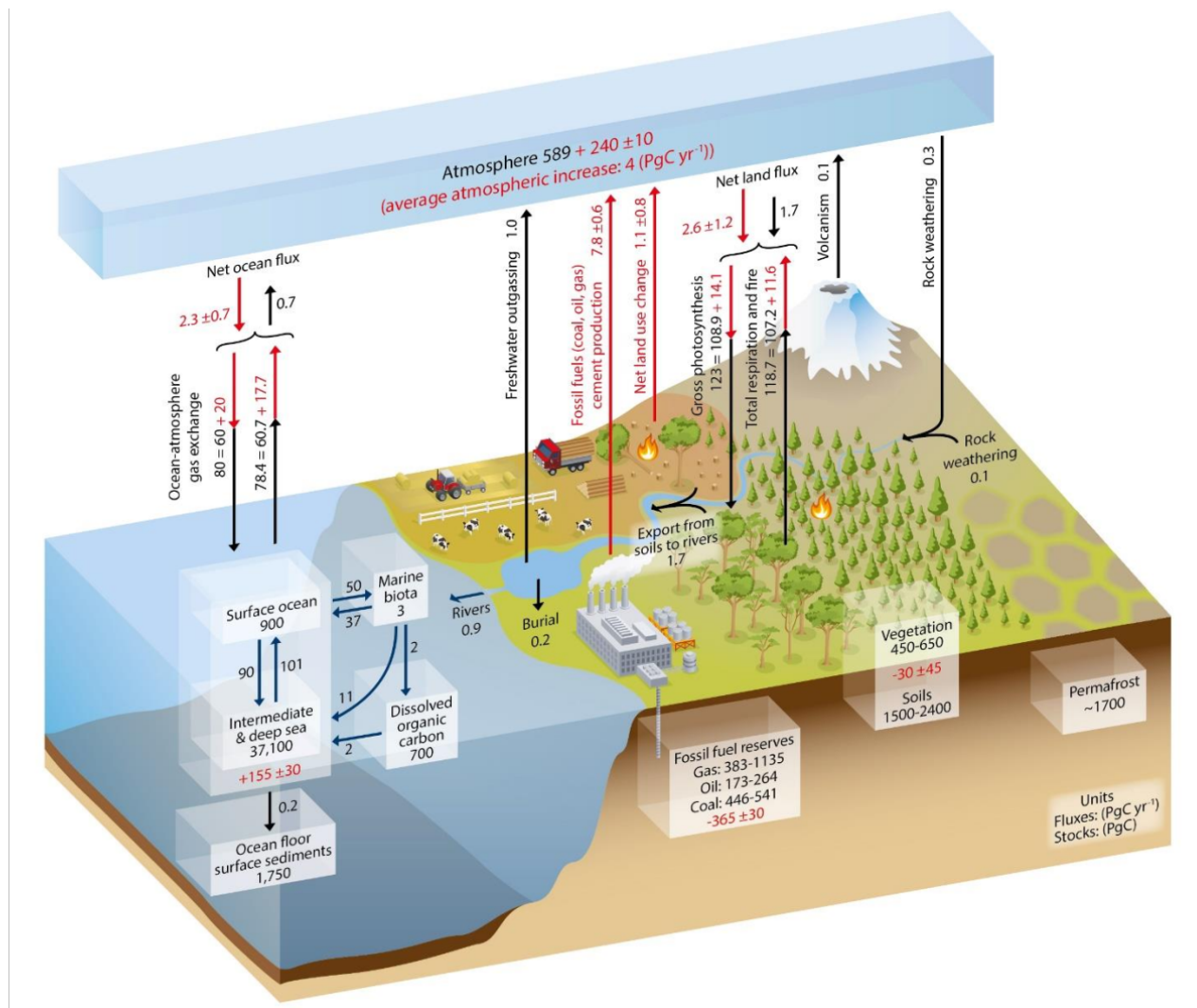


Figure 1.2 Simplified schematic presentation of the global C cycle and its anthropogenic perturbations. The numbers represent reservoir mass, also called C stocks (in Pg C) and annual C exchange fluxes (in Pg C yr⁻¹). Black numbers and arrows indicate reservoir mass and exchange fluxes estimated for the time prior to the industrial era, ~1750. Red arrows and numbers indicate annual anthropogenic C fluxes averaged over the 2000–2009 timespan. These fluxes are an anthropogenic perturbation of the C cycle during the industrial era, after 1750. Red numbers in the reservoirs indicate cumulative changes of anthropogenic C over the Industrial Era, 1750–2011. By convention, a positive cumulative change means that a reservoir has gained C since 1750. Uncertainties are reported as 90% CI. Source: IPCC (2013)

Global soil erosion and leaching release 1.9–5.1 Pg C yr⁻¹ from land to inland waters (Drake et al., 2018; Sawakuchi et al., 2017; Tranvik et al., 2009). Terrestrial and autochthonous (i.e., produced in inland waters) C is: (1) exported to the sea, (2) buried in sediments of inland waters, and (3) emitted to the atmosphere as CO₂ and CH₄ (Cole et al., 2007; Tranvik et al., 2009). The export rate of terrestrial C to the sea through inland waters

is better constrained and falls in a narrow range of 0.9–0.95 Pg C yr⁻¹ (Drake et al., 2018; Tranvik et al., 2009). However, the global estimates of the burial rate of C in sediments of inland waters are highly variable; 0.2–1.6 Pg C yr⁻¹ (Battin et al., 2009; Cole et al., 2007; Regnier et al., 2013). The large difference between the lower and higher bound estimates of C burial in inland waters stresses the scarcity of observational data to constrain this flux at the global scale. Due to this large uncertainty, 0.6 Pg C yr⁻¹ was adopted as the global burial rate of C in inland waters; floodplains, lakes, ponds, and reservoirs (Drake et al., 2018; Regnier et al., 2013; Tranvik et al., 2009).

Inland waters are net emitters of CO₂ and CH₄ to the atmosphere (Keller et al., 2020; Raymond et al., 2013; Rosentreter et al., 2021). Global CO₂ emissions from inland waters are 1.8 Pg C yr⁻¹ from lotic inland waters (Raymond et al., 2013), 0.02–0.15 Pg C yr⁻¹ from natural ponds (Holgerson & Raymond, 2016), 0.29 Pg C yr⁻¹ from lakes (Raymond et al., 2013), 0.27 Pg C yr⁻¹ from reservoirs (Deemer et al., 2016), and 0.12 Pg C yr⁻¹ from dry inland waters (Keller et al., 2020), while wetlands are a net sink of atmospheric CO₂, ~0–0.83 Pg C yr⁻¹ (Li et al., 2023; Mitsch et al., 2013). Lotic inland waters emit more CO₂ than lakes and reservoirs combined although their global surface area, 624,000 km², is about five times lower than the global surface area of lakes and reservoirs, 3,000,000 km² (Raymond et al., 2013). Lotic inland waters are hotspots for CO₂ emissions because of their higher gas transfer velocity compared with lakes and reservoirs (Raymond et al., 2013). Global CH₄ emissions from inland waters are (mean ± 95% confidence interval) 398.1 ± 79.4 Tg CH₄ yr⁻¹; 150.9 ± 73 Tg CH₄ yr⁻¹ from lakes, 148.6 ± 15.2 Tg CH₄ yr⁻¹ from freshwater wetlands, 30.5 ± 17.1 Tg CH₄ yr⁻¹ from rivers, 29.8 Tg CH₄ yr⁻¹ from rice cultivation, 24.3 ± 8 Tg CH₄ yr⁻¹ from reservoirs, and 14 ± 18.8 Tg CH₄ yr⁻¹ from agricultural ponds (Rosentreter et al., 2021). Thus, inland waters contribute ~50% of global CH₄ emissions from anthropogenic and natural sources, 500–600 Tg CH₄ yr⁻¹ (Forster et al., 2007; Saunois et al., 2016).

1.3.2. Processes of C cycling in inland waters

Carbon dioxide and CH₄ emitted by inland waters are received from terrestrial ecosystems or produced in inland waters (Zhang et al., 2022). For instance, 85% of CO₂ emissions in European rivers results from terrestrial CO₂ inputs (Zhang et al., 2022). Carbon dioxide is produced in inland waters through carbonate and metabolic reactions (Gruca-Rokosz & Koszelnik, 2018; Khan et al., 2022; Marcé et al., 2015). Carbonate reactions drive CO₂ supersaturation where an alkalinity threshold is above 1 mequiv L⁻¹, encompassing 57% of the global surface area of lakes and reservoirs (Marcé et al., 2015). Metabolic reactions leading to the production of CO₂ include, among others, the decomposition of organic matter (OM).

The decomposition of OM is the physical breakdown and biochemical transformations of complex organic molecules into simpler organic and/or compounds, such as CO₂ (Weathers et al., 2013). The decomposition rate of OM depends on its intrinsic factors and extrinsic factors. Two intrinsic factors of OM are its content and molecular composition (Catalán et al., 2016, 2021; Kothawala et al., 2021). The low content of some

compounds under low concentrations of OM can limit microbial production, some specific metabolic pathways, and thus the decomposition of OM (Arrieta et al., 2015; Čapek et al., 2019). The molecular composition (i.e., the chemical composition of OM, including its chemodiversity, optical characteristics, elemental composition, functional group composition, or isomeric diversity) is a relevant factor for the decomposition of OM (Kellerman et al., 2015; Kothawala et al., 2021). For instance, molecular composition explains 41% of the variability in the decomposition of OM in freshwater ecosystems (Catalán et al., 2016). In inland waters, the molecular composition of OM depends on its decomposition stage (highly decomposed OM tends to be more recalcitrant) and origin. Autochthonous OM is usually more bioreactive than allochthonous OM because the latter contains, for instance, higher concentrations of aromatic compounds and C:N ratio (Weathers et al., 2013).

Extrinsic factors influencing the decomposition rate of OM are, among others, oxygen (O_2), temperature, inorganic nutrients, diversity of OM decomposers, and light availability (Čapek et al., 2019; Cory et al., 2014; del Giorgio & Williams, 2005). For instance, the decomposition rate of OM increases with the concentration of O_2 , temperature, inorganic nutrients, diversity of OM decomposers, and light availability (Čapek et al., 2019; Cory et al., 2014; del Giorgio & Williams, 2005; Gudas et al., 2010; Weathers et al., 2013). Sediments contain 1,000 times more C and nutrients than the overlying water layer (del Giorgio & Williams, 2005). Thus, the abundance and production rates of bacteria in sediments are 2–3 orders of magnitude higher than in the overlying water column (Kuznetsov, 1958) and 30–80% of hypolimnetic O_2 consumption in lakes is attributed to sediment respiration (Cornett & Rigler, 1887). Sediment respiration is also influenced by sediment texture or size. Fine sediments increase the decomposition rate of OM because they provide a larger habitat for larger microbial populations and retain OM and sediment moisture to a greater degree than coarse sediments (Coyne et al., 1997). The decomposition rate of OM influences the production and emissions of CO_2 and CH_4 .

Methane is produced in inland waters through acetoclastic, methylotrophic, and hydrogenotrophic methanogenesis (Berghuis et al., 2019; Likens, 2009; Vincent et al., 2021). Hydrogenotrophic methanogenesis is the dominant pathway of CH_4 production (Berghuis et al., 2019). The production of CH_4 is carried out by methanogenic archaea (Buan, 2018). Methanogens are anaerobic organisms, and CH_4 is produced preferentially in anoxic environments, but oxic CH_4 production also happens in aquatic ecosystems (Günthel et al., 2019). Methanotrophs are archaea that consume or oxidize CH_4 in a process called methanotrophy (Venkiteswaran et al., 2013). Methanotrophy or CH_4 oxidation/consumption is aerobic or anaerobic. Aerobic oxidation of CH_4 occurs at the oxic–anoxic interface or close to the oxycline, i.e., the threshold between the oxic and anoxic water layers (Likens, 2009). Aerobic oxidation of CH_4 consumes 50–95%, while 12–87% of CH_4 produced in inland waters is consumed through anaerobic oxidation of CH_4 (Guérin & Abril, 2007; Likens, 2009; Martinez-Cruz et al., 2018).

Inland waters emit CO_2 and CH_4 through two main pathways: (1) ebullition and (2) diffusion, and three minor pathways: (3) storage flux, (4) plant-mediated flux, and (5) degassing (Bastviken et al., 2004; Deemer et al., 2016). Storage and plant-mediated fluxes

usually occur during lake overturn and in highly vegetated ecosystems, respectively (Bastviken et al., 2004). Degassing is the gas evasion from waters discharged at turbines and spillways of reservoirs (Deemer et al., 2016). Due to its high solubility in water (Yalkowsky et al., 2010), ~100% of CO₂ is emitted through diffusion (Deemer et al., 2016). Diffusive CO₂ comprised 75% of gaseous C emissions from the water surface of reservoirs in the 20th century (Soued et al., 2022). In contrast, the low solubility of CH₄ in water (Yalkowsky et al., 2010) makes CH₄ ebullition more important. Methane ebullition, also called bubbling, accounts for 40–60%, 65%, and 53% of CH₄ emissions from lakes, reservoirs, and all inland waters, respectively (Bastviken et al., 2004; Bastviken et al., 2011; Deemer et al., 2016). However, the contribution of CH₄ ebullition to total CH₄ fluxes in aquatic systems is highly uncertain, 0–100% in reservoirs and 10–80% of CH₄ emitted from rivers (Baulch et al., 2011; Deemer et al., 2016), which may be due to its high spatial and temporal heterogeneity (Wik et al., 2016).

The high spatial and temporal heterogeneity of CH₄ ebullition results in hotspots and hot moments of CH₄ ebullition. Hotspots of CH₄ ebullition in inland waters are shallow zones close to river inflows (replenishing the system with fresh OM), and zones with large sediments and/or OM storages (DelSontro et al., 2010; Deshmukh et al., 2018; Hilgert et al., 2019). Most CH₄ that emerges from sediments through ebullition bypasses oxidation along the water column (McGinnis et al., 2006), while 50–90% of CH₄ that leaves lake sediments through diffusion undergoes oxidation (Bastviken et al., 2008). Methane oxidation is more significant in deep, stratified waters that subject CH₄ to the oxycline and a longer oxidation pathway and residence time (Guérin & Abril, 2007). Hot moments of CH₄ ebullition include high air, sediment, and bottom water temperature, low hydrostatic pressure (i.e., the downward force exerted by the overlying water column due to gravity), and low barometric pressure (DelSontro et al., 2010; Kosten et al., 2018; Maeck et al., 2013). High sampling effort is necessary to detect the hotspots and hot moments of CH₄ ebullition. To achieve a high spatial and temporal resolution of CH₄ ebullition, CH₄ fluxes must be measured at numerous sites over a long-term framework.

Another C flux pathway that has received increasing interest since recently is emissions from air-exposed sediments. Exposed sediments are hotspots for CO₂ emissions due to their closer coupling between CO₂ production and emissions. Sediment drying increases the contact between deeper layers of exposed sediments and atmospheric O₂ and, thus, CO₂ production (Fromin et al., 2010; Keller et al., 2020; Kosten et al., 2018). Limited primary productivity restricts the consumption of produced CO₂, resulting in higher areal CO₂ fluxes in exposed sediments than in inundated lentic ecosystems (Gómez-Gener et al., 2015; Keller et al., 2020; Marcé et al., 2019). The global mean areal CO₂ flux in exposed sediments of dry inland waters, 186 mmol CO₂ m⁻² d⁻¹ (Keller et al., 2020), is equivalent to the global mean areal CO₂ flux in soils, 179 mmol m⁻² d⁻¹ (Bond-Lamberty & Thomson, 2012), higher than the global mean range of areal CO₂ flux on the water surfaces of lentic waters, range: 18–35 mmol CO₂ m⁻² d⁻¹ (Deemer et al., 2016; Holgerson & Raymond, 2016; Raymond et al., 2013), but lower than the global mean areal CO₂ flux from lotic waters, 663 mmol CO₂

$\text{m}^{-2} \text{d}^{-1}$ (Raymond et al., 2013). However, C cycling in exposed sediments of inland waters remains an important blind spot in the global C budget (Marcé et al., 2019).

In a recent study by Paranaíba et al. (2021), the importance of including CH_4 fluxes was stressed to gain comprehensive understanding of C cycling in air-exposed sediments. The increased availability of O_2 due to the exposure to the air and oxic metabolism reduces CH_4 production and emissions from exposed sediments. However, anoxia can still prevail a few millimetres deep in some microhabitats of wet and drying exposed sediments, which can sustain CH_4 production (Koschorreck & Darwich, 2003; Serrano-Silva et al., 2014). The global mean areal flux of CH_4 from air-exposed sediments of inland waters is (mean \pm SD) $2.5 \pm 5 \text{ mmol CH}_4 \text{ m}^{-2} \text{ d}^{-1}$ (Paranaíba et al., 2021). The global mean areal CH_4 flux in exposed sediments is lower than areal CH_4 fluxes from the water surfaces of lentic, $0.75\text{--}10 \text{ mmol CH}_4 \text{ m}^{-2} \text{ d}^{-1}$ (Holgerson & Raymond, 2016; Rosentreter et al., 2021) and lotic, $4.32\text{--}7 \text{ mmol CH}_4 \text{ m}^{-2} \text{ d}^{-1}$, inland waters (Rosentreter et al., 2021; Stanley et al., 2016). It is, however, higher than the global areal CH_4 flux in soils, $0.1 \pm 0.4 \text{ mmol CH}_4 \text{ m}^{-2} \text{ d}^{-1}$, which may be due to low soil moisture (Paranaíba et al., 2021). Low sediment/soil moisture can inhibit CO_2 and CH_4 emissions by inducing osmotic stress for microorganisms and/or restricting the contact between OM and microorganisms (Schimel, 2018). Thus, rewetting of exposed sediments is a hot moment for the leaching of DOM and nutrients, the decomposition of OM, and CO_2 and CH_4 emissions (Harjung et al., 2018; Kosten et al., 2018; von Schiller et al., 2019).

1.3.3. Carbon biogeochemical processes in reservoirs

Reservoirs have characteristics that are intermediate between rivers and lakes, earning them the designation of river-lake hybrids (Thornton et al., 1990). They are typically long, shallow, and narrow and receive water and sediments from a single large tributary river. Rivers exhibit longitudinal gradients in channel morphology, water velocity, water temperature, substrate type, and biotic communities, according to the river continuum concept (Cummins et al., 1983; Vannote et al., 1980). Natural lakes have a notable degree of vertical gradients in physical (e.g., light and temperature), chemical (e.g., dissolved substances), and biological (e.g., production and decomposition of OM) properties (Wetzel, 2001). Reservoirs combine these longitudinal and vertical gradients (Thornton et al., 1990). Due to the longitudinal gradients, three zones are typically distinguished in reservoirs: the riverine zone, the transition zone, and the lacustrine zone. These zones have different physico-chemical and biological properties, such as the rate of primary production.

Primary production in reservoirs is carried out by several biological groups: planktonic algae (phytoplankton), planktonic photoautotrophic bacteria and, to a much lesser extent, attached algae (periphyton) and rooted macrophytes (Thornton et al., 1990). Turbidity and the fluctuation of the water depth restrict the development of periphyton and macrophytes and their contribution to primary production in reservoirs (Thornton et al., 1990). Due to higher nutrient inputs, primary production is typically higher in reservoirs than in lakes, respectively, 400 and $200 \text{ g C m}^{-2} \text{ yr}^{-1}$ (Dean & Gorham, 1998). The global mean primary productivity in reservoirs is $23.76 \pm 6.48 \text{ Tg C yr}^{-1}$ (Maavara et al., 2017). High

turbidity limits primary production in the riverine zone of reservoirs, while it is limited by nutrient shortages in the lacustrine zone. The transition zone, due to the high penetration of light and nutrient availability, has the highest autotrophic productivity and biomass in reservoirs (Forbes et al., 2012; Thornton et al., 1990). High primary production and inputs of allochthonous OM (i.e., the input of OM from terrestrial ecosystems) fuel C burial in reservoir sediments.

Reservoir sediments are hotspots for the burial of allochthonous and autochthonous C, which contribute ~75% and 25% of C buried in reservoir sediments, respectively (Maavara et al., 2017). About 30% of allochthonous C and 34% of autochthonous C inputs are buried in reservoir sediments (Maavara et al., 2017). The burial rate of allochthonous C peaks in the riverine zone and declines progressively towards the dam, whereas the burial rate of autochthonous OM culminates in the transition zone (Thornton et al., 1990). Globally, reservoirs and lakes bury 0.15 Pg C yr⁻¹ of which 40% (0.06 Pg C yr⁻¹) is buried in reservoir sediments (Mendonça et al., 2017). However, the surface area used to determine the global mean rate of C burial in reservoir, 354,033 km², is 10 times lower than the surface area used to determine the global mean rate of C burial in lake sediments, 3,769,669 km² (Maavara et al., 2017; Mendonça et al., 2017; Raymond et al., 2013). Thus, the mean rate of areal C burial in reservoir sediments is six (range: 4–12) times higher than in lakes (Mendonça et al., 2017).

The higher areal C burial rate in reservoirs may be explained by two key factors: reservoirs (1) have a higher catchment area and (2) are closer to human activities than lakes (Deemer et al., 2016; Thornton et al., 1990). Reservoirs have a higher catchment area to reservoir area ratio because they are generally built on large tributary rivers (mainly 6th–9th order rivers) in the lower section of the basin (Thornton et al., 1990). However, lakes are in the upper part of the hydrological basin where they are recharged by low-order tributaries (Thornton et al., 1990). Thus, the average watershed area upstream of reservoirs is >12,000 km² compared to 617 km² for lakes (Maavara et al., 2020; Messenger et al., 2016). Furthermore, the ratio of the catchment area to the reservoir area is, for instance, ~500 for reservoirs in Kansas, while it is ~10 for lakes in Michigan (Thornton et al., 1990). The high catchment area increases the input of sediments from the catchment into reservoirs because sediment yield is proportional to the catchment size (Thornton et al., 1990). Human activities can increase the amount of sediments arriving from the catchment to the water body through, for instance, soil erosion (Anderson et al., 2013).

Increased inputs of sediments from the catchment area increase sedimentation rate in reservoirs. Sedimentation is the process by which materials transported in suspension settle as the sediment (Duda & Bellmore, 2022). The global mean sedimentation rate in reservoirs is 2 cm yr⁻¹ and 4.4 cm yr⁻¹ in reservoirs of the Conterminous US, while it is 0.3 cm yr⁻¹ in lakes of the temperate region (Clow et al., 2015; Dean & Gorham, 1998; Mulholland & Elwood, 1982). The high sedimentation rate in reservoirs creates better conditions for OM burial by reducing the penetration depth of O₂ and the exposure time of OM to O₂. For instance, the penetration depth of O₂ in the Wohlen Reservoir was 1–7 mm, while it can be even >50 mm in natural lakes (Sobek et al., 2009, 2012). Thus, the mean exposure time of OM to O₂ was 16 days in the Wohlen Reservoir, while it can even reach 93 years in natural

lakes (Sobek et al., 2012, 2009). The low penetration depth of O₂ and exposure time of OM to O₂ can increase C burial efficiency. Carbon burial efficiency is the ratio between C deposition (i.e., C settling on the surface of sediments) and C burial (i.e., C storage in sediments for decades or longer) (Sobek et al., 2009). Accordingly, C burial efficiency was, for instance, 87% in the Wohlen Reservoir and 48% in natural lakes (Sobek et al., 2009, 2012).

Global estimates of C burial in reservoirs are highly uncertain because studies on C burial in reservoirs are scarce and unevenly distributed across geographic zones. The global mean range of C burial rate in reservoirs is 35–200 Tg C yr⁻¹ (Dean & Gorham, 1998; Maavara et al., 2017; Mulholland & Elwood, 1982). Global rates of C burial in reservoirs are extremely different because these studies did not use a standardized method, i.e., they used different reservoir areas and did not cover the same geographic range. For instance, the datasets are dominated by data from Europe and North America (Dean & Gorham, 1998; Mendonça et al., 2017). However, areal C burial rates in lakes and reservoirs differ between geographic zones (Mendonça et al., 2017). Thus, the extrapolation of areal C burial rates in reservoir sediments in the temperate region to a global scale may be highly uncertain. More studies are required on C burial in reservoirs in warmer and drier regions. An accurate estimate of the global burial rate of OM can help to understand the role of reservoirs in the global C budget as a C sink and a source of CO₂ and CH₄ emissions.

Knowledge of C cycling in reservoirs has evolved from initially considering hydropower reservoirs as a GHG-neutral source of energy and a long-term C sink, to recognizing reservoirs as a significant source of CO₂ and CH₄ emissions to the atmosphere (Deemer et al., 2016; Hoffert et al., 1998; Lima et al., 1998; Soued et al., 2022) (Fig.1.3). The global mean range of CO₂ emissions from the water surface of reservoirs is 36.8–273 Tg C CO₂ yr⁻¹ (Deemer et al., 2016; Fearnside, 1995; St. Louis et al., 2000). The global mean range of CH₄ emissions from the water surface of reservoirs is 3–52 Tg C CH₄ yr⁻¹ (Deemer et al., 2016; Fearnside, 1995; Rosentreter et al., 2021; St. Louis et al., 2000). Carbon dioxide and CH₄ emissions from reservoirs corresponded, respectively, to 0.2% and 5.2% of global anthropogenic CO₂ and CH₄ emissions in 2020 (Soued et al., 2022). Furthermore, the radiative forcing of reservoirs is comparable to the radiative forcing of the aviation sector, which is 3.5% of total anthropogenic forcing (Soued et al., 2022). Although the Paris Agreement had promoted hydroelectricity as a green source of energy (Hermoso, 2017), the global C flux from water surfaces of reservoirs was included in the global inventories of anthropogenic GHGs (IPCC, 2019) (Fig.1.3).

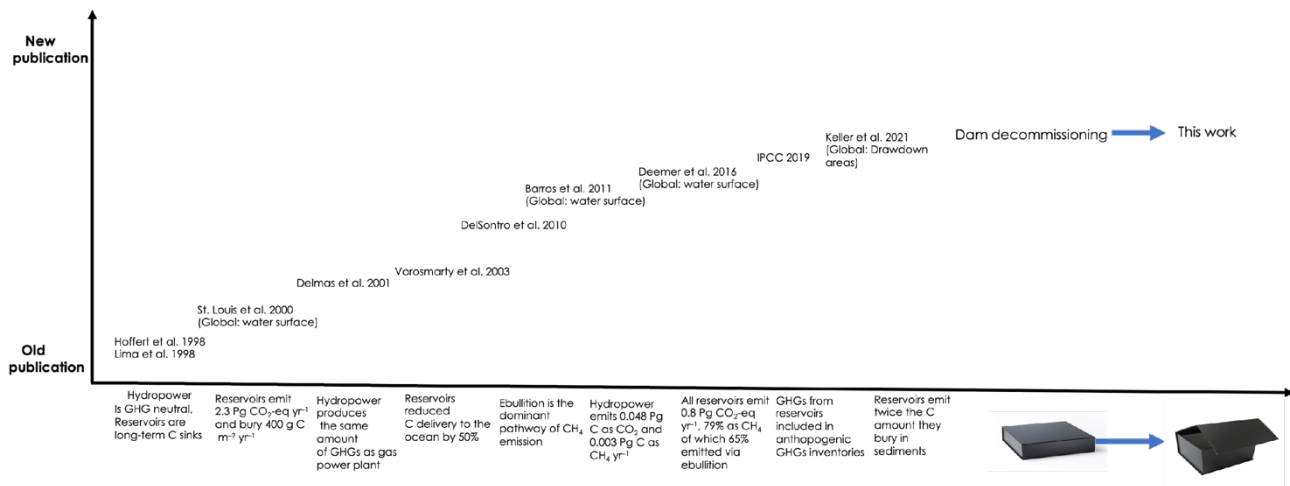


Figure 1.3 Publications representative of the evolution of our knowledge about C cycling in reservoirs. The effect of dam decommissioning on C cycling in reservoirs is depicted in the figure as a closed black box that this study aims to slightly open

Reservoirs are substantial emitters of CO₂ and CH₄ due to three key factors: (1) large stocks of flooded terrestrial OM, (2) great fluctuations in the water depth, and high inputs of OM and nutrients from the catchment area (Deemer et al., 2016; Keller et al., 2021; Thornton et al., 1990). The decomposition of newly flooded terrestrial OM results in high C emissions from young reservoirs, i.e., reservoirs of ≤15 years old, while allochthonous and autochthonous OM fuels C emissions in old reservoirs (Barros et al., 2011; Maavara et al., 2017; St. Louis et al., 2000). For instance, global reservoirs emitted 40 Tg C yr⁻¹ in 1970 to which flooded OM contributed 75% (Maavara et al., 2017). The role of flooded OM in C emissions decreases as reservoirs age and emissions reach baseline levels (Barros et al., 2011). Baseline C emissions from reservoirs are comparable to C emissions from lakes and considered non-anthropogenic (Soued et al., 2022). However, anoxic conditions created by the decomposition of flooded biomass may enhance CH₄ production and the burial of OM through a process called feed-forward loop (Thornton et al., 1990). Clearing vegetation and biomass before flooding can be an effective way to reduce CO₂ emissions in young reservoirs, C burial in reservoir sediments, and CH₄ production in old reservoirs.

Methane accounts for most of CO₂-equivalent (CO₂-eq) emissions from reservoirs due to its high global warming potential (GWP). The GWP of a GHG is the radiative forcing of a unit of mass of that GHG, relative to that of CO₂, over a given time horizon (IPCC, 2013). Methane has a GWP 25 times higher than CO₂ over 100 years (IPCC, 2013). The product of GWP of a gas and its molar mass gives its CO₂-eq. Of the 1,080 Tg CO₂-eq yr⁻¹ emitted from reservoirs in 2020, CO₂ contributed 31%, i.e., 330 Tg CO₂-eq yr⁻¹, while CH₄ contributed 69%, i.e., 750 Tg CO₂-eq yr⁻¹ (Soued et al., 2022). Emissions of CH₄ via ebullition and degassing are increasing mainly due to a high construction rate of hydroelectric dams in the tropics and subtropics and the rise of CH₄ emissions with reservoir age (Soued et al., 2022;

Zarfl et al., 2015). Any mitigation effort aiming to reduce CH₄ emissions from reservoirs through ebullition and degassing would be an effective way to reduce the C footprint of reservoirs.

1.3.4. Effects of water level fluctuations on CO₂ and CH₄ emissions in reservoirs

Reservoirs experience greater fluctuations in the water depth than natural lakes (Thornton et al., 1990). Most aquatic systems undergo natural changes in water levels, but the amplitude and/or frequency of these changes are extreme in reservoirs (Zohary & Ostrovsky, 2011). For instance, a study of 6,794 reservoirs showed that 15% of the global surface area of reservoirs was dry between 1985 and 2015 due to reservoir drawdown (Keller et al., 2021). The change of the water depth in reservoirs is due to flood inflow characteristics, land uses, channelization of primary influents, flood control, and large, irregular water withdrawal to produce hydroelectricity (Thornton et al., 1990). The magnitude of water drawdown in inland waters is expected to increase due to the combined effects of climate change and human activities, such as water diversion and abstraction (Pekel et al., 2016; Yao et al., 2023).

Water-level fluctuations affect C cycling in reservoirs by creating areas with shallow waters. Shallow waters are hotspots for CO₂ and CH₄ emissions due to the strong interaction between their sediments and the atmosphere and low hydrostatic pressure. For instance, shallow inland waters emit higher CO₂ fluxes due to elevated O₂ and temperature in sediments (Deshmukh et al., 2018). Hydrostatic pressure determines the timing, the ratio of CH₄ to CO₂, and the CH₄ flux pathway (Harrison et al., 2017; Holgerson et al., 2017; Li et al., 2020). High hydrostatic pressure delays CH₄ in sediments and the water column, increasing its dissolution in water and oxidation to CO₂ (McGinnis et al., 2006). Small, shallow waters are also more prone to eutrophication due to high areal nutrient loads and a low physical self-cleaning capacity. Autochthonous OM produced in eutrophic waters is more favorable for methanogenesis than allochthonous OM (Deemer et al., 2016; Grasset et al., 2018; West et al., 2012). Furthermore, nutrients drawn from the littoral zone during water drawdown can enhance the growth of phytoplankton in the pelagic zone. The return of water to the normal level can lead to the flooding and decomposition of the newly established phytoplankton and C emissions. Extreme water drawdown events exacerbate CO₂ emissions from reservoirs by replacing shallow water with exposed sediments.

Drawdown areas covered 15% of the global surface area of reservoirs between 1985 and 2015 (Keller et al., 2021). The exposed sediments of these drawdown areas contributed 53% of global CO₂ emissions from reservoirs (Keller et al., 2021). However, Keller et al. (2021) did not consider the effect of vegetation growth on C fluxes in dry sediments of reservoirs. Vegetation involves, in the long-term, C cycling by sequestering atmospheric CO₂ in above- and below-ground vegetation biomass and soil OM. For instance, terrestrial ecosystems are autotrophic, i.e., primary productivity is higher than ecosystem respiration due to vegetation (Bond-Lamberty & Thomson, 2010, 2012). Hence, exposed sediments under terrestrialization (i.e., transition from an aquatic to a terrestrial stage due to the growth

of terrestrial vegetation) can evolve from net emitters to net sinks of atmospheric CO₂ (Bolpagni et al., 2017). However, the time scales for C sinks in exposed sediments are not known and may depend on several factors, such as the replacement of annual herbaceous vegetation by perennial woody vegetation (Albrecht & Kandji, 2003; Jansson et al., 2010). The replacement of herbaceous plants by woody plants may be a long-term effect of water management in reservoirs, such as dam decommissioning.

1.4. Dam decommissioning: a new global challenge

1.4.1. Dam ageing and dam decommissioning as an unavoidable action

Dam ageing is the deterioration that occurs more than five years after the beginning of the operational phase of a dam (Zamarrón-Mieza et al., 2017). The deterioration of a dam before five years is attributed to the inadequacy of design, construction, or operation (Zamarrón-Mieza et al., 2017). Many dams have exceeded their lifetime of 50–100 years and, thus, the world faces an unprecedented challenge of dam ageing (Perera et al., 2021). In the northern hemisphere many dams have exceeded the alert age threshold of 50 years and will soon reach 100 years (ICOLD WRD, 2022; Perera et al., 2021) (Fig.1.4). For instance, North America and Asia have ~16,000 large dams in the range 50–100 years and ~2,300 large dams older than 100 years (ICOLD WRD, 2022). The average age of 90,580 dams in the US is 56 years, and more than 85% of these dams reached the end of their lifetime in 2020 (Hansen et al., 2019). The average age of dams in the UK is 100 years (Perera et al., 2021). About 20 dams are in the range of 130 (e.g., Proserpina Dam in Spain) and 1,470 (e.g., Otakiine Dam in Japan) years worldwide (ICOLD WRD, 2022). Of the 1.2 million dams built in Europe, 200,000 dams (17%) are no longer efficient, safe, or suitable for their intended purposes (Dam Removal Europe, 2020). Thus, dam ageing is an emerging global problem with multifaceted effects.

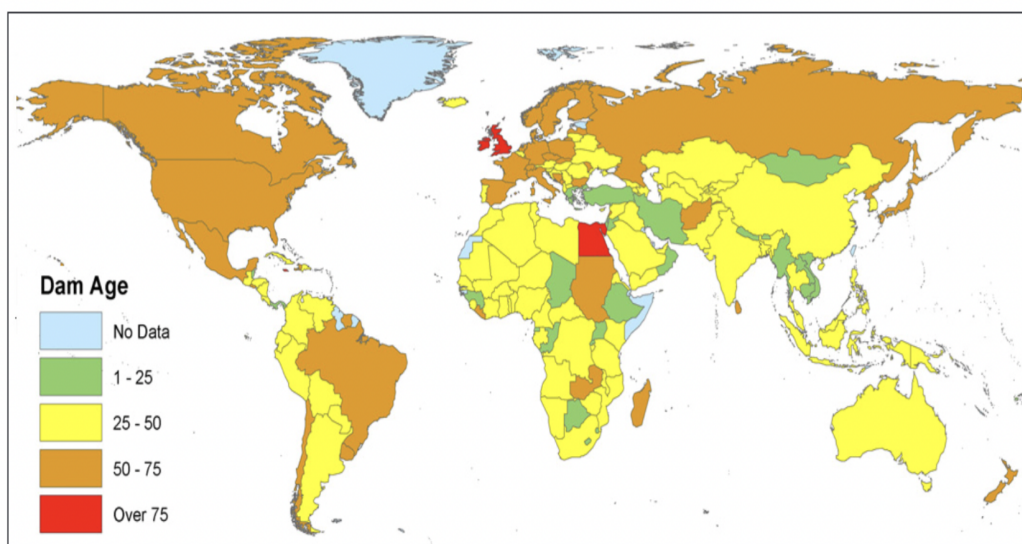


Figure 1.4 The median age of large dams by country. Source: Perera et al. (2021)

Negative effects of old dams include, among others, high repair and maintenance costs, loss of function and effectiveness, and a threat to public safety (Perera et al., 2021). Thus, an old dam is either repaired and its primary function maintained, retained but with its primary function amended (i.e., re-operationalization), or partially or fully decommissioned (Perera et al., 2021). Dam decommissioning (DD) is the partial or full removal of a dam and its ancillary facilities so that the statutory definition of a dam is no longer met, or the structure is no longer a source of danger (Pacca, 2007; USSD, 2015). Dam decommissioning can be cheaper than repairing and maintaining old dams. For instance, removing dams in the US would cost 10.5 billion USD by 2050, while their maintenance would be 10–30 times more expensive (Habel et al., 2020). However, decision-makers must consider many technical, environmental, and socio-economic concerns before DD. Thus, DD of even a small dam requires years (often decades), expert and public participation, and long regulatory reviews (Habel et al., 2020; Perera et al., 2021). Since it is also associated with significant financial costs and landscape alteration, DD frequently faces fervent resistance.

1.4.2. Resistance to DD

Dam decommissioning, especially the removal of large dams, is not yet a common practice nor an easy task. Thus, most of the removed dams in the US are small with a median height of ~3 m (Bellmore et al., 2017). Dams ≤ 2.5 m high constitute 43% and those 2.5–7.5 m high constitute 42.7% of the 1,250 dams removed with a reported height between 1968 and 2019 in the US (Habel et al., 2020). Dams ≤ 2.5 –7.5 m high constitute ~95% of 342 dams removed between 1996 and 2019 in Europe (Habel et al., 2020). Only six dams higher than 30 m were removed in the US and in Europe, only one dam 36 m high, Vezins Dam on the Sélune River in France, was removed in 2019 (Habel et al., 2020). The Enobieta Reservoir (42 m high) has been partially removed since 2017 (Atristain et al., 2022;

Larrañaga et al., 2019). Small dams dominate the list of removed dams because they are the most numerous, oldest, and their removal causes less social and economic problems.

Social and economic problems caused by DD affect local livelihoods, heritage, property value, recreation, and aesthetics (Fox et al., 2016; Habel et al., 2020; Perera & North, 2021). These problems cause resistance to DD. Resistance to DD is stronger in Europe than in the US because dams have existed in Europe since the medieval age, while the history of dams is relatively recent in the US (Brykała & Podgórski, 2020; Pohl, 2002). Due to the strong economic dependence on large dams and the long history of dams in the landscape, DD is often considered an unnecessary cost in Europe (Habel et al., 2020). Thus, the maintenance approach of old dams is more prevalent in Europe where, for instance, new dams are built upstream or downstream to mitigate the potential harmful effects of old dams. However, indigenous people who depend economically and culturally on and have strong spiritual ties to the pristine environment, such as several tribes in the US, are key supporters of DD (Habel et al., 2020). The biggest concerns in fighting against DD in developed countries are cultural heritage, aesthetics, recreation, and property value (Habel et al., 2020; Perera & North, 2021; Perera et al., 2021). These concerns can be mitigated through education, commemoration, and the creation of attractive green spaces near the removed dams. The motives to oppose DD may be different in low-income and arid nations where people depend on dams for water supply, irrigation, and electricity.

To conduct DD in harmony, this process must be conducted in a sound economic, geographic, and social context. Although DD may differ for each country due to its politics, economy, and social and cultural aspects, it should involve all stakeholders (i.e., people affected by DD: public administration, scientific experts, businesspeople, environmental NGOs, local communities, politicians, and indigenous communities). It should also include all aspects of the discussion, such as economic (e.g., energy, transport, profit, concessions, maintenance, fishing, tourism, agriculture, water provision, employment, the value of real estate), environmental (e.g., biodiversity, ecological conditions, habitat heterogeneity, river continuum), and social (e.g., local customs, recreation, safety, cultural heritage, cultural landscape) (Duda & Bellmore, 2022; Habel et al., 2020; Perera & North, 2021). Local communities should have alternative options related to development means for areas covered by removed reservoirs. These new development plans should provide greater social and economic benefits than the removed dam. Dam decommissioning should also include a phase of informing the stakeholders about the probable positive and negative environmental effects of DD.

1.4.3. Environmental effects of DD

Dam decommissioning causes short-term environmental effects on the fluvial system mainly because of erosion of the reservoir sediments. Ecological conditions, relative to pre-dam decommissioning conditions, deteriorate due to the release of sediments and contaminants from the reservoir (Bednarek, 2001). The release of sediments causes turbidity, suffocation, and abrasion of habitats and organisms, scouring of insects and algae,

and sediments can cover the food sources of some organisms (Bednarek, 2001). These effects depend on many factors, including sediment composition or grain size (erodibility and cohesion), hydrology, DD approach, and geomorphology of the river valley, and riverbed gradient (Randle et al., 2015; Wilcox et al., 2014). A sound approach to DD can limit the impact of eroded sediments on downstream environments (Larrañaga et al., 2019; Ritchie et al., 2018). The flux of nutrients in sediments can cause eutrophication in coastal watersheds and negative effects on estuaries (Gold et al., 2016). Furthermore, although DD restores the dispersal and movement of migratory fish, it can also enable the dispersal of exotic species (De Rego et al., 2020). However, sediment release during DD, by lasting only hours to months; mainly causes short-term effects (Bellmore et al., 2019; Duda & Bellmore, 2022).

The short-term effects of DD are followed by long-term responses, which take years to decades to appear. These long-term responses after DD are, for instance, increased access to habitat, sediment and water flow continuity, ecosystem heterogeneity, vegetation succession in the riparian zone, and the development of the food web (Duda & Bellmore, 2022). These long-term effects of DD lead to high biodiversity (Mapes, 2016), which is economically profitable, such as for fisheries (Allen et al., 2016; Hardiman & Allen, 2015; Lovett, 2014). However, studies on the effects of DD on ecosystem changes in the biological, chemical, and physical conditions of rivers and the final impact on river restoration are limited. For instance, of the 1,200 dams removed in the US, <10% have been studied, and most of these studies were on a short time scale (<4 years) (Bellmore et al., 2017) and focused on the impact of sediment release on rivers and their deltas (Ritchie et al., 2018). These studies had limited (1–2 years) or no monitoring before DD (Bellmore et al., 2019). Finally, previous studies did not assess how DD affects the large stocks of OM buried in reservoir sediments and the C footprint of reservoirs. The impact of DD on the C footprint of reservoirs may depend on the content and decomposition rate of the OM buried in reservoir sediments.

1.4.4. Potential effect of DD on C cycling in reservoirs

Three reasons drive the interest in the effect of DD on C cycling in reservoirs: (1) the massive ageing of dams, (2) the large stocks of OM buried in reservoir sediments, and (3) the high C emissions during reservoir drawdown. Tens of thousands of dams built in the 19th and early 20th centuries have become obsolete and pose several economic and social problems (Perera et al., 2021). The most viable option to address socio-economic challenges caused by old dams is DD. However, reservoirs bury large amounts of OM in their anoxic sediments during their operational phase (Maavara et al., 2017; Mendonça et al., 2017). Dam decommissioning subjects sediment OM to three hotspots of CO₂ and CH₄ emissions: (1) shallow water, (2) exposed sediments, and (3) lotic water. Shallow waters are hotspots for CO₂ and CH₄ emissions, while exposed sediments and lotic waters are hotspots for CO₂ emissions (Harrison et al., 2017; Kosten et al., 2018; Marcé et al., 2019; Raymond et al., 2013).

Thus, DD should be expected to affect C cycling in reservoirs by creating shallow impounded waters, which are emission hotspots for CO₂ and CH₄ due to increased interaction between the atmosphere and sediments, low hydrostatic pressure, and reduced CH₄ oxidation at low water depth, exposed sediments that are emission hotspots for CO₂ because of reduced CO₂ consumption by primary production and high CO₂ production due to the increased concentration of O₂ in sediments. The high concentration of O₂ in sediments can enhance the decomposition of sediment OM but limit CH₄ fluxes in exposed sediments. Dam decommissioning may also alter C cycling in reservoirs by increasing the surface area of lotic waters in the former reservoirs. Lotic waters show higher areal CO₂ emission rates due to their higher gas transfer velocity and concentration of O₂ than impounded waters. In addition, CO₂ and CH₄ emissions may increase downstream by increasing the export of OM and CO₂ and CH₄ from the reservoir. Sediment exposure may also lead to high terrestrialization of exposed sediments due to high contents of OM and nutrients buried in reservoir sediments. Terrestrialization can reduce CO₂ emissions from exposed sediments by incorporating atmospheric CO₂ into vegetation biomass.



2. Objectives and hypotheses of the study

The overall objective of this thesis is to explore the effects of DD on C cycling in reservoirs because there are many dams under removal and many more predicted in the near future. To answer this question, we conducted this study in the Enobieta Reservoir (Navarre, N Iberian Peninsula) that underwent drawdown between 2017 and 2019. The central objectives are addressed in the main three chapters (chapters 3, 4, and 5), each corresponding to a separate article publication that addresses several specific objectives.

Overall question: This thesis will answer the overarching question of how DD affects C dynamics in reservoirs by altering water depth, impoundment status, and vegetation cover through terrestrialization.

Chapter 3: This chapter aimed to assess the effects of the drawdown phase of DD on CO₂ and CH₄ emissions in the Enobieta Reservoir. The specific objectives of this chapter were (1) to compare CO₂ and CH₄ emissions among impounded water, exposed sediment, and lotic water, (2) to examine the influence of water depth on CO₂ and CH₄ emissions in reservoirs, (3) to constrain spatial and temporal trends of CO₂ and CH₄ emissions in exposed sediment after reservoir drawdown, and (4) to assess how reservoir drawdown affects CO₂ and CH₄ emissions in the river reach downstream of reservoirs.

Hypotheses for chapter 3: We expected that (1) CO₂ emissions will be highest in lotic water, followed by exposed sediment, and lowest in impounded water, while CH₄ emissions will be highest in impounded water due to higher anoxia, followed by lotic water, and lowest in exposed sediment, (2) shallow water will exhibit higher CO₂ and CH₄ emissions than deep impounded water, (3) CO₂ and CH₄ emissions in exposed sediment will vary over space and time due to spatial and temporal changes in the content and reactivity of sediment OM, and (4) reservoir drawdown will increase CO₂ and CH₄ emissions in the river reach downstream of the reservoir due to enhanced transport of OM and those gases downstream from the reservoir.

Chapter 4: This chapter sought to estimate the content and reactivity of sediment OM in the study reservoir. The specific objectives of this chapter were (1) to understand the temporal changes in the content and reactivity of sediment OM in exposed sediments, (2) to compare the decomposition efficiency of bulk sediment OM and sediment water-extractable organic matter (WEOM), and (3) to compare the content and reactivity of sediment OM in reservoir sediments with the content and reactivity of sediment OM in other inland waters and soils.

Hypotheses for chapter 4: We predicted that (1) the content and reactivity of sediment OM will change with sediment exposure time due to the consumptive loss of sediment OM, (2) the decomposition efficiency will be lower for bulk sediment OM compared to WEOM because WEOM is the most bioavailable fraction of OM, and (3) the content and reactivity

of sediment OM in the Enobieta Reservoir and other lentic inland waters will be comparable, but higher than in lotic inland waters.

Chapter 5: This chapter aimed to understand how vegetation biomass affects CO₂ fluxes in the exposed sediment of the study reservoir. The specific objectives were to (1) assess spatial and temporal dynamics of terrestrialization of exposed sediment after reservoir drawdown, (2) compare CO₂ fluxes between bare sediment and sediment with vegetation, and (3) assess how the incorporation of C into vegetation biomass affects C fluxes in exposed sediment.

Hypotheses for chapter 5: We expected that (1) stable (e.g., flat) and old (i.e., with long sediment exposure time) environments will exhibit greater terrestrialization than steep and young environments, (2) CO₂ fluxes from sediment with vegetation will be higher than from bare sediment due to the supply of labile OM by the growing vegetation and its contribution to respiration, and (3) the incorporation of C into vegetation biomass will reduce C fluxes in exposed sediment.

Supervisors' report

Dr. Biel Obrador and Dr. Daniel von Schiller, professors in the Section of Ecology of the Department of Evolutionary Biology, Ecology and Environmental Sciences, at the University of Barcelona, as supervisors of the Doctoral Thesis presented by Amani MABANO entitled: *Effects of dam decommissioning on carbon cycling in reservoirs. Case study of the Enobieta Reservoir, N Iberian Peninsula*,

INFORM:

That the research studies developed by Amani MABANO for his Doctoral Thesis have been organized in three chapters, which correspond to three scientific papers, two published and one to submit for publication.

The list of the published papers indicating the Impact of Factor of Journals according to SCI of ISI Web of Science is the following:

Amani, M, von Schiller, D, Suárez, I, Atristain, M, Elosegí, A, Marcé, R, García-Baquero, G, & Obrador, B (2022). The drawdown phase of dam decommissioning is a hot moment of gaseous carbon emissions from a temperate reservoir. *Inland Waters*, 12, 451–462. DOI: 10.1080/20442041.2022.2096977. Impact factor (2022): 3.1; Quartile: Q1.

Amani, M, Obrador, B, Fandos, D, Butturini, A & von Schiller, D (2024). Exposed sediments in a temperate-cimate reservoir under dam decommissioning contains large stocks of highly bioreactive organic matter. *Limnetica*, 43, 000-000. DOI: 10.23818/limn.43.11. Impact factor (2022): 1.4; Quartile: Q3.

The manuscript to be submitted is:

Amani, M, von Schiller, D, Minaudo, C, Badia, M, Suárez-Velasquez, I, Elosegí, A, Aldezabal, A, Atristain, M, Obrador, B. Vegetation growth partially offsets carbon dioxide emissions from exposed sediments: a study in a decommissioned reservoir.

And CERTIFY:

That Amani MABANO has participated actively in the development of the research and the elaboration associated with each of the listed papers. His contribution included the following tasks:

- Setting objectives and experimental design,
- Sampling design and field work,
- Laboratory analysis and data processing,

- Statistical data analysis and interpretation of results, and
- Writing, reviewing, and editing of the manuscripts.

We finally certify that the co-authors of the papers that conform this Doctoral Thesis will not use any of the manuscripts in any other Doctoral Thesis.

Barcelona, September 2023

A handwritten signature in blue ink, appearing to be 'B. Obrador', written in a cursive style.

Dr. Biel Obrador

A handwritten signature in blue ink, appearing to be 'D. von Schiller', written in a cursive style.

Dr. Daniel von Schiller



3. The drawdown phase of dam decommissioning is a hot moment of gaseous carbon emissions from a temperate reservoir

Amani, M, von Schiller, D, Suárez, I, Atristain, M, Elozegi, A, Marcé, R, García-Baquero, G, Obrador, O (2022). The drawdown phase of dam decommissioning is a hot moment of gaseous carbon emissions from a temperate reservoir. *Inland Waters*, 12, 451–462. DOI: 10.1080/20442041.2022.2096977

3.1. Abstract

Dam decommissioning (DD) is a viable management option for thousands of ageing dams. Reservoirs are great carbon sinks, and reservoir drawdown results in important carbon dioxide (CO₂) and methane (CH₄) emissions. We studied the effects of DD on CO₂ and CH₄ fluxes from impounded water, exposed sediment, and lotic water before, during, and 3–10 months after drawdown of the Enobieta Reservoir, north Iberian Peninsula. During the study period, impounded water covered 0–100%, exposed sediment 0–96%, and lotic water 0–4% of the total reservoir area (0.14 km²). Areal CO₂ fluxes in exposed sediment (mean ± SE: 295.65 ± 74.90 mmol m⁻² d⁻¹) and lotic water (188.11 ± 86.09) decreased over time but remained higher than in impounded water (-36.65 ± 83.40). Areal CH₄ fluxes did not change over time and were noteworthy only in impounded water (1.82 ± 1.11 mmol m⁻² d⁻¹). Total ecosystem carbon (CO₂ + CH₄) fluxes (kg CO₂-eq d⁻¹) were higher during and after than before reservoir drawdown because of higher CO₂ fluxes from exposed sediment. The reservoir was a net sink of carbon before reservoir drawdown and became an important emitter of carbon along the first ten months after reservoir drawdown. Future studies should examine mid- and long-term effects of DD on carbon fluxes, identifying the drivers of areal CO₂ fluxes from exposed sediment and incorporating DD in the carbon footprint of reservoirs.

Keywords: Ageing dams; carbon dioxide fluxes; dam removal; exposed sediment; reservoir drawdown; water reservoirs

Resumen

El desmantelamiento de presas (DP) es una opción de gestión viable para miles de presas envejecidas. Los embalses son grandes sumideros de carbono, y el vaciado de los embalses genera importantes emisiones de dióxido de carbono (CO₂) y metano (CH₄). Estudiamos los efectos del DP en los flujos de CO₂ y CH₄ del agua embalsada, los sedimentos expuestos y el agua lótica antes, durante y entre 3 y 10 meses después del vaciado del embalse de Enobieta, situado en el norte de la Península Ibérica. Durante el período de estudio, el agua embalsada cubrió del 0 al 100%, los sedimentos expuestos del 0 al 96% y el agua lótica del 0 al 4% del área total del embalse (0,14 km²). Los flujos areales de CO₂ en sedimentos expuestos (media ± SE: 295,65 ± 74,90 mmol m⁻² d⁻¹) y agua lótica (188,11 ± 86,09) disminuyeron con el tiempo, pero permanecieron más altos que en el agua embalsada (-36,65 ± 83,40). Los flujos areales de CH₄ no cambiaron con el tiempo y solo fueron notables en el agua embalsada (1,82 ± 1,11 mmol m⁻² d⁻¹). Los flujos de carbono total (CO₂ + CH₄) del ecosistema (kg CO₂-eq d⁻¹) fueron más altos durante y después que antes del vaciado del embalse debido a los flujos más altos de CO₂ de los sedimentos expuestos. El embalse era un sumidero neto de carbono antes del

vaciado y se convirtió en un importante emisor de carbono durante los primeros diez meses después del vaciado. Los estudios futuros deberían examinar los efectos a mediano y largo plazo del DP en los flujos de carbono, identificando las variables que controlan los flujos de CO₂ en las zonas de sedimentos expuestos e incorporando el DP en la huella de carbono de los embalses.

Palabras clave: Envejecimiento de presas; flujos de dióxido de carbono; remoción de presas; sedimento expuesto; vaciado de embalses; embalses

3.2. Introduction

Reservoirs influence the global carbon (C) cycle and climate system because they are large sinks of organic (C) and great emitters of carbon dioxide (CO₂) and methane (CH₄) greenhouse gases (GHGs) (Deemer et al., 2016; Downing et al., 2008; Mendonça et al., 2017). Emissions of GHGs during the operational phase of reservoirs, ~0.8 Pg CO₂ equivalents (CO₂-eq) yr⁻¹ (Deemer et al., 2016), have been included in the global inventories of anthropogenic GHGs (IPCC, 2019) because they play a significant role in global warming. The global carbon emissions from reservoirs are lower than the organic C burial in their sediments (Deemer et al., 2016; Mendonça et al., 2017), although this has been recently challenged (Keller et al., 2021). In addition, during the removal of a dam and its ancillary facilities (i.e., dam decommissioning), the large stocks of organic C in the sediments of the reservoir may decompose and emit more CO₂ and CH₄ (Keller et al., 2021; Pacca, 2007).

Dam decommissioning is becoming a credible management solution for tens of thousands of dams that have reached or exceeded their engineered life expectancies of 50–100 years (Doyle et al., 2003; Perera et al., 2021; Stanley & Doyle, 2003). Dams are removed for several reasons, including environmental restoration, increasing maintenance costs, gradual reservoir sedimentation, and public safety (Perera et al., 2021). The process of DD has gained high research interest, which has focused mostly on the effects of river connectivity on ecological processes such as migration and dispersion of living organisms (Bednarek, 2001; Bellmore et al., 2019; Marks et al., 2010). Although reservoir sediments are important repositories of organic C, previous studies have not examined the fate of that sediment organic C following DD (Pacca, 2007). Dam decommissioning may be a relevant component of the C balance in a reservoir because reservoir drawdown is hot moment for the decomposition of sediment organic C to CO₂ and CH₄ (Deshmukh et al., 2018; Keller et al., 2021; Paranaíba et al., 2021).

The reservoir drawdown phase of DD is likely to first increase CO₂ and CH₄ fluxes from a reservoir through the formation of shallow waters (Deshmukh et al., 2018; Harrison et al., 2017; Li et al., 2020). Small patches of shallow waters can emit, for instance, 75% and 90% of, respectively, the annual CO₂ and CH₄ fluxes from reservoirs (Deshmukh et al., 2018; Harrison et al., 2017). Approximately 35% of total CH₄ fluxes from the surface waters of reservoirs is emitted via diffusion while 65% is emitted via ebullition (Deemer et al., 2016), which is higher in shallow waters (Baulch et al., 2011). Shallow waters emit higher areal C fluxes due to conditions such as increased aeration and temperature that facilitate gas production in sediments, and shallow depth that results in low hydrostatic pressure and readily allows gases to be transported to the overlying water layer and the water-atmosphere interface (Harrison et al., 2017; Li et al., 2020). Dam decommissioning may promote C emissions to the atmosphere due to the increased areal extension in shallow waters resulting from reservoir drawdown.

Reservoir drawdown can furthermore produce high carbon fluxes when it exposes sediments to the atmosphere. Exposed sediment is a hotspot for CO₂ emissions whose areal fluxes in reservoirs, 4–1533 mmol m⁻² d⁻¹ (Gómez-Gener et al., 2016; Jin et al., 2016; Obrador et al., 2018) are higher than CO₂ fluxes from surface waters of lentic waters, 18–55 mmol m⁻² d⁻¹ (Deemer et al., 2016; Holgerson et al., 2017; Raymond et al., 2013), and even comparable to areal CO₂ fluxes from lotic water, 120–633 mmol m⁻² d⁻¹ (Borges et al., 2015; Gómez-Gener et al., 2015; Raymond et al., 2013). Lotic water emits higher C fluxes than impounded water because of its highly turbulent water columns of and, hence, higher gas exchange coefficients (Gómez-Gener et al., 2015). Furthermore, the higher CO₂ emissions from exposed sediment are related to a closer coupling of CO₂ production and fluxes and increased CO₂ production due to high oxygen availability (Fromin et al., 2010; Keller et al., 2020).

Increased redox potentials in exposed sediment reduce CH₄ production and increase CH₄ oxidation, which results in lower CH₄ fluxes. Thus, CH₄ fluxes from exposed sediment, 0.1–1 mmol m⁻² d⁻¹ (Deshmukh et al., 2018; Gómez-Gener et al., 2015; Yang et al., 2014) are lower than CH₄ fluxes from lotic waters, 4.2 ± 8.4 mmol m⁻² d⁻¹ (Stanley et al., 2016) and surface waters of lakes and reservoirs, 3–10 mmol m⁻² d⁻¹ (Deemer et al., 2016). Fluxes of CH₄ from a flooded site may even be three orders of magnitude higher than CH₄ fluxes from a non-flooded site of the same reservoir (Yang et al., 2014). Though areal CO₂ fluxes are higher than CH₄ fluxes from reservoirs, CH₄ has a global warming potential 25 times higher than that of CO₂ over a timespan of 100 years and, thus, 79% of the annual CO₂-eq emissions from reservoirs occurs as CH₄ (Deemer et al., 2016). In summary, when exposed sediment replaces impounded water during DD, CO₂ emissions may increase, whereas CH₄ emissions may decrease. However, to our knowledge, there is no empirical evidence on the effects of DD on carbon fluxes in reservoirs. This knowledge would help inform regional and global scale estimates of the carbon footprint of reservoirs and their perception as a carbon-neutral source of energy (Barros et al., 2011).

Here, we assessed short-term effects of DD on CO₂ and CH₄ fluxes before, during, and after drawdown of a temperate reservoir. We measured CO₂ and CH₄ fluxes in exposed sediment, deep and shallow zones of impounded water, and lotic water. We hypothesize a temporal change in CO₂ and CH₄ fluxes for the three environments along reservoir drawdown, CO₂ fluxes highest in exposed sediment, CH₄ fluxes highest in impounded water, higher CO₂ and CH₄ fluxes from the shallow zone than the deep zone of impounded water, and higher ecosystem C fluxes due to higher areal carbon fluxes from exposed sediment and lotic water after reservoir drawdown.

3.3. Materials and Methods

3.3.1. Study site

The Enobieta Reservoir is in the valley of Artikutza (Navarre, N Iberian Peninsula), where human activities are restricted since 1919, when the municipality of Donostia-San Sebastián bought the land to ensure the supply of high-quality drinking water. The mean annual air temperature is 12.2 °C with an average rainfall of 2,604 mm yr⁻¹ (average 1954–2019; Gobierno de Navarra (2019)). The dam was constructed between 1947 and 1953 on the Enobieta Stream. The reservoir had an initial storage capacity of 2.66 hm³, length of 1.1 km, maximum depth of 25.5 m, a concrete dam height of 42 m, and an area of 0.14 km². Geotechnical problems appeared during its construction, forcing a reduction in its storage capacity to 1.40 hm³, and the construction of a larger reservoir (Añarbe Reservoir, 43.8 hm³) downstream in 1976, after which Enobieta Reservoir was no longer used as a water supply facility (Larrañaga et al., 2019). In addition, Artikutza is part of the Natura 2000 Network and, since 2014, it is a special conservation zone. The high conservation status of the valley and the structural instability of the dam led to a DD of the Enobieta Reservoir, a process that began in 2017 and extended along 2018 and 2019 (Fig.S.3.1). To date, the decommissioning has been partial, as the reservoir has been completely emptied of water and the river runs freely through a hole in the dam, but the concrete structure of the dam (the physical structure retaining the water) is still standing.

3.3.2. Sampling design

We measured CO₂ and CH₄ fluxes in three environments: impounded water, exposed sediment, and lotic water, before, during, and after reservoir drawdown. We conducted eight sampling campaigns on 16 June 2016, 07 July 2018, 10 September 2018, 22 October 2018, 21 January 2019, 09 April 2019, 02 July 2019, and 18 February 2020 (Table 3.1, Fig.S.3.1). Exposed sediment and lotic water completely replaced impounded water on 25 February 2019. The campaigns we conducted before 25 February 2019 correspond to the periods Before and During reservoir drawdown, while the campaigns after this date correspond to the period After reservoir drawdown. Thus, we sampled two times prior to drawdown (days -984 and -233), three times during drawdown (days -168, -126, and -35), and three times after drawdown was complete (days 43, 127, and 358 days). We identified these days by taking the sampling date minus 25 February 2019 (for instance, 16 June 2016 - 25 February 2019 = -984 days, Table 3.1).

Impounded water was sampled from day -984 to day -35 (i.e., when it was present) in two zones: deep water (>4 m) and shallow water (<4 m) (Harrison et al., 2017) (Fig.3.1, Table 3.1, Fig.S.3.1). The location of the shallow water zone changed over time as water level decreased along drawdown. Before exposed sediment and lotic water completely

replaced impounded water (day -233 to -35), we measured CO₂ and CH₄ fluxes in lotic water at the stream-reservoir transition inlet (one site). After complete reservoir drawdown (day 43–58), we measured the fluxes in lotic water at two sites across the reservoir. For both impounded water and lotic water, we measured CO₂ and CH₄ fluxes by triplicate (three samples at each site).

We sampled CO₂ and CH₄ fluxes in exposed sediment from day -233 to day 358 (when it was present; Table 1). To measure CO₂ and CH₄ fluxes in exposed sediment, we used four cross-sectional transects (A, B, C, and D; Fig.3.1), comprising between one and five sites (Table S.3.1). We measured three CO₂ fluxes and one CH₄ flux at each site. The number of transects and the number of sites for some transects increased with time, as water retracted from the edge to the center and toward the dam of the reservoir. For instance, because impounded water covered most of the reservoir on day -233, we had only transect A with one site (thus, the sample size (*n*) in this campaign was three for CO₂ and one for CH₄). Moreover, the number of sites among transects varied because the distance from the center to the edge of the reservoir was not the same across the reservoir. Consequently, the number and length of transects changed with reservoir drawdown (Table 3.1). During reservoir drawdown (days -168 to -35), we used three transects (A, B and C), with three sites each (*n* = 27 for CO₂ and *n* = 9 for CH₄). After reservoir drawdown (i.e., from day 43 onward), we used four transects, with three (A and D), four (B), and five (C) sites each (*n* = 45 for CO₂ and *n* = 15 for CH₄) (Fig.3.1, Table S.3.1).

3.3.3. Determination of CO₂ fluxes

We determined CO₂ fluxes from exposed sediment and impounded water using the chamber method (Frankignoulle, 1988). We measured CO₂ fluxes from exposed sediment with an enclosed opaque soil respiration chamber (SRC-1, PP-Systems, USA). For impounded water, we estimated CO₂ fluxes across the water-air interface with a custom-made floating enclosed opaque chamber. We monitored the partial pressure of CO₂ (*p*CO₂) in the chambers every second with an infrared gas analyser (IRGA-EGM-5, PP-Systems, Amesbury, USA, 1 % accuracy). We waited for *p*CO₂ in chambers to change by at least 10 µatm, which took 120–300 s in exposed sediment and 300–600 s in impounded water. We calculated CO₂ fluxes from exposed sediment and impounded water by a linear regression of *p*CO₂ in the chambers over time corrected for temperature and pressure as:

$$FCO_2 = \left(\frac{dpCO_2}{dt} \right) \left(\frac{V}{RTS} \right), \quad (3.1)$$

where *FCO₂* is CO₂ flux (mol m⁻² d⁻¹), *dpCO₂/dt* is the slope of the regression of *p*CO₂ in the chamber over time (atm d⁻¹), *V* is the volume of the chamber (1.171 × 10⁻³ m³ for exposed sediment, 0.027 m³ for impounded water), *S* is the area of the chamber (7.8 × 10⁻³ m² for exposed sediment and 0.194 m² for impounded water), *T* is temperature (K), and *R* is the ideal gas constant (m³ atm K⁻¹ mol⁻¹). All fluxes reported here follow the

convention that efflux to the atmosphere corresponds to a positive flux, and uptake or influx corresponds to a negative flux.

We determined the direction and magnitude of CO₂ fluxes from lotic water by applying Fick's first law of gas diffusion:

$$FCO_{2stream} = kCO_2 \times \beta \times (pCO_{2w} - pCO_{2a}) \quad (3.2)$$

where $FCO_{2stream}$ is the CO₂ flux from lotic water (mol m⁻² d⁻¹), kCO_2 is the transfer velocity of CO₂ (m d⁻¹), β is the solubility coefficient of CO₂ (mol m⁻³ atm⁻¹), and pCO_{2w} and pCO_{2a} are, respectively, the partial pressures of CO₂ (atm) in surface water and air.

We determined pCO_{2w} and pCO_{2a} by triplicate at each sampling site. The pCO_{2w} was determined by means of a membrane gas exchanger (MiniModule, Liqui-Cel, USA) coupled to an IRGA. We circulated sampled water via gravity through the membrane contactor at a rate of 300 mL min⁻¹ while recirculating an enclosed volume of gas between the membrane and the IRGA. We determined the solubility of CO₂, for the temperature and salinity of each sample (Bastviken et al., 2004). We estimated kCO_2 (m d⁻¹) in the lotic water as:

$$kCO_2 = k_{600} \left(\frac{ScCO_2}{600} \right)^{-\frac{2}{3}} \quad (3.3)$$

where $ScCO_2$ is a Schmidt number of CO₂ (dimensionless) and k_{600} (m d⁻¹) is k of CO₂ at a Schmidt number (Sc) of 600,

$$k_{600} = 5.14 \times d \times \frac{Vel}{d^{1.33}} \left(\frac{600}{ScCO_2} \right)^{-\frac{2}{3}}, \quad (3.4)$$

d is depth of the water column (m) and Vel denotes the velocity of lotic water (m s⁻¹), noting that this equation is an empirical adjustment of k_{600} in lotic water.

We estimated the velocity of lotic water by the time-conductivity curve that we obtained in instantaneous additions of tracer (NaCl) at a turbulent point in the channel, 200 m downstream of the point of addition, using a field conductivity-meter (WTW 340i, Germany). We recorded changes in electrical conductivity generated by the tracer pulse, then we used the changes to calculate the speed by dividing the distance by time that electrical conductivity takes to reach the maximum peak (Gordon et al., 2004).

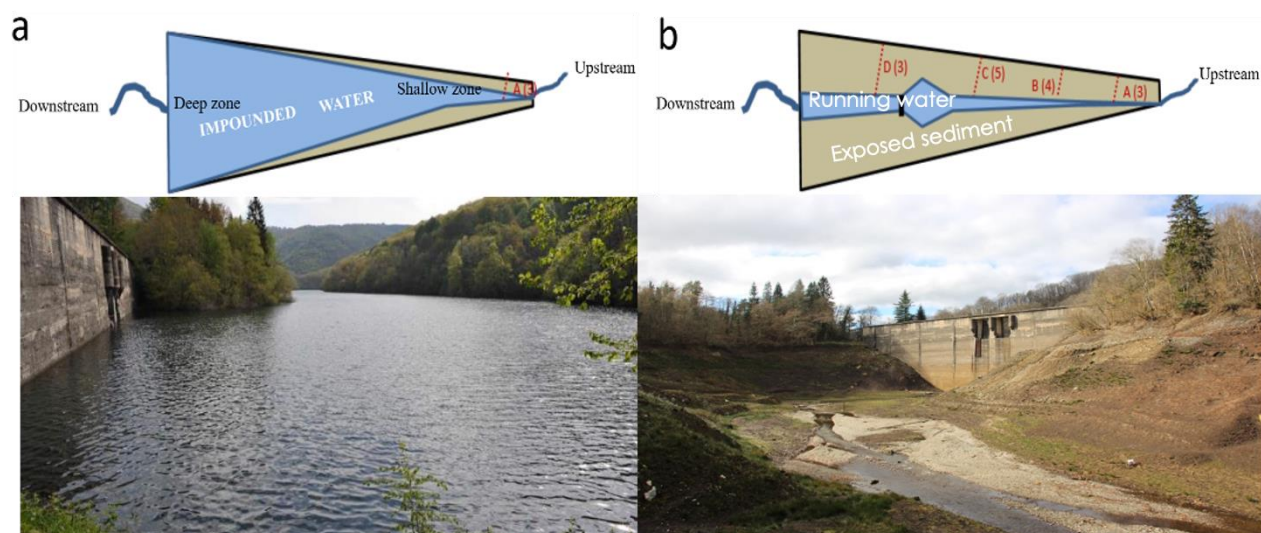


Figure 3.1 Simplified schematic and photographic view of the sampling design showing the state of the Enobieta Reservoir when (a) it was full: photo taken on day -233, July 2018; and (b) when it was empty: photo taken on day 358, February 2020. The scheme shows the three sampled environments: exposed sediment, running water, and impounded water. The red dashed lines are the cross-sectional transects used to measure CO_2 and CH_4 fluxes from exposed sediment. The numbers in brackets are the numbers of sites sampled for each transect of exposed sediment each day. Photos taken by M. Amani and B. Obrador

3.3.4. Determination of CH_4 fluxes

3.3.4.1. Determination of diffusive CH_4 fluxes in water

We determined diffusive CH_4 fluxes from impounded water and lotic water using the gradient of $p\text{CH}_4$ between water and air. We collected three samples of $p\text{CH}_4$ in surface water at each sampling site using the headspace technique equilibrated *in situ* with air (Bastviken et al., 2004). Briefly, we collected 30 mL of water with a 60 mL plastic syringe, which created a headspace with ambient air at 1:1 ratio (collected water: ambient air). We manually shook the syringe for one minute and then submerged it at each sampling site for five minutes, to maintain constant equilibration temperature. Thereafter, we transferred 20 mL of the gas mixture from the plastic syringe to a pre-evacuated vial (Exetainer, Labco Limited, UK). We took ambient air samples to correct for CH_4 concentration in the headspace.

In the laboratory, we determined $p\text{CH}_4$ in the gaseous mixture using a gas chromatograph equipped with a Flame Ionising Detector (FID) (Agilent 7820A GC), with an accuracy of 4%. We routinely ran six point standard curves obtained from a standard of 15 ppm CH_4 (Crystal, Air Liquide SA, Paris, France).

We determined diffusive CH₄ fluxes as for CO₂ (equation 3.2). In impounded water, the CH₄ transfer coefficient (kCH₄, in m d⁻¹) was obtained as:

$$kCH_4 = k_{600} \left(\frac{ScCH_4}{600} \right)^{-0.5} \quad (3.5)$$

with

$$k_{600} = 0.228 \times U_{10}^{2.2} + 0.168 \quad (3.6)$$

where $ScCH_4$ is the Schmidt number for CH₄ and U_{10} corresponds to the wind speed (m s⁻¹) at a height of 10 m above impounded water. To find U_{10} we measured the wind speed *in situ* at 1 m with a portable anemometer (Kestrel 4000, Kestrel Meters, UK) and converted it to U_{10} following (Crusius & Wanninkhof, 2003). We determined $ScCH_4$ in impounded water and lotic water at the measured water temperature (Gómez-Gener et al., 2015; Howard & Howard, 1993). We calculated CH₄ fluxes from lotic water the same way we calculated CO₂ fluxes, using $ScCH_4$ instead of $ScCO_2$ in equation 3 to estimate kCH₄.

3.3.4.2. Determination of ebullitive CH₄ fluxes from impounded water

We measured ebullitive CH₄ fluxes from impounded water with eight inverted funnel collectors: four funnels in deep water and four funnels in shallow water. We maintained the funnels for 6–23 h (DelSontro et al., 2010) to get a measurable flux (i.e., a detectable signal). The funnels (collection area of 0.44 m²) had a collector bottle where the gas accumulated during the entire sampling period. We closed the collectors of each funnel underwater and weighed them on the shore to determine the volume of gas, defined as the difference in weight between the collector after collection and the same collector filled with water. We estimated that the detection limit was ~10 mL for the gas collected using the gravimetric method. The collected gas was sampled and stored in pre-evacuated vials. We analysed pCH_4 in the gas samples with a gas chromatograph as detailed earlier for the diffusive CH₄ fluxes. We determined ebullitive CH₄ fluxes based on pCH_4 in the gas mixture, the volume of the collected gas, the collection time of the funnel and the surface area of the funnel.

3.3.4.3. Determination of diffusive CH₄ fluxes from exposed sediment

We determined diffusive CH₄ fluxes in exposed sediment with enclosed opaque chambers equipped with gas inlet and outlet valves, in a closed mode (no open vent). We installed the chambers (verifying a correct seal between sediments and the atmosphere) in fixed sampling sites within the transects where we installed fixed collar rings (Fig.3.1). We sampled the chamber three times during each measure: at time 0 (T0), time 1 (T1 ≥55 min), and time 2: (T2 ≤654 min). We determined pCH_4 in the gas samples using a gas chromatograph as detailed earlier. We determined areal CH₄ fluxes (mmol m⁻² d⁻¹) based

on the variation of $[\text{CH}_4]$ using the linear regression slope of the $p\text{CH}_4$ -time relationship, the area (0.0168 m^2) and the volume ($1.388 \times 10^{-3} \text{ m}^3$) of the chamber (equation 3.1). For this calculation, we included only the variations in $p\text{CH}_4$ above the detection limit (> 0.05 ppmv: parts per million by volume).

3.3.4.4. Upscaling carbon fluxes to the ecosystem level

We multiplied the mean areal C flux ($\text{mmol m}^{-2} \text{ d}^{-1}$) of each environment by the surface area (m^2) it occupied during each sampling campaign (Table 3.1) to quantify ecosystem carbon fluxes (mol d^{-1}). We obtained surface areas of impounded water and exposed sediment using satellite Sentinel images (Miranda, Mutiara, & Wibowo, 2018) taken in the period closest to each sampling campaign, mostly 2–3 days, and maximum one week. We extracted the surface areas of the reservoir and lotic water, respectively, using pixel-based classification and a Digital Elevation Model using Erdas Image 2020 and ArcMap 10.8 (Maathuis & Wang, 2006; Rathore et al., 2018). Finally, we multiplied ecosystem C fluxes by the molar mass of each GHG (16 g for CH_4 and 44 g for CO_2) by the global warming potential of each GHG (25 for CH_4 and 1 for CO_2 considering a time span of 100 years) to find CO_2 equivalents, $\text{CO}_2\text{-eq}$; in $\text{kg CO}_2\text{-eq d}^{-1}$ (IPCC, 2013).

Table 3.1 Sampling campaigns, sampling date (day/month/year), time (d) before or after exposed sediment completely replaced impounded water, phase of DD (pre = before, peri = during, post = after), average reservoir water depth (RWD), surface area percentage (%) area of each environment, and zone (DS = deep and shallow, S = only shallow) sampled within impounded water, transects (A, B, C, and D) sampled for exposed sediment, (n is the sample size of CO_2 fluxes in exposed sediment while the sample size for CH_4 fluxes is three times less that of CO_2 for each sampling), NA = not applicable.

Sampling date	Time	Phase	RWD (m)	Impounded water			Exposed sediment			Running water	
				Area (m^2)	% area	Depth	Area (m^2)	% area	Transect (n)	Area (m^2)	% area
16/06/16	−984	pre	20	141 400	100	DS	0	0	NA	0	0
07/07/18	−233	pre	19.8	140 800	99.6	DS	526	0.4	A (3)	74	0.1
10/9/18	−168	peri	14.8	101 200	71.5	DS	39 385	28	ABC (27)	815	0.5
22/10/18	−126	peri	9.8	71 500	50.6	DS	69 400	48.4	ABC (27)	1500	1
21/01/19	−35	peri	4.8	15 000	10.6	S	122 500	86.6	ABC (27)	3900	2.8
09/04/19	43	post	0	0	0	NA	135 800	96	ABCD (45)	5600	4
02/07/19	127	post	0	0	0	NA	135 800	96	ABCD (45)	5600	4
18/02/20	358	post	0	0	0	NA	135 800	96	ABCD (45)	5600	4

3.3.4.5. Statistical analyses

We assessed the effect of environment type and time on CO_2 and CH_4 flux rates using mixed effects models (Madsen & Thyregod, 2010; Pinheiro & Bates, 2000) with the R package *nlme* (Pinheiro & Bates, 2018) in R version 4.0.5 (R Core Team, 2021). Environment, a categorical factor with three levels (exposed sediment, impounded water, and lotic water) and time, a numerical variable, were fixed factors. We explored the

potential presence of spatial structure, such as differences in C fluxes among transects and sites of exposed sediment via spatial correlograms, but we found no significant spatial pattern. Thus, we applied spatially explicit methods of analysis by using a random factor “Site” within the framework of mixed modeling to account for spatial variability; therefore, site was the random effect. To consider the temporal autocorrelation present in the data and avoid wrong inference, temporal autocorrelation within each site was accounted for by means of a wide purpose correlation structure (compound symmetry). We included a variance function that allowed for different standard deviations per environment level to control for heteroscedasticity.

3.4. Results

3.4.1. Spatial extent of the environments and areal CO₂ and CH₄ fluxes

Before reservoir drawdown impounded water occupied almost 100% of the surface area of the reservoir (Table 3.1). During reservoir drawdown, exposed sediment covered between 28% and 87% of the reservoir. After reservoir drawdown, exposed sediment covered 96%, and lotic water 4% of the surface area of the Enobieta Reservoir.

Environment ($p < 0.001$), time ($p = 0.006$), and their interaction ($p < 0.001$) influenced areal CO₂ fluxes (Table 3.2, Fig.3.2a, Fig.S.3.3a). Areal CO₂ fluxes (mean \pm SE) from exposed sediment (295.65 ± 74.90 mmol m⁻² d⁻¹) and lotic water (188.11 ± 86.09 mmol m⁻² d⁻¹) decreased over time but remained higher than areal CO₂ fluxes from impounded water (-36.65 ± 83.40 mmol m⁻² d⁻¹) (Fig.3.2a, Table S.3.2, Fig.S.3.3a). Areal CO₂ fluxes in impounded water slightly increased from negative to positive values over time (Fig.3.2a, Table S.3.2, Fig.S.3.3a).

Table 3.2 Mixed modeling results for areal CO₂ and areal CH₄ (diffusion + ebullition) fluxes (mmol m⁻² d⁻¹): hypothesis testing for fixed factors (environment and time). df (num) is the numerator degrees of freedom for the F test for the fixed variables, while df (den) displays the denominator degrees of freedom for the F test for the fixed variables, and EnvXTime represents the interaction between environment and time. Significant p -values are shown in bold.

Source	df (num)	CO ₂ df (den)	F-value	p-value	df (num)	CH ₄ df (den)	F-value	p-value
Intercept	1	255	37.71	<0.001	1	35	164.76	<0.001
Env	2	255	13.91	<0.001	2	35	316.78	<0.001
Time	1	255	7.82	0.006	1	35	0.40	0.531
EnvXTime	2	255	8.70	<0.001	2	35	0.40	0.676

Environment ($p < 0.001$) but not time ($p = 0.531$) influenced the areal CH_4 fluxes (Table 3.2, Fig.3.2b, Fig.S.3.3b). The sum of areal diffusive and ebullitive CH_4 fluxes from impounded water ($1.82 \pm 1.11 \text{ mmol m}^{-2} \text{ d}^{-1}$) were higher than areal diffusive CH_4 fluxes from exposed sediment ($0.06 \pm 0.10 \text{ mmol m}^{-2} \text{ d}^{-1}$) and lotic water ($-0.96 \pm 1.72 \text{ mmol m}^{-2} \text{ d}^{-1}$) (Table S.3.3). Ebullition was the dominant pathway of areal CH_4 fluxes (i.e., 63% of areal diffusive + ebullitive CH_4 fluxes), while the shallow zone emitted 93% of areal CH_4 fluxes from impounded water (Fig.3.2).

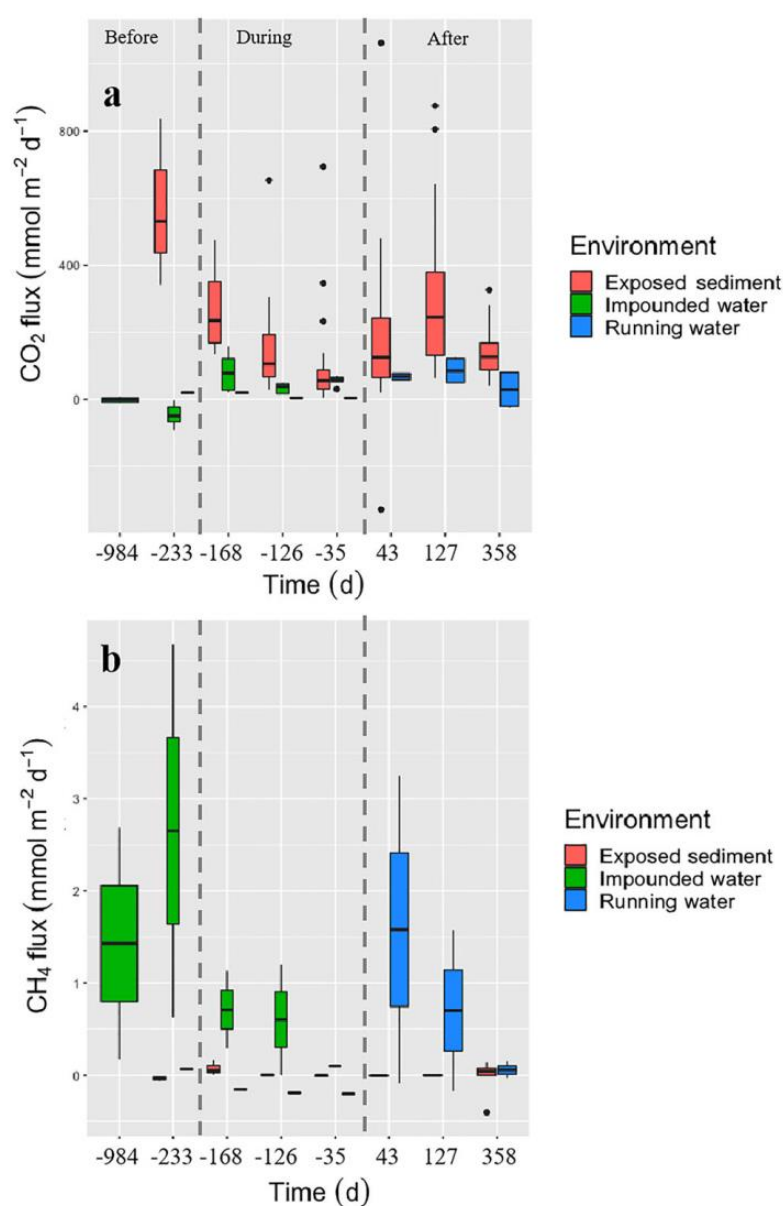


Figure 3.2 Areal CO_2 (a) and CH_4 (b) fluxes from impounded water (green), exposed sediment (red), and running water (blue). Boxplots display 25th, 50th, and 75th percentiles,

whiskers show minimum and maximum values, the points beyond the minimum and maximum are outliers. The x-axis describes the eight sampling campaigns which are divided into three categories: Before (days -984 and -233), During (days -168, -126, and -35), and After (days 43, 127, and 358) reservoir drawdown

3.4.2. Ecosystem CO₂ and CH₄ fluxes

The total ecosystem C flux was slightly positive, 74 mol d⁻¹ (day -984) or even negative, -5,904 mol d⁻¹ (day -233) before drawdown (i.e., when the reservoir was almost fully covered by impounded water; Fig.3.3a). During reservoir drawdown, total ecosystem C fluxes were 18,718 mol d⁻¹ (day -168), 12,540 mol d⁻¹ (day -126), and 12,393 mol d⁻¹ (day -35; Fig.3.3a). After reservoir drawdown, total ecosystem C fluxes were, respectively, 23,669 mol d⁻¹ (day 43) 38,713 mol d⁻¹ (day 127), and 18,568 mol d⁻¹ (day 358; Fig.3.3a). On average, the total ecosystem C fluxes were -2,915 mol day⁻¹ before, 14,550 mol d⁻¹ during, and 26,983 mol d⁻¹ after reservoir drawdown. Thus, ecosystem C fluxes from the reservoir were 2 and 10 times higher after than, respectively, during and before reservoir drawdown.

Exposed sediment contributed most of total ecosystem C fluxes, and its contribution over time followed the same temporal pattern as total ecosystem C fluxes. The mean of total ecosystem C fluxes from exposed sediment, impounded water, and lotic water were, respectively, 16,047 mol d⁻¹ (93% of total C flux), 1,071 mol d⁻¹ (6%), and 154 mol d⁻¹ (1%). Thus, exposed sediment contributed most to total ecosystem C fluxes because of its high areal CO₂ fluxes and surface area, while lotic water had the lowest contribution to the total ecosystem C fluxes because of its small surface area.

Ecosystem CO₂ and CH₄ fluxes contributed, respectively, 99% and 1% of total ecosystem C fluxes. Ecosystem CO₂ and ecosystem CO₂-eq fluxes followed the temporal pattern of total ecosystem C fluxes in exposed sediment because this environment contributed most of total ecosystem C fluxes, and ecosystem CO₂ fluxes predominated over ecosystem CH₄ fluxes (Fig.3.3b, c, and d). By contrast, impounded water emitted 98% of ecosystem CH₄ fluxes (Fig.3.3d). Thus, ecosystem CH₄ fluxes from impounded water were higher before reservoir drawdown and then they decreased along DD as impounded water was replaced by exposed sediment and lotic water. Exposed sediment contributed 87%, impounded water 12%, and lotic water 1% of total C fluxes expressed in CO₂-eq (814 kg CO₂-eq d⁻¹) over a span of 100 years. The average of C flux after reservoir drawdown was 8 g CO₂-eq m⁻² d⁻¹.

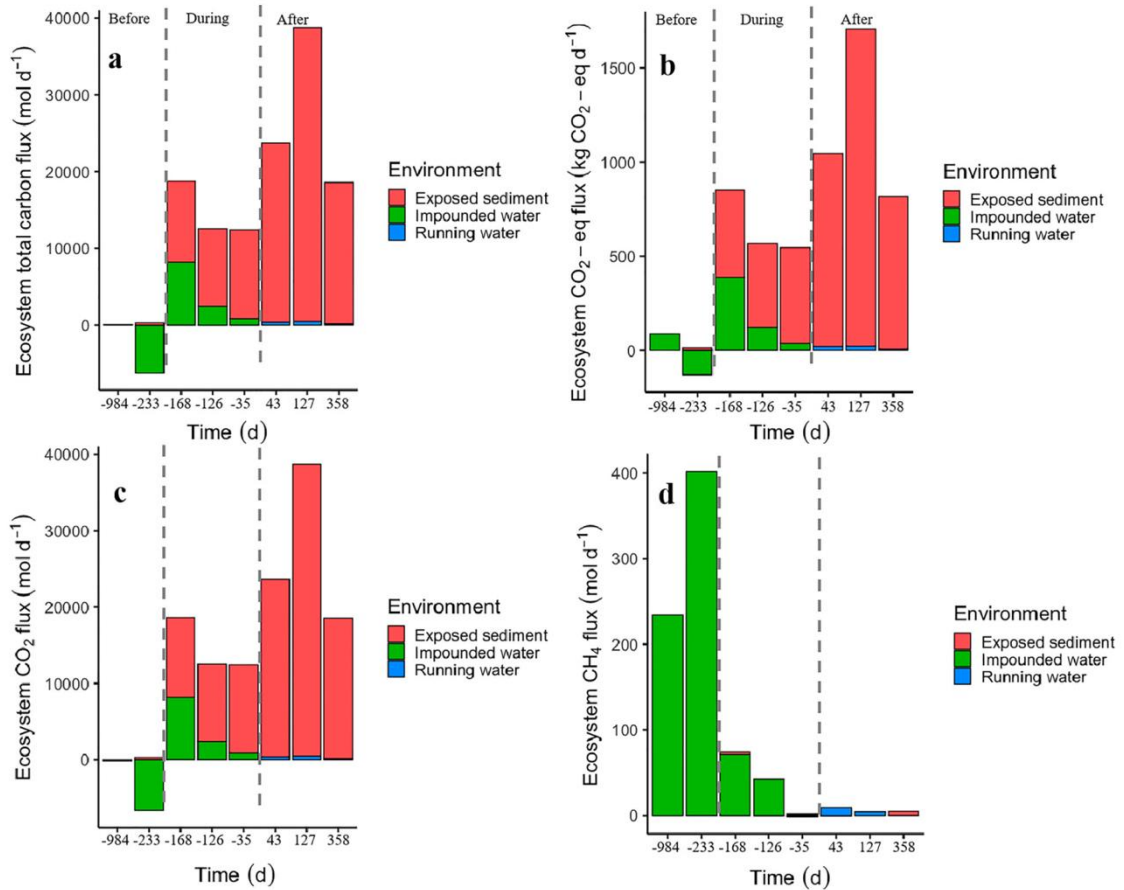


Figure 3.3 (a) Ecosystem total carbon flux, (b) carbon CO₂-eq, (c) ecosystem CO₂ flux, and (d) ecosystem CH₄ flux in exposed sediment, impounded water, and running water. Ecosystem CH₄ fluxes in impounded water are a sum of diffusion and ebullition but are only emitted via diffusion for exposed sediment and running water. The values below y = 0 indicate negative carbon fluxes or carbon uptake by the reservoir. Each vertical bar corresponds to a sampling campaign. The x-axis describes the eight sampling campaigns, which are divided into three categories: Before (days -984 and -233), During (days -168, -126, and -35), and After (days 43, 127, and 358) reservoir drawdown

3. 5. Discussion

As we hypothesized, the drawdown phase of DD increased total ecosystem C (CO₂ + CH₄) fluxes from the reservoir because of higher fluxes from exposed sediment. Exposed sediment emitted, on average, 93% of the CO₂ flux and 87% of the flux expressed in CO₂-eq. At the ecosystem scale, CO₂ fluxes contributed 99% of total C fluxes while the remaining 1% was contributed by CH₄ fluxes. Most of the CH₄ fluxes (98% on average) arose from impounded water and mostly emitted via ebullition. The rates of CO₂ and CH₄ emissions from shallow impounded water were higher than from deep impounded water.

3.5.1. The drawdown phase of DD increased CO₂ and CH₄ fluxes from the reservoir

Before drawdown (days -984 and -233), the reservoir was a net sink of atmospheric CO₂ but a net source of CH₄. Because impounded water took more CO₂ than the CH₄ it emitted, the Enobieta Reservoir was a net sink of C before reservoir drawdown. Note that we conducted these samplings during summer, a season of high primary production in the northern hemisphere and therefore CO₂ fixation via photosynthesis (Teodoru et al., 2011).

During reservoir drawdown (days -168, -126, and -35), the reservoir became a net source of carbon to the atmosphere, especially as CO₂. Areal CO₂ fluxes from impounded water were comparable to areal CO₂ fluxes measured elsewhere in lakes, ponds, and reservoirs (Deemer et al., 2016; Holgerson & Raymond, 2016; Raymond et al., 2013). They were, however, lower than fluxes from exposed sediment and lotic water, in agreement with previous studies (Keller et al., 2020; Kosten et al., 2018; Raymond et al., 2013). Impounded waters typically emit lower areal CO₂ fluxes than lotic waters and exposed sediments because of higher CO₂ uptake by primary producers (Gómez-Gener et al., 2015; Howard & Howard, 1993). Carbon emissions from reservoirs are typically highest during their first 10 to 20 years, when flooded labile C is still available for microbial respiration (Barros et al., 2011; St. Louis et al., 2000). Thus, low areal CO₂ fluxes from impounded water were expected in this oligotrophic reservoir of more than 60 years of existence.

As we expected, areal CH₄ fluxes were lower in exposed sediment and lotic water than in impounded water and higher in shallow than in deep impounded water. Impounded waters are important emitters of CH₄ because of their increased anaerobic microbial functioning (Deemer et al., 2016). Methane is produced in anoxic conditions by anaerobic archaea and bacteria and emitted mainly via ebullition (Bastviken et al., 2004; Baulch et al., 2011; Deemer et al., 2016). Ebullition was the dominant pathway of CH₄ fluxes from impounded water in this study, consistent with other findings (DelSontro et al., 2016; West et al., 2016), mainly in shallow impounded water. Shallow impounded waters are hotspots for CH₄ emissions because they have lower capacity to dissolve, trap, and oxidize CH₄. Ebullition might, however, have been underestimated due to its high spatial and temporal heterogeneity (Wik et al., 2016). Impounded water in this study emitted most of CH₄ fluxes; thus, the contribution of CH₄ to total ecosystem C fluxes decreased along reservoir drawdown as impounded water was replaced by exposed sediment.

Exposed sediments emit areal CO₂ fluxes to the atmosphere at higher rates than emissions from the water surface during the flooded periods (Catalán et al., 2014; Gómez-Gener et al., 2016; Obrador et al., 2018). Areal CO₂ fluxes from exposed sediments are higher because of their increased CO₂ diffusivity, higher microbial respiration due to higher oxic conditions, and lower CO₂ uptake by primary producers compared with inundated environments (Gómez-Gener et al., 2015; Howard & Howard, 1993; Marcé et al., 2019). In this study, exposed sediment emitted most of the CO₂ fluxes within the reservoir. During the drawdown phase, these CO₂ emissions declined between days -168 and -35, likely

reflecting seasonal variations in temperature and humidity. The sampling days were conducted in October (day -126) and January (day -35), the coldest and wettest period in the study area. Lower temperature and higher humidity might have limited oxygen diffusivity and, thus, microbial respiration and CO₂ production in exposed sediment, during reservoir drawdown on days -126 and -35.

After reservoir drawdown, total C fluxes at the scale of the reservoir increased and peaked on day 127, following the trend in ecosystem CO₂ fluxes. Microbial respiration and thus CO₂ production are higher in exposed sediments with higher content and quality of organic matter (Almeida et al., 2019; Keller et al., 2020; von Schiller et al., 2019). The areal CO₂ fluxes from exposed sediment decreased with time in this study, probably due to the reduction in quantity and quality of sediment organic carbon. Unfortunately, we did not assess temporal changes in the content and chemical composition of sediment organic C to support this hypothesis. While the underlying mechanisms for this temporal pattern remain unclear at this stage, they provide evidence for areal emissions to be higher after than before DD.

As we assumed, areal CO₂ fluxes were lower in impounded water than areal CO₂ fluxes from exposed sediment and lotic water. However, we did not expect areal CO₂ fluxes from exposed sediment to be equal to areal CO₂ fluxes from lotic water. Lotic water, because of its high turbulence, should emit higher areal CO₂ fluxes than exposed sediment (Borges et al., 2015; Gómez-Gener et al., 2015; Raymond et al., 2013). The low *p*CO₂ and gas transfer velocity measured in this study might have limited emissions of CO₂ from the lotic water. We reported an average *p*CO₂ in lotic water that is 791 µatm, nearly four times lower than the average *p*CO₂ = 3100 µatm reported from 6,798 streams on a global scale (Raymond et al., 2013). In addition, the average gas transfer velocity (*k*₆₀₀) of 2.6 m d⁻¹ in the lotic water of this study is lower than the mean of *k*₆₀₀ values = 35.0 m d⁻¹ reported in a review on gas exchanges in streams (Ulseth et al., 2019).

Carbon dioxide and CH₄ contributed on average 99% and 1% of total ecosystem C fluxes, respectively. Expressed in CO₂-eq, the contribution of CH₄ rose to 6% of total ecosystem C fluxes, because of the higher global warming potential of CH₄ compared to CO₂ (IPCC, 2013). Ecosystem CH₄ fluxes are responsible for ~ 60%–79% of CO₂-eq from surface waters of lakes, ponds, and reservoirs (Deemer et al., 2016; DelSontro et al., 2016; van Bergen et al., 2019) whereas exposed sediments are poor emitters of CH₄ due to their increased aerobic conditions (Arce et al., 2021; Marcé et al., 2019; Obrador et al., 2018; Paranaíba et al., 2021). Impounded water emitted 98% of CH₄ fluxes while the remaining 2% was contributed by the combined exposed sediment and lotic water. Although exposed sediment occupied a large surface area, its contribution to ecosystem CH₄ fluxes was low because of its low areal CH₄ fluxes. The contribution of lotic water to ecosystem CH₄ fluxes was low because it occupied a negligible surface area.

3.5.2. Conclusion: implication of DD for the carbon footprint of the reservoir and future perspectives

The average ecosystem C flux in CO₂-eq after reservoir drawdown was 8 g CO₂-eq m⁻² d⁻¹, slightly higher than the flux reported on a global scale in surface waters of reservoirs; between 4.25 g CO₂-eq m⁻² d⁻¹ (St. Louis et al., 2000) and 6.64 g CO₂-eq m⁻² d⁻¹ (Deemer et al., 2016). The flux reported in this study is also higher than the flux from hydroelectric reservoirs worldwide; 2.55–7.64 g CO₂-eq m⁻² d⁻¹ (Deemer et al., 2016). Hydropower was considered a green source of energy, but GHG emissions from reservoirs contribute to the global C budgets (Barros et al., 2011; Deemer et al., 2016; St. Louis et al., 2000) even before considering their C emissions during and after DD. The high CO₂ fluxes from exposed sediment reported in this study indicate the importance of the drawdown phase of DD as a hot moment for CO₂ and CH₄ emissions from a reservoir. Thus, the exclusion of GHGs related to the end-of-life of dams may result in an underestimation of the C footprint of reservoirs.

The decrease in CO₂ fluxes in exposed sediment may be a seasonal specific feature that warrants further investigation beyond the short-term duration of this study. Furthermore, exposed sediments are amenable environments for vegetation growth, which may overturn the effects of DD on the C emissions of a reservoir by fixing atmospheric CO₂. However, we lack empirical evidence to clarify the role of plant regrowth on the C dynamics in reservoirs following DD. Thus, we underline a need to know the drivers of CO₂ fluxes from exposed sediments, mid- and long-term effects of DD on C emissions in reservoirs, including the role of plant recolonization, and to include DD in the C footprint of reservoirs. To conclude, this study sets the table for promising future studies to improve our understanding of how the C dynamics of reservoirs are affected by DD.

3.6. Acknowledgements

This study was funded by the projects Alteration of carbon sinks and sources in shrinking inland waters (Alter-C), the Spanish Ministry of Science, Innovation and Universities (refs: PID2020-114024GB-C31 funded by MCIN/AEI /10.13039/501100011033/) and Effects of the drawdown of Enobieta Reservoir (Navarre) on the biodiversity and functioning of river ecosystems (DESEMBALSE), Foundation BBVA (ref: PI064-17). AM was supported by an FI grant from the Agència de Gestió d'Ajuts Universitaris i de Recerca (AGAUR) of the Generalitat de Catalunya. DvS and BO acknowledge support through the Consolidated Research Group 2017SGR0976. RM acknowledges support by the Generalitat de Catalunya through the Consolidated Research Group 2017SGR1124, and by the CERCA program. AE and MA support of the Basque Government through the Consolidated Research Group IT951-16. AM got a predoctoral grant from the University of the Basque Country (UPV/EHU). DvS is a Serra Húnter Fellow.



4. Exposed sediments in a temperate-climate reservoir under dam decommissioning contain large stocks of highly bioreactive organic matter

Amani, M, Obrador, O, Fandos, D, Butturini, A, von Schiller, D (2024). Exposed sediments in a temperate-climate reservoir under dam decommissioning contain large stocks of highly bioreactive organic matter. *Limnetica*, 43 (1), 000–0000. DOI: 10.23818/limn.43.11

4.1. Abstract

Dam decommissioning (DD) is used to solve economic and social problems posed by old dams. However, we ignore the effect of DD on the content and reactivity of large stocks of organic matter (OM) buried in reservoir sediments. We explored temporal changes in the content and reactivity of sediment OM during the first 580 days after the drawdown phase of DD of a large reservoir in the N Iberian Peninsula. We determined the content of sediment OM as organic carbon (OC) in bulk sediment OM and water-extractable OM (WEOM). We estimated the reactivity of bulk sediment OM as its respiration rate and carbon-to-nitrogen ratio, and that of sediment WEOM as its respiration rate, percent biodegradable dissolved OC (%BDOC), and SUVA₂₅₄. The content of bulk sediment OM was 84 ± 5.1 (mean \pm SE) mg OC g⁻¹ dry sediment, comparable to the values in the literature on sediment OM in dry sediments from lentic, but higher than in lotic ecosystems. The content of sediment WEOM was 0.81 ± 0.05 mg DOC g⁻¹ dry sediment, higher than the values in the literature on sediment WEOM from lakes, soils, and rivers. On average, 41% of WEOM was consumed by microorganisms in two days of incubation, showing the great reactivity of this OM fraction. The content of bulk sediment OM and the respiration rate of WEOM showed a nonlinear temporal trend, while %BDOC increased linearly with sediment exposure time. The labile OM produced by the vegetation that rapidly recolonized the reservoir and photoreactions may explain the temporal increase in %BDOC. Our results suggest that exposed sediments can be a source of labile OM and high C emissions in river segments downstream of the reservoir after DD.

Keywords: Ageing dams, dam removal, exposed sediments, sediment organic matter, water reservoirs

Resumen

El desmantelamiento de presas (DP) resuelve los problemas económicos y sociales que suponen las presas antiguas. Sin embargo, ignoramos el efecto del DP en la materia orgánica (OM) enterrada en los sedimentos del embalse, sobre todo en su contenido y reactividad. En un experimento de incubación, exploramos cambios temporales en el contenido y reactividad de la OM del sedimento durante los 580 días posteriores a la fase de vaciado de un gran embalse en el Norte de la Península Ibérica. Determinamos el contenido de OM del sedimento como carbono orgánico (OC) en sedimento y en materia orgánica extraíble en agua (WEOM) del sedimento. Determinamos la reactividad de la OM en el sedimento como su tasa de respiración y la ratio C:N, y la reactividad de la WEOM del sedimento como su tasa de respiración, el porcentaje de OC disuelto biodegradable

(%BDOC), y $SUVA_{254}$. El contenido de OC en la OM en peso seco de sedimento fue de 84 ± 5.1 (promedio \pm error estándar) mg OC g^{-1} de sedimento seco, comparable a los valores de la literatura de materia orgánica presente en el sedimento en lagos, estanques y presas, pero mayor que en los ríos. El contenido de WEOM del sedimento fue de 0.81 ± 0.05 mg DOC g^{-1} sedimento seco, superior a los valores de la literatura de WEOM del sedimento de lagos, suelos y ríos. En promedio, el 41% de la WEOM fue consumida por microorganismos en dos días, lo que demuestra la gran reactividad de esta fracción de OM. El contenido de OM del sedimento seco y la tasa de respiración de la WEOM mostraron una tendencia temporal no lineal, mientras que el %BDOC aumentó linealmente con el tiempo de exposición del sedimento. La OM lábil producida por la vegetación que rápidamente recolonizó el embalse y las fotoreacciones pueden explicar el incremento temporal de %BDOC. Nuestros resultados sugieren que los sedimentos expuestos pueden ser una fuente de OM lábil, que puede alterar las emisiones de C en tramos de río aguas abajo de las presas sujetas a desmantelamiento.

Palabras clave: Presas en envejecimiento, desmantelamiento de presas, sedimentos expuestos, materia orgánica del sedimento, embalses

4.2. Introduction

Ageing dams and the growing interest in river restoration have increased the practice of dam decommissioning (DD). Dam decommissioning is a widely hailed option to restore riverine connectivity, biodiversity, and ecosystem function (Allen et al., 2016; Bednarek, 2001; Magilligan et al., 2016). However, DD can also allow the downstream export and decomposition of organic matter (OM) buried in reservoir sediments (i.e., sediment OM) into greenhouse gases (GHGs) (Amani et al., 2022; Pacca, 2007). The decomposition rate of sediment OM depends on extrinsic environmental factors and the content and reactivity of sediment OM (Keller et al., 2020; Obrador et al., 2018; Paranaíba et al., 2021). Thus, DD can affect extrinsic factors of the decomposition of OM in sediments, and hence the content and reactivity of sediment OM by exposing the anoxic sediments to the atmosphere. For instance, exposed sediments in a large temperate reservoir under DD were reported to be a hotspot for carbon dioxide (CO₂) emissions (Amani et al., 2022). These CO₂ emissions decreased with sediment exposure time, hypothetically, due to a decrease in the content and reactivity of sediment OM. However, we lack empirical evidence of the effect of DD on the content and reactivity of the large stocks of OM buried in sediments of reservoirs during their life cycle (Downing et al., 2008; Maavara et al., 2017; Mendonça et al., 2017). The reactivity of sediment OM can affect its fate and shape the role of reservoirs in regional and global carbon (C) budgets (Kothawala et al., 2021). Reactive sediment OM can decompose into CO₂ in the reservoir or in the river reach downstream of the reservoir and, thus, remain in the short-term atmosphere-biosphere C loop. However, recalcitrant sediment OM may remain buried in the reservoir after terrestrialization (i.e., the transition from an aquatic to a terrestrial system) and/or reach coastal marine sediments and, thus, enter the long-term geological C pool. To include DD in the C footprint of reservoirs on a regional and global scale, it is necessary to test how the content and reactivity of sediment OM in reservoirs change over time after DD.

Reservoir sediments are hotspots for OM burial because, relative to lakes, they receive higher loads of sediment, OM, and nutrients from their relatively larger catchment area (Downing et al., 2008; Mendonça et al., 2017; Thornton et al., 1990). The catchment area to the waterbody area ratio is higher for reservoirs than lakes, implying higher inputs of terrestrial materials and a higher sedimentation rate in reservoirs (Thornton et al., 1990). The higher sedimentation rate in reservoirs creates better conditions for OM preservation because it potentially implies, compared to lakes, a shorter exposure time of sediment OM to oxygen (O₂) (Clow et al., 2015; Sobek et al., 2009, 2012). The shorter exposure time of sediment OM to O₂ and a large portion of allochthonous OM increase the burial efficiency of OM (i.e., the ratio of OM burial to OM deposition) and the areal burial rate of OM (Sobek et al., 2009, 2012). The areal burial rate of OM is six times higher in reservoirs than in lakes worldwide (Mendonça et al., 2017). The global burial rate of OM in reservoir sediments is estimated at 35.43 Tg C yr⁻¹, of which 75% is contributed by

allochthonous OM (Maavara et al., 2017). However, when this occlusion of OM in sediments is removed due to, for instance, DD, this sediment OM can become highly bioreactive (Bastviken et al., 2004; Freeman et al., 2001; Kothawala et al., 2021).

The bioreactivity of OM depends on its content and molecular composition and extrinsic environmental factors (Amani et al., 2019; Catalán et al., 2013; Webster & Benfield, 1986). The content of organic carbon (OC) is an important factor in the decomposition of OM because low concentrations of some molecules can be below the threshold of energetic requirements of decomposers and, thus, limit some catabolic reactions (Arrieta et al., 2015; Kothawala et al., 2021). The molecular composition of OM affects its decomposition by providing the energy and chemical elements required for the growth and reproduction of decomposers. Organic matter is a complex mixture of several molecules of different molecular size, structure, oxidation degree, hydrolysis degree, and aromaticity (Kellerman et al., 2014; Stubbins et al., 2014) and often characterized using optical techniques (Miller & McKnight, 2010; Stubbins et al., 2014; Weishaar et al., 2003). More bioreactive or labile OM contains molecules with low aromaticity, low carbon-to-nitrogen (C:N) ratio, and low molecular weight (Gudasz et al., 2010; Koehler et al., 2012; Miller & McKnight, 2010). Water-extractable OM (WEOM: OM obtained by extracting a given mass of soil/sediment with an aqueous solution (Zsolnay, 1996)) represents only a small fraction of sediment OM, but it is often the most mobile, leachable, and biodegradable fraction (Bolan et al., 2011; Boyer & Groffman, 1996; Chantigny, 2003). Extrinsic environmental factors that affect the decomposition of sediment OM include temperature, O₂, the structure and function of microbial communities, the texture and moisture of the sediment, and exposure to solar radiation (Baumann et al., 2013; Keller et al., 2020; von Schiller et al., 2019; Walz et al., 2017). Dam decommissioning can alter some of these extrinsic environmental factors, and thus the content and reactivity of sediment OM during sediment exposure to the atmosphere.

Sediment exposure can affect the content and reactivity of sediment OM by mainly reducing sediment moisture, increasing sediment texture, increasing exposure to solar radiation, and promoting plant recolonization of exposed sediments. Low sediment moisture increases O₂ concentration in deeper layers of exposed sediments and the decomposition rate of sediment OM (Gómez-Gener et al., 2015; Kosten et al., 2018; Marcé et al., 2019). However, since extreme desiccation can reduce the decomposition rate of OM through a limited supply of OM to microorganisms (Schimel, 2018), the availability of C substrates, the activity of extracellular enzymes, and, thus, the decomposition rate of OM increase with sediment and soil moisture (Coulson et al., 2022; Manzoni & Katul, 2014; Manzoni et al., 2016). Since DD is a hot moment for the erosion of reservoir sediments (Duda & Bellmore, 2022; Ritchie et al., 2018), sediment texture may increase during sediment exposure due to the loss of fine-sized sediments, which are more susceptible to the erosion and transport downstream (Duda & Bellmore, 2022; Warrick et al., 2012). Furthermore, solar radiation (Granéli et al., 1996; Wetzel et al., 1995) and plant recolonization can alter the content and reactivity of sediment OM by providing labile OM (Shaver & Chapin III, 1986; Shaver et al., 1992). Therefore, temporal changes in the content and reactivity of sediment OM can

depend on the balance between the decomposition of OM and factors such as exposure to solar radiation and vegetation growth after DD. However, there is no clear characterization of how these factors affect the content and reactivity of sediment OM after DD in decommissioned reservoirs.

Here, we assessed how the content and reactivity of the sediment OM changed during the first 580 days of sediment exposure after the drawdown phase of DD of the Enobieta Reservoir, a large (42 m high) temperate-climate reservoir in the North Iberian Peninsula. We collected sediment samples during six sampling campaigns between 2018 and 2020. We predicted that (1) the content of sediment OM would be high and highly bioreactive, (2) sediment WEOM would be more bioreactive than bulk sediment OM, and (3) the content and reactivity of sediment OM would decrease with sediment exposure time because high precipitation in the region should support OM decomposition in exposed sediments after reservoir drawdown. To contextualize our results in a wider framework of environments, we compared the content and reactivity of sediment OM in the Enobieta Reservoir with literature data about dry soils and dry sediments of lentic and lotic inland waters.

4.3. Materials and Methods

4.3.1. Study site

The Enobieta Reservoir (coordinates: 43°13'03''N 1°47'15''W, elevation: 345 m) was constructed in the Artikutza Valley (Navarre, N Iberian Peninsula) between 1947 and 1953 on the Enobieta Stream to regulate water supply to the municipality of Donostia-San Sebastián. The mean annual air temperature is 12.2 °C with an average rainfall of 2,604 mm yr⁻¹ (period 1954–2019) (Gobierno de Navarra, 2019). This rainfall rate makes the Artikutza Valley, perhaps, the most humid region of the Cantabrian cornice. The hydrological network of the Artikutza Valley has a drainage basin of 3,683 ha, with a geology dominated by acidic rocks, such as granite and schist (Atristain et al., 2022). The Artikutza Valley is mainly covered by mature forests dominated by beech (*Fagus sylvatica* L.) and oak (*Quercus robur* L.) stands, dense autochthonous riparian vegetation with alder (*Alnus glutinosa* (L.) Gaertner) and ash (*Fraxinus excelsior* L.), some old exotic plantations of conifers and red oaks (*Quercus rubra* L.), and pasturelands on the highest terrain (Lozano & Latasa, 2019). The reservoir had an initial storage capacity of 2.66 hm³ and an area of ~0.14 km². Geotechnic problems noticed during dam construction required the reduction of storage capacity to 1.63 hm³ and the construction, downstream in the same catchment, of the Añarbe Reservoir in 1976. Subsequently, the Enobieta Reservoir was not used to provide water (Larrañaga et al., 2019) and was not maintained properly to the point that it became a safety problem. Due to the early structural instability and the conservation status of the Artikutza Valley (it is part of the Natura 2000 Network and a special conservation zone), the decommissioning of the Enobieta Reservoir began in 2017 and continued throughout

2018 and 2019 (Amani et al., 2022). The phase of reservoir drawdown of the Enobieta Reservoir ended on 25 February 2019.

4.3.2. Sampling strategy and treatment of sediment samples

We collected sediment samples during and after the drawdown of the Enobieta Reservoir during six sampling campaigns (C₁–C₆): on 10 September 2018, 22 October 2018, 21 January 2019, 09 April 2019, 02 July 2019, and 18 February 2020 (Table S.4.1). To assess how the content and reactivity of sediment OM changed over time, we used the sampling date minus the last inundation date of each site to find sediment exposure time (in days) for each site (Table S.4.1). We determined the last inundation date for each site from the site elevation (Table S.4.2), the reservoir bathymetry, and the daily evolution of water level in the reservoir (available in Amani et al. (2022)). The range of sediment exposure time was 9–580 days (Table S.4.1). We collected sediment samples using six sites (A, B, C, D, E, and F), which were close to the tail of the reservoir, in the section exposed to the atmosphere for a longer time (see Table S.4.2 for coordinates). We collected three samples in a 1 × 1 m plot in each site when sediments were still bare and during the early recolonization of the bare sediments by vegetation. Thus, we collected 108 sediment samples: 6 sites × 3 replicate plots per site × 6 sampling campaigns. We lost one sample and, thus, we performed the incubation experiment and other analyses with 107 sediment samples.

In the field, we stored sediment samples in clean polyethylene falcon tubes that we transported in dark portable refrigerators to the laboratory. In the laboratory, we froze the sediment samples at -18 °C. Before all analyses and the incubation experiment performed in this study (Fig.4.1), we freeze-dried all sediment samples for 48 h in a Telstar LyoQuest at a vacuum pressure of 0.05 mbar and a temperature between -50 and -55 °C. We sieved the freeze-dried sediment samples with a steel sieve of a 2-mm mesh to retain the fine fraction of the sediments. We cleaned the steel sieve between samples with a plastic brush, taking maximum care to avoid contamination. We kept the sieved, freeze-dried sediment samples in clean polyethylene falcon tubes in the laboratory at -18 °C until the incubation experiment and other analyses.

4.3.3. Sediment texture

We assessed the mean sediment size with 0.5 g of sieved freeze-dried sediment using a laser light diffraction instrument (Coulter LS, 230, Beckman-Coulter, USA) after removing organic C (OC) with H₂O₂ (Arriaga et al., 2006).

4.3.4. Content of bulk sediment OM and sediment WEOM

We determined the content of bulk sediment OM as the amount of OC in the sediments. We determined the percentage of OC content (%OC) and the percentage of total nitrogen content (%N) on a 0.1 g dry sediment sample with an Elemental Analyzer (Model

1108, Carlo-Erba, Italy) after sediment acidification with 2M HCl to remove inorganic C and preserve OM. We reported the content of bulk sediment OM in mg OC g⁻¹ dry sediment.

We determined the content of sediment WEOM as sediment water-extractable OC (WEOC: mg DOC g⁻¹ dry sediment). We obtained WEOM by shaking a dry sediment aliquot of 2 g with 180 mL of mineral water (Font Vella) in 250-mL plastic bottles, in a dark incubator for 24 h at 4 °C and 150 rpm. We filtered the sediment-water mixture through glass fibre filters (0.7 µm pore size; Whatman GF/F, GE Healthcare, UK), pre-ashed for 4 h at 450 °C, into clean polyethylene falcons of 50 mL. We used a different filter for each sample. We acidified the filtered samples to pH 2–3 with HCl 10% to remove dissolved inorganic C and preserve OM. We used the high-temperature catalytic oxidation method to determine the concentration of DOC in a Shimadzu instrument (TOC-VCSH, Tokyo, Japan). We calculated WEOC as the product of [DOC] (mg L⁻¹) and the volume of water (L) used to extract WEOM divided by the mass (g) of each dry sediment sample:

$$\text{WEOC} = \frac{[\text{DOC}] \left(\frac{\text{mg}}{\text{L}} \right) \times \text{water volume (L)}}{\text{mass dry sediment (g)}} \quad (4.1)$$

4.3.5. Reactivity of bulk sediment OM and sediment WEOM

We assessed the reactivity of bulk sediment OM using three parameters: (1) respiration rate of bulk sediment OM, (2) respiration efficiency of bulk sediment OM, and (3) the mass ratio of %OC to %N (i.e., %OC/%N = C:N ratio, which was used as a proxy for reactivity). We determined the respiration rate of bulk sediment OM from the rate of dissolved O₂ consumption during incubation (von Schiller et al., 2019). We introduced 2.5 g of sediment samples into pre-washed 100 mL incubation glass bottles. We sealed the glass bottles with hexagonal glass stoppers (M-29/32, Scharlau, Spain) to avoid contamination of the samples. We left the sealed bottles on a laboratory benchtop for 24 h for the samples to acclimate to laboratory conditions. We aerated the water we used for incubation, Font Vella mineral water (spring: Sant Hilari Sacalm-Girona, Spain, [HCO₃¹⁻]: 143 mg L⁻¹, [Ca]: 42 mg L⁻¹, [Mg]: 11.3 mg L⁻¹, [Na]: 12.5 mg L⁻¹, and conductivity: 286 µS cm⁻¹), overnight in an open plastic jerrycan placed in a benchtop incubator (Optic Ivymen System, Spain) at 15 °C and a rotation speed of 150 rpm. We used the air-saturated water to fill the bottles containing sediments and four control bottles without sediments (i.e., with mineral water only). We ensured that no air bubbles formed or stayed in the incubation bottles, which we sealed with the stoppers throughout the incubations.

We incubated the samples and controls for 24 h at 15 °C in the dark benchtop incubator at 150 rpm. The temperature of 15 °C was close to the mean annual temperature of 12.2 °C in the Artikutza Valley (Gobierno de Navarra, 2019). We conducted the incubation of bulk sediment OM for 24 h because preliminary experiments had shown that more time could result in anoxia. We measured the O₂ concentration four times during the incubations (at 2, 4, 8, and 24 h) with O₂ optode spots (model PSt3, PreSens) attached to the interior of each bottle using a standalone, portable, fiberoptic O₂ meter (Microx 4 trace, PreSens,

Regensburg, Germany). We vigorously shook each incubation bottle before each measurement to ensure homogeneous O₂ concentrations inside the bottles. We calculated the respiration rate of the bulk sediment OM (R-BOM; μg O₂ g⁻¹ dry sediment h⁻¹) as:

$$R - BOM = \frac{(O_{2sample}^{2h} - O_{2sample}^{24h}) - (O_{2control}^{2h} - O_{2control}^{24h})}{incubation\ time\ (h)} \times \frac{volume\ resp.\ bottle\ (L)}{mass\ of\ dry\ sediment\ (g)} \quad (4.2)$$

where O₂ is [O₂] (mg L⁻¹), subscripts sample and control refer to each analytical replicate and the mean [O₂] in the four control bottles, and superscripts 2 h and 24 h correspond to the measurement times (respectively, 2 h and 24 h). The volume of the bottle was 100 mL, the incubation time was 22 h, the sediment mass was 2.5 g. To estimate the respiration efficiency of the bulk sediment OM (Reff-BOM; μg O₂ g⁻¹ OC h⁻¹), we replaced the mass of dry sediment in the equation (2) by the mass of OC in each sediment sample. The consumption rate of O₂ over incubation time was linear and, thus, we used the initial (2 h) and final (24 h) values, to estimate the decomposition rate of sediment OM.

We determined the reactivity of sediment WEOM using four variables: (1) respiration rate of sediment WEOM, (2) respiration efficiency of sediment WEOM, (3) biodegradable DOC (BDOC), and (4) a chromophoric index; SUVA₂₅₄. We determined the respiration rate of sediment WEOM by incubating the WEOM extract, which was not filtered. We used a syringe to carefully collect the supernatant, avoiding the intake of the sediment and other particles. We conducted the incubation experiment for 48 h (which was the time it took to consume at least 1 mg O₂ L⁻¹ in our preliminary experiments) under the same conditions as for the bulk sediment OM; dark conditions, at 15 °C and 150 rpm. We measured [O₂] at 2 h, 24 h, and 48 h using the same PreSens O₂ optodes. We calculated the respiration rate of sediment WEOM (R-WEOM; μg O₂ g⁻¹ dry sediment h⁻¹) as:

$$R - WEOM = \frac{(O_{2sample}^{2h} - O_{2sample}^{48h}) - (O_{2control}^{2h} - O_{2control}^{48h})}{incubation\ time\ (h)} \times \frac{resp.\ bottle\ volume\ (L)}{mass\ of\ dry\ sediment\ (g)} \quad (4.3)$$

We estimated the respiration efficiency of sediment WEOM (Reff-WEOM; μg O₂ g⁻¹ of DOC h⁻¹) by replacing, in the equation (3), mass of dry sediment with the mass of DOC (g) in each WEOM extract. To determine the fraction of biodegradable DOC (BDOC), we measured [DOC] in the samples before and after incubation, and we filtered each WEOM extract using a different filter with a pore size of 0.7 μm before determining [DOC]. We then calculated BDOC as the difference in [DOC] before ([DOC]_i) and after incubation ([DOC]_f) and expressed it as % of [DOC]_i, i.e., %BDOC as:

$$\%BDOC = \left(\frac{[DOC]_i - [DOC]_f}{[DOC]_i} \right) \times 100 \quad (4.4)$$

We analyzed the optical property of WEOM by filtering 10 mL of the WEOM extract with a 0.2 μm filter (Whatman GF/F, GE Healthcare, UK). We used a PharmaSpec UV-1700 spectrophotometer (Shimadzu, Tokyo, Japan) to obtain ultraviolet-visible (UV-Vis)

spectroscopy (200–600 nm) using a 1 cm quartz cuvette (Obrador et al., 2018). We determined a qualitative property of WEOM: the specific ultraviolet absorbance at 254 nm ($SUVA_{254}$: $L\ mg\ C^{-1}\ m^{-1}$). We determined $SUVA_{254}$, which is a descriptor of DOC aromaticity (Shao, He, Zhang, & Shao, 2009), as in Weishaar et al. (2003):

$$SUVA_{254} = \frac{abs_{254} \times \ln_{(10)}}{[DOC] \times l} \quad (4.5)$$

where abs_{254} is the absorbance at 254 nm, $[DOC]$ is in $mg\ C\ L^{-1}$, and l is the path length of the cuvette in m.

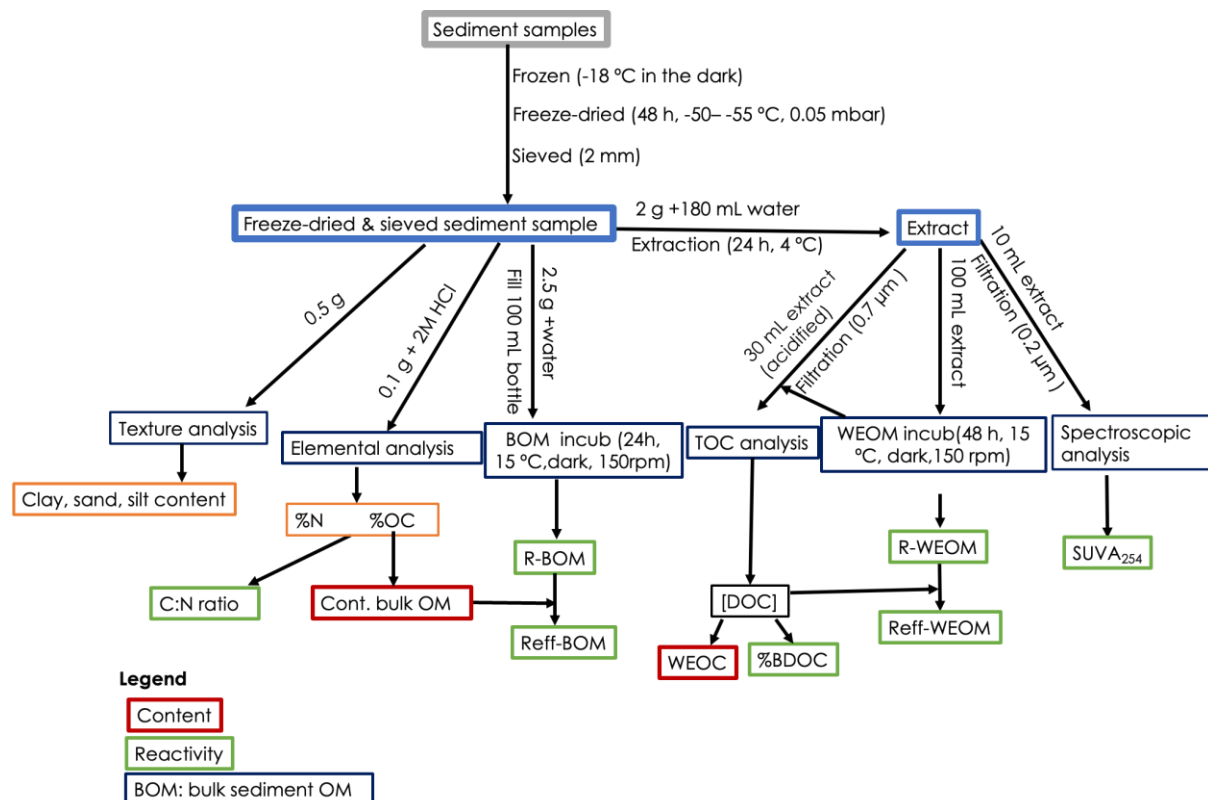


Figure 4.1 Schematic representation of the experiments conducted in this study

4.3.6. Meteorological and vegetation data

We evaluated how the accumulated precipitation (a proxy for sediment moisture) and temperature in the Artikutza Valley, and the vegetation growth in the Enobieta Reservoir after drawdown changed with time during our sampling period. We obtained daily precipitation and temperature data from the nearest meteorological station (Artikutza Station of Meteorology and Climate of Navarre). We assessed how the temperature changed during the sampling period using the mean daily temperature ($^{\circ}C$) that was recorded on our sampling dates. We used the sum of daily precipitation for seven days (six days preceding the sampling date plus the precipitation on our sampling date) to obtain the accumulated

weekly precipitation (mm). We used the sampling date to assess the temporal changes in precipitation during the sampling period. We assessed the temporal change in vegetation recolonization of the exposed sediments using Sentinel 2-Multipectral Instrument (MSI) imaging data taken on the 15th of each sampling month, which was mostly 3–7 days before or after the sampling date, a maximum of 13 days. The Sentinel 2-MSI data were preprocessed using Google Earth Engine. We used these satellite images of the whole reservoir to obtain the normalized difference vegetation index (NDVI, dimensionless). We did not have NDVI values for the first and third sampling campaigns because we could not find satellite images for the two sampling campaigns. We determined sediment exposure time for NDVI, precipitation, and temperature using the sampling date for each variable minus the earliest last inundation date.

4.3.7. Statistical analyses

We determined temporal changes in the content and reactivity of sediment OM during the first 9–580 days of sediment exposure after the drawdown phase of DD of the Enobieta Reservoir using generalized additive mixed models (GAMMs), with the R package *mgcv* (mixed GAM computational vehicle) in R version 4.0.5 (R Core Team, 2021). We considered as response variable the content and reactivity of sediment OM, and as explanatory variable time as a fixed factor. We used site as a random factor. We visually explored temporal trends of precipitation, temperature, and NDVI during sediment exposure time. We additionally ran a correlation analysis to explore the direction and significance of the temporal trend in NDVI. We used the paired samples t-test to test the difference between the means of the respiration rates for bulk sediment OM and sediment WEOM and their respiration efficiency. Statistical tests were considered significant when the *p*-value was ≤ 0.05 .

4.4. Results

4.4.1. Sediment texture

The mean sediment size in the Enobieta Reservoir (Table 4.1) changed with sediment exposure time. The mean sediment size decreased between the beginning of our sampling campaign and ~200 days of sediment exposure, then increased from ~200 days to ~400 days before slightly decreasing and increasing again (Fig.S.4.1).

4.4.2. Content of bulk sediment OM and sediment WEOM

The content of bulk sediment OM (Table 4.1) changed with sediment exposure time (Fig.4.2a). The content of bulk sediment OM decreased between the beginning of our sampling period and ~200 days, increased between ~200 and 400 days, and then, between

~400 and 580 days of sediment exposure, it reached a plateau. Sediment WEOC (Table 4.1) did not change with sediment exposure time (Fig.4.2b).

Table 4.1 Descriptive statistics of sediment texture and the content and reactivity of sediment OM in the Enobieta Reservoir. Bulk OM content is the content of bulk sediment OM and SE is the standard error of the mean.

Factor	Variable	Mean	SE	Range
Sed. texture	Mean sediment size (μm)	33.7	1.0	21.0–43.3
Content	Bulk OM content (mg OC g^{-1} dry sediment)	84	5.1	20–143
	Sediment WEOC (mg DOC g^{-1} dry sediment)	0.81	0.1	0.29–1.6
Reactivity	R-BOM ($\mu\text{g O}_2 \text{ g}^{-1}$ dry sediment h^{-1})	2.8	0.2	0.5–5.1
	Reff-BOM ($\mu\text{g O}_2 \text{ g}^{-1}$ OC h^{-1})	32.1	2.4	9.5–78.4
	R-WEOM ($\mu\text{g O}_2 \text{ g}^{-1}$ dry sediment h^{-1})	2.4	0.1	0.6–8.1
	Reff-WEOM ($\mu\text{g O}_2 \text{ g}^{-1}$ DOC h^{-1})	1,103	63	566–1,860
	BDOC (%)	41.4	2.0	17.5–64.8
	SUVA ₂₅₄ ($\text{L mg C}^{-1} \text{ m}^{-1}$)	2.91	0.1	1.23–5.7
	C:N ratio (dimensionless)	16.2	1.0	5.1–28.6

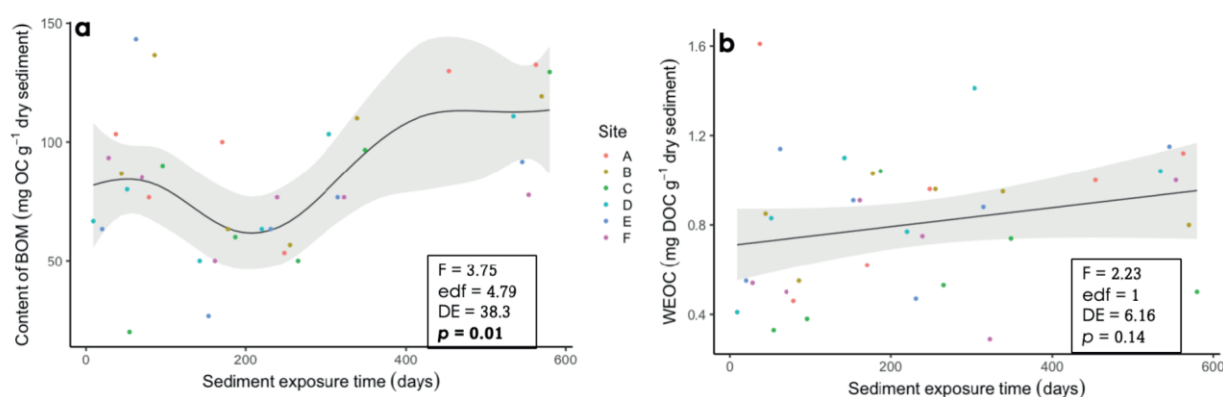


Figure 4.2 Temporal changes in the content of bulk sediment OM (a) and sediment WEOC (b) along sediment exposure time. The lines and shaded areas represent, respectively, the mean and 95% confidence interval of GAMMs; each point represents the average of three sediment samples collected at each site for each sampling date; edf is effective degrees of freedom; DE is deviance explained (%); significant p-values are shown in bold

4.4.3. Reactivity of bulk sediment OM and WEOM

R-BOM and R-WEOM were not different ($t(35.0) = 0.85$, $p = 0.40$), while Reff-WEOM was 34.4 times higher than Reff-BOM ($t(35.0) = 16.9$, $p < 0.01$). Reff-WEOM , and %BDOC changed with sediment exposure time, while other parameters for the reactivity of sediment OM did not (Fig.4.3 and 4). R-WEOM decreased between the beginning of our sampling and ~200 days; it also increased between ~400 days and 580 days of sediment exposure to form a nearly U-shaped curve (Fig.4.3b). Reff-WEOM showed almost the same temporal trend as R-WEOM, but its increase between ~400 and 580 days was not as strong as for R-WEOM (Fig.4.3d). Furthermore, %BDOC increased linearly with sediment exposure time (Fig.4.4a).

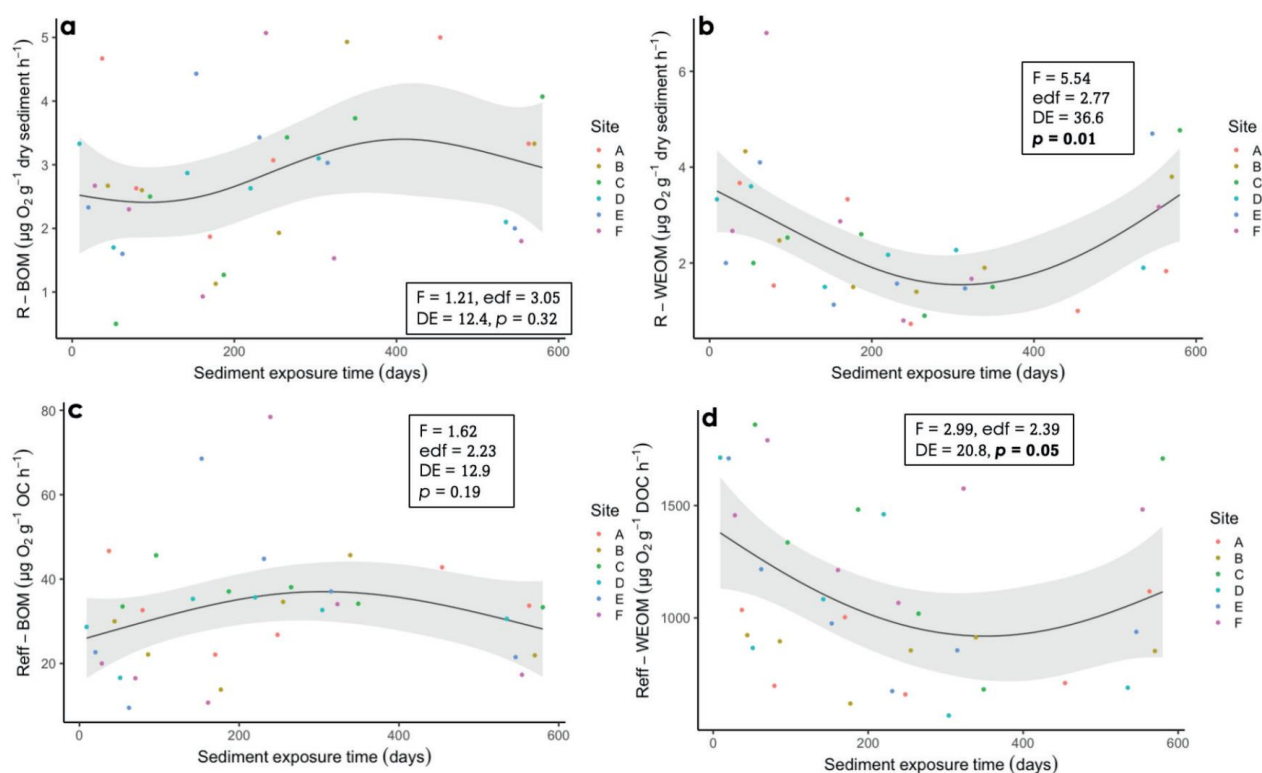


Figure 4.3 Temporal changes in the respiration rate for bulk sediment OM (R-BOM, a), the rate of microbial respiration for sediment WEOM (R-WEOM, b), respiration efficiency for bulk sediment OM (Reff-BOM , c), and respiration efficiency for sediment WEOM (Reff-WEOM , d) along sediment exposure time. The lines and shaded areas represent, respectively, the mean and 95% confidence interval of the GAMMs; each point represents the average of three sediment samples collected for each sampling date at each site; edf is effective degrees of freedom; DE is deviance explained (%); significant p-values are shown in bold

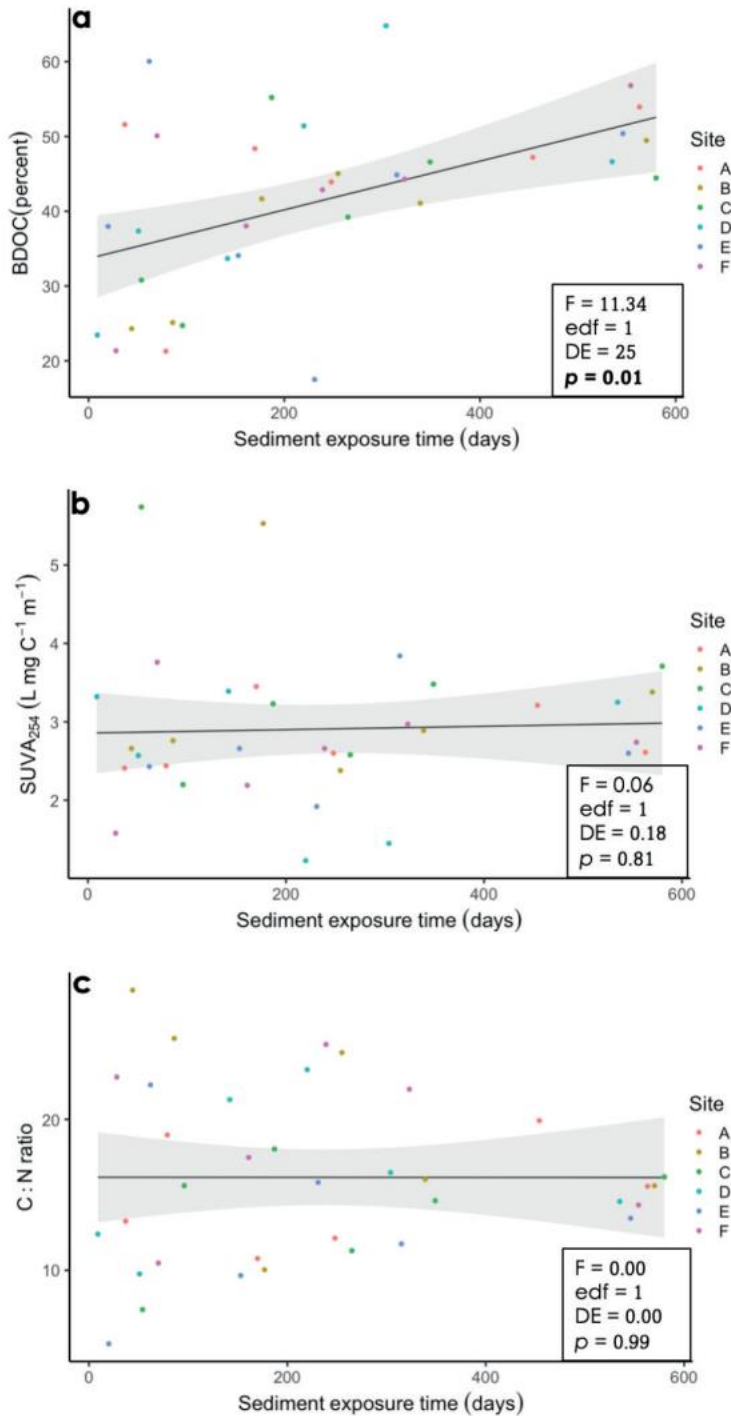


Figure 4.4 Temporal changes of BDOC (a), $SUVA_{254}$ (b), and C: N ratio (c) during sediment exposure time. The lines and shaded areas represent the mean and 95% confidence interval of the GAMMs; each point represents the average of three sediment samples collected for each sampling date at each site; edf is effective degrees of freedom; DE is deviance explained (%); significant p-values are shown in bold

4.4.4. Meteorological and vegetation data

The accumulated weekly precipitation was 73 ± 11 (0.0–170) mm [mean \pm SE (range)], the temperature was 11.7 ± 0.9 (5.5–18.5) °C during the study period. Precipitation decreased from 18.8 to 0.0 mm between 54 and 96 days, increased from 0.0 to 148 mm between 96 and 265 days, decreased from 148 to 20.9 mm between 265 and 349 days, and increased from 20.9 to 170 mm between 349 and 580 days of sediment exposure (Fig.S.4.2a). Temperature decreased from 18.5 to 5.5 °C between 54 and 187 days, increased from 5.5 to 8.7 °C between 187 and 265 days, between 256 and 349 days it increased from 8.7 to 18.2 °C, and then decreased from 18.2 to 7.0 °C between 349 and 580 days of sediment exposure (Fig.S.4.2b). Correlation analysis showed that NDVI increased with sediment exposure time ($r = 0.9$ $p < 0.01$). Vegetation continuously increased during sediment exposure, but the growth rate was greater between 362 and 577 days of sediment exposure (Fig.4.5).

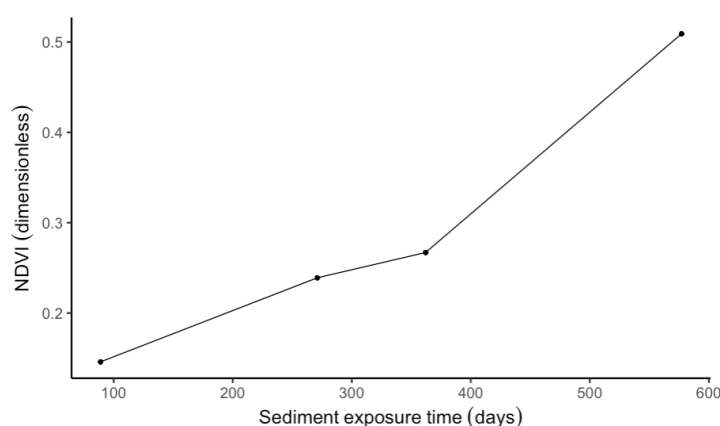


Figure 4.5 Temporal changes in NDVI (dimensionless) with sediment exposure time

4.5. Discussion

As expected, we report a high content of highly bioreactive bulk sediment OM and sediment WEOM in the Enobieta Reservoir. However, in contrast to what we expected, the content and reactivity of sediment OM did not decrease with sediment exposure time. For instance, %BDOC increased linearly with sediment exposure time, while the content of bulk sediment OM, R-WEOM, and Ref-WEOM showed complex temporal trends. A common trend for R-WEOM and Ref-WEOM is that they began to increase when vegetation became abundant between 362 and 577 days, while the content of bulk sediment OM reached a plateau at ~400 days of sediment exposure. The linear increase in %BDOC with sediment exposure time and the late increases in R-WEOM and Ref-WEOM may be due to the input of labile OM produced by plants recolonizing the reservoir and the conversion of high molecular, recalcitrant OM to low molecular, labile OM through photodegradation.

The content of bulk sediment OM in the Enobieta Reservoir (84 ± 5.1 mg OC g^{-1} dry sediment) was comparable to the global content of sediment OM in ponds (mean \pm SD in mg OC g^{-1} dry sediment), 180 ± 200 , lakes, 140 ± 170 , and reservoirs, 100 ± 110 , but higher than in streams, 30 ± 40 (Keller et al., 2020). However, sediment WEOC (0.81 ± 0.05 mg DOC g^{-1} dry sediment) in the Enobieta Reservoir was higher than WEOC in lakes, mean \pm SE in mg C g^{-1} dry sediment, 0.52 ± 0.06 (Table S.4.3), soils, 0.35 ± 0.03 (Table S.4.4), and rivers, 0.29 ± 0.02 (Table S.4.5). The mean content of sediment OM in the Enobieta Reservoir may be comparable to the global mean content of sediment OM in ponds due to a high perimeter-to-area ratio of ponds that may lead to higher input and burial of OM in the sediments of ponds (Keller et al., 2020). Since the areal C burial rate in natural lakes is 4–12 times lower than in reservoirs (Mendonça et al., 2017), the content of bulk sediment OM in the Enobieta Reservoir should be higher than in lakes. However, our findings are consistent with those of Keller et al. (2020) who found no difference between the content of sediment OM in lakes and reservoirs worldwide. Furthermore, as found in this study, a previous study reported a higher content of sediment OM in reservoirs than in streams (Keller et al., 2020). High inputs of sediment and OM from the catchment increases C burial and content in reservoir sediments.

The content of bulk sediment OM decreased between the first sampling campaign and ~ 200 days of sediment exposure, which may be due to a rapid decomposition of labile OM contained in sediments that were mostly bare (with almost no vegetation) (Gómez-Gener et al., 2015; Kosten et al., 2018; Marcé et al., 2019). The content of bulk sediment OM increased between ~ 200 and 400 days of sediment exposure, which may be due to the input of OM produced by plants recolonizing the exposed sediment. However, the content of bulk sediment OM reached a plateau at ~ 400 days of sediment exposure. At this stage, we do not have a clear explanation of why the content of bulk sediment OM reached this plateau, especially because vegetation continued to grow. We can speculate that there may have been a developing microbial community associated with root development. These microorganisms could have compensated for the effect of vegetation regrowth, a potential new source of OM, on the content of bulk sediment OM by increasing heterotrophic respiration. The balance between the supply of OM by plants and the loss through respiration could have led to a plateau of bulk sediment OM at ~ 400 days of sediment exposure. However, the role of vegetation recolonization in C content and microbial structure and function in exposed sediments after DD deserves further research.

Sediment OM in the Enobieta Reservoir was highly bioreactive. The mean O_2 consumption rate for bulk sediment OM (mean \pm SE in $\mu g O_2 g^{-1}$ dry sediment h^{-1} : 2.76 ± 0.20) was lower than the global mean of the O_2 consumption rate of bulk soil OM in dry soils of wetlands, 3.74 ± 0.39 (Table S.4.6), but was ~ 2 times higher than the global mean of the O_2 consumption rate in dry sediments of streams, 1.43 ± 0.31 (Table S.4.7). The mean decomposition rate of OM in dry soils of wetlands may be higher than in dry sediments of reservoirs because wetlands are more likely to bury large stocks of bioreactive OM due to

high primary productivity and low O₂ concentration (due to soil water saturation), which inhibits the decomposition of OM in wetlands (Freeman et al., 2001; Mitsch et al., 2013). Carbon buried in wetlands comprises ~33% of wetland soils (Villa & Bernal, 2018) and the decomposition of OM increases with the content of OM (Keller et al., 2020; Kothawala et al., 2021; Paranaíba et al., 2021). Thus, the lower amount of sediment OM may explain its lower decomposition rate in streams than in the Enobieta Reservoir. By comparing the C:N ratio, we may also infer that sediment OM in the Enobieta Reservoir (C:N ratio = 16.2 ± 1.0) was more bioreactive than sediment OM in streams, C:N ratio: 26.0 ± 2.2 (von Schiller et al., 2019). The C:N ratio in the Enobieta Reservoir was, however, higher than in lakes (Dean & Gorham, 1998). In addition, we report %BDOC for a two-day incubation, 41.4 ± 2.0%, which is 1.4 times lower than %BDOC in dry sediments of three reservoirs in the Three Gorges Reservoir region in China and dry soils from a wetland in Southeastern China, which were, however, incubated for an average time of 28 days at 28 °C, mean: 58.0% (Table S.4.3). Since the decomposition of sediment OM increases with temperature (Gudasz et al., 2010, 2015), %BDOC in the Enobieta Reservoir would be comparable or even higher than %BDOC in the three reservoirs and one wetland if the incubation temperature and time were equal. Furthermore, %BDOC in the Enobieta Reservoir was ~2 times higher than the global mean %BDOC in dry soils incubated for an average time of 50 days at 16.9 °C, 22.1 ± 1.4% (Table S.4.4). Thus, although the experimental approaches adopted to estimate %BDOC differ among studies, our results highlight that reservoir sediments may be hotspots of highly biodegradable OM.

Reff-WEOM was 34.4 times higher than Reff-BOM. This result reinforces the idea that WEOM is the most bioavailable fraction of OM (Boyer & Groffman, 1996; Chantigny, 2003), and that most of the degradation of OM in bulk sediments is based on WEOM. Furthermore, our results suggest that C burial in reservoir sediments is due to conditions not favorable for C decomposition, rather than the inherent C recalcitrance (Catalán et al., 2016; Kellerman et al., 2015; Kothawala et al., 2021). If the OM buried in the sediments of the Enobieta Reservoir was inherently recalcitrant against microbial decomposition, we should have reported low decomposition rates in our incubation experiment. Since we conducted our incubation experiment with the native microbial community under dark conditions, at a temperature close to the temperature in the region of the Enobieta Reservoir and without the addition of nutrients, we may speculate that the key factor that restricted the decomposition of sediment OM during the operational phase of the Enobieta Reservoir was anoxia. The high sedimentation rate and the limited exposure time of sediment OM to O₂ (Sobek et al., 2009, 2012) can result in the burial of inherently bioreactive OM in reservoir sediments. However, we expected that the content and reactivity of sediment OM would decrease with sediment exposure time, as increased availability of O₂ would increase the microbial decomposition of OM during sediment exposure.

Interestingly, %BDOC increased linearly with sediment exposure time, while the content of bulk sediment OM, R-WEOM and Reff-WEOM exhibited complex temporal trends during the first 9–580 days of sediment exposure. The linear increase in %BDOC with sediment exposure time may be explained by the rapid recolonization of exposed sediments by vegetation and the effect of photodegradation. As shown by the NDVI values, vegetation rapidly recolonized the reservoir after reservoir drawdown. Growing plants may supply an important amount of fresh and labile OM. For instance, depending on plant species, roots release 10–250 mg C g⁻¹ root produced as root exudates (McNear, 2013; Vranova et al., 2013). Root exudates comprise labile, low molecular weight organic compounds, such as amino acids, peptides, and sugars (Rovira, 1969). These root exudates can also increase microbial biomass (Eisenhauer et al., 2017; Sung et al., 2006; Wang et al., 2012), which can contribute to the labile C pool. However, the labile OM of microbial biomass and plants that recolonize exposed sediments after drawdown can also increase the bioreactivity of old recalcitrant OM buried in sediments, a process called the priming effect (Bianchi et al., 2015; Guenet et al., 2010, 2014). Thus, the priming effect due to labile OM produced by microorganisms and regrowing plants could lead to a decrease in the content and reactivity of sediment OM. Furthermore, high-molecular weight, recalcitrant molecules in sediment OM of exposed sediments may also be converted into low-molecular weight, bioreactive molecules, due to sediment exposure to solar radiation (Granéli et al., 1996; Lindell et al., 1995; Wetzel et al., 1995). Though photoreactions produce mainly inorganic C (CO₂), they also produce organic compounds of low molecular weight and low aromaticity called biologically available photoproducts (Backlund, 1992; Catalán et al., 2013; Kieber et al., 1989; Mopper & Stahovec, 1986). Since sediment exposure is a hot moment of OM decomposition, aromaticity should have increased with sediment exposure time (Hansen et al., 2016). Thus, we expect photodegradation to be one of the reasons why sediment exposure time did not affect the aromaticity of sediment OM. However, future studies should assess the specific effect of solar exposure on the molecular weight of sediment OM after DD.

Other parameters of the content and reactivity of sediment OM showed non-linear temporal trends. R-WEOM and Reff-WEOM showed almost the same temporal trend as the content of bulk sediment OM but did not reach a plateau at ~400 days of sediment exposure. The effects of terrestrialization and associated development of the microbial community and solar radiation may explain why R-WEOM and Reff-WEOM continued to increase with sediment exposure time. With current data, we cannot, beyond speculation, explain why other factors, such as the decomposition rate for bulk sediment OM and its respiration efficiency, SUVA₂₅₄, sediment WEOC, and the C: N ratio did not change with time. However, SUVA₂₅₄ in sediment WEOM of the Enobieta Reservoir was in the range of SUVA₂₅₄ of dissolved OM reported from sediments of different types of inland waters (0.2–3.7 L mg C⁻¹ m⁻¹, Chen & Hur (2015)), but lower than SUVA₂₅₄ of dissolved OM in waters collected from a range of aquatic systems, 3.2–10.6 L mg C⁻¹ m⁻¹ (Helms et al., 2008).

The observed temporal trend of the sediment texture was not expected since water withdrawal should result in rapid transport of fine-sized sediment, which would increase the mean size of the sediment during the early sampling campaigns. The late increase in mean sediment size may be explained by a higher transport of fine sediment and the accumulation of coarse sediment in the reservoir. Furthermore, sediment texture did not affect the content and reactivity of sediment OM in the Enobieta Reservoir, and previous studies also reported conflicting results on the role sediment texture in the reactivity of sediment OM (Mendoza-Lera et al., 2017; von Schiller et al., 2019).

Amani et al. (2022) hypothesized that the areal CO₂ fluxes in exposed sediments decreased with the sediment exposure time due to a decrease in the content and reactivity of sediment OM in the Enobieta Reservoir after the drawdown phase of DD. This study rejects the hypothesis that the content and reactivity of sediment OM in the Enobieta Reservoir decreased with sediment exposure time. Decreasing areal CO₂ fluxes in exposed sediments due to reduced C availability and microbial activity due to sediment drying should not be expected in a humid region, such as the Artikutza Valley with a rainfall of 2604 mm yr⁻¹ (Atristain et al., 2022). However, a decrease in temperature over the last two sampling campaigns shown in this study may explain why areal CO₂ emissions in exposed sediments and running water decreased during the sampling period in Amani et al. (2022).

4.6. Conclusion

This study explored the content and reactivity of bulk sediment OM and sediment WEOM in a reservoir under DD. We reported a high content of highly bioreactive sediment OM, with the respiration efficiency of sediment WEOM being higher than that of bulk sediment OM. Sediment OM in exposed sediments during and after DD is susceptible to erosion and lateral transport downstream of the reservoir. Our results suggest that exposed sediments may be a great source of labile OM in downstream river reaches. Lateral transport of labile OM from the reservoir can imply higher C respiration and CO₂ fluxes in the river network downstream of the reservoir, therefore, interfering in the final OM delivered to the coastal ocean after a reservoir DD. It is necessary to know how the lateral transport of C from the reservoir alters the dynamics of C in the river segments downstream from the removed reservoir. Future studies should also examine the effects of vegetation recolonization on the C dynamics in the reservoir and the lateral transport of C downstream of the reservoir after DD.

4.7. Acknowledgements

This study was funded by the project PID2020-114024GB-C31 (*Alteration of carbon sinks and sources in shrinking inland waters – Alter-C*) funded by MCIN/AEI /10.13039/501100011033/. Additional support was provided by Agència de Gestió d'Ajuts Universitaris i de Recerca (AGAUR), and Institut de Recerca de l'Aigua (IdRA). DvS is a Serra Húnter Fellow. The authors also acknowledge Montse Badia, Miren Atristain, and Arturo Elosegui for their valuable help with field and laboratory activities, and Camille Minaudo for helping with statistics and NDVI data.



5. Vegetation growth partially offsets carbon dioxide emissions from exposed sediments: a study in a decommissioned reservoir

Amani, M, von Schiller, D, Minaudo, C, Badia, M, Suárez-Velasquez, I, Elozegi, A, Aldezabal, A, Atristain, M, Obrador, B. Vegetation growth partially offsets carbon dioxide emissions from exposed sediments: a study in a decommissioned reservoir. *To be submitted.*

5.1. Abstract

Climate change and human activities are increasing the spatiotemporal extent of dry inland waters and their exposed sediments. Exposed sediments are conducive environments for carbon dioxide (CO₂) emissions and vegetation growth. Vegetation affects CO₂ fluxes through its biomass respiration and fixation of atmospheric CO₂, but knowledge of its effect on carbon (C) cycling in exposed sediments is limited. We determined the spatiotemporal dynamics of vegetation growth and its effect on C fluxes four months after drawdown of the Enobieta Reservoir, north Iberian Peninsula. We explored vegetation biomass, biomass density, and plant species diversity at 25 sites and CO₂ fluxes in dark and light conditions at 5 of the 25 sites in bare sediments and sediments covered by vegetation in 5 environments of the reservoir. We identified 31 plant species that covered 31% of the reservoir area. Old (with longer sediment exposure time) and more stable (flat) environments had higher plant species diversity, cover, and biomass density than young and steep environments. Hourly and daily areal CO₂ emissions from bare sediments were always positive and equal in dark and light conditions and equal to hourly and daily areal CO₂ emissions from sediments covered by vegetation. Carbon dioxide emissions in light conditions were lower than in dark conditions in sediments covered by vegetation, probably, due to photosynthesis. Accounting for C in vegetation biomass reduced the ecosystem C flux by 52%. Our results suggest that vegetation regeneration can mitigate CO₂ emissions from exposed sediments, with relevant implications for dam decommissioning projects.

Keywords: Bare sediments, carbon sink, dam decommissioning, reservoirs, terrestrialization

Resumen

El cambio climático y las actividades humanas están aumentando la extensión espaciotemporal de las aguas continentales secas y sus sedimentos expuestos. Los sedimentos expuestos son entornos propicios para las emisiones de dióxido de carbono (CO₂) y el crecimiento de la vegetación. La vegetación afecta los flujos de CO₂ a través de la respiración de su biomasa y la fijación del CO₂ atmosférico, pero el conocimiento de su efecto sobre el ciclo del carbono (C) en los sedimentos expuestos es limitado. Determinamos la dinámica espaciotemporal del crecimiento de la vegetación y su efecto sobre los flujos de C cuatro meses después del vaciado del embalse de Enobieta, norte de la Península Ibérica. Exploramos la biomasa vegetal, la densidad de biomasa y la diversidad de especies de plantas en 25 sitios y los flujos de CO₂ en condiciones de luz y oscuridad en 5 de los 25 sitios en sedimentos desnudos y sedimentos cubiertos por vegetación en 5 ambientes del embalse. Identificamos 31 especies de plantas que cubrían el 31% del área del embalse. Los ambientes antiguos (con mayor tiempo de exposición a los sedimentos) y más estables (planos) tenían una mayor diversidad de especies de plantas, cobertura y densidad de

biomasa que los ambientes jóvenes y empinados. Las emisiones horarias y diarias de CO₂ por área de los sedimentos desnudos siempre fueron positivas e iguales en condiciones de luz y oscuridad y similares a las emisiones horarias y diarias de CO₂ por área de los sedimentos cubiertos por vegetación. Las emisiones CO₂ en condiciones de luz fueron menores que en condiciones de oscuridad en sedimentos cubiertos por vegetación, probablemente debido a la fotosíntesis. Contabilizar el C en la biomasa vegetal redujo el flujo de C del ecosistema en un 52%. Nuestros resultados sugieren que la regeneración de la vegetación puede mitigar las emisiones de CO₂ de los sedimentos expuestos, lo cual tiene importantes implicaciones para los proyectos de desmantelamiento de presas.

Palabras clave: Sedimentos desnudos, sumidero de carbono, desmantelamiento de presas, embalses, terrestrialización

5.2. Introduction

Climate change and increased water abstraction, damming, and diversion are increasing the surface area of dry inland waters (Konapala et al., 2020; Pekel et al., 2016; Yao et al., 2023). Dry inland waters are sections of lentic (i.e., standing or non-flowing waters: lakes, ponds, and reservoirs) and lotic (i.e., flowing waters: rivers and streams) ecosystems that are, due to the absence of surface water, covered by air-exposed sediments (Marcé et al., 2019). Exposed sediments of inland waters are widely reported hotspots of carbon dioxide (CO₂) emissions (Keller et al., 2020; Marcé et al., 2019; von Schiller et al., 2019). Carbon dioxide emissions from exposed sediments can, however, be affected by vegetation growth because these systems are suitable for terrestrialization (Orr & Stanley, 2006). Terrestrialization is the passage from the aquatic stage to the terrestrial stage due to the establishment of terrestrial vegetation in dry aquatic ecosystems (Marcé et al., 2019). Terrestrialization can increase CO₂ emissions from exposed sediments through the increased supply of organic matter (OM), autotrophic respiration, gas diffusion due to the alteration of sediment texture and porosity by vegetation, aeration of anoxic microhabitats by aerenchymatous plants, hydraulic lift in dry regions and transport of water and nutrients through interspecific mycorrhizal networks (Cable et al., 2008; Luo & Zhou, 2010; Van Andel et al., 1993). Conversely, terrestrialization can offset CO₂ emissions from exposed sediments by converting atmospheric CO₂ to vegetation biomass (Bolpagni et al., 2017). Nonetheless, previous studies have rarely explored the effect of terrestrialization on C cycling in exposed sediments (Obrador et al., 2018). A better understanding of the effect of terrestrialization on C cycling in dry inland waters is necessary to better constrain the role of exposed sediments in the local, regional, and global C budgets of inland waters.

Natural and artificial inland waters are affected by drying, which is increasing in frequency and intensity due to the combined effects of climate change and human actions (Keller et al., 2020; Konapala et al., 2020; Pekel et al., 2016). For instance, ~90,000 and ~800,000 km² of inland waters have dried in the last three decades or experience seasonal drying, respectively (Pekel et al., 2016). Globally, there are 16.7 million small dams and 58,700 large dams that span 507,102–1,500,000 km² (Lehner et al., 2011; Perera et al., 2021; St. Louis et al., 2000). A recent study reported that 15% of the global surface area of reservoirs was dry between 1985 and 2015 (Keller et al., 2020). Furthermore, tens of thousands of dams have reached their engineered life expectancies (Perera et al., 2021; Zamarrón-Mieza et al., 2017). Old dams pose various economic, environmental, and social problems, including high expenses associated with dam maintenance, environmental damage due to dam failures, and a threat to public safety (Perera & North, 2021; Perera et al., 2021). The most viable management option to solve problems caused by old dams is dam decommissioning (DD) (Stanley & Doyle, 2003). Dam decommissioning is a partial or full removal of a dam and its ancillary facilities (Amani et al., 2022; Perera et al., 2021). Given the large number of old dams, DD can contribute to the increasing surface area of dry inland

waters. Dry inland waters are, however, not included in the C budgets of inland waters or soils and, thus, represent a potential blind spot in the global C budget (Marcé et al., 2019).

Dry inland waters can alter the role of inland waters in the global C cycle by increasing the spatiotemporal extent of exposed sediments. There is a certain understanding of the magnitude and drivers of CO₂ emissions from exposed sediments of dry lentic and lotic inland waters worldwide (Keller et al., 2020; von Schiller et al., 2019). For instance, areal CO₂ emissions from exposed sediments increase with temperature, the content of sediment OM and moisture, and the proportion of fine sediments (Keller et al., 2020; von Schiller et al., 2019). Furthermore, although exposed sediments of inland waters are widely reported to undergo rapid terrestrialization (Orr & Stanley, 2006; Shafroth et al., 2002; Stanley & Doyle, 2003), previous studies deliberately avoided including CO₂ emissions from sediments covered by vegetation (Keller et al., 2020) or did not include C incorporated into vegetation biomass in their estimates of dry C fluxes (Catalán et al., 2014; Obrador et al., 2018). Exposed sediments can be viewed as young soils that are maturing toward a soil-like stage (Arce et al., 2019). Thus, sediments covered by vegetation can act as terrestrial ecosystems, which, despite high areal CO₂ emissions from soils, are net sinks of atmospheric CO₂ (Bond-Lamberty & Thomson, 2012; Janssens et al., 2003; Zhao et al., 2017). Plants can be a short-term C sink by storing C in biomass and a long-term C sink when C in plant biomass enters the soil C pool. However, the time scales for C sinks in exposed sediments are not clear and may depend on the turnover rate of annual herbaceous species to perennial woody species (Albrecht & Kandji, 2003; Jansson et al., 2010).

Here, we explore the effect of terrestrialization on C fluxes measured under dark and light conditions in bare sediments and sediments covered by vegetation in five environments of the Enobieta Reservoir, north Iberian Peninsula, four months after its drawdown. We expected that terrestrialization descriptors (e.g., diversity of plant species, biomass, biomass density, and vegetation cover) and C fluxes would be different between the five environments because factors of terrestrialization and CO₂ fluxes (e.g., OM content, sediment texture, and the time of sediment exposure) would vary between the environments. Additionally, we expected that areal CO₂ fluxes from bare sediments, which are assumed to result mainly from heterotrophic respiration, would be lower than areal CO₂ fluxes from sediments covered by vegetation, which are assumed to result from autotrophic plus heterotrophic respiration (Cable et al., 2008). We also expected that areal CO₂ fluxes in dark conditions would be higher than in light conditions for sediments covered by vegetation due to photosynthesis but equal in both conditions for bare sediments. Consequently, we expected that terrestrialization would substantially reduce the whole-ecosystem C flux.

5.3. Materials and Methods

5.3.1. Study site

We conducted this study in the Enobieta Reservoir, a recently partially decommissioned reservoir in the Artikutza Valley (Fig.5.1) (Amani et al., 2022, 2024). The Artikutza Valley is mainly covered by mature forests, dense autochthonous riparian vegetation, some exotic plantations, and pasturelands on the highest terrain of the catchment (Amani et al., 2024; Lozano & Latasa, 2019). The catchment area of the hydrological network in the Artikutza Valley is 3,683 ha, with a geology dominated by acidic rocks, such as granite and schist (Atristain et al., 2022). The mean annual air temperature and rainfall in the Artikutza Valley are, respectively, 12.2 °C and 2,604 mm yr⁻¹ (period 1954–2019) (Amani et al., 2024; Gobierno de Navarra, 2019). The dam was built on the Enobieta Stream between 1947 and 1953 to supply drinking water to the city of Donostia-San Sebastian. The reservoir had a length of 1,100 m from the tail to the dam, a dam height of 42 m, a surface area of 141,361.98 m², and a water storage capacity of 2,660,000 m³ (Amani et al., 2022, 2024). Its use ended in the 1970s when a larger reservoir (Añarbe) was built some kilometers downstream (Larrañaga et al., 2019). The city council of Donostia-San Sebastian started decommissioning the reservoir in 2017 to promote the conservation of the Artikutza Valley and solve safety-related problems caused by the ageing dam. A progressive decrease in the inundated area was interrupted by some increases in water level until November 2018. The reservoir drawdown ended on 25 February 2019 when the water level reached its lowest level (326 m) (Amani et al., 2022, 2024).

5.3.2. Sampling design

We collected vegetation biomass and measured CO₂ fluxes in exposed sediments in July 2019, four months after the end of the drawdown phase of the Enobieta Reservoir (Fig.5.1a). We collected vegetation and CO₂ samples in five geomorphological environments present in the former reservoir (i.e., in the descending order of their exposure times, tail, old slope, young slope, plain, and dam, hereinafter referred to as environments) (Table S.5.1, Fig.5.1b). The five environments were differentiated by their location, elevation, substrate, and timing of exposure to the atmosphere along the decline in water level in the reservoir (Table S.5.1). We randomly selected 25 sites, i.e., five sites in each environment, to collect vegetation biomass and five sites, i.e., one site in each environment, drawn from the 25 random sites to measure CO₂ fluxes (Table S.5.1, Fig.5.1, Fig.5.2). Each of the five sites used to measure CO₂ fluxes had bare sediments and at least one of the three most abundant plant taxa, *Gnaphalium* spp., *Juncus* spp., and *Persicaria* spp. Bare sediments and plant taxa were designated as colonization type. Each site was a square with a side of 0.5 m.

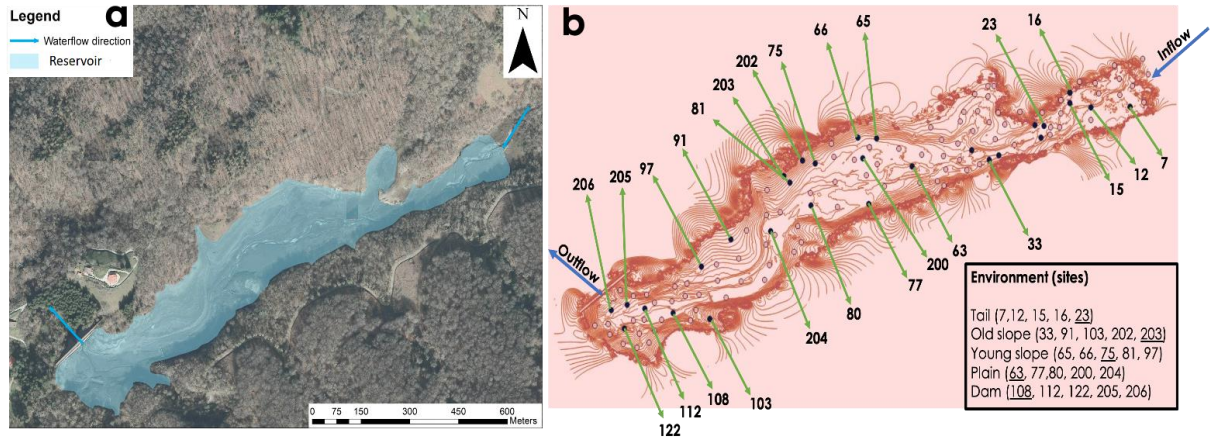


Figure 5.1 The Enobieta Reservoir and the surrounding forest (a) and the five environments and 25 sites used to collect samples of vegetation biomass (b) in the reservoir. The five underlined sites were used to measure CO₂ fluxes in bare sediments and sediments covered by vegetation

5.3.3. Vegetation sampling

We collected the above- and belowground vegetation biomass of all plant species, which we identified at the lowest taxonomical level possible. When we found several species of the same genus, we aggregated them to the genus level (Table S.5.2). We stored the biomass samples at -18 °C in the laboratory for their preservation. To determine vegetation dry biomass, we weighed vegetation samples that we had dried at 65 °C for 24 hours. We obtained the above- and belowground biomass density (g m⁻²) of each plant taxon and site by multiplying the vegetation biomass in each site by 4, because each site was 0.25 m², i.e., 0.5 × 0.5 m². To obtain the biomass density in each environment, we calculated the average of the biomass density of all sites in the environment. We obtained total vegetation biomass of each species in each environment (kg) by multiplying its mean biomass density by the area occupied by the environment (Table S.5.1). We determined the total vegetation biomass in the reservoir as the sum of the average vegetation biomass in the five environments. Furthermore, we determined the vegetation cover at each site using top-down photographs that we took before harvesting vegetation biomass. We processed the photographs in ImageJ (Schneider et al., 2012) to obtain the percent surface within the sampling frame that was either covered by bare sediments or by vegetation. We assigned the percent cover to total vegetation cover rather than to individual taxa.

5.3.4. Instantaneous CO₂ fluxes

We measured 24 instantaneous CO₂ fluxes for each of the 5 sites/environment. That is, 5 sites/environment (tail, old slope, young slope, plain, and dam) × 4 colonization types

(3 most abundant plant taxa + bare sediments for each site) \times 2 conditions (dark and light for each colonization type) \times 3 replicates for each condition, which is 120 CO₂ flux measurements for the whole reservoir (Fig.5.2). We measured CO₂ fluxes on the 3 most abundant plant taxa because dominant species of a plant community largely drive the functional component of an ecosystem, such as C cycling (Grime et al., 1987; Van Andel et al., 1993). We determined CO₂ fluxes using enclosed custom-made transparent methacrylate chambers. We used two chambers of different sizes (a small chamber with a volume of $1.77 \times 10^{-3} \text{ m}^3$ and a surface area of 0.0118 m^2 , and a big chamber with a volume of 0.039 m^3 and a surface area of 0.049 m^2) depending on the size of plants. We connected the chamber to an infrared gas analyzer (IRGA model EGM-5, PP-Systems, Amesbury, USA) that recorded the CO₂ concentration in the chamber every second with an accuracy of 1%. We inserted the chambers \sim 1 cm into sediments to avoid gas leakage during the measurements. We determined the dark and light fluxes sequentially using the same chamber and sampling spot. Once placed on the substrate, we covered the chamber with an opaque blanket for the first 120 s to determine the flux in dark conditions. At 120 s the blanket was removed and the CO₂ flux in light conditions was determined during the next 120 s. Time around the inflection, due to the shift from dark to light conditions, was discarded during data analysis. After the measurement of CO₂ fluxes, we collected the above- and belowground biomass of plant species within the chamber to estimate their biomass.

We obtained the rate of change of the partial pressure of CO₂ ($p\text{CO}_2$) in the chamber by linear regression between $p\text{CO}_2$ and time ($\frac{dp\text{CO}_2}{dt}$, in $\mu\text{atm s}^{-1}$) during each measurement. We used only periods with a linear trend duration of at least 60 s and with $R^2 \geq 0.9$. We reported instantaneous hourly areal CO₂ fluxes ($\text{mmol CO}_2 \text{ m}^{-2} \text{ h}^{-1}$), net daily areal CO₂ fluxes ($\text{mmol CO}_2 \text{ m}^{-2} \text{ d}^{-1}$), and net daily ecosystem C fluxes (kg C d^{-1}). The instantaneous hourly areal CO₂ flux was determined as:

$$FCO_2 = \left(\frac{dp\text{CO}_2}{dt} \right) \times \left(\frac{V}{RTS} \right), \quad (5.1)$$

where V is the volume of the chamber (L), S is the surface area of the chamber (m^2), T is air temperature (K) and R is the ideal gas constant ($\text{L atm K}^{-1} \text{ mol}^{-1}$). Conventionally, positive fluxes reported here correspond to CO₂ efflux to the atmosphere, and negative fluxes correspond to CO₂ uptake or influx.

We calculated net daily CO₂ fluxes as the sum of an instantaneous hourly areal CO₂ flux in light conditions multiplied by 15 h plus an instantaneous hourly areal CO₂ flux in dark conditions multiplied by 9 h. We used 15 h for light and 9 h for dark times according to the sunrise and sunset times in July 2019 in the Artikutza Valley.

5.3.5. Upscaling C fluxes to the ecosystem level

We used instantaneous hourly areal CO₂ flux, vegetation biomass, and area to obtain the total ecosystem C flux (Fig.5.2). The instantaneous hourly areal CO₂ flux for each of the 3 most abundant plant taxa (i.e., plant associated flux + heterotrophic CO₂ flux) minus the average of the instantaneous hourly areal CO₂ fluxes in bare sediments (i.e., heterotrophic CO₂ flux) of each environment for dark and light conditions gave the autotrophic CO₂ flux (mmol CO₂ m⁻² h⁻¹). The plant associated CO₂ flux multiplied by 9 h for dark conditions and 15 h for light conditions gave the net daily areal plant associated CO₂ flux (mmol CO₂ m⁻² d⁻¹). The net daily areal plant associated CO₂ flux divided by the total (above + belowground) biomass density of each of the three most abundant plant taxa gave the net daily biomass-specific CO₂ flux (mmol CO₂ g⁻¹ d⁻¹) of the three most abundant plant taxa. The net daily biomass-specific CO₂ flux multiplied by the vegetation biomass of the three most abundant plant taxa in each environment and the molar weight of C gave the vegetation C flux (kg C d⁻¹) for the 3 most abundant plant taxa. The vegetation C flux for the three most abundant plant taxa plus the C flux for other species (species that we did not use to measure CO₂ fluxes) gave the total vegetation C flux (kg C d⁻¹). We calculated the C flux for other species as the product of the vegetation biomass of other species in each environment and the average net daily biomass-specific CO₂ flux of the three most abundant taxa in each environment. The product of the average net daily CO₂ fluxes for each environment in bare sediments, the atomic mass of C (12 g mol⁻¹), and the area of each environment gave the total C flux for bare sediments (kg C d⁻¹). The sum of C fluxes in bare sediments and sediments covered by vegetation gave the total ecosystem C flux (kg C d⁻¹). We divided the total C flux for bare sediments and sediments covered by vegetation by the surface area of the Enobieta Reservoir to obtain the daily areal C flux (g C m⁻² d⁻¹) for bare sediments and sediments covered by vegetation, respectively.

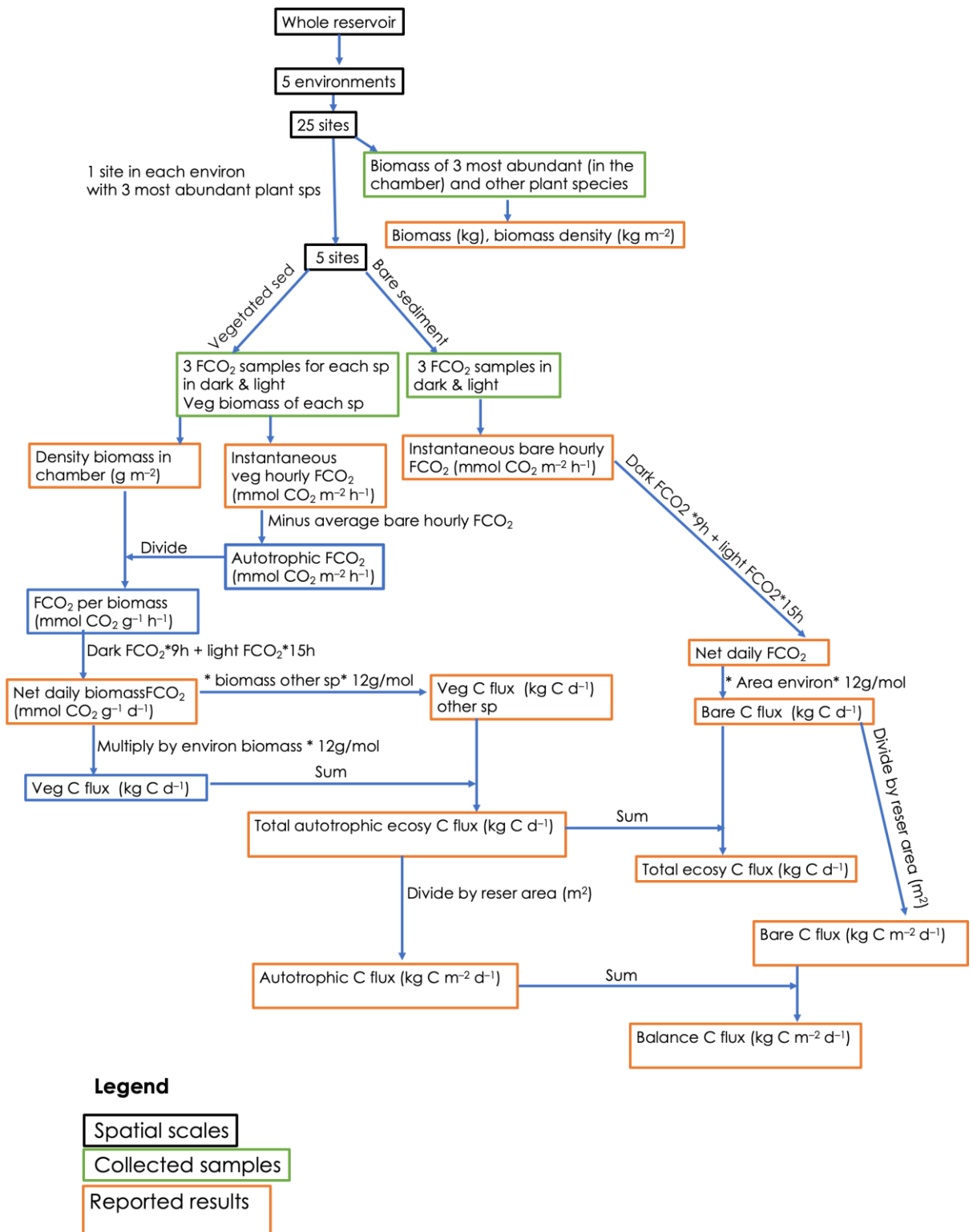


Figure 5.2 Schematic representation of sampling design and upscaling methods

5.3.6. Statistical analysis

Since our data did not meet the requirements for the parametric analysis even after data transformation, we used non-parametric tests in R version 4.0.5 (R Core Team, 2021).

We tested the effect environment with five levels (tail, old slope, young slope, plain, and dam), colonization type with four levels (three most abundant plant taxa + bare sediments), and condition with two levels (dark and light) on hourly and daily areal CO₂ fluxes. To test for the combined effect of environment and colonization type on instantaneous hourly areal CO₂ fluxes, we used the Friedman test. We used the Kruskal-Wallis test to test for the effect of environment and colonization type on instantaneous hourly areal CO₂ fluxes. As the effect of environment was significant, we conducted pairwise comparisons between the five environments using Dwass-Steel-Critchow-Flinger pairwise comparisons. To test for the effect of dark and light conditions (paired samples) on areal CO₂ fluxes between the four colonization types, we used the Wilcoxon signed-rank test. To test for the difference between areal CO₂ fluxes in bare sediments and sediments covered by vegetation, we used the Mann-Whitney U test. We also ran a correlation test to explore the relationship between vegetation biomass and sediment exposure time.

5.4. Results

5.4.1. Vegetation dynamics

Old and flat environments showed higher plant diversity, vegetation cover, and biomass density than young and steep environments (Fig.5.3a, b, c). Terrestrial vegetation colonized the five environments and 23 of the 25 sites, i.e., 92% of the sampled sites. The two sampling sites that were not colonized by terrestrial vegetation were in the dam environment. Bare sediment covered 68.8% and vegetation covered 31.2% of the reservoir (Table S.5.1). We identified 31 plant species, which we aggregated in 23 genera because some genera had more than one species (Table S.5.2). We observed the highest vegetation cover (80%), diversity (15 plant taxa) and biomass density (~1,000 g m⁻²) in the tail environment. The old slope and plain environments showed lower terrestrial colonization, with 30–40% vegetation cover, 10–11 plant taxa, and biomass density ~300 g m⁻². The dam and young slope environments had the lowest vegetation cover (<5%), plant taxa (5–6), and biomass density (<50 g m⁻²). Old and plain environments generally showed higher between-site patchiness, as shown by the higher variability in vegetation cover (higher relative standard deviation: RSD, Fig.5.3b). Above-ground biomass accounted for 75% of total biomass in all environments. The three most abundant species contributed 70% of vegetation biomass of all plant species. There was no correlation between total vegetation biomass and sediment exposure time, $p = 0.273$ (Fig.5.3d).

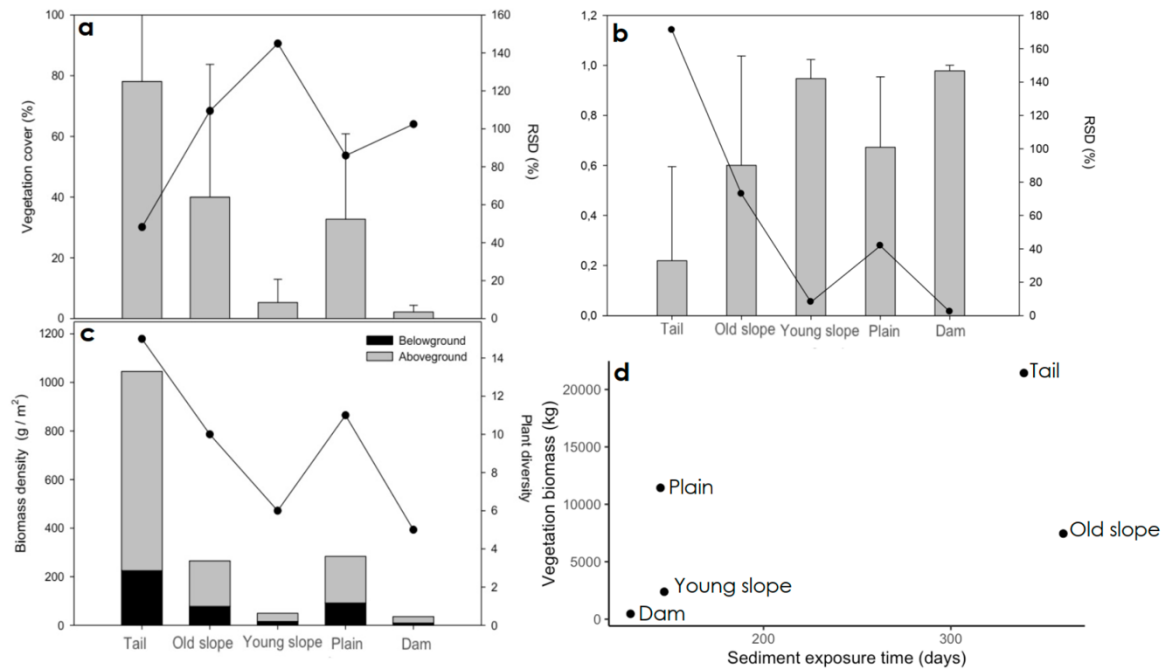


Figure 5.3 Percent vegetation cover (a), relative standard deviation (RSD, %) of vegetation cover (b), above- and below-ground vegetation biomass density and distribution of total biomass (g) by plant functional types (c), and correlation between total vegetation biomass and sediment exposure time (d) in the five environments of the reservoir. Percentage of vegetation cover and relative standard deviation are indicators of vegetation patchiness

5.4.2. Carbon fluxes

The Kruskal-Wallis test showed that environment significantly affected hourly areal CO_2 fluxes, $\chi^2(4) = 40.9$, $p < 0.001$. Dwass-Steel-Critchow-Flinger pairwise comparisons showed that average of (dark and light conditions combined) instantaneous hourly areal CO_2 fluxes were equal for three pairs of environments: the young slope and old slope, dam and plain, and dam and young slope environments, while the average of hourly areal CO_2 fluxes from the tail environment was higher than from dam, $p = 0.001$, plain, $p = 0.005$, old slope, $p < 0.001$, and the young slope, $p < 0.001$, environments, the average of hourly areal CO_2 fluxes from the plain environment was higher than from the old slope, $p < 0.001$, and young slope, $p = 0.04$, environments, the average of hourly areal CO_2 fluxes from the dam was higher than from the old slope environment, $p < 0.001$. The Kruskal-Wallis test showed that the colonization type did not affect instantaneous hourly areal CO_2 fluxes, $\chi^2(3) = 7.37$, $p = 0.06$. Thus, the Mann-Whitney U test showed that instantaneous hourly areal CO_2 fluxes in bare sediments, 19.2 ± 3.16 (4.94–60.5), and sediments covered by vegetation, 20.4 ± 3.18 (-36.9–138) did not differ, $U = 1,244$, $p = 0.921$. Instantaneous hourly areal CO_2 fluxes in bare sediments were always positive (i.e., emissions) and did not differ between dark, 19.3 ± 4.55 (5.47–60.5) and light, 19.2 ± 4.55 (4.94–55.4) conditions, Wilcoxon signed-rank test: $W = 94.0$, $p = 0.07$ (Table S.5.3.). On the other hand, instantaneous hourly areal CO_2 fluxes under light conditions were a mix of negative (i.e., uptake) and positive fluxes for

sediments covered by vegetation (Table S.5.3). Thus, the overall mean instantaneous areal CO₂ flux under dark, 34.4 ± 4.83 (0.00–138), was five times higher than under light, 6.32 ± 2.84 (-36.9–47.2), conditions in sediments covered by vegetation, $W = 861$, $p < 0.001$. The Friedman test showed that the interaction between environment and colonization type did not affect instantaneous hourly areal CO₂ fluxes (Fig.5.4a), $\chi^2(3) = 3.4$, $p < 0.334$.

The Mann-Whitney U test showed that the net daily areal CO₂ flux in bare sediments, mean \pm SE mmol CO₂ m⁻² d⁻¹ (range): 435 ± 111 (123–1,376) and sediments covered by vegetation, 414 ± 63.5 (-180–1,400) did not differ, $U = 271$, $p = 0.767$ (Fig.4b). The Kruskal-Wallis test showed that the colonization type did not affect net daily areal CO₂ fluxes, $\chi^2(3) = 7.233$, $p = 0.06$. The Kruskal-Wallis test showed that the environment affected net daily areal CO₂ fluxes, $\chi^2(4) = 38.8$, $p < 0.001$. Dwass-Steel-Critchlow-Fligner pairwise comparisons showed that net daily areal CO₂ fluxes were higher in the tail environment than the dam, $p < 0.001$, old slope, $p = 0.002$, plain, $p = 0.003$, and young slope, $p < 0.001$, environments, net daily areal CO₂ fluxes were higher in the dam environment than the old slope, $p = 0.002$, and the young slope, $p < 0.001$, environment, and higher in the plain environment than the young slope environment, $p = 0.04$. There was no difference for other pairs.

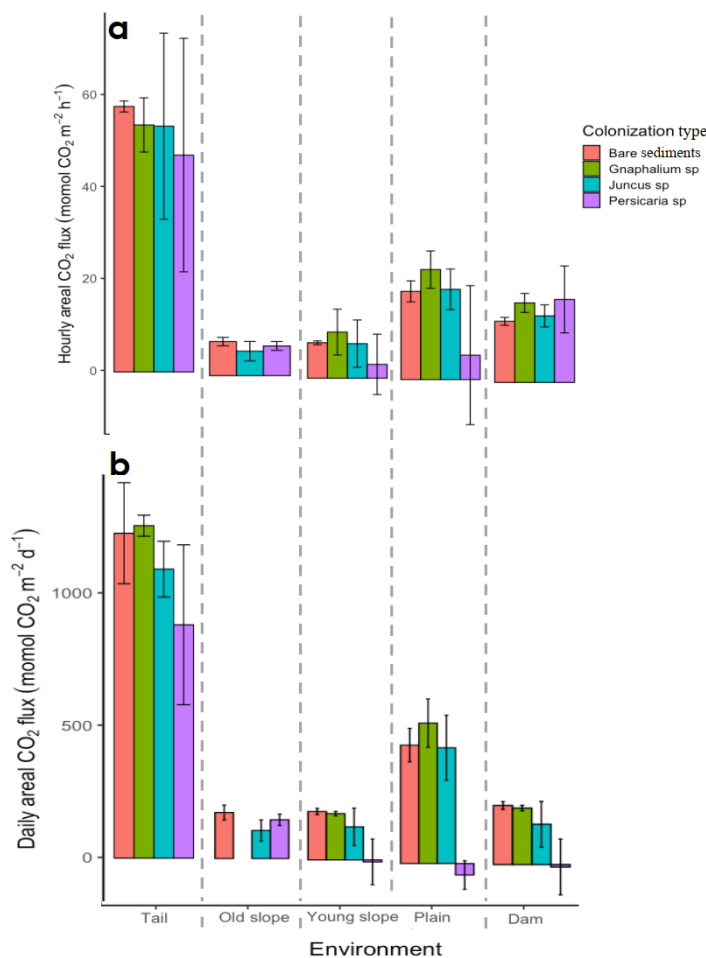


Figure 5.4 Mean instantaneous hourly (a) and net daily areal CO₂ flux (b) emitted by bare sediments and sediments covered by the three vegetation taxa. The error bars show the

standard error (SE) of the mean. The mean instantaneous hourly areal CO₂ flux is the mean of the dark and light CO₂ fluxes

Bare sediments in the tail, old slope, young slope, plain, and dam environments emitted 336.9, 61.9, 82.7, 216.4, and 49.1 kg C d⁻¹, respectively. However, vegetation in these environments fixed, respectively, 267.7, 27.5, 18.5, 77.8 kg C d⁻¹, except for the dam environment where vegetation emitted 0.7 kg C d⁻¹ (Fig.5.5a). The total emission rate from the reservoir was 747 kg C d⁻¹ and total C fixation rate by vegetation was 391 kg C d⁻¹, which is a reduction of 52%. The balance C emission was 356 kg C d⁻¹ (Fig.5.5b).

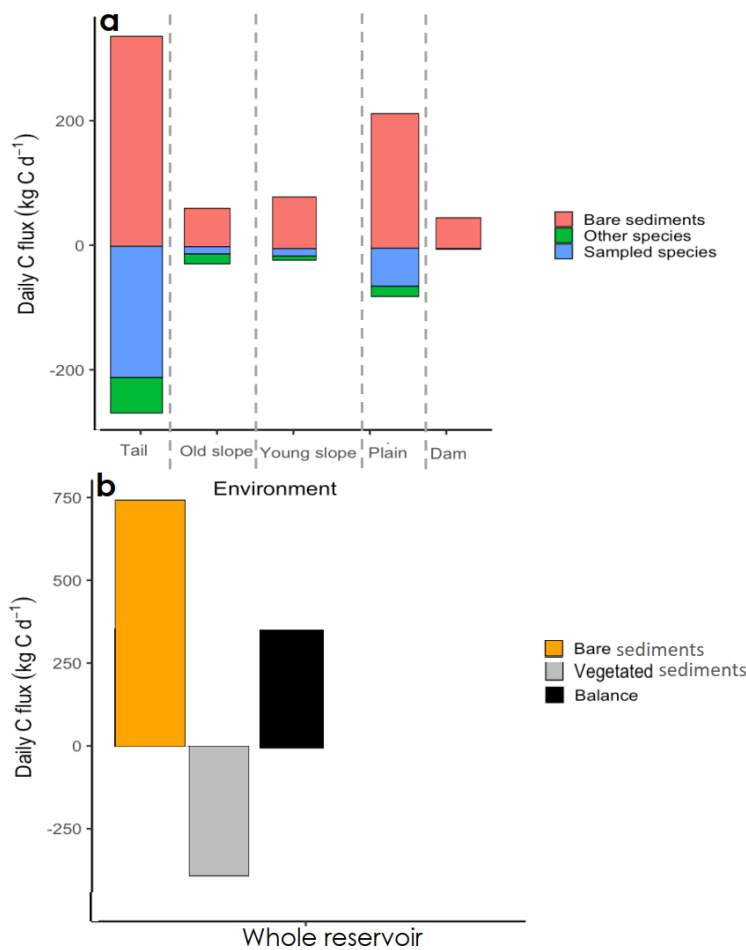


Figure 5.5 Total net daily C flux (kg C d⁻¹) in bare sediments and sediments covered by sampled plant species and other plant species in the five reservoir environments (a), and total flux corresponding to bare sediments, sediments covered by vegetation, and the balance for the whole reservoir (b)

5.5. Discussion

The goal of this study was to understand the spatiotemporal dynamics of terrestrialization and its effect on C fluxes in exposed sediments in the Enobieta Reservoir four months after its drawdown. Thirty-one plant species colonized 92% of the 25 sampled sites and covered 31% of the reservoir area. As expected, the old and flat environments exhibited higher terrestrialization, i.e., higher plant species diversity, vegetation biomass, and biomass density, than young and steep environments. Instantaneous hourly areal CO₂ fluxes in bare sediments were always positive and equal in dark and light conditions. However, instantaneous hourly areal CO₂ fluxes in sediments covered by vegetation were higher in dark conditions than in light conditions. Interestingly, instantaneous hourly and net daily areal CO₂ fluxes were equal between bare sediments and sediments covered by vegetation. The inclusion of C fixed into vegetation biomass reduced the ecosystem C flux by 52%.

Our findings are consistent with the findings of studies that reported rapid terrestrialization of exposed sediments after DD (Orr & Stanley, 2006; Shafroth et al., 2002). Removed dams can rapidly terrestrialize due to large stocks of OM and nutrients buried in reservoir sediments during their operational time (Maavara et al., 2017; Mendonça et al., 2017). The prompt terrestrialization of the Enobieta Reservoir may be favoured by the high moisture in the Artikutza Valley, high content of sediment OM, restricted human activities, and the presence of an adjacent mature forest (Amani et al., 2024, 2022; Lozano & Latasa, 2019). Rapid natural terrestrialization of exposed sediments during the first growing was also recorded in weeks after DD in humid regions (Shafroth et al., 2002). The adjacent forest can be a source of seeds and a habitat for seed dispersers to the former reservoir because propagules of pioneer plant species may be present in seed banks or imported from nearby habitats. Dispersion via air and via the stream might be relevant.

Terrestrialization levels were different between geomorphological environments of the Enobieta Reservoir reflecting stability and exposure time after its drawdown. Old and flat environments exhibited a higher terrestrialization level than young and steep environments. For instance, the tail environment exhibited the highest plant diversity, vegetation cover, and biomass density. This may be because sediments in the tail environment were exposed for a longer time than in other environments. The recovery period may be important for vegetation growth and, thus, soil stability and the creation of other favorable conditions for vegetation establishment. The establishment of some plant species can enhance the growth of other plants or species through direct facilitation, also called plant-to-plant interaction, or indirect facilitation, also called indirect facilitation such as improving microclimatic and edaphic conditions amenable for, for instance, seed germination (Van Andel et al., 1993). Another study on terrestrialization after DD of five dams in Wisconsin, US, recorded low species diversity dominated by large, monotypic stands of pioneer plant species at young sites (Lenhart, 2000). Additionally, tails of reservoirs can be rapidly terrestrialized because they contain higher contents of

allochthonous OM and nutrients than other zones (Thornton et al., 1990). Furthermore, flat environments in the reservoir may be highly productive because they may receive nutrients, OM, fine sediments, and seeds from steep environments, while natural terrestrialization takes many years in less productive settings (Shafroth et al., 2002). The slow terrestrialization of steep environments may explain why we did not find a positive relationship between vegetation biomass and the terrestrialization time of the environments. Different environments in the Enobieta Reservoir could have terrestrialized at different rates because they may exhibit heterogeneities in abiotic and biotic factors.

Four months after the removal of the Enobieta Reservoir, vegetation was dominated by three herbaceous plant taxa. The three most abundant plant taxa (*Gnaphalium* spp., *Juncus* spp., and *Persicaria* spp.) contributed 70% while the remaining 28 plant taxa contributed 30% of the vegetation biomass. Species change over time should progress from early successional pioneer taxa to climax or later successional flora. This pattern can be predictable because, in natural ecological succession, developing communities tend to resemble those in adjacent undisturbed areas (Orr & Stanley, 2006). For instance, tree species and canopy cover increased with time since DD, while grasses and forbs dominated in recently removed reservoirs (Shafroth et al., 2002). The replacement of herbaceous by woody species may be expected in the Enobieta Reservoir because woodland is the typical vegetation in the Artikutza Valley (Lozano & Latasa, 2019). However, our projection must be considered tentative because it is based on data collected from early succession during a single campaign. Furthermore, riparian ecosystems may not fully recover to their pre-dam condition because ecosystem restoration may depend on several factors, including climate, flood regime, geology, fluvial processes associated with vegetation growth, and human activities (Shafroth et al., 2002). Thus, ecosystem restoration may result in pre-dam vegetation or novel stage (s) (Shafroth et al., 2002). Long-term studies are required to assess vegetation dynamics and development towards the target vegetation community after DD.

Instantaneous areal CO₂ fluxes in bare sediments were always positive and equal under dark and light conditions, but negative and positive and lower under light than dark conditions in sediments covered by vegetation. Absent or limited photosynthesis may be responsible for the equal and always positive CO₂ fluxes in dark and light conditions in bare sediments. Conversely, sediments covered by vegetation emitted lower CO₂ fluxes in light than dark conditions, due to photosynthesis. Respiration in sediments covered by vegetation is mainly a combination of autotrophic and heterotrophic respiration, and heterotrophic respiration rates can be equal between bare sediments and sediments covered by vegetation (Cable et al., 2008). Thus, we had predicted that areal CO₂ fluxes would be higher in sediments covered by vegetation than in bare sediments due to autotrophic respiration (Cable et al., 2008). However, instantaneous hourly areal CO₂ fluxes were equal between bare sediments and sediments covered by vegetation. Our results suggest that heterotrophic respiration by the sediment microbial community dominated CO₂ fluxes during early terrestrialization of the Enobieta Reservoir.

Areal CO₂ fluxes in flat environments were higher than areal CO₂ fluxes in steep environments. Flat environments may exhibit higher CO₂ fluxes because they may contain

higher content of sediment OM and moisture and fine sediments that increase CO₂ emissions in exposed sediments (Keller et al., 2020; von Schiller et al., 2019). For instance, the tail environment exhibited the highest areal CO₂ fluxes, which may be due to large vegetation biomass reported in this study and stocks of allochthonous OM and nutrients in riverine zones of reservoirs (Thornton et al., 1990). Furthermore, net daily areal CO₂ emissions from bare sediments and sediments covered by vegetation of the Enobieta Reservoir were in the range of areal CO₂ emissions from bare sediments of the Enobieta Reservoir (Amani et al., 2022), bare sediments and sediments covered by vegetation of other inland waters (Catalán et al., 2014; Marcé et al., 2019), and soils (Bond-Lamberty & Thomson, 2010, 2012).

Sediments covered by vegetation corresponded to 31% of the surface area of the Enobieta Reservoir, but vegetation reduced the ecosystem C flux to the atmosphere by 52%. Most autotrophic CO₂ fluxes were negative (i.e., an uptake of atmospheric CO₂ by vegetation), except for the dam environment. Positive autotrophic CO₂ fluxes in the dam environment could have been related to a sampling artifact, as this environment was sampled between 8 and 9 pm. At this time, ecosystem metabolism may be dominated by respiration, while photosynthesis may be light limited. Exposed sediments of dry inland waters are considered young soils that evolve toward a soil-like stage (Arce et al., 2019), and soils are a net sink of atmospheric CO₂ (Bond-Lamberty & Thomson, 2012). Our results may suggest that the Enobieta Reservoir will become a net sink for atmospheric CO₂ when vegetation will cover the whole reservoir and perennial woody plants will replace fast-growing annual herbaceous plants (Jansson et al., 2010; Stanley & Doyle, 2003).

5.6. Conclusion

Exposed sediments in the Enobieta Reservoir rapidly terrestrialized, especially in flat environments. A persistent open mudflat in the former reservoir is the great concern of DD opponents (Johnson & Graber, 2002). Our results suggest that repugnant exposed bare sediments may be a short-term effect of DD. Plant-free exposed sediments, such as steep environments, may be easily colonized by deleterious alien species (Orr & Stanley, 2006). Limiting sediment erosion and assisted or active revegetation by adding soil, nutrients, and seeds can support ecosystem restoration in less productive environments. Vegetation covered approximately a third of the reservoir area and reduced the ecosystem C flux by more than a half only 4 months after reservoir drawdown. These results highlight the effectiveness of vegetation growth as a management option to reduce CO₂ emissions from exposed sediments. Thus, high CO₂ emissions from exposed sediments can be a short-term effect of DD. More research is required to identify factors that promote vegetation regeneration so that they can be applied in the assisted ecological recovery of disturbed ecosystems, such as removed dams.

5.7. Acknowledgements

This study was funded by the project PID2020-114024GB-C31 (*Alteration of carbon sinks and sources in shrinking inland waters – Alter-C*) funded by MCIN/AEI /10.13039/501100011033/. Additional support was provided by Agència de Gestió d'Ajuts Universitaris i de Recerca (AGAUR), and Institut de Recerca de l'Aigua (IdRA). DvS is a Serra Húnter Fellow.



Chapter 6

6. General discussion

Dam ageing is an emerging global problem for water management because of tens of thousands of existing old dams (Perera et al., 2021). Old dams incur high maintenance costs for repair and maintenance and threaten public safety (Perera & North, 2021; Perera et al., 2021). For instance, the repair of a small dam in the US called the Gray Reservoir would cost 1.5 million USD, but its removal cost 0.3 million USD (Grabowski et al., 2018). The maintenance of all old dams in the US would cost 105–300 billion USD, while their removal would cost 10.5 billion USD by 2050 (Habel et al., 2020). Furthermore, old dams are less effective than young dams in serving their primary purposes, and their failure results in substantial financial losses and harmful environmental effects (Perera et al., 2021). Dam failures are expected to become more frequent in the future because of climate change, which is expected to increase the frequency and intensity of flooding (Arnell & Lloyd-Hughes, 2014). By embracing proactive measures such as DD as part of a comprehensive strategy, challenges posed by old dams can be addressed, public safety enhanced, and the sustainable management of water resources promoted (Fig.6.1).

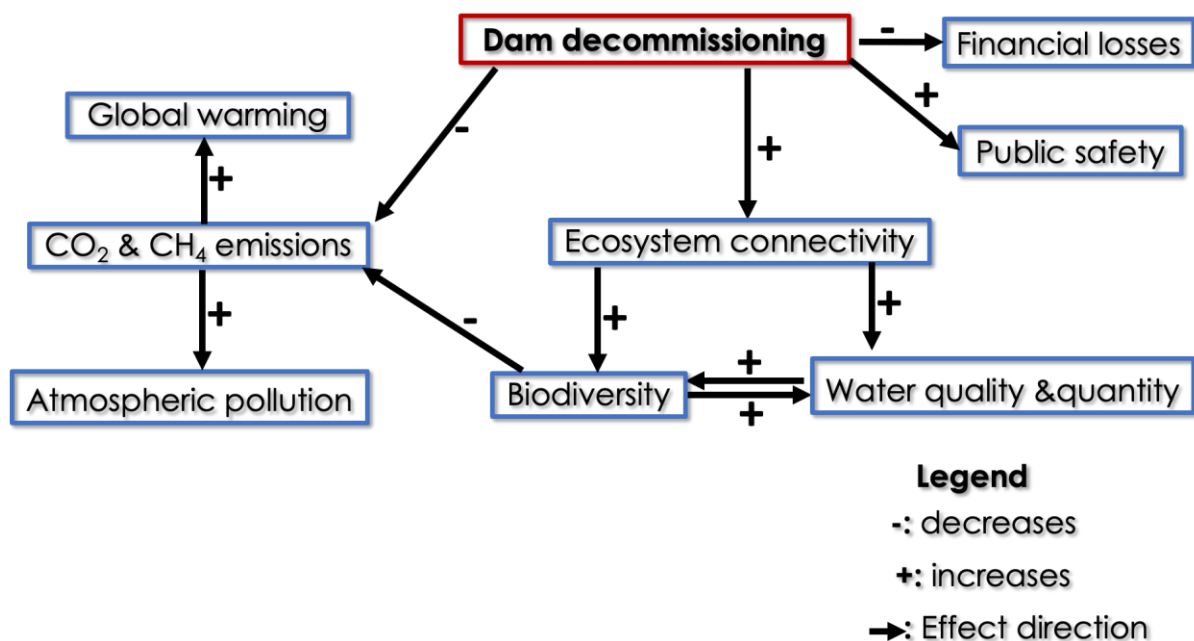


Figure 6.1 Schematic presentation of the background on which the hypothesis of this study was built

6.1. Dam decommissioning: mitigation of C emissions from reservoirs

The drawdown phase of the Enobieta Reservoir decreased CH₄ emissions by replacing impounded water with exposed sediments and lotic water, while terrestrialization reduced CO₂ emissions from exposed sediments. The decrease in CH₄ emissions from reservoirs may be relevant because reservoirs contribute ~5% of the global anthropogenic

CH₄ emissions (Soued et al., 2022). Methane emissions correspond to 69–79% of global CO₂-eq emissions from water surfaces of reservoirs (Deemer et al., 2016; Harrison et al., 2017; Soued et al., 2022), due to its higher GWP than CO₂ (IPCC, 2013). In the Enobieta Reservoir, CH₄ emissions constituted 100% of the CO₂-eq emissions prior to reservoir drawdown, when the reservoir acted as a CO₂ sink (Fig.6.2). However, CH₄ emissions contributed on average only 1% of the CO₂-eq emissions during, and after reservoir drawdown. This is because areal CH₄ fluxes from exposed sediments were lower than areal CH₄ fluxes from impounded water. Impounded water and exposed sediments were, in terms of area, the most important environments in the reservoir. Thus, the replacement of impounded water with exposed sediments through DD presents a promising policy option to effectively reduce CH₄ emissions from reservoirs. This finding emphasizes the potential benefits of DD in mitigating GHG emissions and highlights the importance of considering such a measure in reservoir management.

Methane emissions from exposed sediments in the Enobieta Reservoir (range: 0.01–0.41 mmol CH₄ m⁻² d⁻¹) were, however, not equal to zero as was assumed by Keller et al. (2020) who estimated the role of drawdown areas in the global C budget of reservoirs. Our findings align with the findings of a recent global study that highlighted the relevance of CH₄ emissions from exposed sediments (Paranaíba et al., 2021). While dry exposed sediments are not conducive to methanogenesis because they have a deep oxic layer, CH₄ can be produced in anoxic microhabitats that persist in humid exposed sediments (Serrano-Silva et al., 2014). Humid exposed sediments emit, thus, higher areal CH₄ fluxes than dry exposed sediments (Paranaíba et al., 2021). The high humidity in the Artikutza Valley could have sustained the low but measurable CH₄ emissions from exposed sediments in the Enobieta Reservoir. Furthermore, CH₄ emissions from exposed sediments of inland waters increase with the content and reactivity of sediment OM (Dalal et al., 2008; Serrano-Silva et al., 2014). The high content and reactivity of sediment OM reported in the fourth chapter of this thesis could have contributed to CH₄ emissions from exposed sediments in the Enobieta Reservoir. It can be speculated that exposing sediments to air may be more effective in reducing CH₄ emissions from reservoirs characterized by low content and refractory sediment OM, especially, in xeric environments than a humid ecosystem containing large stocks of highly bioreactive OM like the Enobieta Reservoir. Further investigations are warranted to assess the reactivity of sediment OM in anaerobic conditions, which sustain CH₄ emissions, as we tested it in aerobic conditions in the Enobieta Reservoir.

The findings of this study suggest that proper management of water depth in reservoirs can reduce their C footprint. Water drawdown, a characteristic feature of reservoirs distinguishing them from natural lakes, is driven by natural hydrological dynamics and human activities related to water management (Thornton et al., 1990). Our results show that reservoir drawdown, which creates shallow water, may have a stronger effect on CH₄ than CO₂ emissions, probably, due to reduced CH₄ oxidation in shallow water (McGinnis et al., 2006). For instance, areal CO₂ emissions from deep impounded water in this study were, 14.33 mmol CO₂ m⁻² d⁻¹, approximately three times lower than areal CO₂

emissions from shallow impounded water, $39.37 \text{ mmol CO}_2 \text{ m}^{-2} \text{ d}^{-1}$ (Fig.6.2a). On the other hand, areal CH_4 emissions from deep areas of impounded water were, $0.16 \text{ mmol CH}_4 \text{ m}^{-2} \text{ d}^{-1}$, approximately five times lower than areal CH_4 emissions from shallow impounded water, $0.78 \text{ mmol CH}_4 \text{ m}^{-2} \text{ d}^{-1}$ (Fig.6.2b). Thus, carefully managing water level (such as avoiding reservoir drawdown during the dry period) can reduce C emissions, particularly in the form of CH_4 , from reservoirs. For instance, deferring reservoir drawdown from the end of the stratified time to a period when reservoir water is well mixed could reduce CH_4 emissions by enhancing CH_4 oxidation at the water-sediment interface and in the water column (Harrison et al., 2017). This assumption requires more empirical evidence because it can have a significant effect on the C footprint of reservoirs, mainly in relation to hydroelectricity that is promoted as a clean source of energy by the Paris Agreement (Hermoso, 2017). Continued research and careful management practices are necessary to mitigate C emissions associated with reservoirs and ensure alignment with sustainable energy policies.

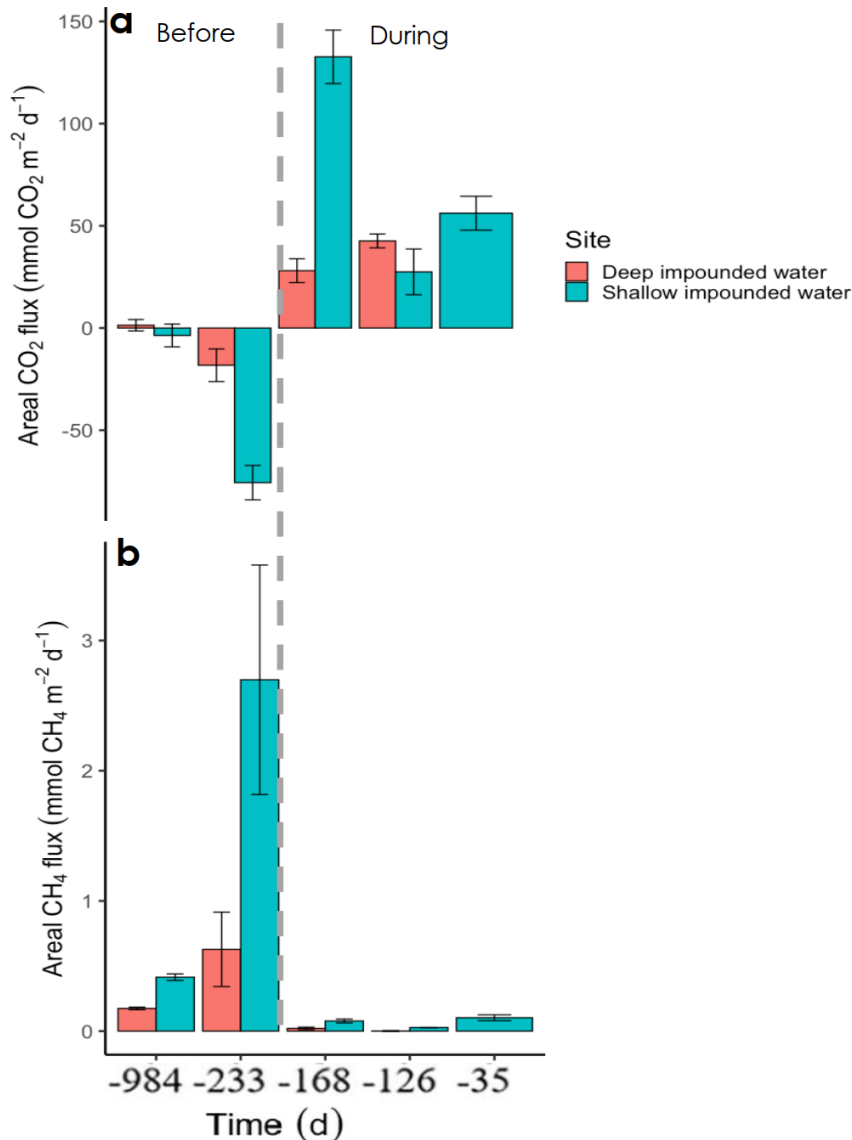
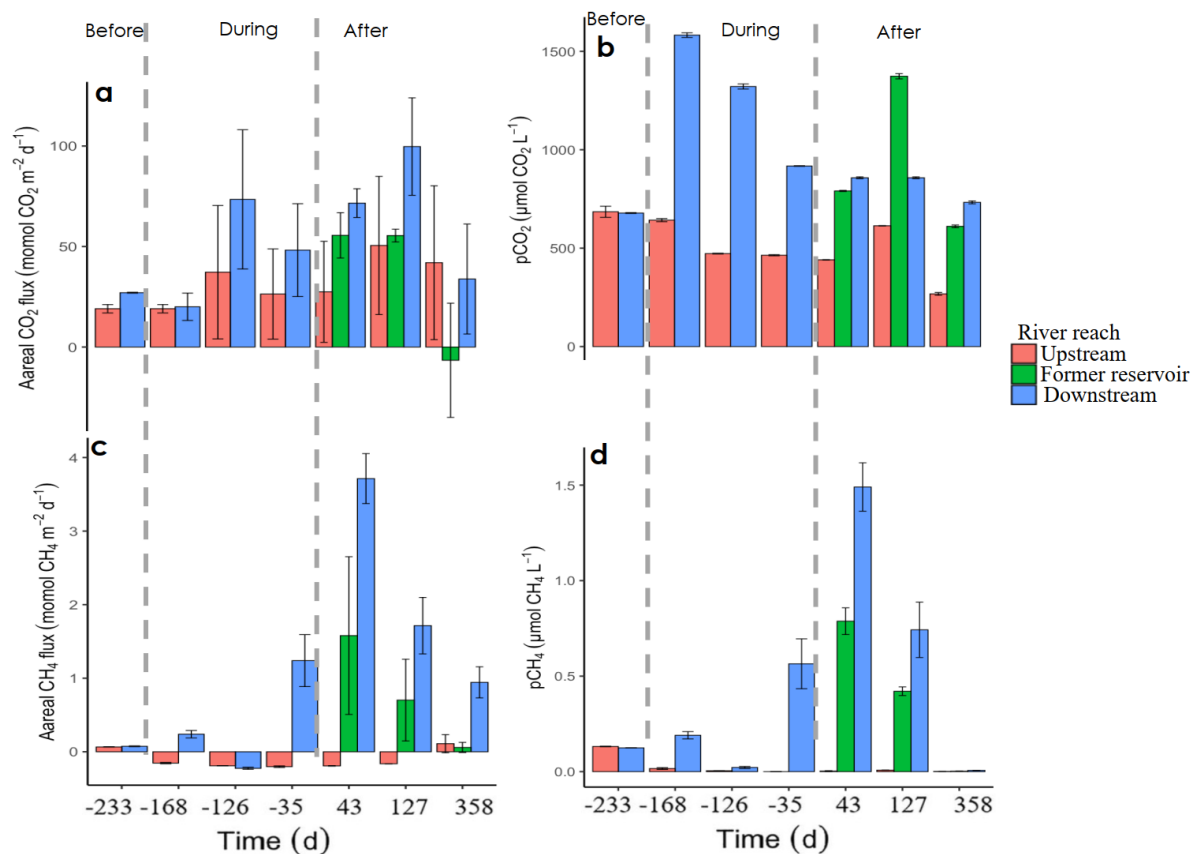


Figure 6.2 Areal CO₂ (a) and CH₄ (b) fluxes in deep and shallow impounded water before and during reservoir drawdown. The error bars represent standard error (SE). The x-axis describes the 5 sampling campaigns, which are divided into 2 categories: Before (days -984 and -233) and During (days -168, -126, and -35) reservoir drawdown

It is important to acknowledge, however, that maintaining high-water depths in reservoirs may not always be feasible or compatible with the various demands for water supply, including industrial and domestic use, hydroelectricity, and irrigation (Keller et al., 2021). To balance these competing needs, there is a need for a close collaboration among civil engineers, decision-makers, policymakers, scientists, and water managers to ensure that dams are built and operate in an environmentally friendly manner. In addition to collaborative efforts, public awareness and providing education about environmental impacts of reservoirs and the importance of sustainable water management can be critical in reducing water abstraction from reservoirs (Damerell et al., 2013; Nourredine et al., 2023; Sarkar et al., 2007). By promoting water conservation, responsible usage practices, and the adoption of sustainable approaches at the individual and community levels,

education campaigns can play a pivotal role in reducing excessive water abstraction from reservoirs. Fostering a sense of environmental responsibility and empowering individuals to make informed choices regarding water usage can contribute to long-term sustainability of reservoirs and their associated ecosystems.

Reservoir drawdown can be a short-term hot moment of CO₂ and CH₄ emissions in the river reach downstream of the reservoir due to, probably, the mobilization of large amounts of sediment OM and CO₂ and CH₄ from the reservoir. The drawdown of the Enobieta Reservoir increased CO₂ and CH₄ fluxes downstream of the reservoir, especially CH₄ emissions, that increased 17 times (0.07 before, to 1.30 mmol CH₄ m⁻² d⁻¹ during and after drawdown; Fig.6.3a, c). The high content and reactivity of the sediment OM stored in sediments of the Enobieta Reservoir can be the origin of the high areal CO₂ and CH₄ fluxes in the river reach downstream of the reservoir during the drawdown. The emissions downstream of the reservoir could have been the result of CO₂ and CH₄ produced in the reservoir or in the river reach itself, because *p*CO₂ and *p*CH₄ in the river reach downstream were comparable to those upstream before, but higher during drawdown (Fig.6.3b, d). Since the Enobieta Reservoir was sometimes stratified, opening the low gate could have released hypolimnetic water with high concentrations of CO₂ and CH₄ during drawdown. These CO₂ and CH₄ contained in water from the reservoir could have contributed to the higher *p*CO₂ and *p*CH₄ downstream than upstream. Furthermore, despite the large SE for CO₂ fluxes, C fluxes, mainly CH₄, tended to be higher downstream than upstream, which was a sink to atmospheric CH₄. Since *p*CO₂ and *p*CH₄ were higher downstream than in the former reservoir reach after drawdown, it can be inferred that the production of CO₂ and CH₄ in the former reservoir and in the river reach downstream contributed to their emissions in that reach. However, the prompt decline in *p*CH₄ and CH₄ emissions in the river reach downstream after drawdown, while, for instance, CO₂ emissions increased ~127 days after drawdown, may mean that most CH₄ emitted in the river reach downstream was produced in the reservoir while there was a significant contribution of CO₂ production to its emissions in this river reach. This discussion highlights the dynamic nature of CO₂ and CH₄ emissions during reservoir drawdown and underscores the complex interplay between the reservoir, sediment OM, and the river reach downstream of the reservoir. It is essential to consider these factors when assessing the environmental implication of reservoir drawdown and to develop management strategies that minimize downstream impacts of C emissions while ensuring the sustainable operation of reservoirs.



Figure

6.3 Areal flux (a) and water partial pressure (b) of CO₂ and areal flux (c) and water partial pressure (d) of CH₄ in the river reach upstream, river reach flowing through the former reservoir, and downstream of the reservoir before, during, and after reservoir drawdown. The x-axis describes the 7 campaigns when we sampled lotic water, which are divided into 3 categories: Before (day -233), During (days -168, -126, and -35), and After (days 43, 127, and 358) reservoir drawdown. The error bars represent standard error (SE). There was no river reach crossing the reservoir before and during reservoir drawdown

Interestingly, CO₂ and CH₄ emissions started to decrease at the last sampling date, ~300 days after drawdown, but did not reach the pre-drawdown levels. One year after drawdown, CO₂ and CH₄ emissions in the river reach downstream of the reservoir were still higher than the pre-drawdown levels, which may be due to the legacy of reservoir drawdown. Studies other than this short-term study should test the time it takes for CO₂ and CH₄ emissions in the river reach downstream after drawdown recover to before and during impoundment levels. As we measured CO₂ and CH₄ fluxes downstream close to the dam, it would be also interesting to know how these fluxes vary longitudinally further downstream. Such a study can complement a recently completed PhD study that addressed longitudinal responses to DD of the Enobietta Reservoir on other functional descriptors in the river reach downstream of the reservoir (Atristain, 2023). Furthermore, downstream emissions of CO₂ and CH₄ produced in reservoirs can exacerbate the increasing contribution of the degassing pathway to C emissions from reservoirs (Soued et al., 2022). However, downstream degassing remains among the least understood pathways of CO₂ and CH₄

emissions in reservoirs (Soued et al., 2022). It should be compulsory to address how reservoir drawdown during DD affects CO₂ and CH₄ emissions through degassing at the dam outlet. By addressing these research gaps and expanding research efforts on downstream emissions and degassing, we can gain a more comprehensive understanding of the environmental implications of reservoirs and develop effective strategies for managing C emissions due to reservoir drawdown. Such studies are essential for informing sustainable reservoir management practices and ensuring long-term environmental integrity of these crucial water management structures.

The export of fine sediments, which are more susceptible to erosion (Grabowski et al., 2011; Warrick et al., 2012), can increase CO₂ and CH₄ emissions in the river reach downstream of the reservoir because they provide habitat for microbial populations and sorb large stocks of OM (Coyne et al., 1997). However, sediment export and the influence of the reservoir on C emissions in the river reach downstream of the reservoir may be a short-term effect of DD due to the quick ecosystem terrestrialization (Atristain et al., 2022; Bellmore et al., 2019; Duda & Bellmore, 2022). Terrestrialization of exposed sediment can reduce erosion by stabilizing sediments. Sediment stability and, thus, reduced erosion may be the reason CO₂ and CH₄ emissions downstream of the reservoir began to decrease in the last sampling campaign. This may be true because the content and reactivity of sediment OM, discussed in the fourth chapter of this study, did not decrease with sediment exposure time. However, the low temperature reported in the fourth chapter of this study recorded in the last two sampling campaigns may partially explain the sharp decrease in CH₄ emissions in the river reach downstream between days 127 and 358 after reservoir drawdown. Yet, it is not clear why CO₂ emissions remained high ~127 days after drawdown, which may be partly explained by the legacy effect of increased turbidity and reduced biofilm gross primary productivity reported in the river reach downstream of the Enobieta Reservoir during its drawdown (Atristain et al., 2022). To gain a more comprehensive understanding of the temporal evolution of CO₂ and CH₄ emissions in the river reach downstream of the reservoir after reservoir drawdown, further research is needed. It is crucial to establish connections between temporal changes in C emissions from the river reach downstream of the reservoir after drawdown with processes such as terrestrialization and sediment stability. Future studies should consider existing knowledge on temporal patterns of sediment erosion after drawdown (Bellmore et al., 2019; Duda & Bellmore, 2022), which can serve as a guide for exploring the dynamics of C cycling in the river reach downstream of the reservoir after drawdown. By delving into these temporal dynamics, we can enhance our understanding of the factors driving C emissions and develop more informed strategies for managing reservoir drawdown and its impacts on downstream ecosystems.

The temporal extent of the high areal CO₂ fluxes may be shortened by terrestrialization. Areal CO₂ fluxes from exposed sediments were an order of magnitude higher than areal CO₂ fluxes from impounded water of the Enobieta Reservoir. This finding is consistent with the findings of previous studies that reported exposed sediments of inland waters to emit more CO₂ than the same systems in their inundated phase (Gómez-Gener et

al., 2015; Kosten et al., 2018; Obrador et al., 2018). However, studies on CO₂ emissions from exposed sediments did not include CO₂ fluxes in sediments covered by vegetation (Keller et al., 2020) or vegetation biomass in their estimates (Catalán et al., 2014; Obrador et al., 2018). The inclusion of the C sink in vegetation biomass in this study showed that vegetation growth can partially overturn CO₂ emissions from exposed sediments (chapter 5). Considering the temporal evolution of terrestrialization in the Enobieta Reservoir (Fig.6.4), the reservoir may already be a net sink of atmospheric CO₂. The increase in NDVI from 0.35 in July 2019 when we sampled vegetation biomass to 0.77 in January 2022 indicates a rapid terrestrialization of the Enobieta Reservoir. Pictures taken in 2023 showed that some perennial trees are replacing annual herbaceous trees (Fig.6.4b), which will increase C sink in the vegetation biomass in the reservoir (Albrecht & Kandji, 2003; Jansson et al., 2010). Regions with humid climates, such as the Artikuza Valley, exhibit typical succession towards a woodland, which takes 20–25 years for most disturbed ecosystems in Central Europe (Prach, 2003; Prach et al., 2014). Thus, it is reasonable to expect continued vegetation growth and increased C sink in the Enobieta Reservoir as it undergoes further terrestrialization. Understanding the dynamics of terrestrialization and its impact on C cycling in reservoirs is crucial for assessing their potential as C sinks and for informing management strategies. Continued research in this area will enhance our knowledge of the role of reservoirs in the global C cycle and the contribution of their terrestrialization to mitigating climate change.

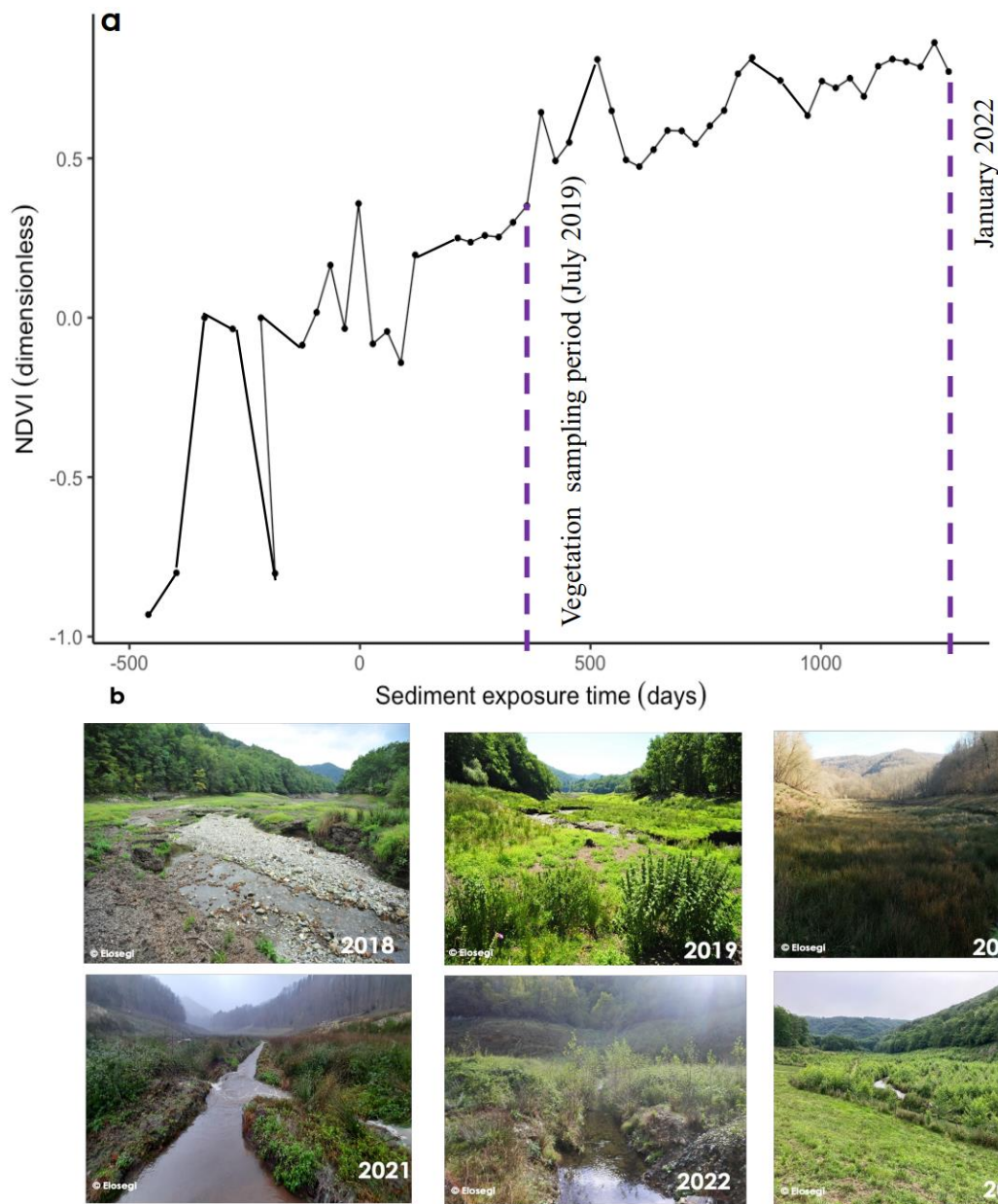


Figure 6.4 Normalized Difference Vegetation Index (NDVI), a proxy of vegetation biomass (a) and pictures (b) showing the temporal evolution of terrestrialization of the exposed sediment in the Enobieta Reservoir. The x-axis in (a) shows time before (below zero days) and after (above zero days) complete reservoir drawdown. The graph shows NDVI data spanning between 2018 and 2022, but, as shown by the first vertical dashed line our sampling period for the fifth chapter was in July 2019, while the second vertical dashed line shows the value of NDVI in January 2022, the last date we could find good satellite images

6.2. Counteracting reservoir sedimentation: a move to relatively sustainable reservoirs

The high sedimentation rate increases the rate of dam ageing, C burial efficiency, and CH₄ emissions in reservoirs (Perera et al., 2021; Sobek et al., 2009, 2012). Sediments

of inland waters contain high contents of OM, nutrients, and microbial biomass and diversity, and are, thus, hotspots of biogeochemical activities (Cornett & Rigler, 1987; del Giorgio & Williams, 2005; Kuznetsov, 1958). These intense biogeochemical activities drive the high areal CH₄ emissions from the water surfaces and CO₂ emissions from exposed sediments of reservoirs (Deemer et al., 2016; Keller et al., 2020; Soued et al., 2022). Additionally, sedimentation restricts the effectiveness and life of reservoirs and leads to reduced sediment transport downstream (Bednarek, 2001; Perera et al., 2021).

Sediment management can be implemented at the catchment and reservoir levels prior to dam construction, during the operational phase of dams, and during and after DD using four strategies: (1) reducing the amount of sediment entering reservoirs from the upstream catchment, (2) routing sediment through or around reservoirs, and (3) removing sediments accumulated in reservoirs. Sediments can be intercepted before they reach the reservoir and used to increase soil fertility using sediment basins, ponds, check dams, and sediment warping (Kondolf et al., 2014; Mekonnen et al., 2015; Verstraeten & Poesen, 2001). Sediment routing through (by building off-channel reservoir storage) or around (by using a sediment bypass) and drawdown routing or sluicing can prevent reservoir sedimentation and sediment starvation downstream (Espa et al., 2019; Kondolf et al., 2014). Catchment management, such as erosion control through sustainable land use and soil conservation, can minimize sediment loads in reservoirs (Anderson et al., 2014; Anderson et al., 2013; Smith & Muirhead, 2023).

Techniques such as sediment dredging or removal from the reservoir bed using scrapers, dump trucks, and suction with hydraulic pumps can be applied to remove deposited sediments (De Vincenzo et al., 2018; Kantoush et al., 2021; Kondolf et al., 2014). Sediments removed from reservoirs or sediment traps can be used for land reclamation or restoration, construction, or food production, if they are not contaminated (Kantoush et al., 2021). Mechanical sediment removal may be implemented after reservoir drawdown during DD, but it can also be best adapted to reservoirs that are dry for some parts of the year, such as flood control reservoirs (Kondolf et al., 2014). Proper sediment management during and after the drawdown phase of DD can reduce the effects of DD on water quality, turbidity, ecosystem heterogeneity, organisms and their food sources, and the geomorphology of the river due to erosion of riverbanks and river braiding due to sediment deposition in the riverbed (Habel et al., 2020; Ritchie et al., 2018; Wik, 1995). The release of nutrients and contaminants associated with exported sediments can also cause several harmful effects downstream of the reservoir (Gold et al., 2016). Various strategies, such as gradual drawdown, building structures that trap sediments in reservoirs, such as silt fences, sediment basins, and sediment ponds at strategic sites in reservoirs, can be implemented to limit sediment export downstream during and after DD. For instance, gradual drawdown led to the retention of 92% of sediments in the Enobieta Reservoir (Atristain et al., 2022; Larrañaga et al., 2019). Another restoration policy that should be implemented to limit sedimentation erosion after the drawdown phase of DD is terrestrialization.

6.3. Terrestrialization: a potential positive long-term effect of DD

We observed rapid terrestrialization of exposed sediments after the drawdown phase of the Enobieta Reservoir. The rapid terrestrialization of the Enobieta Reservoir, mainly in its stable (flat) environments, may be due to high humidity in this region, a well-protected surrounding forest, and low human activities and herbivory (Orr & Stanley, 2006; Shafroth et al., 2002). Yet, we realized that terrestrialization of steep environments in the Enobieta Reservoir was slow. Slow terrestrialization in steep environments of the Enobieta Reservoir can be caused by a low content of sediments (mainly fine-sized sediments), seedbanks, sediment moisture, OM, and nutrients due to erosion. These vegetation-free spaces can be suitable for invasion by alien species and sediment erosion. The invasion of exotic species and sediment erosion can be a threat, respectively, to native biodiversity and water quality. Thus, assisted vegetation regeneration by the addition of soil, nutrients, and propagules can support ecosystem restoration and alleviate the threat of alien species and sediment erosion to water quality. Other bioengineering techniques, such as contour wattling and mulching, can be implemented to reduce sediment erosion from areas more susceptible to erosion (Singh, 2010). It is necessary to identify factors of terrestrialization of exposed sediments to inform the restoration of inland waters fragmented by reservoirs.

Terrestrialization and ecosystem connectivity after DD can result in several benefits for people and the environment, including increased biodiversity, water quality, value of adjacent property, and C sequestration in vegetation biomass (Allen et al., 2016; Lovett, 2014; Orr & Stanley, 2006). The composition and biodiversity of plant species in the former reservoir can be expected to change from early successional to late successional plant species and increase, respectively, over time after DD (Orr & Stanley, 2006). These plant species can provide habitat for many animal species and spawning grounds for aquatic and terrestrial organisms. When a dam is removed, the riparian areas can be frequently flooded, which can improve the growth of riparian vegetation and the formation of wetlands, which are habitats for a wide array of organisms and C sinks (Bednarek, 2001; Mitsch et al., 2013; Smith & Muirhead, 2023). Additionally, small, temporary pools and backwater areas, used as nurseries and spawning grounds by some organisms, may return due to the resumption of natural water flow (Bednarek, 2001). Dam decommissioning can also benefit terrestrial species, including large carnivores, that require abundant riparian vegetation. Furthermore, terrestrialization and the resumption of natural flow can improve water quality through increased sediment stabilization, heat dissipation, and O₂ availability due to increased water turbulence in lotic ecosystems (Randle et al., 2015; Warrick et al., 2019; Wilcox et al., 2014).

Dam removal can increase biodiversity in unfettered rivers by increasing ecosystem connectivity and heterogeneity (Bednarek, 2001; Bellmore et al., 2019; Duda & Bellmore, 2022). Longitudinal connectivity of the fluvial network restores spatial and temporal variations in frequency, magnitude, duration, and regularity of water flow, creating an environment favorable for high biodiversity (Bednarek, 2001). For instance, river connectivity can enhance the return of species of commercial interest, such as anadromous

fishes moving to or from their reproduction sites in the upper reach of the river. Sediment export can also increase the integrity of estuaries (which are nurseries for fish and shrimp) and food production in river floodplains and deltas. Ecosystem heterogeneity of the fluvial system is achieved through the reappearance of riffle/pool sequences, boulders, cobbles, and gravels that provide a habitat for a range of macroinvertebrates and periphyton (Bednarek, 2001). However, long-term studies on ecosystem changes in biological, chemical, and physical conditions of rivers and riparian ecosystems and the final impact on river restoration are limited (Bellmore et al., 2017; Habel et al., 2020). Long-term, multidisciplinary studies with robust study designs must be conducted to inform the decision-making phase of DD and understand the resistance and resilience of inland water ecosystems.

Vegetation growth, as a long-term effect of DD, may be expected to reduce C emissions in exposed sediments and downstream and increase C sequestration in the former reservoir. Vegetation regrowth may increase areal CO₂ emissions from exposed sediments through autotrophic respiration, OM subsidies for microorganisms, changes in sediment moisture, texture, redox potentials, and porosity (Cable et al., 2008; Luo & Zhou, 2010; Van Andel et al., 1993). However, like soil, sediment respiration can be counteracted through primary production by overlying vegetation, which may result in a net ecosystem autotrophy (Bond-Lamberty & Thomson, 2010, 2012). Vegetation restoration is of chief importance to mitigate climate change because 90% of total C stock in terrestrial systems, i.e., 3,170 Pg C, is stored in forests (Cable et al., 2008). Furthermore, 99.9% of the C sink in the world's biota is contributed by vegetation and microorganisms (Cable et al., 2008). However, the size of this C sink in disturbed ecosystems can depend on the turnover rate of annual, herbaceous plant species to a vegetation community dominated by perennial, woody plant species (Albrecht & Kandji, 2003; Jansson et al., 2010).

The uptake rate of atmospheric CO₂ and the final vegetation structure of vegetation succession in a reservoir may depend on many factors, including the level of disturbance, human activities, the content of sediment OM and nutrients, sediment stability, adjacent environments, the size of seedbanks, interactions between plant individuals and/or species, and sediment humidity (Orr & Stanley, 2006; Prach, 2003; Prach et al., 2014; Van Andel et al., 1993). In humid regions, the vegetation community tends to evolve from an early vegetation community dominated by herbaceous plants to a later plant community composed of predominantly woody plants (Orr & Stanley, 2006). In Central Europe, disturbed ecosystems need 20–25 years to recover to woodland ecosystems (Prach, 2003; Prach et al., 2014) and temperate woodlands take 50–160 years to mature (Broughton et al., 2021; Fuentes-Montemayor et al., 2022). The Artikutza Valley is highly humid and mainly covered by mature forests dominated by beech (*Fagus sylvatica* L.) and oak (*Quercus robur* L.) stands and dense autochthonous riparian vegetation with alder (*Alnus glutinosa* (L.) Gaertner) and ash (*Fraxinus excelsior* L.) (Lozano & Latasa, 2019) and the valley is strictly preserved. In addition, the reservoir sediments are rich in OM. Thus, we can predict that exposed sediments will be easily replaced by woodland in the Enobieta Reservoir. This transition will alter C cycling in the river network by sequestering atmospheric CO₂ in the

above- and belowground vegetation biomass and soil OM but also by reducing the export of sediment C downstream.

Terrestrialization can mitigate sediment erosion by (1) shielding soil against direct raindrops by intercepting and dispersing raindrops and minimizing their erosive force for soil splash due to the presence of the plant canopy and litter, (2) minimizing the velocity of surface runoff through increased surface roughness, (3) increasing water infiltration due to the presence of roots, plant residue, and high biological processes, (4) enhancing transpiration of soil water through changes in soil structure and the need for plants to grow, and (5) increasing the cohesion of soil particles and by acting as mechanical barriers against soil, water, and wind movement (Pimentel et al., 1995; Woo et al., 1997; Yang et al., 2023). Thus, we expect that the long-term effect of DD of the Enobieta Reservoir will be the colonization of exposed sediments by a woodland ecosystem, which will enhance C sequestration in vegetation biomass and soil OM and reduce CO₂ and CH₄ emissions in the river reach downstream by acting as a shield against erosion.

6.4. Study limitations and future research agenda

Emissions of CO₂ and CH₄ from the water surface of deep impounded water in the Enobieta Reservoir were lower than in shallow impounded water. The increase in areal CH₄ emissions from shallow waters is counterintuitive because they should have contrasting effects on CH₄ emissions. On the one hand, shallow waters should increase CH₄ production and emissions by increasing sediment temperature and reducing hydrostatic pressure and residence time of CH₄ in the reservoir. On the other hand, the formation of shallow water should increase CH₄ oxidation by potentially increasing the concentration of dissolved O₂ in the water column. However, this and other studies have reported CH₄ emissions to increase at shallow water depth in reservoirs and other aquatic systems (Harrison et al., 2017; McGinnis et al., 2006). We did not assess the effects of reservoir drawdown on biological, chemical, and physical properties that led to high CH₄ emissions from shallow water. Mechanisms driving high C emissions deserve special attention because water drawdown periods in inland waters are expected to increase (Jaeger et al., 2014; Pekel et al., 2016; Wang et al., 2018). Future studies should, for instance, constrain the mechanisms by which drawdowns short-circuit connections between CH₄ production and oxidation to increase CH₄ emissions from shallow inland waters.

The drawdown phase increased CO₂ and CH₄ emissions in the river reach located downstream of the Enobieta Reservoir (Fig.6.3). Future studies should explore whether these GHGs are produced in the reservoir or in the river reach itself. These emissions probably resulted from CO₂ and CH₄ produced in exposed or inundated sediments of the reservoir or groundwater because reservoir drawdown reduced the decomposition of OM downstream of the Enobieta Reservoir (Atristain et al., 2022). The export of CO₂ and CH₄ from the reservoir during drawdown could have increased their degassing at the dam outlet. Future studies should constrain C degassing downstream of reservoirs, especially due to

DD, because it is becoming an important but least understood C emission pathway in reservoirs (Soued et al., 2022). Many studies addressed the effects of sediment export, but they did not assess how sediment erosion affects C cycling in the river reach downstream of removed reservoirs (Duda & Bellmore, 2022; Ritchie et al., 2018; Wilcox et al., 2014). We suggest that downstream emissions will decrease over time, but we do not have much data to test our hypothesis. Long-term studies should quantify C that is exported downstream from reservoirs due to DD and explore the temporal evolution of this C export and how it is affected by terrestrialization of exposed sediments, to have an integrative assessment of the effect of DD on C emissions. Also, as reservoir drawdown may affect local water table, it should be interesting to know the contribution of groundwater to CO₂ and CH₄ emissions following DD.

The study of C emissions following DD is a recent topic in the C biogeochemistry of inland waters. This is the first empirical study assessing the role of DD on C cycling in reservoirs, which contrasts with the abundance of data on C emissions from water surfaces of reservoirs during their operational stage (Deemer et al., 2016; Maavara et al., 2017; Soued et al., 2022). Thus, data collection on C emissions during and after DD should be a research priority for the next few years. Studies on the effects of DD on C cycling in reservoirs are particularly recommended in the temperate region, which is the current hotspot of DD (Perera et al., 2021). The findings of such research in the temperate region could guide DD in low-latitude regions, which will need specific attention in a few decades because they are hotspots of the current dam construction (Zarfl et al., 2015) and C burial (Mendonça et al., 2017).

We did not constrain drivers of CO₂ emissions from exposed sediments after DD, which should be addressed by future studies. Drivers of CO₂ emissions from exposed sediments are important to predict CO₂ fluxes in different ecosystems (Keller et al., 2020). Recent global studies did not show differences in CO₂ and CH₄ emissions from dry inland waters between climate zones, but local characteristics of exposed sediments (e.g., sediment moisture, OM, and temperature) explained substantial variability in CO₂ and CH₄ emissions between locations (Keller et al., 2020; Paranaíba et al., 2021). Thus, an important research area should be to identify drivers of CO₂ emissions from exposed sediments after DD. More studies on CO₂ emissions and their drivers in individual reservoirs are required to acquire data that will be needed to upscale CO₂ emissions after DD to regional and global scales. It should be also important to understand the effects of sediment exposure on the composition and activity of microbial communities involved in C cycling after DD. Furthermore, we assumed CO₂ emissions from exposed sediments to result from the respiration of the large stock of bioreactive OM, but we did not address the potential role of other sources (e.g., groundwater) or biogeochemical processes beyond aerobic microbial respiration. An important knowledge gap is to examine the origin of the emitted CO₂ and whether this origin changes with DD.

We did not find a clear spatial trend in CO₂ and CH₄ emissions from exposed sediments after reservoir drawdown. However, future studies should test the spatial variability in C emissions from exposed sediments after DD. Spatial heterogeneity of C

emissions from exposed sediments is required because drivers of CO₂ emissions in dry inland waters, such as the content and composition of OM, sediment texture, and sediment moisture, are different between the three zones of reservoirs (Thornton et al., 1990). Eutrophic reservoirs may exhibit higher spatial variability than oligotrophic reservoirs in C emissions from exposed sediments due to DD because stocks of buried autochthonous OM may be higher in transition and lacustrine zones, while sediments in the tail water zone may contain larger stocks of allochthonous OM (Thornton et al., 1990). Furthermore, spatial heterogeneity in C emissions from exposed sediments may depend on the length and shape of reservoirs, with longer reservoirs potentially exhibiting greater differences between the three zones of reservoirs.

We did not explore long-term effects of reservoir drawdown on C emissions from exposed sediments. Exposed sediments in this study emitted higher areal CO₂ in summer than in other seasons, which may reflect seasonal variability in temperature and sediment moisture. Thus, a wider temporal coverage is required to constrain uncertainties that may be produced by the seasonal and long-term dynamics of CO₂ emissions after DD. Those temporal resolutions should link CO₂ emissions from exposed sediments with the presumed consumptive loss of sediment OM (Keller et al., 2020). Furthermore, CO₂ emissions from exposed sediments in this study can be conservative because we did not purposely incorporate CO₂ fluxes upon sediment rewetting. Rewetting events are short periods of biogeochemical hot moments (Kosten et al., 2018; Schimel, 2018; von Schiller et al., 2019). The effect of rewetting on C cycling is well documented in soil, but more effort is needed in dry inland waters (Gallo et al., 2014; Muñoz et al., 2018). For instance, empirical evidence on mechanisms that drive pulses of CO₂ fluxes in exposed sediments should be a research priority for future studies. A comprehensive understanding of the balance between the biological and physicochemical mechanisms driving the pulses of CO₂ emissions after the rewetting of the dry sediments of inland waters deserves more research attention (Schimel, 2018).

Since relying on data collected by individual research teams can require many years to obtain robust regional and global C emission data, there is a need to establish global collaborative sampling teams. The collaborative approach can allow for a more efficient and coordinated effort in data collection, enabling the generation of robust regional and global C emission datasets in a shorter timeframe. These studies should also estimate the global area of removed dams that can be used to upscale C emissions from dam removal to a global scale. Recent advances in remote sensing (Pekel et al., 2016) may help to estimate the area of removed reservoirs. Furthermore, to improve the understanding of the effects of DD on C cycling in reservoirs, there is a need to know the amount of C in reservoir sediments (which can be known from the volume of sediments and %C in reservoir sediments), the proportion that is decomposed during sediment exposure, the proportion of sediment C exported and emitted downstream, and the proportion of sediment C that remains buried in reservoir sediments. For instance, a recent global study showed that reservoir sediments become net C sources by considering areas covered by exposed sediments (Keller et al., 2021).

We could have overestimated the content of sediment OM in the Enobieta Reservoir (fourth chapter) by collecting sediment samples in the section close to the tail. The content of allochthonous OM in reservoirs decreases exponentially from the tail towards the dam (Thornton et al., 1990). By collecting sediments close to the tail of the reservoir, where the burial of allochthonous OM peaks, we could have reported a higher content of sediment OM. The compromise in spatial resolution happened because sediments at sites far from the tail were exposed later along reservoir drawdown, while the focus was on capturing the temporal pattern of the content and reactivity of sediment OM. Future studies should explore how the content of sediment OM and C emissions changes spatially from the riverine zone to the lacustrine zone.

Because we conducted just one sampling campaign in the fifth chapter, we could not investigate successional or temporal patterns of plant species colonizing exposed sediments. It would be interesting to understand temporal changes in species composition of plants from early successional to late successional species. It would also be critical to assess the effect of terrestrialization on sediment conditions, such as sediment moisture, the content of OM and nutrients, which can affect C cycling and set the trajectory of terrestrialization. Understanding factors that drive terrestrialization can also inform assisted recolonization where conditions are not suitable for natural terrestrialization. The findings of these studies will inform ecological restoration projects, increase the understanding of succession dynamics, and shed light onto the recovery and resilience of inland water ecosystems after disturbances. Additionally, long-term data are needed to understand changes, patterns, and trends of long timespans in biodiversity and ecological processes. They are crucial to know complex systems and support policy and decision-making for effective management strategies.



Chapter 7

7. General conclusions

This thesis is the first study to study the effects of DD on C cycling in reservoirs. We addressed this topic in the Enobieta Reservoir, a temperate-climate reservoir that was emptied and partially decommissioned between 2017 and 2019. The research objectives were addressed through three complementary chapters; chapters 3, 4, and 5. The third chapter assessed CO₂ and CH₄ emissions in three environments: deep and shallow impounded water, exposed sediments, and lotic water, before, during, and after the drawdown phase of the Enobieta Reservoir. The fourth chapter investigated the temporal change in the content and reactivity of sediment OM in the Enobieta Reservoir. The fifth chapter examined the role of vegetation growth in C cycling in the Enobieta Reservoir. The main conclusions of this thesis are the following:

1. The drawdown phase of DD was a hot moment of CO₂ and CH₄ emissions because the ecosystem C flux was higher during and after than before the reservoir drawdown phase of DD.
2. Areal CO₂ and CH₄ emissions from shallow impounded water were higher than from deep impounded water.
3. Due to their higher surface area than lotic water and higher areal CO₂ fluxes than impounded water, exposed sediments emitted most of CO₂ emissions, which contributed 99% of the ecosystem C flux in CO₂-eq before, during, and after the drawdown phase of DD.
4. Thus, DD may be a sustainable strategy to mitigate CH₄ fluxes, which comprise 69–69% of CO₂-eq emissions from the water surfaces of reservoirs.
5. Areal CO₂ emissions from exposed sediments decreased with sediment exposure time, but they did not show a clear spatial pattern.
6. Exposed sediment in the Enobieta Reservoir contained a large content of highly biodegradable and leachable OM. The respiration efficiency of sediment WEOM was higher than that of bulk sediment OM. Some parameters of the content and reactivity of sediment OM showed different trends; linear and complex.
7. The high content and reactivity of sediment OM, especially, sediment WEOM reported in this study imply that reservoir drawdown can result in important C emissions in the reservoir and downstream of the reservoir.
8. Vegetation rapidly recolonized exposed sediment after the drawdown. Thirty-one plant species already covered 31% of the reservoir four months after the

drawdown phase of DD. The vegetation community was dominated by three herbaceous plant taxa: *Juncus* spp., *Gnaphalium* spp., and *Persicaria* spp.

9. Accounting for the C sink in vegetation biomass reduced CO₂ emissions from the reservoir to the atmosphere by 52%. The C sink in vegetation biomass is predicted to increase when annual herbaceous plants are replaced with perennial woody plant taxa.
10. The findings of this study imply that high C emissions related to reservoir drawdown may be a short-term effect of DD, while terrestrialization may be a long-term sink of atmospheric CO₂ and a sustainable strategy for ecosystem restoration and climate mitigation.
11. Long-term studies are needed to track temporal changes in C cycling in reservoirs and river reaches downstream after DD.

8. References

- Afan, H. A., El-shafie, A., Mohtar, W. H. M. W., & Yaseen, Z. M. (2016). Past, present and prospect of an Artificial Intelligence (AI) based model for sediment transport prediction. *Journal of Hydrology*, *541*, 902–913. <https://doi.org/10.1016/j.jhydrol.2016.07.048>
- Albrecht, A., & Kandji, S. T. (2003). Carbon sequestration in tropical agroforestry systems. *Agriculture, Ecosystems and Environment*, *99*, 15–27. [https://doi.org/10.1016/S0167-8809\(03\)00138-5](https://doi.org/10.1016/S0167-8809(03)00138-5)
- Allen, M. B., Engle, R. O., Zendt, J. S., Shrier, F. C., Wilson, J. T., & Connolly, P. J. (2016). Le saumon et la truite arc-en-ciel dans la rivière White Salmon après la destruction du barrage de Condit – résultats des travaux de planification et de la recolonisation. *Fisheries*, *41*(4), 190–203. <https://doi.org/10.1080/03632415.2016.1150839>
- Almeida, R. M., Paranaíba, J. R., Barbosa, Í., Sobek, S., Kosten, S., Linkhorst, A., Mondençã, R., Quadra, G., Roland, F., & Barros, N. (2019). Carbon dioxide emission from drawdown areas of a Brazilian reservoir is linked to surrounding land cover. *Aquatic Sciences*, *81*, 1–9. <https://doi.org/10.1007/s00027-019-0665-9>
- Amani, M., Ferreira, V., & Graça, M. A. S. (2019). Effects of elevated atmospheric CO₂ concentration and temperature on litter decomposition in streams: A meta-analysis. *International Revi*, *2019*, 1–12. <https://doi.org/10.1002/iroh.201801965>
- Amani, M., Obrador, B., Fandos, D., Butturini, A., & von Schiller, D. (2024). Exposed sediments in a temperate-climate reservoir under dam decommissioning contain large stocks of highly bioreactive organic matter. *Limnetica*, *43*, 000–000. <https://doi.org/10.23818/limn.43.11>
- Amani, M., von Schiller, D., Suárez, I., Atristain, M., Elozegi, A., Marcé, R., Barcía-Baquero, G., & Obrador, B. (2022). The drawdown phase of dam decommissioning is a hot moment of gaseous carbon emissions from a temperate reservoir. *Inland Waters*, *12*, 451–462. <https://doi.org/10.1080/20442041.2022.2096977>
- Anderson, N. J., Bennion, H., & Lotter, A. F. (2014). Lake eutrophication and its implications for organic carbon sequestration in Europe. *Global Change Biology*, *20*, 2741–2751. <https://doi.org/10.1111/gcb.12584>
- Anderson, N. J., Dietz, R. D., & Engstrom, D. R. (2013). Land-use change, not climate, controls organic carbon burial in lakes. *Proceedings of the Royal Society B: Biological Sciences*, *280*(1769). <https://doi.org/10.1098/rspb.2013.1278>
- Arce, M. I., Mendoza-Lera, C., Almagro, M., Catalán, N., Romani, A. M., Martí, E., Gómez, R., Bernal, S., Foulquier, A., Mutz, M., Marcé, R., Zoppini, A., Gionchetta, G., Weigelhofer, G., del Campo, R., Robinson, C. T., Gilmer, A., Rulik, M., Obrador, B., Shumilova, O., Zlatanovic, S., Arnon, S., Baldrian, P., Singer, G., Datry, T., Skoulikidis, N., Tietjen, B., & von Schiller, D. (2019). A conceptual framework for understanding the biogeochemistry of dry riverbeds through the lens of soil science. *Earth-Science Reviews*, *188*, 441–453.

<https://doi.org/10.1016/j.earscirev.2018.12.001>

- Arce, M. I., Bengtsson, M. M., von Schiller, D., Zak, D., Täumer, J., Urich, T., & Singer, G. (2021). Desiccation time and rainfall control gaseous carbon fluxes in an intermittent stream. *Biogeochemistry*, *155*, 381–400. <https://doi.org/10.1007/s10533-021-00831-6>
- Arnell, N. W., & Lloyd-Hughes, B. (2014). The global-scale impacts of climate change on water resources and flooding under new climate and socio-economic scenarios. *Climatic Change*, *122*, 127–140. <https://doi.org/10.1007/s10584-013-0948-4>
- Arriaga, F. J., Lowery, B., & Mays, M. D. (2006). A fast method for determining soil particle size distribution using a laser instrument. *Soil Science*, *171*, 663–674. <https://doi.org/10.1097/01.ss.0000228056.92839.88>
- Arrieta, J. M., Mayol, E., Hansman, R. L., Herndl, G. J., Dittmar, T., & Duarte, C. M. (2015). Dilution limits dissolved organic carbon utilization in the deep ocean. *Science*, *348*, 331–333. <https://doi.org/10.1126/science.1258955>
- Atristain, M. V. (2023). Effects of the decommissioning of the Enobieta Dam (Navarre, North Iberian Peninsula) on stream ecosystem structure and functioning. [PhD thesis, Departamento: Biología Vegetal y Ecología, University of the Basque Country]. Fecha de la defensa: 18 de julio de 2023 a las 10:00 horas, en la Sala Adela Moyua de la Facultad
- Atristain, M., von Schiller, D., Larrañaga, A., & Elozegi, A. (2022). Short-term effects of a large dam decommissioning on biofilm structure and functioning. *Restoration Ecology*. <https://doi.org/10.1111/rec.13779>
- Backlund, P. (1992). Degradation of aquatic humic material by ultraviolet light. *Chemosphere*, *25*, 1869–1878. [https://doi.org/10.1016/0045-6535\(92\)90026-N](https://doi.org/10.1016/0045-6535(92)90026-N)
- Barros, N., Cole, J. J., Tranvik, L. J., Prairie, Y. T., Bastviken, D., Huszar, V. L. M., del Giorgio, P., & Roland, F. (2011). Carbon emission from hydroelectric reservoirs linked to reservoir age and latitude. *Nature Geoscience*, *4*, 593–596. <https://doi.org/10.1038/ngeo1211>
- Banadkooki, F. B., Ehteram, M., Ahmed, A. N., Teo, F. Y., Ebrahimi, M., Fai, C. M., Huang, Y. F., & Schulz, M. (2020). Suspended sediment load prediction using artificial neural network and ant lion optimization algorithm. *Environmental Science and Pollution Research*, *27*, 38094–38116. <https://doi.org/10.1007/s11356-020-09876-w>/Published
- Bastviken, D., Cole, J. J., Pace, M. L., & Van de-Bogert, M. C. (2008). Fates of methane from different lake habitats: Connecting whole-lake budgets and CH₄ emissions. *Journal of Geophysical Research: Biogeosciences*, *113*, G02024. <https://doi.org/10.1029/2007JG000608>
- Bastviken, D., Cole, J., Pace, M., & Tranvik, L. (2004). Methane emissions from lakes: Dependence of lake characteristics, two regional assessments, and a global estimate. *Global Biogeochemical Cycles*, *18*, 1–12. <https://doi.org/10.1029/2004GB002238>
- Bastviken, D., Persson, L., Odham, G., & Tranvik, L. (2004). Degradation of dissolved

- organic matter in oxic and anoxic lake water. *Limnology and Oceanography*, *49*, 109–116. <https://doi.org/10.4319/lo.2004.49.1.0109>
- Bastviken, D., Tranvik, L. J., Downing, J. A., Crill, P. M., & Enrich-prast, A. (2011). Freshwater methane emissions offset the continental carbon sink. *Science*, *331*, 50. <https://doi.org/10.1126/science.1196808>
- Battin, J. T., Butturini, A., & Sabater, F. (1999). Immobilization and metabolism of dissolved organic carbon by natural sediment biofilms in a Mediterranean and temperate stream. *Aquatic Microbial Ecology*, *19*, 297–305. <https://doi.org/10.3354/ame019297>
- Battin, T. J., Luysaert, S., Kaplan, L. A., Aufdenkampe, A. K., Richter, A., & Tranvik, L. J. (2009). The boundless carbon cycle. *Nature Geoscience*, *2*, 598–600. <https://doi.org/10.1038/ngeo618>
- Baulch, H. M., Dillon, P. J., Maranger, R., & Schiff, S. L. (2011). Diffusive and ebullitive transport of methane and nitrous oxide from streams: Are bubble-mediated fluxes important? *Journal of Geophysical Research: Biogeosciences*, *116*, G04028. <https://doi.org/10.1029/2011JG001656>
- Baumann, K., Dignac, M. F., Rumpel, C., Bardoux, G., Sarr, A., Steffens, M., & Maron, P. A. (2013). Soil microbial diversity affects soil organic matter decomposition in a silty grassland soil. *Biogeochemistry*, *114*, 201–212. <https://doi.org/10.1007/s10533-012-9800-6>
- Bednarek, A. T. (2001). Undamming rivers: A review of the ecological impacts of dam removal. *Environmental Management*, *27*, 803–814. <https://doi.org/10.1007/s002670010189>
- Bellmore, J. R., Duda, J. J., Craig, L. S., Greene, S. L., Torgersen, C. E., Collins, M. J., & Vittum, K. (2017). Status and trends of dam removal research in the United States. *Wiley Interdisciplinary Reviews: Water*, *4*, e1164. <https://doi.org/10.1002/WAT2.1164>
- Bellmore, J. R., States, U., Pess, G. R., Oceanic, N., Duda, J. J., States, U., ... Cruz, S. (2019). Conceptualizing ecological responses to dam removal: if you remove it, what's to come? *BioScience*, *69*, 26–39. <https://doi.org/10.1093/biosci/biy152>
- Berghuis, B. A., Yu, F. B., Schulz, F., Blainey, P. C., Woyke, T., & Quake, S. R. (2019). Hydrogenotrophic methanogenesis in archaeal phylum Verstraetearchaeota reveals the shared ancestry of all methanogens. *Proceedings of the National Academy of Sciences of the United States of America*, *116*, 5037–5044. <https://doi.org/10.1073/pnas.1815631116>
- Bianchi, T. S., Thornton, D. C. O., Yvon-Lewis, S. A., King, G. M., Eglinton, T. I., Shields, M. R., Ward, N. D., & Curtis, J. (2015). Positive priming of terrestrially derived dissolved organic matter in a freshwater microcosm system. *Geophysical Research Letters*, *42*, 5460–5467. <https://doi.org/10.1002/2015GL064765>
- Bolan, N. S., Adriano, D. C., Kunhikrishnan, A., James, T., McDowell, R., & Senesi, N. (2011). Dissolved organic matter. Biogeochemistry, dynamics, and environmental significance in soils. In *Advances in Agronomy* (Vol. 110, pp. 1–75).

- <https://doi.org/10.1016/B978-0-12-385531-2.00001-3>
- Bolpagni, R., Folegot, S., Laini, A., & Bartoli, M. (2017). Role of ephemeral vegetation of emerging river bottoms in modulating CO₂ exchanges across a temperate large lowland river stretch. *Aquatic Sciences*, *79*, 149–158. <https://doi.org/10.1007/s00027-016-0486-z>
- Bond-Lamberty, B., & Thomson, A. (2010). A global database of soil respiration data. *Biogeosciences*, *7*, 1915–1926. <https://doi.org/10.5194/bg-7-1915-2010>
- Bond-Lamberty, B., & Thomson, A. M. (2012). A global database of soil respiration data, version 3.0. Oak Ridge, Tennessee. <https://doi.org/https://doi.org/10.3334/ORNLDAAC/1235>
- Borges, A. V., Darchambeau, F., Teodoru, C. R., Marwick, T. R., Tamoo, F., Geeraert, N., Omengo, F. O., Guérin, F., Lambert, T., Morana, C., Okulu, E., & Bouillon, S. (2015). Globally significant greenhouse-gas emissions from African inland waters. *Nature Geoscience*, *8*, 637–642. <https://doi.org/10.1038/ngeo2486>
- Boyer, J. N., & Groffman, P. M. (1996). Bioavailability of water extractable organic carbon fractions in forest and agricultural soil profiles. *Soil Biology & Biogeochemistry*, *28*, 783–790. [https://doi.org/10.1016/0038-0717\(96\)00015-6](https://doi.org/10.1016/0038-0717(96)00015-6)
- Broughton, R. K., Bullock, J. M., George, C., Hill, R. A., Hinsley, S. A., Maziarz, M., Melin, M., Mountford, J. O., Sparks, T. H., & Pywell, R. F. (2021). Long-term woodland restoration on lowland farmland through passive rewilding. *PLoS ONE*, *16*, 1–24. <https://doi.org/10.1371/journal.pone.0252466>
- Brouns, K., Verhoeven, J. T. A., & Hefting, M. M. (2014). The effects of salinization on aerobic and anaerobic decomposition and mineralization in peat meadows: The roles of peat type and land use. *Journal of Environmental Management*, *143*, 44–53. <https://doi.org/10.1016/j.jenvman.2014.04.009>
- Brykała, D., & Podgórski, Z. (2020). Evolution of landscapes influenced by watermills, based on examples from Northern Poland. *Landscape and Urban Planning*, *198*. <https://doi.org/10.1016/j.landurbplan.2020.103798>
- Buan, N. R. (2018). Methanogens: Pushing the boundaries of biology. *Emerging Topics in Life Sciences*, *2*, 629–646. <https://doi.org/10.1042/ETLS20180031>
- Cable, J. M., Ogle, K., Williams, D. G., Weltzin, J. F., & Huxman, T. E. (2008). Soil texture drives responses of soil respiration to precipitation pulses in the sonoran desert: Implications for climate change. *Ecosystems*, *11*, 961–979. <https://doi.org/10.1007/s10021-008-9172-x>
- Čapek, P., Starke, R., Hofmockel, K. S., Bond-Lamberty, B., & Hess, N. (2019). Apparent temperature sensitivity of soil respiration can result from temperature driven changes in microbial biomass. *Soil Biology and Biochemistry*, *135*, 286–293. <https://doi.org/10.1016/j.soilbio.2019.05.016>
- Catalán, N., Marcé, R., Kothawala, D. N., & Tranvik, L. J. (2016). Organic carbon decomposition rates controlled by water retention time across inland waters. *Nature Geoscience*, *9*, 501–504. <https://doi.org/10.1038/ngeo2720>
- Catalán, N., Obrador, B., Felip, M., & Pretus, J. L. (2013). Higher reactivity of

- allochthonous vs. autochthonous DOC sources in a shallow lake. *Aquatic Sciences*, *75*, 581–593. <https://doi.org/10.1007/s00027-013-0302-y>
- Catalán, N., Pastor, A., Borrego, C. M., Casas-Ruiz, J. P., Hawkes, J. A., Gutiérrez, C., von Schiller, D., & Marcé, R. (2021). The relevance of environment vs. composition on dissolved organic matter degradation in freshwaters. *Limnology and Oceanography*, *66*, 306–320. <https://doi.org/10.1002/lno.11606>
- Catalán, N., Von Schiller, D., Marcé, R., Koschorreck, M., Gomez-Gener, L., & Obrador, B. (2014). Carbon dioxide efflux during the flooding phase of temporary ponds. *Limnetica*, *33*, 349–360. <https://doi.org/10.23818/limn.33.27>
- Chantigny, M. H. (2003). Dissolved and water-extractable organic matter in soils: A review on the influence of land use and management practices. *Geoderma*, *113*, 357–380. [https://doi.org/10.1016/S0016-7061\(02\)00370-1](https://doi.org/10.1016/S0016-7061(02)00370-1)
- Chantigny, M. H., Harrison-Kirk, T., Curtin, D., & Beare, M. (2014). Temperature and duration of extraction affect the biochemical composition of soil water-extractable organic matter. *Soil Biology and Biochemistry*, *75*, 161–166. <https://doi.org/10.1016/j.soilbio.2014.04.011>
- Chen, M., & Hur, J. (2015). Pre-treatments, characteristics, and biogeochemical dynamics of dissolved organic matter in sediments: A review. *Water Research*, *79*, 10–25. <https://doi.org/10.1016/j.watres.2015.04.018>
- Clow, D. W., Stackpoole, S. M., Verdin, K. L., Butman, D. E., Zhu, Z., Krabbenhoft, D. P., & Striegl, R. G. (2015). Organic carbon burial in lakes and reservoirs of the conterminous United States. *Environmental Science and Technology*, *49*, 7614–7622. <https://doi.org/10.1021/acs.est.5b00373>
- Cole, J. J., Prairie, Y. T., Caraco, N. F., Mcdowell, W. H., Tranvik, L. J., Striegl, R. G., Duarte, C. M., Kortelainen, P., Downing, J. A., Middelburg, J. J., & Melack, J. (2007). Plumbing the global carbon cycle: Integrating inland waters into the terrestrial carbon budget. *Ecosystems*, *10*, 171–184. <https://doi.org/10.1007/s10021-006-9013-8>
- Cornett, R. J., & Rigler, F. H. (1987). Decomposition of seston in the hypolimnion. *Canadian Journal of Fisheries and Aquatic Sciences*, *44*, 146–151. <https://doi.org/10.1139/f87-019>
- Cory, R. M., Ward, C. P., Crump, B. C., & Kling, G. W. (2014). Sunlight controls water column processing of carbon in arctic fresh waters. *Science*, *345*, 925–928. <https://doi.org/10.1126/science.1255006>
- Coulson, L. E., Weigelhofer, G., Gill, S., Hein, T., Griebler, C., & Schelker, J. (2022). Small rain events during drought alter sediment dissolved organic carbon leaching and respiration in intermittent stream sediments. *Biogeochemistry*, *159*, 159–178. <https://doi.org/10.1007/s10533-022-00919-7>
- Couto, T. B. A., & Olden, J. D. (2018). Global proliferation of small hydropower plants – science and policy. *Frontiers in Ecology and the Environment*, *16*, 91–100. <https://doi.org/10.1002/fee.1746>
- Coyne, M. S., Howell, J. M., Cornelius, P. L., Coyne, M. S. ; Howell, J. M. ; & Coyne, M. S. (1997). Particle size and temperature affect fecal bacteria survival in sediment.

- Agronomy*, 30, 1–4. <https://doi.org/10.2134/jeq1996.00472425002500060007x>
- Craft, J. A., Stanford, J. A., & Pusch, M. (2002). Microbial respiration within a floodplain aquifer of a large gravel-bed river. *Freshwater Biology*, 47, 251–261. <https://doi.org/10.1046/j.1365-2427.2002.00803.x>
- Crenshaw, C. L., Valett, H. M., & Webster, J. R. (2002). Effects of augmentation of coarse particulate organic matter on metabolism and nutrient retention in hyporheic sediments. *Freshwater Biology*, 47, 1820–1831. <https://doi.org/10.1046/j.1365-2427.2002.00928.x>
- Crusius, J., & Wanninkhof, R. (2003). Gas transfer velocities measured at low wind speed over a lake. *Limnology and Oceanography*, 48, 1010–1017. <https://doi.org/10.4319/lo.2003.48.3.1010>
- Cummins, K. W., Sedell, J. R., Swanson, F. J., Minshall, G. W., Fisher, S. G., Cushing, C. E., Petersen, R. C., & Vannote, R. L. (1983). Organic matter budgets for stream ecosystems: problems in their evaluation. In *Stream Ecology* (pp. 299–353). Boston, MA: Springer, Boston, MA. https://doi.org/10.1007/978-1-4613-3775-1_13
- Dalal, R. C., Allen, D. E., Livesley, S. J., & Richards, G. (2008). Magnitude and biophysical regulators of methane emission and consumption in the Australian agricultural, forest, and submerged landscapes: A review. *Plant and Soil*, 309, 43–76. <https://doi.org/10.1007/s11104-007-9446-7>
- Dam Removal Europe. (2020). *Dam removal Europe progress 2020*.
- Damerell, P., Howe, C., & Milner-Gulland, E. J. (2013). Child-orientated environmental education influences adult knowledge and household behaviour. *Environmental Research Letter*, 8, 015016. <https://doi.org/10.1088/1748-9326/8/1/015016>
- De Rego, K., Lauer, J. W., Eaton, B., & Hassan, M. (2020). A decadal-scale numerical model for wandering, cobble-bedded rivers subject to disturbance. *Earth Surface Processes and Landforms*, 45, 912–927. <https://doi.org/10.1002/esp.4784>
- De Vincenzo, A., Covelli, C., Molino, A. J., Pannone, M., Ciccaglione, M., & Molino, B. (2018). Long-term management policies of reservoirs: Possible re-use of dredged sediments for coastal nourishment. *Water (Switzerland)*, 11, 15. <https://doi.org/10.3390/w11010015>
- Dean, W. E., & Gorham, W. (1998). Magnitude and significance of carbon burial in lakes, reservoirs, and peatlands. *Geology*, 26, 535–538. [https://doi.org/10.1130/0091-7613\(1998\)026<0535:MASOCB>2.3.CO;2](https://doi.org/10.1130/0091-7613(1998)026<0535:MASOCB>2.3.CO;2)
- Deemer, B. R., Harrison, J. A., Li, S., Beaulieu, J. J., Delsontro, T., Barros, N., Fezerra-Neto, J. F., Powers, S. M., Dos Santos, M. A., & Vonk, J. A. (2016). Greenhouse gas emissions from reservoir water surfaces: A new global synthesis. *BioScience*, 66, 949–964. <https://doi.org/10.1093/biosci/biw117>
- del Giorgio, P. A., & Williams, P. J. le B. (2005). *Respiration in aquatic ecosystems*. New York.
- DelSontro, T., Boutet, L., St-pierre, A., Giorgio, P. A., & Prairie, Y. T. (2016). Methane ebullition and diffusion from northern ponds and lakes regulated by the interaction between temperature and system productivity. *Limnology and Oceanography*, 61,

- S62–S77. <https://doi.org/10.1002/lno.10335>
- DelSontro, T., McGinnis, D. F., Sobek, S., Ostrovsky, I., & Wehrli, B. (2010). Extreme methane emissions from a swiss hydropower Reservoir: Contribution from bubbling sediments. *Environmental Science and Technology*, *44*, 2419–2425. <https://doi.org/10.1021/es9031369>
- Deshmukh, C., Guérin, F., Vongkhamkao, A., Pighini, S., Oudone, P., Sopraseuth, S., Godon, A., Rode, W., Guédant, P., Oliva, P., Audry, S., Zouiten, C., Galy-Lacaux, C., Robain, H., Ribolzi, O., Kansal, A., Chanudet, V., Dscloux, S., & Serça, D. (2018). Carbon dioxide emissions from the flat bottom and shallow Nam Theun 2 Reservoir : drawdown area as a neglected pathway to the atmosphere. *Biogeosciences*, *15*, 1775–1794. <https://doi.org/https://doi.org/10.5194/bg-15-1775-2018>
- Dong, Y., Li, Y., Kong, F., Zhang, J., & Xi, M. (2020). Source, structural characteristics and ecological indication of dissolved organic matter extracted from sediments in the primary tributaries of the Dagu River. *Ecological Indicators*, *109*. <https://doi.org/10.1016/j.ecolind.2019.105776>
- Downing, J. A., Cole, J. J., Middelburg, J. J., Striegl, R. G., Duarte, C. M., Kortelainen, P., Prairie, Y. T., & Laube, K. A. (2008). Sediment organic carbon burial in agriculturally eutrophic impoundments over the last century. *Global Biogeochemical Cycles*, *22*, 1–10. <https://doi.org/10.1029/2006GB002854>
- Downing, J. A., Prairie, Y. T., Cole, J. J., Duarte, C. M., Tranvik, L. J., Striegl, R. G., McDowell, W. H., Kortelainen, P., Caraco, N. F., Melack, J. M., & Middelburg, J. J. (2006). The global abundance and size distribution of lakes, ponds, and impoundments. *Limnology and Oceanography*, *51*, 2388–2397. <https://doi.org/10.4319/lo.2006.51.5.2388>
- Doyle, M. W., Stanley, E. H., Harbor, J. M., & Grant, G. S. (2003). Dam removal in the united states: Emerging needs for science and policy. *Eos*, *93*, 425–426. <https://doi.org/10.1029/2003EO040001>
- Drake, T. W., Raymond, P. A., & Spencer, R. G. M. (2018). Terrestrial carbon inputs to inland waters: A current synthesis of estimates and uncertainty. *Limnology and Oceanography Letters*, *3*, 132–142. <https://doi.org/10.1002/lol2.10055>
- Duda, J. J., & Bellmore, J. R. (2022). Dam removal and river restoration. In T. Tockner, K., Mehner (Ed.), *Encyclopedia of Inland Waters* (Second, pp. 576–585). Oxford, UK: Elsevier. <https://doi.org/10.1016/b978-0-12-819166-8.00101-8>
- Duval, T. P., & Radu, D. D. (2018). Effect of temperature and soil organic matter quality on greenhouse-gas production from temperate poor and rich fen soils. *Ecological Engineering*, *114*, 66–75. <https://doi.org/10.1016/j.ecoleng.2017.05.011>
- Eisenhauer, N., Lanoue, A., Strecker, T., Scheu, S., Steinauer, K., Thakur, M. P., & Mommer, L. (2017). Root biomass and exudates link plant diversity with soil bacterial and fungal biomass. *Scientific Reports*, *7*, 44641. <https://doi.org/10.1038/srep44641>
- Espa, P., Batalla, R. J., Brignoli, M. L., Crosa, G., Gentili, G., & Quadroni, S. (2019). Tackling reservoir siltation by controlled sediment flushing: Impact on downstream

- fauna and related management issues. *PLoS ONE*, *14*, e0218822. <https://doi.org/10.1371/journal.pone.0218822>
- Fearnside, P. M. (1995). Hydroelectric dams in the Brazilian Amazon as sources of 'greenhouse' gases. *Environmental Conservation*, *22*, 7–19. <https://doi.org/10.1017/S0376892900034020>
- Ferreira, V., Bini, L. M., González Sagrario, M. de los Á., Kovalenko, K. E., Naselli-Flores, L., Padial, A. A., & Padisák, J. (2023). Aquatic ecosystem services: an overview of the Special Issue. *Hydrobiologia*, *850*, 2473–2483. <https://doi.org/10.1007/s10750-023-05235-1>
- Findlay, S., & Sinsabaugh, L. R. (2003). Response of hyporheic biofilm metabolism and community structure to nitrogen amendments. *Aquatic Microbial Ecology*, *33*, 127–136. <https://doi.org/10.3354/ame033127>
- Forbes, M. G., Doyle, R. D., Scott, J. T., Stanley, J. K., Huang, H., Fulton, B. A., & Brooks, B. W. (2012). Carbon sink to source: Longitudinal gradients of planktonic P:R ratios in subtropical reservoirs. *Biogeochemistry*, *107*, 81–93. <https://doi.org/10.1007/s10533-010-9533-3>
- Forster, P., Ramaswamy, V., Artaxo, P., Bernsten, T., Betts, R., Fahey, D. W., Haywood, J., Lean, J., Lowe, D. C., Myhre, G., Nganga, J., Prinn, R., Raga, G., Schulz, M., & Van Dorland, R. (2007). *Changes in atmospheric constituents and in radiative forcing. In: Climate change 2007: The physical science basis. Contribution of working group I to the Fourth Assessment Report of the Intergovernmental Panel on Climate Change [Solomon, S., D. Qin, M. Ma.*
- Foulquier, A., Malard, F., Mermillod-Blondin, F., Datry, T., Simon, L., Montuelle, B., & Gibert, J. (2010). Vertical change in dissolved organic carbon and oxygen at the water table region of an aquifer recharged with stormwater: Biological uptake or mixing? *Biogeochemistry*, *99*, 31–47. <https://doi.org/10.1007/s10533-009-9388-7>
- Fox, C. A., Magilligan, F. J., & Sneddon, C. S. (2016). “You kill the dam, you are killing a part of me”: Dam removal and the environmental politics of river restoration. *Geoforum*, *70*, 93–104. <https://doi.org/10.1016/j.geoforum.2016.02.013>
- Fox, P. M., Nico, P. S., Tfaily, M. M., Heckman, K., & Davis, J. A. (2017). Characterization of natural organic matter in low-carbon sediments: Extraction and analytical approaches. *Organic Geochemistry*, *114*, 12–22. <https://doi.org/10.1016/j.orggeochem.2017.08.009>
- Frankignoulle, M. (1988). Field measurements of air-sea CO₂ exchange. *Limnology and Oceanography*, *33*, 313–322. <https://doi.org/10.4319/lo.1988.33.3.0313>
- Freeman, C., Ostle, N., & Kang, H. (2001). An enzymatic latch on a global carbon store. *Nature*, *409*, 149. <https://doi.org/10.1038/35051650>
- Fromin, N., Pinay, G., Montuelle, B., Landais, D., Ourcival, J. M., Joffre, R., & Lensi, R. (2010). Impact of seasonal sediment desiccation and rewetting on microbial processes involved in greenhouse gas emissions. *Ecohydrology*, *3*, 339–348. <https://doi.org/10.1002/eco.115>
- Fuentes-Montemayor, E., Park, K. J., Cordts, K., & Watts, K. (2022). The long-term

- development of temperate woodland creation sites: From tree saplings to mature woodlands. *Forestry*, *95*, 28–37. <https://doi.org/10.1093/forestry/cpab027>
- Gallo, E. L., Lohse, K. A., Ferlin, C. M., Meixner, T., & Brooks, P. D. (2014). Physical and biological controls on trace gas fluxes in semi-arid urban ephemeral waterways. *Biogeochemistry*, *121*, 189–207. <https://doi.org/10.1007/s10533-013-9927-0>
- Gernaat, D. E. H. J., Bogaart, P. W., Vuuren, D. P. V., Biemans, H., & Niessink, R. (2017). High-resolution assessment of global technical and economic hydropower potential. *Nature Energy*, *2*, 821–828. <https://doi.org/10.1038/s41560-017-0006-y>
- Gerull, L., Frossard, A., Gessner, M. O., & Mutz, M. (2011). Variability of heterotrophic metabolism in small stream corridors of an early successional watershed. *Journal of Geophysical Research*, *116*, G02012. <https://doi.org/10.1029/2010JG001516>
- Gerull, L., Frossard, A., Gessner, M. O., & Mutz, M. (2012). Effects of shallow and deep sediment disturbance on whole-stream metabolism in experimental sand-bed flumes. *Hydrobiologia*, *683*, 297–310. <https://doi.org/10.1007/s10750-011-0968-x>
- Glatzel, S., Basiliko, N., & Moore, T. (2004). Carbon dioxide and methane production potentials of peats from natural and harvested sites, eastern Québec, Canada. *Wetlands*, *24*, 261–267. [https://doi.org/10.1672/0277-5212\(2004\)024\[0261:CDAMPP\]2.0.CO;2](https://doi.org/10.1672/0277-5212(2004)024[0261:CDAMPP]2.0.CO;2)
- Gleeson, T., Wada, Y., Bierkens, M. F. P., & Van Beek, L. P. H. (2012). Water balance of global aquifers revealed by groundwater footprint. *Nature*, *488*, 197–200. <https://doi.org/10.1038/nature11295>
- Gobierno de Navarra. (2019). *Ficha climática de la estación—Meteo Navarra*. http://meteo.navarra.es/climatologia/fichasclimaticas_estacion.cfm?IDestacion=74.
- Gold, A. J., Addy, K., Morrison, A., & Simpson, M. (2016). Will dam removal increase nitrogen flux to estuaries. *Water*, *8*, 522. <https://doi.org/10.3390/w8110522>
- Gómez-Gener, L., Obrador, B., Marcé, R., Acuña, V., Catalán, N., Casas-Ruiz, J. P., Sabater, S., Muñoz, I., & von Schiller, D. (2016). When water vanishes: Magnitude and regulation of carbon dioxide emissions from dry temporary streams. *Ecosystems*, *19*, 710–723. <https://doi.org/10.1007/s10021-016-9963-4>
- Gómez-Gener, L., Obrador, B., von Schiller, D., Marcé, R., Casas-Ruiz, J. P., Proia, L., Acuña, V., Catalán, N., Muñoz, I., & Koschorreck, M. (2015). Hot spots for carbon emissions from Mediterranean fluvial networks during summer drought. *Biogeochemistry*, *125*, 409–426. <https://doi.org/10.1007/s10533-015-0139-7>
- Gordon, N. D., McMahon, T. A., Finlayson, B. L., Gippel, C. J., Nathan, R. J., & Knight, S. (2004). *Stream hydrology: An introduction for ecologists*. (John Wiley and Sons Ltd, Ed.) (Second). Chichester, England: John Wiley and Sons Ltd.
- Grabowski, R. C., Droppo, I. G., & Wharton, G. (2011). Erodibility of cohesive sediment: The importance of sediment properties. *Earth-Science Reviews*, *105*, 101–120. <https://doi.org/10.1016/j.earscirev.2011.01.008>
- Grabowski, Z. J., Chang, H., & Granek, E. F. (2018). Fracturing dams, fractured data: Empirical trends and characteristics of existing and removed dams in the United

- States. *River Research and Applications*, *34*, 526–537.
<https://doi.org/10.1002/rra.3283>
- Grace, J. (2013). Carbon cycle. In *Encyclopedia of Biodiversity: Second Edition* (pp. 674–684). Elsevier Inc. <https://doi.org/10.1016/B978-0-12-384719-5.00306-3>
- Granéli, W., Lindell, M., & Tranvik, L. (1996). Photo-oxidative production of dissolved inorganic carbon in lakes of different humic content. *Limnology and Oceanography*, *41*, 698–706. <https://doi.org/10.4319/lo.1996.41.4.0698>
- Grasset, C., Mendonça, R., Villamor Saucedo, G., Bastviken, D., Roland, F., & Sobek, S. (2018). Large but variable methane production in anoxic freshwater sediment upon addition of allochthonous and autochthonous organic matter. *Limnology and Oceanography*, *63*, 1488–1501. <https://doi.org/10.1002/lno.10786>
- Gregorich, E. G., Beare, M. H., Stoklas, U., & St-Georges, P. (2003). Biodegradability of soluble organic matter in maize-cropped soils. *Geoderma*, *113*, 237–252. [https://doi.org/10.1016/S0016-7061\(02\)00363-4](https://doi.org/10.1016/S0016-7061(02)00363-4)
- Grigg, N. S. (2019). Global water infrastructure: state of the art review. *International Journal of Water Resources Development*, *35*, 181–205. <https://doi.org/10.1080/07900627.2017.1401919>
- Grill, G., Lehner, B., Lumsdon, A. E., Macdonald, G. K., Zarfl, C., & Reidy Liermann, C. (2015). An index-based framework for assessing patterns and trends in river fragmentation and flow regulation by global dams at multiple scales. *Environmental Research Letters*, *10*, 015001. <https://doi.org/10.1088/1748-9326/10/1/015001>
- Gruca-Rokosz, R., & Koszelnik, P. (2018). Production pathways for CH₄ and CO₂ in sediments of two freshwater ecosystems in south-eastern Poland. *PLoS ONE*, *13*, e0199755. <https://doi.org/10.1371/journal.pone.0199755>
- Gu, N., Song, Q., Yang, X., Yu, X., Li, X. M., & Li, G. (2020). Fluorescence characteristics and biodegradability of dissolved organic matter (DOM) leached from non-point sources in southeastern China. *Environmental Pollution*, *258*, 113807. <https://doi.org/10.1016/j.envpol.2019.113807>
- Gudasz, C., Bastviken, D., Steger, K., Premke, K., Sobek, S., & Tranvik, L. J. (2010). Temperature-controlled organic carbon mineralization in lake sediments. *Nature*, *466*, 478–481. <https://doi.org/10.1038/nature09186>
- Gudasz, C., Sobek, S., Bastviken, D., Koehler, B., & Tranvik, L. J. (2015). Temperature sensitivity of organic carbon mineralization in contrasting lake sediments. *Journal of Geophysical Research G: Biogeosciences*, *120*, 1215–1225. <https://doi.org/10.1002/2015JG002928>
- Guenet, B., Danger, M., Abbadie, L., Gé, A., & Lacroix, R. (2010). Priming effect: bridging the gap between terrestrial and aquatic ecology. *Ecology*, *91*, 2850–2861. <https://doi.org/10.1890/09-1968.1>
- Guenet, B., Danger, M., Harrault, L., Allard, B., Jauset-Alcala, M., Bardoux, G., Benest, D., Abbadie, L., & Lacroix, G. (2014). Fast mineralization of land-born C in inland waters: First experimental evidences of aquatic priming effect. *Hydrobiologia*, *721*, 35–44. <https://doi.org/10.1007/s10750-013-1635-1>

- Guérin, F., & Abril, G. (2007). Significance of pelagic aerobic methane oxidation in the methane and carbon budget of a tropical reservoir. *Journal of Geophysical Research: Biogeosciences*, *112*, 1–14. <https://doi.org/10.1029/2006JG000393>
- Guigue, J., Mathieu, O., Lévêque, J., Mounier, S., Laffont, R., Maron, P. A., Navarro, N., Chateau, C. Amiotte-Suchet, P., & Lucas, Y. (2014). A comparison of extraction procedures for water-extractable organic matter in soils. *European Journal of Soil Science*, *65*, 520–530. <https://doi.org/10.1111/ejss.12156>
- Günthel, M., Donis, D., Kirillin, G., Ionescu, D., Bizic, M., McGinnis, D. F., Grossart, H. P., & Tang, K. W. (2019). Contribution of oxic methane production to surface methane emission in lakes and its global importance. *Nature Communications*, *10*, 5497. <https://doi.org/10.1038/s41467-019-13320-0>
- Habel, M., Mechkin, K., Podgorska, K., Saunes, M., Babiński, Z., Chalov, S., Absalon, D., Podgórski, Z., & Obolewski, K. (2020). Dam and reservoir removal projects: a mix of social-ecological trends and cost-cutting attitudes. *Scientific Reports*, *10*, 19210. <https://doi.org/10.1038/s41598-020-76158-3>
- Han, L., Wang, Y., Xu, Y., Wang, Y., Zheng, Y., & Wu, J. (2021). Water- and base-extractable organic matter in sediments from Lower Yangtze River–Estuary–East China Sea Continuum: Insight into accumulation of organic carbon in the river-dominated margin. *Frontiers in Marine Science*, *8*, 617241. <https://doi.org/10.3389/fmars.2021.617241>
- Hanasaki, N., Kanae, S., & Oki, T. (2006). A reservoir operation scheme for global river routing models. *Journal of Hydrology*, *327*, 22–41. <https://doi.org/10.1016/j.jhydrol.2005.11.011>
- Hansen, A. M., Kraus, T. E. C., Pellerin, B. A., Fleck, J. A., Downing, B. D., & Bergamaschi, B. A. (2016). Optical properties of dissolved organic matter (DOM): Effects of biological and photolytic degradation. *Limnology and Oceanography*, *61*, 1015–1032. <https://doi.org/10.1002/lno.10270>
- Hansen, H. H., Forzono, E., Grams, A., Ohlman, L., Ruskamp, C., Pegg, M. A., & Pope, K. L. (2019). Exit here: strategies for dealing with aging dams and reservoirs. *Aquatic Sciences*, *82*, 1–16. <https://doi.org/10.1007/s00027-019-0679-3>
- Hardiman, J. M., & Brady Allen, M. (2015). *Open-file report 2015-1100 prepared in cooperation with the mid-Columbia fisheries enhancement group salmon habitat assessment for conservation planning in the lower White Salmon River, Washington*.
- Harjung, A., Sabater, F., & Butturini, A. (2018). Hydrological connectivity drives dissolved organic matter processing in an intermittent stream. *Limnologica*, *68*, 71–81. <https://doi.org/10.1016/j.limno.2017.02.007>
- Harrison, J. A., Deemer, B. R., Birch, M. K., & Malley, M. T. O. (2017). Reservoir water-level drawdowns accelerate and amplify methane emission. *Environmental Science & Technology*, *51*, 1267–1277. <https://doi.org/10.1021/acs.est.6b03185>
- Harvey, B. N., Johnson, M. L., Kiernan, J. D., & Green, P. G. (2011). Net dissolved inorganic nitrogen production in hyporheic mesocosms with contrasting sediment size distributions. *Hydrobiologia*, *658*, 343–352. <https://doi.org/10.1007/s10750-010->

- Helms, J. R., Stubbins, A., Ritchie, J. D., Minor, E. C., Kieber, D. J., & Mopper, K. (2008). Absorption spectral slopes and slope ratios as indicators of molecular weight, source, and photobleaching of chromophoric dissolved organic matter. *Limnology and Oceanography*, *53*, 955–969. <https://doi.org/10.4319/lo.2008.53.3.0955>
- Hermoso, V. (2017, September 1). Freshwater ecosystems could become the biggest losers of the Paris Agreement. *Global Change Biology*. Blackwell Publishing Ltd. <https://doi.org/10.1111/gcb.13655>
- Heslop, J., Anthony, K. W., & Zhang, M. (2017). Utilizing pyrolysis GC-MS to characterize organic matter quality in relation to methane production in a thermokarst lake sediment core. *Organic Geochemistry*, *103*, 43–50. <https://doi.org/10.1016/j.orggeochem.2016.10.013>
- Hilgert, S., Vicente, C., Fernandes, S., & Fuchs, S. (2019). Redistribution of methane emission hot spots under drawdown conditions. *Science of the Total Environment*, *646*, 958–971. <https://doi.org/10.1016/j.scitotenv.2018.07.338>
- Hoffert, M. I., Caldeira, K., Jain, A. K., Haites, E. F., Harvey, L. D. D., Potter, S. D., Schlesinger, M. E., Schneider, S. H., Watts, R. G., Wigley, T. M., & Wuebbles, D. J. (1998). Energy implications of future stabilization of atmospheric CO₂ content. *Nature*, *395*, 881–884. <https://doi.org/10.1890/09-1968.1>
- Hogeboom, R. J., Knook, L., & Hoekstra, A. Y. (2018). The blue water footprint of the world's artificial reservoirs for hydroelectricity, irrigation, residential and industrial water supply, flood protection, fishing and recreation. *Advances in Water Resources*, *113*, 285–294. <https://doi.org/10.1016/j.advwatres.2018.01.028>
- Holgerson, M. A., Farr, E. R., & Raymond, P. A. (2017). Gas transfer velocities in small forested ponds. *Journal of Geophysical Research: Biogeosciences*, *122*, 1011–1021. <https://doi.org/10.1002/2016JG003734>
- Holgerson, M. A., & Raymond, P. A. (2016). Large contribution to inland water CO₂ and CH₄ emissions from very small ponds. *Nature Geoscience*, *9*, 222–226. <https://doi.org/10.1038/NGEO2654>
- Howard, D. M., & Howard, P. J. A. (1993). Relationships between CO₂ revolution, moisture content, and temperature for a range of soil types. *Soil Biology & Biogeochemistry*, *25*, 1537–1546. [https://doi.org/10.1016/0038-0717\(93\)90008-Y](https://doi.org/10.1016/0038-0717(93)90008-Y)
- ICOLD WRD. (2022). *World register of dams: General synthesis*. Accessed December 08, 2022 at https://www.icoldd-cigb.org/GB/world_register/general_synthesis.asp.
- Ingendahl, D., Borchardt, D., Saenger, N., & Reichert, P. (2009). Vertical hydraulic exchange and the contribution of hyporheic community respiration to whole ecosystem respiration in the River Lahn (Germany). *Aquatic Sciences*, *71*, 399–410. <https://doi.org/10.1007/s00027-009-0116-0>
- Inglett, K. S., Inglett, P. W., Reddy, K. R., & Osborne, T. Z. (2012). Temperature sensitivity of greenhouse gas production in wetland soils of different vegetation. *Biogeochemistry*, *108*, 77–90. <https://doi.org/10.1007/s10533-011-9573-3>
- IPCC. (2013). Summary for policymakers. *Climate Change 2013: The Physical Science*

- Basis. Contribution of Working Group I to the Fifth Assessment Report of the Intergovernmental Panel on Climate Change*, 33. <https://doi.org/10.1017/CBO9781107415324>
- IPCC. (2019). *2019 Refinement to the 2006 IPCC Guidelines for National Greenhouse Gas Inventories. Volume 4*. <https://www.ipcc-nggip.iges.or.jp/public/2019rf/index.html>, retrieved on December 24, 2019.
- Jaeger, K. L., Olden, J. D., & Pelland, N. A. (2014). Climate change poised to threaten hydrologic connectivity and endemic fishes in dryland streams. *Proceedings of the National Academy of Sciences of the United States of America*, *111*, 13894–13899. <https://doi.org/10.1073/pnas.1320890111>
- Janssens, I. A., Freibauer, A., Ciais, P., Smith, P., Nabuurs, G.-J., Folberth, G., Schlamadinger, B., Hutjes, R. W. A., Ceulemans, R., Schulze, E. D., Valentini, R., & Dolman, A. J. (2003). Europe's terrestrial biosphere absorbs 7 to 12% of European anthropogenic CO₂ emissions. *Science*, *300*, 1538. <https://doi.org/10.1126/science.1083592>
- Jansson, C., Wullschleger, S. D., Kalluri, U. C., & Tuskan, G. A. (2010). Phytosequestration: Carbon biosequestration by plants and the prospects of genetic engineering. *BioScience*, *60*, 685–696. <https://doi.org/10.1525/bio.2010.60.9.6>
- Jin, H., Yoon, T. K., Lee, S., Kang, H., Im, J., & Park, J. (2016). Enhanced greenhouse gas emission from exposed sediments along a hydroelectric reservoir during an extreme drought event. *Environmental Research Letters*, *11*, 124003-undefined. <https://doi.org/10.1088/1748-9326/11/12/124003>
- Johnson, S. E., & Graber, B. E. (2002). Enlisting the social sciences in decisions about dam removal. *Bioscience*, *52*, 731–738. [https://doi.org/10.1641/0006-3568\(2002\)052\[0731:ETSSID\]2.0.CO;2](https://doi.org/10.1641/0006-3568(2002)052[0731:ETSSID]2.0.CO;2)
- Jones, J. B. (1995). Factors controlling hyporheic respiration in a desert stream. *Freshwater Biology*, *34*, 91–99. <https://doi.org/10.1111/j.1365-2427.1995.tb00426.x>
- Juniper, T. (2019). *The ecology book. Big ideas simply explained*. (J. Andrews, A. Doran, S. George, G. Croton, C. Meeus, & A. Mitchell, Eds.) (1st ed.). New York.
- Kantoush, S. A., Mousa, A., Shahmirzadi, E. M., Toshiyuki, T., & Sumi, T. (2021). Pilot Field Implementation of Suction Dredging for Sustainable Sediment Management of Dam Reservoirs. *Journal of Hydraulic Engineering*, *147*, 04020098. [https://doi.org/10.1061/\(asce\)hy.1943-7900.0001843](https://doi.org/10.1061/(asce)hy.1943-7900.0001843)
- Keller, P. S., Catalán, N., von Schiller, D., Grossart, H. P., Koschorreck, M., Obrador, B., Frassl, M. A., Karakaya, N., Barros, N., Howitt, J. A., Mendoza-Lera, C., Pastor, A., Flaim, G., Aben, R., Riis, T., Arce, M. I., Onandia, G., Paranaíba, J. R., Linkhorst, A., del Campo, R., Amado, A. M., Cauvy-Fraunié, S., Brothers, S., Condon, J., Mendonça, R. F., Reverey, F., Room, E.-I., Datry, T., Roland, F., Laas, A., Obertegger, U., Park, J.-H., Wang, H., Kosten, S., Gómez, R., Feijoó, C., Elosegí, A., Sánchez-Montoya, Finlayson, C. M., Melita, M., Oliveira Junior, E. S., Muniz, C. C., Gómez-Gener, L., Leigh, C., Zhang, Q., & Marcé, R. (2020). Global CO₂ emissions from dry inland waters share common drivers across ecosystems. *Nature Communications*,

- 11, 1–8. <https://doi.org/10.1038/s41467-020-15929-y>
- Keller, P. S., Marcé, R., Obrador, B., & Koschorreck, M. (2021). Global carbon budget of reservoirs is overturned by the quantification of drawdown areas. *Nature Geoscience*, *14*, 402–408. <https://doi.org/10.1038/s41561-021-00734-z>
- Kellerman, A. M., Dittmar, T., Kothawala, D. N., & Tranvik, L. J. (2014). Chemodiversity of dissolved organic matter in lakes driven by climate and hydrology. *Nature Communications*, *5*, 3804. <https://doi.org/10.1038/ncomms4804>
- Kellerman, A. M., Kothawala, D. N., Dittmar, T., & Tranvik, L. J. (2015). Persistence of dissolved organic matter in lakes related to its molecular characteristics. *Nature Geoscience*, *8*, 454–457. <https://doi.org/10.1038/NGEO2440>
- Khan, H., Marcé, R., Laas, A., & Obrador, B. (2022). The relevance of pelagic calcification in the global carbon budget of lakes and reservoirs. *Limnetica*, *41*, 17–25. <https://doi.org/10.23818/limn.41.02>
- Kieber, D. J., McDaniel, J., & Mopper, K. (1989). Photochemical source of biological substrates in sea water: implication for carbon cycling. *Nature*, *341*, 637–639. <https://doi.org/10.1038/341637a0>
- Koehler, B., Wachenfeldt, E. Von, Kothawala, D., & Tranvik, L. J. (2012). Reactivity continuum of dissolved organic carbon decomposition in lake water. *Journal of Geophysical Research: Biogeosciences*, *117*, 1–14. <https://doi.org/10.1029/2011JG001793>
- Konapala, G., Mishra, A. K., Wada, Y., & Mann, M. E. (2020). Climate change will affect global water availability through compounding changes in seasonal precipitation and evaporation. *Nature Communications*, *11*, 3044. <https://doi.org/10.1038/s41467-020-16757-w>
- Kondolf, G. M., Rubin, Z. K., & Minear, J. T. (2014). Dams on the Mekong: Cumulative sediment starvation. *Water Resources Research*, *50*, 5158–5169. <https://doi.org/10.1002/2013WR014651>
- Kondolf, G. Mathias, Gao, Y., Annandale, G. W., Morris, G. L., Jiang, E., Zhang, J., Cao, Y., Carling, P., Fu, K., Guo, Q., Hotchkiss, R., Peteuil, C., Sumi, T., Wang, H.-W., Wang, Z., Wu, B., Wu, C., & Yang, C. T. (2014). Sustainable sediment management in reservoirs and regulated rivers: Experiences from five continents. *Earth's Future*, *2*, 256–280. <https://doi.org/10.1002/2013ef000184>
- Koschorreck, M., & Darwich, A. (2003). Nitrogen dynamics in seasonally flooded soils in the Amazon floodplain. *Wetlands Ecology and Management*, *11*, 317–318. <https://doi.org/10.1023/B:WETL.0000005536.39074.72>
- Kosten, S., Berg, S. Van Den, Mendonça, R., Paranaíba, J. R., Roland, F., Sobek, S., Van Den Hoek, J., & Barros, N. (2018). Extreme drought boosts CO₂ and CH₄ emissions from reservoir drawdown areas. *Inland Waters*, *8*, 329–340. <https://doi.org/10.1080/20442041.2018.1483126>
- Kothawala, D. N., Kellerman, A. M., Catalán, N., & Tranvik, L. J. (2021). Organic matter degradation across ecosystem boundaries: The need for a unified conceptualization. *Trends in Ecology and Evolution*, *36*, 113–122.

<https://doi.org/10.1016/j.tree.2020.10.006>

- Kuznetsov, S. I. (1958). A study of the size of bacterial populations and of organic matter formation due to photo- and chemosynthesis in water bodies of different types. *Internationale Vereinigung Für Theoretische Und Angewandte Limnologie: Verhandlungen*, *13*, 156–169. <https://doi.org/10.1080/03680770.1956.11895395>
- Larrañaga, A., Atristain, M., Von Schiller, D., & Elozegi, A. (2019). *Artikutza (Navarra): diagnóstico ambiental de la red fluvial previo al desmantelamiento de un embalse y resultados preliminares del efecto del vaciado*. *Revista Digital del Cedex 193*: 4–15. Retrieved from www.embalses.com
- Lehner, B., Liermann, C. R., Revenga, C., Vörösmarty, C., Fekete, B., Crouzet, P., Döll, P., Endejan, M., Frenken, K., Magome, J., Nilsson, C., Robertson, J. C., Rödel, R., Sindorf, N., & Wisser, D. (2011). High-resolution mapping of the world's reservoirs and dams for sustainable river-flow management. *Frontiers in Ecology and the Environment*, *9*, 494–502. <https://doi.org/doi:10.1890/100125>
- Lenhart, C. F. (2000). *The vegetation and hydrology of impoundments after dam removal in southern Wisconsin*. Master's thesis. University of Wisconsin, Madison, WI.
- Li, J., Jiang, M., Pei, J., Fang, C., Li, B., & Nie, M. (2023). Convergence of carbon sink magnitude and water table depth in global wetlands. *Ecology Letters*, *00*, 1–8. <https://doi.org/10.1111/ele.14199>
- Li, M., Peng, C., Zhu, Q., Zhou, X., Yang, G., Song, X., & Zhang, K. (2020). The significant contribution of lake depth in regulating global lake diffusive methane emissions. *Water Research*, *172*, 115465. <https://doi.org/10.1016/j.watres.2020.115465>
- Li, Y., Wang, S., & Zhang, L. (2015). Composition, source characteristic and indication of eutrophication of dissolved organic matter in the sediments of Erhai Lake. *Environmental Earth Sciences*, *74*, 3739–3751. <https://doi.org/10.1007/s12665-014-3964-4>
- Li, Y., Wang, S., Zhang, L., Zhao, H., Jiao, L., Zhao, Y., & He, X. (2014). Composition and spectroscopic characteristics of dissolved organic matter extracted from the sediment of Erhai Lake in China. *Journal of Soils and Sediments*, *14*, 1599–1611. <https://doi.org/10.1007/s11368-014-0916-2>
- Likens, G. E. (2009). *Biogeochemistry of inland waters*. (G. E. Likens, Ed.) (1st ed.). Amsterdam: Elsevier Science. Retrieved from http://catalog.ub.edu/record=b1953346~S1*cat
- Lima, I. B. T., Novo, E. M. L. M., Ballester, M. V. R., & Ometto, J. P. H. B. (1998). Methane production, transport and emission in Amazon hydroelectric plants. *Verhandlungen Der Internationalen Vereinigung Für Theoretische Und Angewandte Limnologie*, *2529–2531*. <https://doi.org/10.1109/IGARSS.1998.702268>
- Lindell, M., Granéli, W., & Tranvik, L. (1995). Enhanced bacterial growth in response to photochemical transformation of dissolved organic matter. *Limnology and Oceanography*, *40*, 195–199. <https://doi.org/10.4319/lo.1995.40.1.0195>
- Liu, F., Wang, D., Zhang, B., & Huang, J. (2021). Concentration and biodegradability of dissolved organic carbon derived from soils: A global perspective. *Science of the Total Environment*, *782*, 147217. <https://doi.org/10.1016/j.scitotenv.2021.147217>

- Environment*, 754, 142378. <https://doi.org/10.1016/j.scitotenv.2020.142378>
- Liu, H., Wu, Y., Ai, Z., Zhang, J., Zhang, C., Xue, S., & Liu, G. (2019). Effects of the interaction between temperature and revegetation on the microbial degradation of soil dissolved organic matter (DOM) – A DOM incubation experiment. *Geoderma*, 337, 812–824. <https://doi.org/10.1016/j.geoderma.2018.10.041>
- Liu, X., Liu, W., Tang, Q., Liu, B., Wada, Y., & Yang, H. (2022). Global agricultural water scarcity assessment incorporating blue and green water availability under future climate change. *Earth's Future*, 10, e2021EF002567. <https://doi.org/10.1029/2021EF002567>
- Logue, J. B., Robinson, C. T., Meier, C., & Van Der Meer, J. R. (2004). Relationship between sediment organic matter, bacteria composition, and the ecosystem metabolism of alpine streams. *Limnology and Oceanography*, 49, 2001–2010. <https://doi.org/10.4319/lo.2004.49.6.2001>
- Lovett, R. A. (2014). Rivers on the run. *Nature*, 511, 521–523. <https://doi.org/10.1038/511521a>
- Lozano, P., & Latasa, I. (2019). Vegetación. In: Artikutza, natura eta historia. Donostiako udaleko Osasun eta Ingurumen Saila. Donostia - San Sebastian, 50, 334–359. <https://doi.org/10.1029/2022GL102611>
- Luo, Y., & Zhou, X. (2010). *Soil respiration and the environment*. Elsevier Academy Press, Amsterdam.
- Maathuis, B. H. P., & Wang, L. (2006). Digital elevation model based hydro-processing. *Geocarto International*, 21, 21–26. <https://doi.org/10.1080/10106040608542370>
- Maavara, T., Chen, Q., Van Meter, K., Brown, L. E., Zhang, J., Ni, J., & Zarfl, C. (2020). River dam impacts on biogeochemical cycling. *Nature Reviews Earth and Environment*, 1, 103–116. <https://doi.org/10.1038/s43017-019-0019-0>
- Maavara, T., Lauerwald, R., Regnier, P., & Van Cappellen, P. (2017). Global perturbation of organic carbon cycling by river damming. *Nature Communications*, 8, 1–10. <https://doi.org/10.1038/ncomms15347>
- Madsen, H., & Thyregod, P. (2010). *Introduction to general and generalized linear models*. (B. P. Carlin, J. J. Faraway, M. Tanner, & J. Zidek, Eds.) (1st ed.). Boca Raton: CRC Press. <https://doi.org/10.1201/9781439891148>
- Maeck, A., DelSontro, T., McGinnis, D. F., Fischer, H., Flury, S., Schmidt, M., Fietzek, P., & Lorke, A. (2013). Sediment trapping by dams creates methane emission hot spots. *Environmental Science & Technology*, 47, 8130–8137. <https://doi.org/10.1021/es4003907>
- Magilligan, F. J., Graber, B. E., Nislow, K. H., Chipman, J. W., Sneddon, C. S., & Fox, C. A. (2016). River restoration by dam removal: Enhancing connectivity at watershed scales. *Elementa*, 2016, 1–14. <https://doi.org/10.12952/journal.elementa.000108>
- Magnusson, T. (1993). Carbon dioxide and methane formation in forest mineral and peat soils during aerobic and anaerobic incubations. *Soil Biology & Biogeochemistry*, 25, 877–883. [https://doi.org/10.1016/0038-0717\(93\)90090-X](https://doi.org/10.1016/0038-0717(93)90090-X)
- Manzoni, S., & Katul, G. (2014). Invariant soil water potential at zero microbial

- respiration explained by hydrological discontinuity in dry soils. *Geophysical Research Letters*, *41*, 7151–7158. <https://doi.org/10.1002/2014GL061467>
- Manzoni, S., Moyano, F., Kätterer, T., & Schimel, J. (2016). Modeling coupled enzymatic and solute transport controls on decomposition in drying soils. *Soil Biology and Biochemistry*, *95*, 275–287. <https://doi.org/10.1016/j.soilbio.2016.01.006>
- Mapes, L. V. (2016). Elwha: Roaring back to life. *The Seattle Times*, pp. 1–5.
- Marcé, R., Obrador, B., Gómez-Gener, L., Catalán, N., Koschorreck, M., Isabel, M., Singer, G., & von Schiller, D. (2019). Emissions from dry inland waters are a blind spot in the global carbon cycle. *Earth-Science Reviews*, *188*, 240–248. <https://doi.org/10.1016/j.earscirev.2018.11.012>
- Marcé, R., Obrador, B., Morguί, J. A., Lluίs Riera, J., López, P., & Armengol, J. (2015). Carbonate weathering as a driver of CO₂ supersaturation in lakes. *Nature Geoscience*, *8*, 107–111. <https://doi.org/10.1038/ngeo2341>
- Marks, J. C., Haden, G. A., O'Neill, M., & Pace, C. (2010). Effects of flow restoration and exotic species removal on recovery of native fish: Lessons from a dam decommissioning. *Restoration Ecology*, *18*, 934–943. <https://doi.org/10.1111/j.1526-100X.2009.00574.x>
- Martinez-Cruz, K., Sepulveda-Jauregui, A., Casper, P., Anthony, K. W., Smemo, K. A., & Thalasso, F. (2018). Ubiquitous and significant anaerobic oxidation of methane in freshwater lake sediments. *Water Research*, *144*, 332–340. <https://doi.org/10.1016/j.watres.2018.07.053>
- McGinnis, D. F., Greinert, J., Artemov, Y., Beaubien, S. E., & Wüest, A. (2006). Fate of rising methane bubbles in stratified waters: How much methane reaches the atmosphere? *Journal of Geophysical Research: Oceans*, *111*, C09007. <https://doi.org/10.1029/2005JC003183>
- McNear, D. H. (2013). The rhizosphere-roots, soil and everything in between. *Nature Education Knowledge*, *4*, 1. Retrieved from <http://cse.naro.affrc.go.jp>.
- MEA. (2005). *Ecosystems and human well-being: A report of the millennium ecosystem assessment*. Washington, DC. <https://doi.org/10.1196/annals.1439.003>
- Mekonnen, M., Keesstra, S. D., Stroosnijder, L., Baartman, J. E. M., & Maroulis, J. (2015). Soil conservation through sediment trapping: A review. *Land Degradation and Development*, *26*, 544–556. <https://doi.org/10.1002/ldr.2308>
- Mendonça, R., Müller, R. A., Clow, D., Verpoorter, C., Raymond, P., Tranvik, L. J., & Sobek, S. (2017). Organic carbon burial in global lakes and reservoirs. *Nature Communications*, *8*, 1694. <https://doi.org/10.1038/s41467-017-01789-6>
- Mendoza-Lera, C., Frossard, A., Knie, M., Federlein, L. L., Gessner, M. O., & Mutz, M. (2017). Importance of advective mass transfer and sediment surface area for streambed microbial communities. *Freshwater Biology*, *62*, 133–145. <https://doi.org/10.1111/fwb.12856>
- Mendoza-Lera, C., & Mutz, M. (2013). Microbial activity and sediment disturbance modulate the vertical water flux in sandy sediments. *Freshwater Science*, *32*, 26–38. <https://doi.org/10.1899/11-165.1>

- Mermillod-Blondin, F., Mauclaire, L., & Montuelle, B. (2005). Use of slow filtration columns to assess oxygen respiration, consumption of dissolved organic carbon, nitrogen transformations, and microbial parameters in hyporheic sediments. *Water Research*, *39*, 1687–1698. <https://doi.org/10.1016/j.watres.2005.02.003>
- Meshram, S. G., Ghorbani, M. A., Deo, R. C., Kashani, M. H., Meshram, C., & Karimi, V. (2019). New approach for sediment yield forecasting with a two-phase feedforward neuron network-particle swarm optimization model integrated with the gravitational search algorithm. *Water Resources Management*, *33*, 2335–2356. <https://doi.org/10.1007/s11269-019-02265-0>
- Messenger, M. L., Lehner, B., Grill, G., Nedeva, I., & Schmitt, O. (2016). Estimating the volume and age of water stored in global lakes using a geo-statistical approach. *Nature Communications*, *7*, 13603. <https://doi.org/10.1038/ncomms13603>
- Micklin, P. (2007). The Aral Sea disaster. *Annual Review of Earth and Planetary Sciences*, *35*, 47–72. <https://doi.org/10.1146/annurev.earth.35.031306.140120>
- Micklin, P. (2016). The future Aral Sea: hope and despair. *Environmental Earth Sciences*, *75*, 1–15. <https://doi.org/10.1007/s12665-016-5614-5>
- Miller, M. P., & McKnight, D. M. (2010). Comparison of seasonal changes in fluorescent dissolved organic matter among aquatic lake and stream sites in the Green Lakes Valley. *Journal of Geophysical Research*, *115*, 1–14. <https://doi.org/10.1029/2009jg000985>
- Miranda, E., Mutiara, A. B., & Wibowo, W. C. (2018). *Classification of land cover from Sentinel-2 imagery using supervised classification technique (preliminary study). 2018 international conference on information management and technology (ICIMTech). IEEE, 2018.*
- Mitsch, W. J., Bernal, B., Nahlik, A. M., Mander, Ü., Zhang, L., Anderson, C. J., Jorgensen, S. E., & Brix, H. (2013). Wetlands, carbon, and climate change. *Landscape Ecology*, *28*, 583–597. <https://doi.org/10.1007/s10980-012-9758-8>
- Mopper, K., & Stahovec, W. L. (1986). Sources and sinks of low molecular weight organic carbonyl compounds in seawater. *Marine Chemistry*, *19*, 305–321. [https://doi.org/https://doi.org/10.1016/0304-4203\(86\)90052-6](https://doi.org/https://doi.org/10.1016/0304-4203(86)90052-6)
- Mulholland, P. J., & Elwood, J. W. (1982). The role of lake and reservoir sediments as sinks in the perturbed global carbon cycle. *Tellus*, *34*, 490–499. <https://doi.org/10.3402/tellusa.v34i5.10834>
- Muñoz, I., Abril, M., Casas-Ruiz, J. P., Casellas, M., Gómez-Gener, L., Marcé, R., Menendez, M., Obrador, B., Sabater, S., von Schiller, D., & Acuña, V. (2018). Does the severity of non-flow periods influence ecosystem structure and function of temporary streams? A mesocosm study. *Freshwater Biology*, *63*, 613–625. <https://doi.org/10.1111/fwb.13098>
- Nourredine, H., Barjenbruch, M., Million, A., El Amrani, B., & Chakri, N. (2023). Linking urban water management, wastewater recycling, and environmental education: A case study of engaging youth in sustainable water resource management in public school in Casablanca City, Morocco. *Education Sciences*, *13*, 824.

<https://doi.org/10.3390/educsci13080824>

- Obrador, B., Schiller, D. Von, Marcé, R., Gómez-gener, L., Koschorreck, M., Borrego, C., & Catalán, N. (2018). Dry habitats sustain high CO₂ emissions from temporary ponds across seasons. *Scientific Reports*, *8*, 3015. <https://doi.org/10.1038/s41598-018-20969-y>
- Oki, T., & Kanae, S. (2006). Global hydrological cycles and world water resources. *Science*, *1068*, 1128845. <https://doi.org/10.1126/science.112884>
- Orr, C. H., & Stanley, E. H. (2006). Vegetation development and restoration potential of drained reservoirs following dam removal in Wisconsin. *River Research and Applications*, *22*, 281–295. <https://doi.org/10.1002/rra.891>
- Pacca, S. (2007). Impacts from decommissioning of hydroelectric dams: a life cycle perspective. *Climate Change*, *84*, 281–294. <https://doi.org/10.1007/s10584-007-9261-4>
- Paranaíba, J. R., Aben, R., Barros, N., Quadra, G., Linkhorst, A., Amado, A. M., Brothers, S., Catalán, N., Condon, J., Finlayson, C. M., Grossart, H.-P., Howitt, J., Oliveira Junior E. S., Keller, S. P., Koschorreck, M., Laas, A., Leigh, C., Marcé, R., Mendonça, R., Muniz, C. C., Obrador, B., Onandia, G., Raymundo, Reverey, F., Roland, F., Room, E.-I, Sobek, S., von Schiller, D., Wang, H., & Kosten, S. (2021). Cross-continental importance of CH₄ emissions from dry inland-waters. *Science of the Total Environment*, *814*, 151925. <https://doi.org/10.1016/j.scitotenv.2021.151925>
- Pekel, J. F., Cottam, A., Gorelick, N., & Belward, A. S. (2016). High-resolution mapping of global surface water and its long-term changes. *Nature*, *540*, 418–422. <https://doi.org/10.1038/nature20584>
- Perera, D., & North, T. (2021). The socio-economic impacts of aged-dam removal: A review. *Journal of Geoscience and Environment Protection*, *09*, 62–78. <https://doi.org/10.4236/gep.2021.910005>
- Perera, D., Smakhtin, V., Williams, S., North, T., & Curry, A. (2021). *Ageing water storage infrastructure: An emerging global risk*. Ottawa. <https://doi.org/10.13140/RG.2.2.29149.44003>
- Pimentel, D., Harvey, C., Resosudarmo, P., Sinclair, K., Kurz, D., McNair, M., Crist, S., Shpritz, L., Fitton, L., Saffouri, R., & Blair, R. (1995). Environmental and economic costs of soil erosion and conservation benefits. *Science*, *267*(5201), 1117–1123. <https://doi.org/10.1126/science.267.5201.1117>
- Pinheiro, J., & Bates, D. (2018). *nlme: Linear and nonlinear mixed effects models, R package version 3.1-137*. Retrieved from <https://bugs.r-project.org>
- Pinheiro, J. C., & Bates, D. M. (2000). *Mixed effects models in S and S-Plus*. (J. Chambers, W. Eddy, W. Hardle, S. Sheather, & L. Tierney, Eds.) (3rd ed.). New York: Springer.
- Pohl, M. M. (2002). Bringing down our dams: trends in American dam removal rationales. *Journal of the American Water Resources Association*, *38*, 1511–1518.
- Prach, K. (2003). Spontaneous succession in Central-European man-made habitats: What information can be used in restoration practice? *Applied Vegetation Science*,

- 6, 125–129. <https://doi.org/10.1111/j.1654-109X.2003.tb00572.x>
- Prach, K., Řehouňková, K., Lencová, K., Jírová, A., Konvalinková, P., Mudrák, O., Študent, V., Vaněček, Z., Tichý, L., Petřík, P., Šmilauer, P., & Pyšek, P. (2014). Vegetation succession in restoration of disturbed sites in Central Europe: The direction of succession and species richness across 19 seres. *Applied Vegetation Science*, *17*, 193–200. <https://doi.org/10.1111/avsc.12064>
- Pusch, M., & Schwoerbel, J. (1994). Community respiration in hyporheic sediments of a mountain stream (Steina, Black Forest). *Archiv Fur Hydrobiologie*, *130*, 35–52. <https://doi.org/10.1016/j.scitotenv.2005.01.043>
- Pusch, Martin. (1996). The metabolism of organic matter in hyporheic zone of a mountain stream, and its spatial distribution. *Hydrobiologia*, *323*, 107–118. <https://doi.org/10.1007/BF00017588>
- R Core Team. (2021). R: a language and environment for statistical computing. R Foundation for statistical computing, Vienna. Retrieved from: <http://www.R-project.org/>.
- Randle, T. J., Bountry, J. A., Ritchie, A., & Wille, K. (2015). Large-scale dam removal on the Elwha River, Washington, USA: Erosion of reservoir sediment. *Geomorphology*, *246*, 709–728. <https://doi.org/10.1016/j.geomorph.2014.12.045>
- Rathore, R., Kumar, V., Ranjan, A., Tiwari, S., Goswami, A., & Agwan, M. (2018). Extraction of watershed characteristics using GIS and digital elevation model. *International Journal of Research in Engineering*, *1*, 62–65. Retrieved from www.ijresm.com
- Raymond, P. A., Hartmann, J., Lauerwald, R., Sobek, S., McDonald, C., & Hoover, M. (2013). Global carbon dioxide emissions from inland waters. *Nature*, *503*, 5–9. <https://doi.org/10.1038/nature12760>
- Regnier, P., Friedlingstein, P., Ciais, P., Mackenzie, F. T., Gruber, N., Janssens, I. A., Laruelle, G. G., Lauerwald, R., Luyssaert, S., Andersson, A. J., Arndt, S., Arnosti, C., Borges, A. V., Dale, A. W., Gallego-Sala, A., Goddérís, Y., Goossens, N., Hartmann, J., Heinze, C., Ilyina, T., Joos, F., LaRowe, D. E., Leifeld, J., Meysman, F. J. R., Munhoven, G., Raymond, P. A., Spahni, R., Suntharalingam, P., & Thullner, M. (2013). Anthropogenic perturbation of the carbon fluxes from land to ocean. *Nature Geoscience*, *6*. <https://doi.org/10.1038/ngeo1830>
- Richter, B. D., Revenga, C., Scudder, T., Lehner, B., Churchill, A., & Chow, M. (2010). Lost in development's shadow: The downstream human consequences of dams. *Water Alternatives*, *3*, 14–42. Retrieved from www.water-alternatives.org
- Ritchie, A. C., Warrick, J. A., East, A. E., Magirl, C. S., Stevens, A. W., Bountry, J. A., Randle, T. J., Currant, C. A., Hildale, R. C., Duda, J. J., Gelfenbaum, G. R., Miller, I. M., Pess, G. R., Foley, M. M., McCoy, R., & Ogston, A. S. (2018). Morphodynamic evolution following sediment release from the world's largest dam removal. *Scientific Reports*, *8*, 13279. <https://doi.org/10.1038/s41598-018-30817-8>
- Rizinjirabake, F., Tenenbaum, D. E., & Pilesjö, P. (2019). Sources of soil dissolved organic carbon in a mixed agricultural and forested watershed in Rwanda. *Catena*, *181*,

104085. <https://doi.org/10.1016/j.catena.2019.104085>
- Rosentreter, J. A., Borges, A. V., Deemer, B. R., Holgerson, M. A., Liu, S., Song, C., Melack, J., Raymond, P. A., Duarte, C. M., Allen, G. H., Olefeldt, D., Poulter, B., Battin, T. I., & Eyre, B. D. (2021). Half of global methane emissions come from highly variable aquatic ecosystem sources. *Nature Geoscience*, *14*(Rovira), 225–230. <https://doi.org/10.1038/s41561-021-00715-2>
- Rovira, A. D. (1969). Plant root exudates. *The Botanical Review*, *35*, 35–57. <https://doi.org/10.1007/BF02859887>
- Sarkar, S. K., Saha, M., Takada, H., Bhattacharya, A., Mishra, P., & Bhattacharya, B. (2007). Water quality management in the low stretch of the river Ganges, east coast of India: an approach through environmental education. *Journal of Cleaner Production*, *15*, 1559–1567. <https://doi.org/10.1016/j.jclepro.2006.07.030>
- Saunois, M., Bousquet, P., Poulter, B., Peregon, A., Ciais, P., Canadell, J. G., Dlugokencky, E. J., Etiope, G., Bastviken, D., Houweling, S., Janssens-Maenhout, G., Tubiello, F. N., Castaldi, S., Jackson, R. B., Alexe, M., Arora, V. K., Beerling, D. J., Bergamaschi, P., Blake, D. R., Brailsford, G., Brovkin, V., Bruhwiler, L., Crevoisier, C., Cyrill, P.,... Zhu, Q. (2016). The global methane budget 2000-2012. *Earth System Science Data*, *8*, 697–751. <https://doi.org/10.5194/essd-8-697-2016>
- Saviozzi, A., Levi-Minzi, R., & Riffaldi, R. (1994). The effect of forty years of continuous corn cropping on soil organic matter characteristics. *Plant and Soil*, *160*, 139–145. <https://doi.org/10.1007/BF00150355>
- Sawakuchi, H. O., Neu, V., Ward, N. D., Barros, M. de L. C., Valerio, A. M., Gagne-Maynard, W., Cunha, A. C., Less, D. F. S., Diniz, J. E. M., Brito, D. C., Krusche, A. V., & Richey, J. E. (2017). Carbon dioxide emissions along the lower Amazon River. *Frontiers in Marine Science*, *4*, 76. <https://doi.org/10.3389/fmars.2017.00076>
- Schimel, J. P. (2018). Life in dry soils: Effects of drought on soil microbial communities and processes. *Annual Review of Ecology, Evolution, and Systematics*, *49*, 409–432. <https://doi.org/10.1146/annurev-ecolsys-110617>
- Schneider, C. A., Rasband, W., & Eliceiri, K. W. (2012). NIH Image to ImageJ: 25 years of image analysis. *Nature Methods*, *9*, 671–675. <http://dx.doi.org/10.1038/nmeth.2089>
- Serrano-Silva, N., Sarria-Guzmán, Y., Dendooven, L., & Luna-Guido, M. (2014). Methanogenesis and methanotrophy in soil: A review. *Pedosphere*, *24*, 291–307. [https://doi.org/10.1016/S1002-0160\(14\)60016-3](https://doi.org/10.1016/S1002-0160(14)60016-3)
- Shafroth, P. B., Friedman, J. M., Auble, G. T., Scott, M. L., & Braatne, J. H. (2002). Potential responses of riparian vegetation to dam removal. *BioScience*, *52*, 703–712.
- Shao, Z., He, P., Zhang, D., & Shao, L. (2009). Characterization of water-extractable organic matter during the biostabilization of municipal solid waste. *Journal of Hazardous Materials*, *164*, 1191–1197. <https://doi.org/10.1016/j.jhazmat.2008.09.035>
- Shaver, G R, & Chapin III, F. S. (1986). Effect of fertilizer on production and biomass of tussock tundra, Alaska, USA. *Arctic and Alpine Research*, *18*, 261–268. <https://doi.org/10.1080/00040851.1986.12004087>

- Shaver, Gaius R, Billings, W. D., Chapin, F. S., Giblin, A. E., Nadelhoffer, K. J., Oechel, W. C., & Rastetter, E. B. (1992). Global change and the carbon balance of arctic ecosystems. Carbon/nutrient interactions should act as major constraints on changes in global terrestrial carbon cycling. *Bioscience*, *42*, 433–441. <https://doi.org/10.2307/1311862>
- Smith, C. L., & Muirhead, R. W. (2023). A review of the effectiveness of sediment traps for New Zealand agriculture. *New Zealand Journal of Agricultural Research*. <https://doi.org/10.1080/00288233.2023.2184838>
- Sobek, S., Delsontro, T., Wongfun, N., & Wehrli, B. (2012). Extreme organic carbon burial fuels intense methane bubbling in a temperate reservoir. *Geophysical Research Letters*, *39*, 1–4. <https://doi.org/10.1029/2011GL050144>
- Sobek, S., Durisch-Kaiser, E., Zurbrugg, R., Wongfun, N., Wessels, M., Pasche, N., & Wehrli, B. (2009). Organic carbon burial efficiency in lake sediments controlled by oxygen exposure time and sediment source. *Limnology and Oceanography*, *54*, 2243–2254. <https://doi.org/10.4319/lo.2009.54.6.2243>
- Soued, C., Harrison, J. A., Mercier-Blais, S., & Prairie, Y. T. (2022). Reservoir CO₂ and CH₄ emissions and their climate impact over the period 1900–2060. *Nature Geoscience*, *15*, 700–705. <https://doi.org/10.1038/s41561-022-01004-2>
- St. Louis, V. L., Kelly, C. A., Duchemin, E., Rudd, J. W. M., & Rosenberg, D. M. (2000). Measuring fluxes of greenhouse gases from reservoir surfaces. *BioScience*, *50*, 766–775. [https://doi.org/10.1641/0006-3568\(2000\)050\[0766:RSASOG\]2.0.CO;2](https://doi.org/10.1641/0006-3568(2000)050[0766:RSASOG]2.0.CO;2)
- Stanley, E. H., Casson, N. J., Christel, S. T., Crawford, J. T., Loken, L. C., & Oliver, S. K. (2016). The ecology of methane in streams and rivers: Patterns, controls, and global significance. *Ecological Monographs*. Ecological Society of America. <https://doi.org/10.1890/15-1027>
- Stanley, E. H., & Doyle, M. W. (2003). Trading off: the ecological effects of dam removal. *Frontiers in Ecology and Environment*, *3220*, 15–22. <https://doi.org/10.2307/3867960>
- Stiling, P. D. (2002). *Ecology, theories and applications*. (T. Ryu, S. L. Snavelly, & E. Smith, Eds.) (4th ed.). New Jersey: Prentice-Hall, Inc.
- Stubbins, A., Lapierre, J. F., Berggren, M., Prairie, Y. T., Dittmar, T., & Del Giorgio, P. A. (2014). What's in an EEM? Molecular signatures associated with dissolved organic fluorescence in boreal Canada. *Environmental Science and Technology*, *48*, 10598–10606. <https://doi.org/10.1021/es502086e>
- Sung, K., Kim, J., Munster, C. L., Corapcioglu, M. Y., Park, S., Drew, M. C., & Chang, Y. Y. (2006). A simple approach to modeling microbial biomass in the rhizosphere. *Ecological Modelling*, *190*, 277–286. <https://doi.org/10.1016/j.ecolmodel.2005.04.020>
- Syvitski, J. P. M., Kettner, A. J., Overeem, I., Hutton, E. W. H., Hannon, M. T., Brakenridge, G. R., Day, J., Vörösmarty, C., Saito, Y., Giosan, L., & Nicholls, R. J. (2009). Sinking deltas due to human activities. *Nature Geoscience*, *2*, 681–686. <https://doi.org/10.1038/ngeo629>
- Szafranek-Nakonieczna, A., & Stępniewska, Z. (2014). Aerobic and anaerobic respiration in profiles of Polesie Lubelskie peatlands. *International Agrophysics*, *28*, 219–229.

<https://doi.org/10.2478/intag-2014-0011>

- Teodoru, C. R., Prairie, Y. T., & del Giorgio, P. A. (2011). Spatial heterogeneity of surface CO₂ fluxes in a newly created Eastmain-1 reservoir in northern Quebec, Canada. *Ecosystems*, *14*, 28–46. <https://doi.org/10.1007/s10021-010-9393-7>
- Thornton, K., Kimmel, B., & Payne, F. (1990). *Reservoir limnology: Ecological perspectives*. *Critical Reviews in Toxicology* (eds.). Informa Healthcare.
- Tockner, K., Bunn, S. E., Gordon, C., Naiman, R. J., Quinn, G. P., & Stanford, J. A. (2008). *Flood plains: critically threatened ecosystems*. In: *Polunin NVC (Ed). Aquatic ecosystems*. Cambridge, UK: Cambridge University Press.
- Tranvik, L. J., Downing, J. A., Cotner, J. B., Loiselle, S. A., Striegl, R. G., Ballatore, T. J., Dillon, P., Finlay, K., Fortino, K., Knoll, L. B., Kortelainen, P. L., Kutser, T., Larsen, S., Laurion, I., Leech, D. M., McCallister, S. L., McKnight, D. M., Melack, J. M., Overholt, E., Porter, J. A., Prairie, Y., Renwick, W. H., Roland, F., Sherman, B. S., Schindler, D. W., Sobek, S., Tremblay, A., Vanni, M. J., Verschoor, A. M., von Wachenfeldt, E., & Weyhenmeyer, G. A. (2009). Lakes and reservoirs as regulators of carbon cycling and climate. *Limnology and Oceanography*, *54*, 2298–2314.
- Turetsky, M. R., & Ripley, S. (2005). Decomposition in extreme-rich fens of Boreal Alberta, Canada. *Soil Science Society of America Journal*, *69*, 1856–1860. <https://doi.org/10.2136/sssaj2003.0084>
- Uehlinger, U., Naegeli, M., & Fisher, S. G. (2002). A heterotrophic desert stream? The role of sediment stability. *Western North American Naturalist*, *64*, 466–473.
- Ulseth, A. J., Hall, R. O., Boix Canadell, M., Madinger, H. L., Niayifar, A., & Battin, T. J. (2019). Distinct air–water gas exchange regimes in low- and high-energy streams. *Nature Geoscience*, *12*, 259–263. <https://doi.org/10.1038/s41561-019-0324-8>
- UN Water. (2019). *Leaving no one behind: the United Nations world water development report 2019*.
- USSD. (2015). *Guidelines for dam decommissioning projects*. Denver, US. Retrieved from www.ussdams.org
- Van Andel, J., Bakker, J. P., & Grootjans, A. P. (1993). Mechanisms of vegetation succession: a review of concepts and perspectives. *Acta Botanica Neerlandica*, *42*, 413–433. <https://doi.org/10.1111/j.1438-8677.1993.tb00718.x>
- van Bergen, T. J. H. M., Barros, N., Mendonça, R., Aben, R. C. H., Althuizen, I. H. J., Huszar, V., Huszar, V., Lamers, L. P. M., Lüring, M., Roland, F., & Kosten, S. (2019). Seasonal and diel variation in greenhouse gas emissions from an urban pond and its major drivers. *Limnology and Oceanography*, *64*, 2129–2139. <https://doi.org/10.1002/lno.11173>
- Vannote, R. L., Cummins, K. W., & Sedell, J. R. (1980). The river continuum concept. *Canadian Journal of Fisheries and Aquatic Sciences*, *37*, 130–137. <https://doi.org/10.1139/f80-017>
- Venkiteswaran, J. J., Schiff, S. L., St. Louis, V. L., Matthews, C. J. D., Boudreau, N. M., Joyce, E. M., Joyce, E. M., Beaty, K. G., & Bodaly, R. A. (2013). Processes affecting greenhouse gas production in experimental boreal reservoirs. *Global Biogeochemical*

- Cycles*, 27, 567–577. <https://doi.org/10.1002/gbc.20046>
- Vergnoux, A., Di Rocco, R., Domeizel, M., Guiliano, M., Doumenq, P., & Théraulaz, F. (2011). Effects of forest fires on water extractable organic matter and humic substances from Mediterranean soils: UV-vis and fluorescence spectroscopy approaches. *Geoderma*, 160, 434–443. <https://doi.org/10.1016/j.geoderma.2010.10.014>
- Verstraeten, G., & Poesen, J. (2001). Modelling the long-term sediment trap efficiency of small ponds. *Hydrological Processes*, 15, 2797–2819. <https://doi.org/10.1002/hyp.269>
- Villa, J. A., & Bernal, B. (2018). Carbon sequestration in wetlands, from science to practice: An overview of the biogeochemical process, measurement methods, and policy framework. *Ecological Engineering*, 114, 115–128. <https://doi.org/10.1016/j.ecoleng.2017.06.037>
- Vincent, S. G. T., Jennerjahn, T., & Ramasamy, K. (2021). Environmental variables and factors regulating microbial structure and functions. In *Microbial Communities in Coastal Sediments* (pp. 79–117). Elsevier. <https://doi.org/10.1016/b978-0-12-815165-5.00003-0>
- Vitousek, P. M., Mooney, H. a, Lubchenco, J., & Melillo, J. M. (1997). Human domination of Earth's ecosystems. *Science*, 277, 494–499. <https://doi.org/10.1126/science.277.5325.494>
- von Schiller, D., Datry, T., Corti, R., Foulquier, A., Tockner, K., Marcé, R., García-Baquero, G., Odriozola, I., Obrador, B., Elozegi, A., Mendoza-Lera, C., Gessner, M. O., Stubbington, R., Albariño, R., Allen, D. C., Altermatt, F., Arce, M. I., Arnon, S., Banas, D., Banegas-Medina, A., Beller, E., Blanchette, M. L.,...Zoppini, A. (2019). Sediment respiration pulses in intermittent rivers and ephemeral streams. *Global Biogeochemical Cycles*, 33, 1251–1263. <https://doi.org/10.1029/2019GB006276>
- Vörösmarty, C. J., McIntyre, P. B., Gessner, M. O., Dudgeon, D., Prusevich, A., Green, P., Glidden, S., Bunn, S. E., Sullivan, C. A., Liermann, C. R., & Davies, P. M. (2010). Global threats to human water security and river biodiversity. *Nature*, 467, 555–561. <https://doi.org/10.1038/nature09440>
- Vörösmarty, Charles J., Meybeck, M., Fekete, B., Sharma, K., Green, P., & Syvitski, J. P. M. (2003). Anthropogenic sediment retention: Major global impact from registered river impoundments. *Global and Planetary Change*, 39, 169–190. [https://doi.org/10.1016/S0921-8181\(03\)00023-7](https://doi.org/10.1016/S0921-8181(03)00023-7)
- Vranova, V., Rejsek, K., Skene, K. R., Janous, D., & Formanek, P. (2013). Methods of collection of plant root exudates in relation to plant metabolism and purpose: A review. *Journal of Plant Nutrition and Soil Science*, 176, 175–199. <https://doi.org/10.1002/jpln.201000360>
- Wagai, R., & Sollins, P. (2002). Biodegradation and regeneration of water-soluble carbon in a forest soil: Leaching column study. *Biology and Fertility of Soils*, 35, 18–26. <https://doi.org/10.1007/s00374-001-0434-4>
- Walz, J., Knoblauch, C., Böhme, L., & Pfeiffer, E. M. (2017). Regulation of soil organic matter decomposition in permafrost-affected Siberian tundra soils - Impact of oxygen

- availability, freezing and thawing, temperature, and labile organic matter. *Soil Biology and Biochemistry*, *110*, 34–43. <https://doi.org/10.1016/j.soilbio.2017.03.001>
- Wang, H., & He, G. (2022). Rivers: Linking nature, life, and civilization. *River*, *1*, 25–36. <https://doi.org/10.1002/rvr2.7>
- Wang, Jida, Song, C., Reager, J. T., Yao, F., Famiglietti, J. S., Sheng, Y., MacDonald, G. M., Brun, F., Schmied, H. M., Marston, R. A., & Wada, Y. (2018). Recent global decline in endorheic basin water storages. *Nature Geoscience*, *11*, 926–932. <https://doi.org/10.1038/s41561-018-0265-7>
- Wang, Jinli, Li, X., Zhang, J., Yao, T., Wei, D., Wang, Y., & Wang, J. (2012). Effect of root exudates on beneficial microorganisms-evidence from a continuous soybean monoculture. *Plant Ecology*, *213*, 1883–1892. <https://doi.org/10.1007/s11258-012-0088-3>
- Wang, S., Jiao, L., Yang, S., Jin, X., Liang, H., & Wu, F. (2011). Organic matter compositions and DOM release from the sediments of the shallow lakes in the middle and lower reaches of Yangtze River region, China. *Applied Geochemistry*, *26*, 1458–1463. <https://doi.org/10.1016/j.apgeochem.2011.05.019>
- Wang, W., Chen, J., Wang, S., & Li, W. (2022). Differences in the composition, source, and stability of suspended particulate matter and sediment organic matter in Hulun Lake, China. *Environmental Science and Pollution Research*, *30*, 27163–27174. <https://doi.org/10.1007/s11356-022-24096-0>
- Warrick, J. A., Duda, J. J., Magirl, C. S., & Curran, C. A. (2012). River turbidity and sediment loads during dam removal. *Eos, Transactions American Geophysical Union*, *93*, 425–426. <https://doi.org/10.1029/2012eo430002>
- Warrick, J. A., Stevens, A. W., Miller, I. M., Harrison, S. R., Ritchie, A. C., & Gelfenbaum, G. (2019). World’s largest dam removal reverses coastal erosion. *Scientific Reports*, *9*, 13968. <https://doi.org/10.1038/s41598-019-50387-7>
- Weathers, K. C., Strayer, D. L., & Likens, G. E. (2013). *Fundamentals of ecosystem science*. (K. C. Weathers, D. L. Strayer, & G. E. Likens, Eds.) (1st ed.). Amsterdam, The Netherlands: Elsevier.
- Webster, J. R., & Benfield, E. F. (1986). Vascular plant breakdown in freshwater ecosystems. *Annual Review of Ecology and Systematics*, *17*, 567–594. <https://doi.org/https://doi.org/10.1146/annurev.es.17.110186.003031>
- Weishaar, J. L., Aiken, G. R., Bergamaschi, B. A., Fram, M. S., Fujii, R., & Mopper, K. (2003). Evaluation of specific ultraviolet absorbance as an indicator of the chemical composition and reactivity of dissolved organic carbon. *Environmental Science and Technology*, *37*, 4702–4708. <https://doi.org/10.1021/es030360x>
- West, W. E., Coloso, J. J., & Jones, S. E. (2012). Effects of algal and terrestrial carbon on methane production rates and methanogen community structure in a temperate lake sediment. *Freshwater Biology*, *57*, 949–955. <https://doi.org/10.1111/j.1365-2427.2012.02755.x>
- West, W. E., Creamer, K. P., & Jones, S. E. (2016). Productivity and depth regulate lake contributions to atmospheric methane. *Limnology and Oceanography*, *61*, S51–S61.

<https://doi.org/10.1002/lno.10247>

- Wetzel, R. G. (2001). *Limnology, lake and river ecosystems*. (Third edition). San Diego: Academic Press. Retrieved from <http://www.elsevier.com>
- Wetzel, R. G., Hatcher, P. G., & Bianchi, T. S. (1995). Natural photolysis by ultraviolet irradiance of recalcitrant dissolved organic matter to simple substrates for rapid bacterial metabolism. *Limnol. Oceanogr.*, *40*, 1369–1380. <https://doi.org/https://doi.org/10.4319/lo.1995.40.8.1369>
- Wickland, K. P., Waldrop, M. P., Aiken, G. R., Koch, J. C., Jorgenson, M. T., & Striegl, R. G. (2018). Dissolved organic carbon and nitrogen release from boreal Holocene permafrost and seasonally frozen soils of Alaska. *Environmental Research Letters*, *13*, 065011. <https://doi.org/10.1088/1748-9326/aac4ad>
- Wik, M., Thornton, B. F., Bastviken, D., Uhlbäck, J., & Crill, P. M. (2016). Biased sampling methane release from northern lakes: A problem of extrapolation. *Geophysical Research Letters*, *43*, 1256–1262. <https://doi.org/10.1002/2015GL066501>
- Wik, S. J. (1995). Reservoir drawdown: Case study in flow changes to potentially improve fisheries. *Journal of Energy Engineering*, *121*, 89–96. [https://doi.org/10.1061/\(ASCE\)0733-9402\(1995\)121:2\(89\)](https://doi.org/10.1061/(ASCE)0733-9402(1995)121:2(89))
- Wilcox, A. C., O'Connor, J. E., & Major, J. J. (2014). Rapid reservoir erosion, hyperconcentrated flow, and downstream deposition triggered by breaching of 38 m tall Condit Dam, White Salmon River, Washington. *Journal of Geophysical Research: Earth Surface*, *119*, 1376–1394. <https://doi.org/10.1002/2013JF003073>
- Wilczek, S., Fischer, H., Brunke, M., & Pusch, M. T. (2004). Microbial activity within a subaqueous dune in a large lowland (River Elbe, Germany). *Aquatic Microbial Ecology*, *36*, 83–97. <https://doi.org/10.3354/ame036083>
- Winton, R. S., Calamita, E., & Wehrl, B. (2019). Reviews and syntheses: Dams, water quality and tropical reservoir stratification. *Biogeosciences*, *16*, 1657–1671. <https://doi.org/10.5194/bg-16-1657-2019>
- Woo, M. K., Fang, G., & DiCenzo, P. D. (1997). The role of vegetation in the retardation of rill erosion. *Catena*, *29*, 145–159. [https://doi.org/10.1016/S0341-8162\(96\)00052-5](https://doi.org/10.1016/S0341-8162(96)00052-5)
- Wu, Y., & Jiang, Y. (2016). A case study on the method-induced difference in the chemical properties and biodegradability of soil water extractable organic carbon of a granitic forest soil. *Science of the Total Environment*, *565*, 656–662. <https://doi.org/10.1016/j.scitotenv.2016.04.201>
- Xu, P., Zhu, J., Fu, Q., Chen, J., Hu, H., & Huang, Q. (2018). Structure and biodegradability of dissolved organic matter from Ultisol treated with long-term fertilizations. *Journal of Soils and Sediments*, *18*, 1865–1872. <https://doi.org/10.1007/s11368-018-1944-0>
- Yalkowsky, S. H., He, Y., & Jain, P. (2010). *Handbook of aqueous solubility data*. (Second ed). Boca Raton, London, New York: CRC Press.
- Yang, M., Geng, X., Grace, J., Lu, C., Zhu, Y., Zhou, Y., & Lei, G. (2014). Spatial and seasonal CH₄ flux in the littoral zone of Miyun Reservoir near Beijing: The effects of

- water level and its fluctuation. *PloS One*, *9*, e94275. <https://doi.org/10.1371/journal.pone.0094275>
- Yang, R., Yang, S., Chen, L. Ian, Yang, Z., Xu, L., Zhang, X., Zhai, B., Wang, Z., Zheng, W., Li, Z., & Zamanian, K. (2023). Effect of vegetation restoration on soil erosion control and soil carbon and nitrogen dynamics: A meta-analysis. *Soil and Tillage Research*, *230*, 105705. <https://doi.org/10.1016/j.still.2023.105705>
- Yao, F., Livneh, B., Rajagopalan, B., Wang, J., Crétaux, J.-F., Wada, Y., & Berge-Nguyen, M. (2023). Satellites reveal widespread decline in global lake water storage. *Science*, *380*, 743–749. <https://doi.org/10.1126/science.abo2812>
- Zamarrón-Mieza, I., Yepes, V., & Moreno-Jiménez, J. M. (2017). A systematic review of application of multi-criteria decision analysis for aging-dam management. *Journal of Cleaner Production*. Elsevier Ltd. <https://doi.org/10.1016/j.jclepro.2017.01.092>
- Zarfl, C., Lumsdon, A. E., & Tockner, K. (2015). A global boom in hydropower dam construction. *Aquatic Sciences*, *77*, 161–170. <https://doi.org/10.1007/s00027-014-0377-0>
- Zhang, H., Lauerwald, R., Ciais, P., Van Oost, K., Guenet, B., & Regnier, P. (2022). Global changes alter the amount and composition of land carbon deliveries to European rivers and seas. *Communications Earth and Environment*, *3*, 245. <https://doi.org/10.1038/s43247-022-00575-7>
- Zhao, A., Zhang, M., & He, Z. (2013). Spectroscopic characteristics and biodegradability of cold and hot water-extractable soil organic matter under different land uses in Subarctic Alaska. *Communications in Soil Science and Plant Analysis*, *44*, 3030–3048. <https://doi.org/10.1080/00103624.2013.829086>
- Zhao, Z., Peng, C., Yang, Q., Meng, F. R., Song, X., Chen, S., Epule, T. E., Li, P., & Zhu, Q. (2017). Model prediction of biome-specific global soil respiration from 1960 to 2012. *Earth's Future*, *5*, 715–729. <https://doi.org/10.1002/2016EF000480>
- Zhu, T., Duan, P., He, J., Zhao, M., & Li, M. (2017). Sources, composition, and spectroscopic characteristics of dissolved organic matter extracted from sediments in an anthropogenic-impacted river in Southeastern China. *Environmental Science and Pollution Research*, *24*, 25431–25440. <https://doi.org/10.1007/s11356-017-0224-7>
- Zohary, T., & Ostrovsky, I. (2011). Ecological impacts of excessive water level fluctuations in stratified freshwater lakes. *Inland Waters*, *1*, 47–59. <https://doi.org/10.5268/iw-1.1.406>
- Zsolnay, A. (1996). Dissolved humus in soil waters. In *Humic Substances in Terrestrial Ecosystems* (pp. 171–223). <https://doi.org/https://doi.org/10.1016/B978-044481516-3/50005-0>

9. Appendices

9. 1. Supplemental information Chapter 3

Table S.3.1 Sites sampled for CO₂ and CH₄ fluxes within the transects in exposed sediment. The latitude and longitude (°), and elevation (masl: meters above sea level) of each site is shown.

Transect	Site	Latitude (°)	Longitude (°)	Elevation (m)
A	A1	43.21684	-1.784684	340
	A2	43.216885	-1.784684	341
	A3	43.216953	-1.7847	342
B	B1	43.216434	-1.78665	336
	B2	43.216628	-1.786541	337
	B3	43.216686	-1.78645	338
	B4	43.216755	-1.786456	339
C	C1	43.2163	-1.788418	333
	C2	43.216713	-1.788406	335
	C3	43.216904	-1.788108	337
	C4	43.21696	-1.788067	340
	C5	43.21696	-1.788067	340
D	D1	43.214336	-1.790767	329
	D2	43.214417	-1.790907	332
	D3	43.214893	-1.791266	341

Table S.3.2 Mixed modelling results for CO₂ fluxes: parameter estimation. The estimate of the parameter ρ for the compound symmetry correlation structure was $\rho = 0.01$; the coefficients for the strata-specific standard deviations were 1.0 for exposed sediment, 0.11 for impounded water, and 0.34 for running water; between- and within-site (residual) variability were $s_S = 49.45$ and $s_R = 165.17$, respectively, EnvXTime means interaction between environment and time. See Fig.3. 2.

	Parameter estimate	SE parameter	95% parameter	C.I.	df	<i>t</i>	<i>p</i>
Environment							
Exposed Sediment	0.06	0.10	(-0.14, 0.25)		35	0.61	0.545
Impounded water	1.76	1.11	(-0.50, 4.01)		35	1.58	0.122

Running water	-1.02	1.72	(-4.51, 2.48)	35	-0.59	0.559
Time	0.00	0.00	(0.00, 0.00)	35	-0.66	0.517
EnvXTime						
Impounded water	0.00	0.00	(0.00, 0.00)	35	-0.35	0.732
Running water	0.00	0.00	(0.00, 0.00)	35	0.82	0.419

Table S.3.3 Mixed modelling results for total CH₄ fluxes: parameter estimation. The estimate of the parameter ρ for the compound symmetry correlation structure was $\rho = -0.14$; the coefficients for the strata-specific standard deviations were 1.0 (exposed sediment), 13.51 (impounded water), and 19.13 (running water); between- and within-site (residual) variability were $s_S = 0.04$ and $s_R = 0.08$, respectively, EnvXTime means interaction between environment and time.

	Parameter estimate	SE parameter	95% parameter	C.I.	df	<i>t</i>	<i>p</i>
Environment							
Exposed sediment	295.65	74.90	(148.15, 443.16)		25	3.95	<
					5		0.001
Impounded water	-332.30	83.40	(-496.54, -168.06)		25	-3.98	<
					5		0.001
Running water	-107.54	86.09	(-277.07, 61.99)		25	-1.25	
					5		0.213
Time	-0.11	0.07	(-0.24, 0.02)		25	-1.64	
					5		0.103
EnvXTime							
Impounded water	0.15	0.07	(0.00, 0.29)		25	1.98	
					5		0.048
Running water	-0.03	0.07	(-0.17, 0.12)		25	-0.37	
					5		0.711

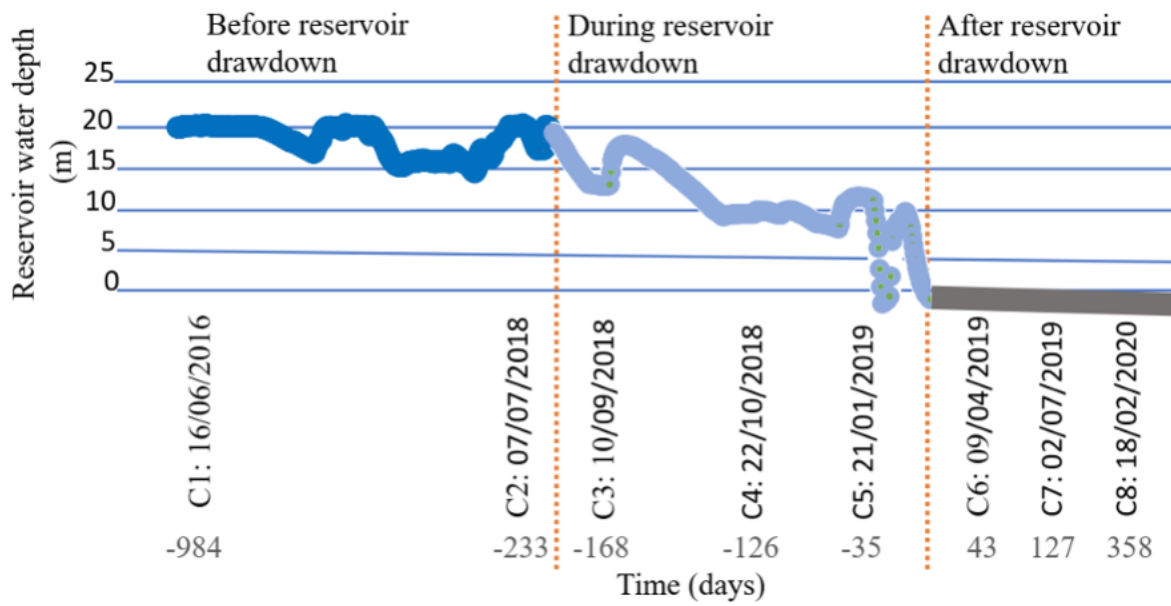


Figure S.3.1 Daily water level dynamics in the Enobieta reservoir before (dark blue), during (light blue), and after reservoir drawdown (grey: when there was not any impounded water). Data from the Donostia- San Sebastian City Council

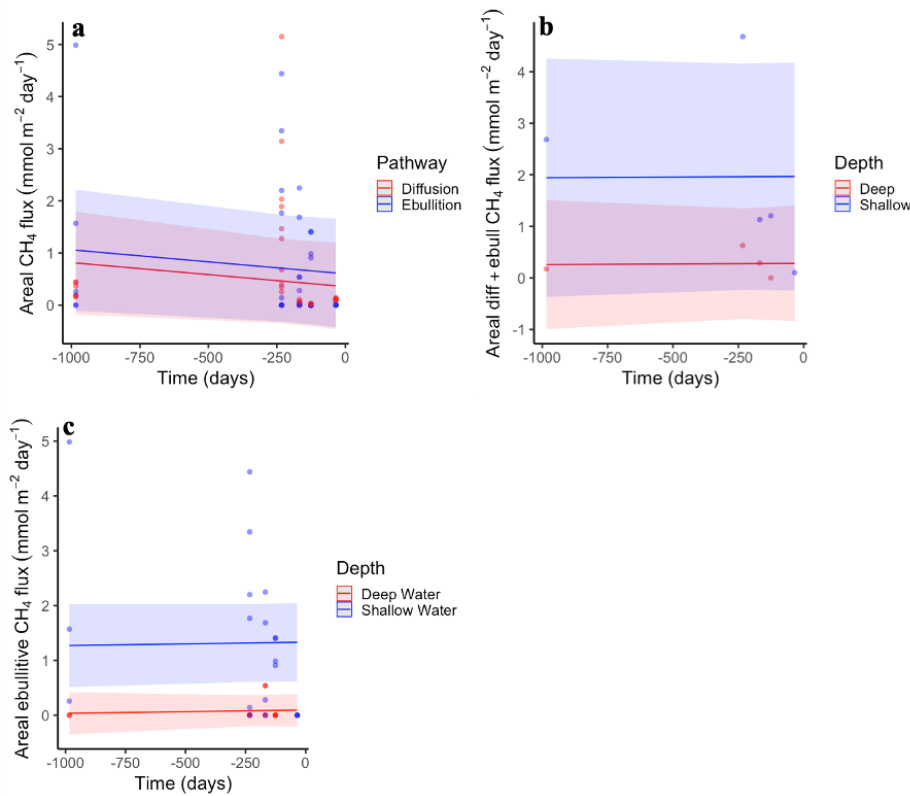


Figure S.3.2 Areal diffusive and ebullitive CH₄ fluxes (a), areal diffusive + ebullitive CH₄ fluxes from deep and shallow impounded water (b), areal ebullitive CH₄ fluxes from deep and shallow water (c), shaded areas correspond to the 95% confidence interval. Lines represent results of the mixed effects modelling

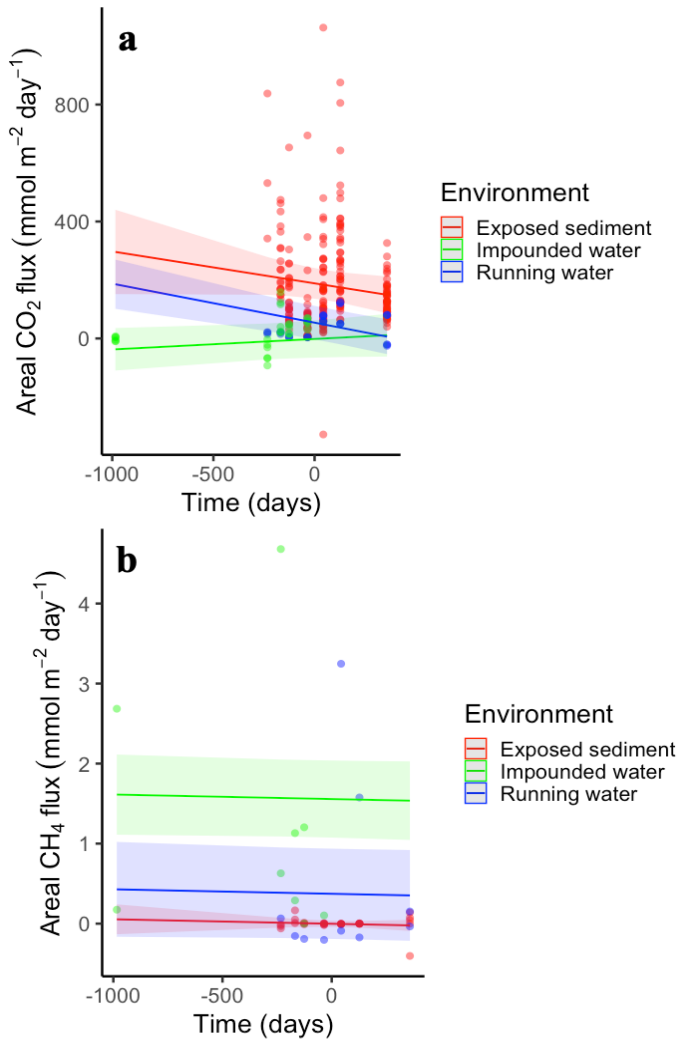


Figure S.3.3 Temporal changes of areal CO₂ (a) and CH₄ (b) fluxes (point estimates and shaded areas correspond to 95% confidence interval) over time for exposed sediment, impounded water and running water. Lines represent results of the mixed effects modelling with available data of all environments. We made the projection to the space where there is no data because the sampling on -984 days was conducted for only impounded water. Each vertical column of data points corresponds to a sampling campaign. The values below $y = 0$ indicate negative CO₂ fluxes or CO₂ uptake by the reservoir

9. 2. Supplemental information Chapter 4

Table S.4.1 Campaign and date (day/month/year) of the samplings, site, and the last inundation date and sediment exposure time (i.e., time since last inundation) for each site.

Campaign	Sampling date	Site		Sediment exposure time
			Last inundation date	
C1	10/09/2018	A	04/08/2018	37
C1	10/09/2018	B	27/07/2018	44
C1	10/09/2018	C	18/07/2018	54
C1	10/09/2018	D	01/09/2018	9
C1	10/09/2018	E	21/08/2018	20
C1	10/09/2018	F	13/08/2018	28
C2	22/10/2018	A	04/08/2018	79
C2	22/10/2018	B	27/07/2018	86
C2	22/10/2018	C	18/07/2018	96
C2	22/10/2018	D	01/09/2018	51
C2	22/10/2018	E	21/08/2018	62
C2	22/10/2018	F	13/08/2018	70
C3	21/01/2019	A	04/08/2018	170
C3	21/01/2019	B	27/07/2018	177
C3	21/01/2019	C	18/07/2018	187
C3	21/01/2019	D	01/09/2018	142
C3	21/01/2019	E	21/08/2018	153
C4	21/01/2019	F	13/08/2018	161
C4	09/04/2019	A	04/08/2018	248
C4	09/04/2019	B	27/07/2018	255
C4	09/04/2019	C	18/07/2018	265
C4	09/04/2019	D	01/09/2018	220
C4	09/04/2019	E	21/08/2018	231
C4	09/04/2019	F	13/08/2018	239
C5	02/07/2019	A	04/08/2018	454
C5	02/07/2019	B	27/07/2018	339
C5	02/07/2019	C	18/07/2018	349
C5	02/07/2019	D	01/09/2018	304
C5	02/07/2019	E	21/08/2018	315
C5	02/07/2019	F	13/08/2018	323
C6	18/02/2020	A	04/08/2018	563
C6	18/02/2020	B	27/07/2018	570
C6	18/02/2020	C	18/07/2018	580
C6	18/02/2020	D	01/09/2018	535

C6	18/02/2020	E	21/08/2018	546
C6	18/02/2020	F	13/08/2018	554

Table S.4.2 Site, number of samples collected at each site for each campaign (n), longitude, latitude, and elevation of each site.

Site	n	Longitude (°)	Latitude (°)	Elevation (m)
A	3	-1.784684	43.21684	339.2
B	3	-1.784684	43.216885	342.3
C	3	-1.7847	43.216953	345.2
D	3	-1.786541	43.216628	335.2
E	3	-1.78645	43.216686	335.2
F	3	-1.786456	43.216755	335.2

Table S.4.3–7 The content and respiration of bulk and water-extractable organic matter (WEOM) in dry sediments from inland waters and dry soils. We calculated the mean, standard error (SE), and the range of each parameter by considering each row as a data point. We converted respiration rates in $\mu\text{g CO}_2 \text{ g}^{-1} \text{ dry sediment/soil h}^{-1}$ to $\mu\text{g O}_2 \text{ g}^{-1} \text{ dry sediment/soil h}^{-1}$ by assuming a respiratory coefficient of 1 between CO_2 and O_2 for aerobic incubation, and, thus, by multiplying the magnitude of respiration rate by 0.73 (32 g of consumed $\text{O}_2/44 \text{ g}$ of produced CO_2).

Table S.4.3 The content of WEOM (mean \pm SE; range: 0.52 ± 0.06 , 0.01–1.06 mg C g^{-1} dry sediment) in dry sediments from lakes, and %BDOC (mean = 57.97 %) in 3 reservoirs and 1 wetland for incubations of an average time of 28 days at 28 °C.

Reference	System	Name, location	Sed/soil	Drying	Extractant	[WEOC]		Incub time (days)	BDOC (%)	Comment
						Mean	Unit			
(Han et al., 2021)	Lake	Yangtze River, China	Sediment	Freeze-dried	Ultrapure water	0.01	mg C/g sed			
(Wang et al., 2022)	Lake	Lake Hulun, China	Sediment	Freeze-dried	Ultrapure water	0.63	mg C/g sed			
	Lake	Dongting Lake, China	Sediment	Freeze-dried	Milli-Q water	0.2	mg C/g sed			
(Li et al., 2014)	Lake	Lake Erhai, China	Sediment	Freeze-dried	Water	0.3	mg C/g sed			
(Gu et al., 2020)	Wetland	Wetland	Soil	Dried at 45 °C	Milli-Q water	0.2	mg C/g sed	30	56.3	
(Li et al., 2015)	Lake	Lake Erhai, China	Sediment	Freeze-dried	Milli-Q water	0.5	mg C/g sed			January-Northern
(Li et al., 2015)	Lake	Lake Erhai, China	Sediment	Freeze-dried	Milli-Q water	0.37	mg C/g sed			January-Central
(Li et al., 2015)	Lake	Lake Erhai, China	Sediment	Freeze-dried	Milli-Q water	0.58	mg C/g sed			January-Southern
(Li et al., 2015)	Lake	Lake Erhai, China	Sediment	Freeze-dried	Milli-Q water	0.54	mg C/g sed			April-Northern
(Li et al., 2015)	Lake	Lake Erhai, China	Sediment	Freeze-dried	Milli-Q water	0.35	mg C/g sed			April-central
(Li et al., 2015)	Lake	Lake Erhai, China	Sediment	Freeze-dried	Milli-Q water	0.23	mg C/g sed			April-southern

(Li et al., 2015)	Lake	Lake Erhai, China	Sediment	Freeze-dried	Milli-Q water	0.47	mg C/g sed		July-Northern
(Li et al., 2015)	Lake	Lake Erhai, China	Sediment	Freeze-dried	Milli-Q water	0.31	mg C/g sed		July-Central
(Li et al., 2015)	Lake	Lake Erhai, China	Sediment	Freeze-dried	Milli-Q water	0.38	mg C/g sed		July-Southern
(Li et al., 2015)	Lake	Lake Erhai, China	Sediment	Freeze-dried	Milli-Q water	0.39	mg C/g sed		October-Northern
(Li et al., 2015)	Lake	Lake Erhai, China	Sediment	Freeze-dried	Milli-Q water	0.34	mg C/g sed		October-Central
(Li et al., 2015)	Lake	Lake Erhai, China	Sediment	Freeze-dried	Milli-Q water	0.39	mg C/g sed		October-Southern
(Wang et al., 2011)	Lake	Lake Poyang, China	Sediment	Freeze-dried	Distilled water	0.76	mg C/g sed		B-1
(Wang et al., 2011)	Lake	Lake Poyang, China	Sediment	Freeze-dried	Distilled water	0.56	mg C/g sed		B-2
(Wang et al., 2011)	Lake	Dongting Lake, China	Sediment	Freeze-dried	Distilled water	0.82	mg C/g sed		
(Wang et al., 2011)	Lake	Lake Hongze, China	Sediment	Freeze-dried	Distilled water	0.76	mg C/g sed		
(Wang et al., 2011)	Lake	Lake Xuanwu, China	Sediment	Freeze-dried	Distilled water	1.04	mg C/g sed		
(Wang et al., 2011)	Lake	Lake Yue, China	Sediment	Freeze-dried	Distilled water	1.06	mg C/g sed		site 1
(Wang et al., 2011)	Lake	Lake Yue, China	Sediment	Freeze-dried	Distilled water	1.06	mg C/g sed		Site 2
(Wang et al., 2011)	Lake	Lake Wuli, China	Sediment	Freeze-dried	Distilled water	1.06	mg C/g sed		
(Wang et al., 2011)	Lake	Lake Gong, China	Sediment	Freeze-dried	Distilled water	0.48	mg C/g sed		
(Wang et al., 2011)	Lake	Lake East Taihu, China	Sediment	Freeze-dried	Distilled water	0.5	mg C/g sed		
(Liu et al., 2019)	Lake	Hafeng Lake of Kaixian, China	Sediment	Air-dried	Distilled water	NA		28	46.6

WEOC in mg L⁻¹

(Heslop et al., 2017)	Lake	Vault Lake, US	Sediment	Oven-dried		0.25				Slurry filtration
(Heslop et al., 2017)	Lake	Vault Lake, US	Sediment	Oven-dried		0.19				Slurry filtration
(Liu et al., 2021)	Reservoir	Zhenxi of Fulin, China	Sediment	Air-dried	Distilled water	NA	28	58.6		WEOC in mg L ⁻¹
(Liu et al., 2021)	Reservoir	Shibaozhai of Zhongxian, China	Sediment	Air-dried	Distilled water	NA	28	59.2		WEOC in mg L ⁻¹
(Liu et al., 2021)	Reservoir	Tujing Zhongxian, China	Sediment	Air-dried	Distilled water	NA	28	57.8		WEOC in mg L ⁻¹

Table S.4.4 The global content of soil WEOM (mean \pm SE, range: 0.35 ± 0.03 , 0–1.7 mg C g⁻¹ dry soil) and %BDOC (22.07 ± 1.36 , 4.08–60.73 %) in dry soils. The average incubation temperature is 16.90 °C and average incubation time is 50 days.

Reference	Ecosystem	Soil layer	Drying method	Extraction medium	Filter size (µm)	Incubation temp (° C)	Incubation time (days)	[WEOC]	BDOC loss	(% Comment)
(Liu et al., 2019)	Arable soil	Top 20 cm	Air dried	Distilled water	0.45	35	60	0.02	39.7	Sloped cropland
(Liu et al., 2019)	Grassland soil	Top 20 cm	Air dried	Distilled water	0.45	35	60	0.04	28.9	Grassland
(Liu et al., 2019)	Shrubland soil	Top 20 cm	Air dried	Distilled water	0.45	35	60	0.06	29.9	Shrubland
(Liu et al., 2019)	Woodland soil	Top 20 cm	Air dried	Distilled water	0.45	35	60	0.04	25.2	Woodland
(Liu et al., 2019)	Arable soil	Top 20 cm	Air dried	Distilled water	0.45	20	60	0.02	32.6	Sloped cropland
(Liu et al., 2019)	Grassland soil	Top 20 cm	Air dried	Distilled water	0.45	20	60	0.04	22.7	Grassland
(Liu et al., 2019)	Shrubland soil	Top 20 cm	Air dried	Distilled water	0.45	20	60	0.06	27	Shrubland
(Liu et al., 2019)	Woodland soil	Top 20 cm	Air dried	Distilled water	0.45	20	60	0.04	22.1	Woodland

(Liu et al., 2019)	Arable soil	Top 20 cm	Air dried	Distilled water	0.45	4	60	0.02	18.2	Sloped cropland
(Liu et al., 2019)	Grassland soil	Top 20 cm	Air dried	Distilled water	0.45	4	60	0.04	15.9	Grassland
(Liu et al., 2019)	Shrubland soil	Top 20 cm	Air dried	Distilled water	0.45	4	60	0.06	23.5	Shrubland
(Liu et al., 2019)	Woodland soil	Top 20 cm	Air dried	Distilled water	0.45	4	60	0.04	19.3	Woodland
(Gu et al., 2020)	Cropland soil	Surface	Dried at 45 °C	Milli-Q water	0.22	NM	30	0.25	46.7	Cropland soil
(Xu et al., 2018)	Arable soil	Surface	Air-dried	Deionized water	0.45	Room Temp (NM)	21	0.02	23.9	Non fertilized soil
(Xu et al., 2018)	Arable soil	Surface	Air-dried	Deionized water	0.45	Room Temp (NM)	21	0.02	28.7	Soil fertilized with NPK
(Xu et al., 2018)	Arable soil	Surface	Air-dried	Deionized water	0.45	Room Temp (NM)	21	0.04	34.2	Soil fertilized with NPK and straw
(Xu et al., 2018)	Arable soil	Surface	Air-dried	Deionized water	0.45	Room Temp (NM)	21	0.06	42.7	Soil fertilized with manure
(Chantigny et al., 2014)	Arable soil	Top 15 cm	Air-dried	Deionized water	NM	NM	NM	0.2	ND	No incubation
(Chantigny et al., 2014)	Arable soil	Top 15 cm	Air-dried	Deionized water	NM	NM	NM	0.25	ND	No incubation
(Chantigny et al., 2014)	Grassland soil	Top 15 cm	Air-dried	Deionized water	NM	NM	NM	0.5	ND	No incubation
(Chantigny et al., 2014)	Grassland soil	Top 15 cm	Air-dried	Deionized water	NM	NM	NM	0.55	ND	No incubation
(Gregorich et al., 2003)	Arable soil	Top 15 cm	Air-dried	Deionized water	0.45	35	40	0.57	40	Fertilized with manure
(Gregorich et al., 2003)	Arable soil	Top 15 cm	Air-dried	Deionized water	0.45	35	40	0.28	40	No fertilizer
(Gregorich et al., 2003)	Arable soil	Top 15 cm	Air-dried	Deionized water	0.45	35	40	0.4	45	Crop rotation + manure
(Gregorich et al., 2003)	Arable soil	Top 15 cm	Air-dried	Deionized water	0.45	35	40	0.4	50	Crop rotation + inorganic fertilizer
(Boyer & Groffman, 1996)	Forest soil	10 cm	Moist soil	Nanopure water	NM (Whatman GF/F)	20	14	0.2	21	Dw estimated

(Boyer & Groffman, 1996)	Arable soil	10 cm	Moist soil	Nanopure water	NM (Whatman GF/F)	20	14	0.4	26	Dw estimated		
(Boyer & Groffman, 1996)	Forest soil	30 cm	Moist soil	Nanopure water	NM (Whatman GF/F)	20	14	0.1	25	Dw estimated		
(Boyer & Groffman, 1996)	Arable soil	30 cm	Moist soil	Nanopure water	NM (Whatman GF/F)	20	14	0.36	17	Dw estimated		
(Boyer & Groffman, 1996)	Forest soil	50 cm	Moist soil	Nanopure water	NM (Whatman GF/F)	20	14	0.2	25	Dw estimated		
(Boyer & Groffman, 1996)	Arable soil	50 cm	Moist soil	Nanopure water	NM (Whatman GF/F)	20	14	0.2	11	Dw estimated		
(Boyer & Groffman, 1996)	Forest soil	70 cm	Moist soil	Nanopure water	NM (Whatman GF/F)	20	14	0.1	11	Dw estimated		
(Boyer & Groffman, 1996)	Arable soil	70 cm	Moist soil	Nanopure water	NM (Whatman GF/F)	20	14	0.1	11	Dw estimated		
(Saviozzi et al., 1994)	Grassland soil	Surface	Air-dried	Distilled water	0.2	ND	ND	0.1	ND	After fire, estimated	sediment	dw
(Saviozzi et al., 1994)	Arable soil	Surface	Air-dried	Distilled water	0.2	ND	ND	0.02	ND	After fire, estimated	sediment	dw
(Vergnoux et al., 2011)	Forest soil	Top 15 cm	Moist soil	Ultrapure water	0.45	ND	ND	0.13	ND	After fire, estimated	sediment	dw
(Vergnoux et al., 2011)	Forest soil	Top 15 cm	Moist soil	Ultrapure water	0.45	ND	ND	0.07	ND	After fire, estimated	sediment	dw
(Vergnoux et al., 2011)	Forest soil	Top 15 cm	Moist soil	Ultrapure water	0.45	ND	ND	0.1	ND	After fire, estimated	sediment	dw
(Vergnoux et al., 2011)	Forest soil	Top 15 cm	Moist soil	Ultrapure water	0.45	ND	ND	0.2	ND	After fire, estimated	sediment	dw
(Vergnoux et al., 2011)	Forest soil	Top 15 cm	Moist soil	Ultrapure water	0.45	ND	ND	0.2	ND	After fire, estimated	sediment	dw
(Vergnoux et al., 2011)	Forest soil	Top 15 cm	Moist soil	Ultrapure water	0.45	ND	ND	0.2	ND	No fire sediment		dw estimated

(Wu & Jiang, 2016)	Forest soil	0–10 cm	Air dried	Distilled water	0.45	20	90	0.1	30.06	Dw estimated
(Wu & Jiang, 2016)	Forest soil	0–10 cm	Air dried	Distilled water	0.45	20	90	0.1	41.03	Dw estimated
(Wu & Jiang, 2016)	Forest soil	0–10 cm	Air dried	Distilled water	0.45	20	90	0.11	24.97	Dw estimated
(Wu & Jiang, 2016)	Forest soil	0–10 cm	Air dried	Distilled water	0.45	20	90	0.15	38.69	Dw estimated
(Wagai & Sollins, 2002)	Forest soil	0–8 cm		Deionized water	0.2	26	90	0.05	38.67	Dw estimated
(Wagai & Sollins, 2002)	Forest soil	0–8 cm		Deionized water	0.2	26	90	0	22.74	Dw estimated
(Wagai & Sollins, 2002)	Forest soil	0–8 cm		Deionized water	0.2	26	90	0	15.93	Dw estimated
(Wagai & Sollins, 2002)	Forest soil	0–8 cm		Deionized water	0.2	26	90	0	12.96	Dw estimated
(Wagai & Sollins, 2002)	Forest soil	0–8 cm		Deionized water	0.2	26	90	0.02	27.36	Dw estimated
(Wagai & Sollins, 2002)	Forest soil	0–8 cm		Deionized water	0.2	26	90	0.02	23.13	Dw estimated
(Wagai & Sollins, 2002)	Forest soil	0–8 cm		Deionized water	0.2	26	90	0.01	17.69	Dw estimated
(Wickland et al., 2018)	Permafrost and seasonally frozen soil	35–50 cm	No drying	Deionized water	NM	5	90	0.05	12	Dw estimated
(Wickland et al., 2018)	Permafrost and seasonally frozen soil	35–50 cm	No drying	Deionized water	NM	5	90	0.11	22	Dw estimated
(Wickland et al., 2018)	Permafrost and seasonally frozen soil	35–50 cm	No drying	Deionized water	NM	5	90	0.03	9	Dw estimated
(Wickland et al., 2018)	Permafrost and seasonally frozen soil	65–80 cm	No drying	Deionized water	NM	5	90	0.03	36	Dw estimated
(Wickland et al., 2018)	Permafrost and seasonally frozen soil	66–80 cm	No drying	Deionized water	NM	5	90	0.17	19	Dw estimated

(Wickland et al., 2018)	Permafrost and seasonally frozen soil	67–80 cm	No drying	Deionized water	NM	5	90	0.06	16	Dw estimated
(Wickland et al., 2018)	Permafrost and seasonally frozen soil	35–50 cm	No drying	Deionized water	NM	5	90	0.49	13	Dw estimated
(Wickland et al., 2018)	Permafrost and seasonally frozen soil	35–50 cm	No drying	Deionized water	NM	5	90	0.43	13	Dw estimated
(Wickland et al., 2018)	Permafrost and seasonally frozen soil	35–50 cm	No drying	Deionized water	NM	5	90	0.45	9	Dw estimated
(Wickland et al., 2018)	Permafrost and seasonally frozen soil	85–100 cm	No drying	Deionized water	NM	5	90	0.61	10	Dw estimated
(Wickland et al., 2018)	Permafrost and seasonally frozen soil	86–100 cm	No drying	Deionized water	NM	5	90	0.52	5	Dw estimated
(Wickland et al., 2018)	Permafrost and seasonally frozen soil	87–100 cm	No drying	Deionized water	NM	5	90	1.04	5	Dw estimated
(Wickland et al., 2018)	Permafrost and seasonally frozen soil	30–45 cm	No drying	Deionized water	NM	5	90	0.02	12	Dw estimated
(Wickland et al., 2018)	Permafrost and seasonally frozen soil	35–50 cm	No drying	Deionized water	NM	5	90	0.15	5	Dw estimated
(Wickland et al., 2018)	Permafrost and seasonally frozen soil	35–50 cm	No drying	Deionized water	NM	5	90	0.14	11	Dw estimated
(Wickland et al., 2018)	Permafrost and seasonally frozen soil	87–102 cm	No drying	Deionized water	NM	5	90	0.48	11	Dw estimated
(Wickland et al., 2018)	Permafrost and seasonally frozen soil	78–90 cm	No drying	Deionized water	NM	5	90	0.43	8	Dw estimated

(Wickland et al., 2018)	Permafrost and seasonally frozen soil	74–89 cm	No drying	Deionized water	NM	5	90	0.16	8	Dw estimated
(Zhao et al., 2013)	Arable and forest soil	0–15 cm	Air dried	Deionized water	0.45	15	21	0.42	14.17	Cold extraction
(Zhao et al., 2013)	Arable and forest soil	0–15 cm	Air dried	Deionized water	0.45	15	21	0.54	12.73	Cold extraction
(Zhao et al., 2013)	Arable and forest soil	0–15 cm	Air dried	Deionized water	0.45	15	21	0.32	17.26	Cold extraction
(Zhao et al., 2013)	Arable and forest soil	0–15 cm	Air dried	Deionized water	0.45	15	21	0.35	4.15	Cold extraction
(Zhao et al., 2013)	Arable and forest soil	0–15 cm	Air dried	Deionized water	0.45	15	21	0.51	13.72	Cold extraction
(Zhao et al., 2013)	Arable and forest soil	0–15 cm	Air dried	Deionized water	0.45	15	21	0.31	10.74	Cold extraction
(Zhao et al., 2013)	Arable and forest soil	0–15 cm	Air dried	Deionized water	0.45	15	21	0.75	13	Cold extraction
(Zhao et al., 2013)	Arable and forest soil	0–15 cm	Air dried	Deionized water	0.45	15	21	0.55	10.62	Cold extraction
(Zhao et al., 2013)	Arable and forest soil	0–15 cm	Air dried	Deionized water	0.45	15	21	0.41	15.21	Cold extraction
(Zhao et al., 2013)	Arable and forest soil	0–15 cm	Air dried	Deionized water	0.45	15	21	0.46	4.08	Cold extraction
(Zhao et al., 2013)	Arable and forest soil	0–15 cm	Air dried	Deionized water	0.45	15	21	0.27	22.07	Cold extraction
(Zhao et al., 2013)	Arable and forest soil	0–15 cm	Air dried	Deionized water	0.45	15	21	0.44	9.06	Cold extraction
(Zhao et al., 2013)	Arable and forest soil	0–15 cm	Air dried	Deionized water	0.45	15	21	0.39	12.07	Cold extraction
(Zhao et al., 2013)	Arable and forest soil	0–15 cm	Air dried	Deionized water	0.45	15	21	0.36	30.21	Hot extraction
(Zhao et al., 2013)	Arable and forest soil	0–15 cm	Air dried	Deionized water	0.45	15	21	1.3	23.04	Hot extraction
(Zhao et al., 2013)	Arable and forest soil	0–15 cm	Air dried	Deionized water	0.45	15	21	1.51	19.33	Hot extraction
(Zhao et al., 2013)	Arable and forest soil	0–15 cm	Air dried	Deionized water	0.45	15	21	0.97	14.17	Hot extraction

(Zhao et al., 2013)	Arable and forest soil	0–15 cm	Air dried	Deionized water	0.45	15	21	1.38	9.91	Hot extraction
(Zhao et al., 2013)	Arable and forest soil	0–15 cm	Air dried	Deionized water	0.45	15	21	1.38	12.24	Hot extraction
(Zhao et al., 2013)	Arable and forest soil	0–15 cm	Air dried	Deionized water	0.45	15	21	0.76	12.1	Hot extraction
(Zhao et al., 2013)	Arable and forest soil	0–15 cm	Air dried	Deionized water	0.45	15	21	1.7	28.11	Hot extraction
(Zhao et al., 2013)	Arable and forest soil	0–15 cm	Air dried	Deionized water	0.45	15	21	1.65	29.77	Hot extraction
(Zhao et al., 2013)	Arable and forest soil	0–15 cm	Air dried	Deionized water	0.45	15	21	1.28	19.37	Hot extraction
(Zhao et al., 2013)	Arable and forest soil	0–15 cm	Air dried	Deionized water	0.45	15	21	0.95	15.79	Hot extraction
(Zhao et al., 2013)	Arable and forest soil	0–15 cm	Air dried	Deionized water	0.45	15	21	0.7	60.73	Hot extraction
(Zhao et al., 2013)	Arable and forest soil	0–15 cm	Air dried	Deionized water	0.45	15	21	0.6	14.67	Hot extraction
(Zhao et al., 2013)	Arable and forest soil	0–15 cm	Air dried	Deionized water	0.45	15	21	0.68	22.31	Hot extraction
(Zhao et al., 2013)	Arable and forest soil	0–15 cm	Air dried	Deionized water	0.45	15	21	0.72	8.18	Hot extraction
(Zhao et al., 2013)	Arable and forest soil	0–10 cm	Air dried	Deionized water	0.45			0.45	ND	
(Zhao et al., 2013)	Arable and forest soil	0–10 cm	Air dried	Deionized water	0.45			0.44	ND	
(Zhao et al., 2013)	Arable and forest soil	0–10 cm	Air dried	Deionized water	0.45			0.38	ND	
(Zhao et al., 2013)	Arable and forest soil	0–10 cm	Field moist	Deionized water	0.45			0.18	ND	Dw estimated
(Zhao et al., 2013)	Arable and forest soil	0–10 cm	Field moist	Deionized water	0.45			0.24	ND	Dw estimated
(Zhao et al., 2013)	Arable and forest soil	0–10 cm	Field moist	Deionized water	0.45			0.16	ND	Dw estimated
(Rizinjirabake et al., 2019)	Soil	0–20 cm	Oven dried	Distilled water	0.45			1.68	ND	Natural forest
(Rizinjirabake et al., 2019)	Soil	0–20 cm	Oven dried	Distilled water	0.45			1.21	ND	Tree plantation

(Rizinjirabake et al., 2019)	Soil	0–20 cm	Oven dried	Distilled water	0.45			1.15	ND	Tea plantation
(Rizinjirabake et al., 2019)	Soil	0–20 cm	Oven dried	Distilled water	0.45			0.75	ND	Cropland soil
(Guigue et al., 2014)	Woodland soil	A-horizon	Air dried	Ultrapure water	0.22	21	48	0.16	17.48	Dystric Andosol
(Guigue et al., 2014)	Forest soil	A-horizon	Air dried	Ultrapure water	0.22	21	48	0.34	18.18	Entic Podzol
(Guigue et al., 2014)	Pastureland soil	A-horizon	Air dried	Ultrapure water	0.22	21	48	0.24	20.28	Dystric Cambisol
(Guigue et al., 2014)	Pastureland soil	A-horizon	Air dried	Ultrapure water	0.22	21	48	0.36	18.18	Gleyic Luvisol
(Guigue et al., 2014)	Arable soil	A-horizon	Air dried	Ultrapure water	0.22	21	48	0.25	42.66	Eutric Cambisol
(Guigue et al., 2014)	Woodland soil	A-horizon	Air dried	Ultrapure water	0.22	21	48	0.04	39.16	Dystric Andosol
(Guigue et al., 2014)	Forest soil	A-horizon	Air dried	Ultrapure water	0.22	21	48	0.09	30.77	Entic Podzol
(Guigue et al., 2014)	Pastureland soil	A-horizon	Air dried	Ultrapure water	0.22	21	48	0.07	42.66	Dystric Cambisol
(Guigue et al., 2014)	Pastureland soil	A-horizon	Air dried	Ultrapure water	0.22	21	48	0.16	23.08	Gleyic Luvisol
(Guigue et al., 2014)	Arable soil	A-horizon	Air dried	Ultrapure water	0.22	21	48	0.03	16.08	Eutric Cambisol
(Guigue et al., 2014)	Woodland soil	A-horizon	Air dried	Ultrapure water	0.22	21	48	0.06	41.26	Dystric Andosol
(Guigue et al., 2014)	Forest soil	A-horizon	Air dried	Ultrapure water	0.22	21	48	0.12	22.38	Entic Podzol
(Guigue et al., 2014)	Pastureland soil	A-horizon	Air dried	Ultrapure water	0.22	21	48	0.08	39.86	Dystric Cambisol
(Guigue et al., 2014)	Pastureland soil	A-horizon	Air dried	Ultrapure water	0.22	21	48	0.16	26.57	Gleyic Luvisol
(Guigue et al., 2014)	Arable soil	A-horizon	Air dried	Ultrapure water	0.22	21	48	0.02	32.17	Eutric Cambisol

Table S.4.5 The content of sediment WEOM (mean \pm SE, range: 0.29 ± 0.02 , 0.01–0.5 mg C/g dry sediment) in dry sediments from rivers.

Reference	System	Name, location	Sed/soil	Drying	Extractant	[WEOC]	Unit	Comment
						Mean		
(Dong et al., 2020)	River	Yunxi River	Sediment	Air-dried	Milli-Q water	0.5	mg C/g sed	
(Dong et al., 2020)	River	Yunxi River	Sediment	Air-dried	Milli-Q water	0.4	mg C/g sed	
(Dong et al., 2020)	River	Yunxi River	Sediment	Air-dried	Milli-Q water	0.3	mg C/g sed	
(Dong et al., 2020)	River	Yunxi River	Sediment	Air-dried	Milli-Q water	0.5	mg C/g sed	
(Dong et al., 2020)	River	Taoyuan River	Sediment	Air-dried	Milli-Q water	0.3	mg C/g sed	
(Dong et al., 2020)	River	Taoyuan River	Sediment	Air-dried	Milli-Q water	0.2	mg C/g sed	
(Dong et al., 2020)	River	Taoyuan River	Sediment	Air-dried	Milli-Q water	0.1	mg C/g sed	
(Dong et al., 2020)	River	Taoyuan River	Sediment	Air-dried	Milli-Q water	0.2	mg C/g sed	
(Dong et al., 2020)	River	Jiaolai River	Sediment	Air-dried	Milli-Q water	0.4	mg C/g sed	
(Dong et al., 2020)	River	Jiaolai River	Sediment	Air-dried	Milli-Q water	0.4	mg C/g sed	
(Dong et al., 2020)	River	Jiaolai River	Sediment	Air-dried	Milli-Q water	0.2	mg C/g sed	
(Dong et al., 2020)	River	Jiaolai River	Sediment	Air-dried	Milli-Q water	0.2	mg C/g sed	
(Fox et al., 2017)	River	Colorado River, US	Sediment	Air-dried	Milli-Q water Distilled	0.04	mg C/g sed	
(Zhu et al., 2017)	River	Hao River, China	Sediment	Air-dried	water	0.2	mg C/g sed	0–10 cm

(Zhu et al., 2017)	River	Hao River, China	Sediment	Air-dried	Distilled water	0.3	mg C/g sed	0–10 cm
(Zhu et al., 2017)	River	Hao River, China	Sediment	Air-dried	Distilled water	0.2	mg C/g sed	0–10 cm
(Zhu et al., 2017)	River	Hao River, China	Sediment	Air-dried	Distilled water	0.25	mg C/g sed	0–10 cm
(Zhu et al., 2017)	River	Hao River, China	Sediment	Air-dried	Distilled water	0.2	mg C/g sed	0–10 cm
(Zhu et al., 2017)	River	Hao River, China	Sediment	Air-dried	Distilled water	0.45	mg C/g sed	0–10 cm
(Zhu et al., 2017)	River	Hao River, China	Sediment	Air-dried	Distilled water	0.4	mg C/g sed	0–10 cm
(Zhu et al., 2017)	River	Hao River, China	Sediment	Air-dried	Distilled water	0.45	mg C/g sed	0–10 cm
(Zhu et al., 2017)	River	Hao River, China	Sediment	Air-dried	Distilled water	0.3	mg C/g sed	10–20 cm
(Zhu et al., 2017)	River	Hao River, China	Sediment	Air-dried	Distilled water	0.3	mg C/g sed	10–20 cm
(Zhu et al., 2017)	River	Hao River, China	Sediment	Air-dried	Distilled water	0.3	mg C/g sed	10–20 cm
(Zhu et al., 2017)	River	Hao River, China	Sediment	Air-dried	Distilled water	0.16	mg C/g sed	10–20 cm
(Zhu et al., 2017)	River	Hao River, China	Sediment	Air-dried	Distilled water	0.5	mg C/g sed	10–20 cm
(Zhu et al., 2017)	River	Hao River, China	Sediment	Air-dried	Distilled water	0.45	mg C/g sed	10–20 cm
(Zhu et al., 2017)	River	Hao River, China	Sediment	Air-dried	Distilled water	0.3	mg C/g sed	10–20 cm
(Zhu et al., 2017)	River	Hao River, China	Sediment	Air-dried	Distilled water	0.25	mg C/g sed	20–30 cm

(Zhu et al., 2017)	River	Hao River, China	Sediment	Air-dried	Distilled water	0.25	mg C/g sed	20–30
(Zhu et al., 2017)	River	Hao River, China	Sediment	Air-dried	Distilled water	0.25	mg C/g sed	20–30
(Zhu et al., 2017)	River	Hao River, China	Sediment	Air-dried	Distilled water	0.3	mg C/g sed	20–30
(Zhu et al., 2017)	River	Hao River, China	Sediment	Air-dried	Distilled water	0.4	mg C/g sed	20–30
(Zhu et al., 2017)	River	Hao River, China	Sediment	Air-dried	Distilled water	0.5	mg C/g sed	20–30
(Zhu et al., 2017)	River	Hao River, China	Sediment	Air-dried	Distilled water	0.3	mg C/g sed	20–30
(Han et al., 2021)	River	Yangtze River, China	Sediment	Freeze-dried	Ultrapure water	0.01	mg C/g sed	
(Han et al., 2021)	River	Yangtze River, China	Sediment	Freeze-dried	Ultrapure water	0.01	mg C/g sed	

Table S.4.6 Respiration rate of bulk OM in dry soils of wetlands (mean \pm SE, range: 3.74 ± 0.39 , 0.30–28.16 $\mu\text{g O}_2 \text{ g}^{-1} \text{ dry soil h}^{-1}$).

Reference	System	Incubation Temp (°C)	Mean resp. rate	Unit	Comment
(Magnusson, 1993)	Wetland (fen)	16	10.04	$\mu\text{g O}_2 \text{ g}^{-1} \text{ dry soil h}^{-1}$	
(Magnusson, 1993)	Wetland (fen)	16	8.53	$\mu\text{g O}_2 \text{ g}^{-1} \text{ dry soil h}^{-1}$	
(Magnusson, 1993)	Wetland (fen)	16	9.00	$\mu\text{g O}_2 \text{ g}^{-1} \text{ dry soil h}^{-1}$	
(Magnusson, 1993)	Wetland (fen)	16	7.04	$\mu\text{g O}_2 \text{ g}^{-1} \text{ dry soil h}^{-1}$	

(Magnusson, 1993)								
		Wetland (fen)	16	7.75	$\mu\text{g O}_2 \text{ g}^{-1} \text{ dry soil h}^{-1}$			
(Szafranek-Nakoneczna & Stêpniewska, 2014)		Wetland (moor)	5	0.91	$\mu\text{g O}_2 \text{ g}^{-1} \text{ dry soil h}^{-1}$		Natural moisture	
(Szafranek-Nakoneczna & Stêpniewska, 2014)		Wetland (moor)	5	0.91	$\mu\text{g O}_2 \text{ g}^{-1} \text{ dry soil h}^{-1}$		Natural moisture	
(Szafranek-Nakoneczna & Stêpniewska, 2014)		Wetland (moor)	5	0.61	$\mu\text{g O}_2 \text{ g}^{-1} \text{ dry soil h}^{-1}$		Natural moisture	
(Szafranek-Nakoneczna & Stêpniewska, 2014)		Wetland (moor)	5	0.61	$\mu\text{g O}_2 \text{ g}^{-1} \text{ dry soil h}^{-1}$		Natural moisture	
(Szafranek-Nakoneczna & Stêpniewska, 2014)		Wetland (moor)	5	1.22	$\mu\text{g O}_2 \text{ g}^{-1} \text{ dry soil h}^{-1}$		Natural moisture	
(Szafranek-Nakoneczna & Stêpniewska, 2014)		Wetland (moor)	5	0.91	$\mu\text{g O}_2 \text{ g}^{-1} \text{ dry soil h}^{-1}$		Natural moisture	
(Szafranek-Nakoneczna & Stêpniewska, 2014)		Wetland (moor)	5	0.61	$\mu\text{g O}_2 \text{ g}^{-1} \text{ dry soil h}^{-1}$		Natural moisture	
(Szafranek-Nakoneczna & Stêpniewska, 2014)		Wetland (moor)	5	0.91	$\mu\text{g O}_2 \text{ g}^{-1} \text{ dry soil h}^{-1}$		Natural moisture	
(Szafranek-Nakoneczna & Stêpniewska, 2014)		Wetland (moor)	5	0.91	$\mu\text{g O}_2 \text{ g}^{-1} \text{ dry soil h}^{-1}$		Natural moisture	
(Szafranek-Nakoneczna & Stêpniewska, 2014)		Wetland (moor)	5	0.61	$\mu\text{g O}_2 \text{ g}^{-1} \text{ dry soil h}^{-1}$		Natural moisture	
(Szafranek-Nakoneczna & Stêpniewska, 2014)		Wetland (moor)	5	0.30	$\mu\text{g O}_2 \text{ g}^{-1} \text{ dry soil h}^{-1}$		Natural moisture	
(Szafranek-Nakoneczna & Stêpniewska, 2014)		Wetland (moor)	5	0.61	$\mu\text{g O}_2 \text{ g}^{-1} \text{ dry soil h}^{-1}$		Natural moisture	
(Szafranek-Nakoneczna & Stêpniewska, 2014)		Wetland (moor)	10	1.52	$\mu\text{g O}_2 \text{ g}^{-1} \text{ dry soil h}^{-1}$		Natural moisture	
(Szafranek-Nakoneczna & Stêpniewska, 2014)		Wetland (moor)	10	1.83	$\mu\text{g O}_2 \text{ g}^{-1} \text{ dry soil h}^{-1}$		Natural moisture	

(Szafranek-Nakoneczna & Stêpniewska, 2014)	Wetland (moor)	10	0.91	$\mu\text{g O}_2 \text{ g}^{-1} \text{ dry soil h}^{-1}$	Natural moisture
(Szafranek-Nakoneczna & Stêpniewska, 2014)	Wetland (moor)	10	1.22	$\mu\text{g O}_2 \text{ g}^{-1} \text{ dry soil h}^{-1}$	Natural moisture
(Szafranek-Nakoneczna & Stêpniewska, 2014)	Wetland (moor)	10	1.83	$\mu\text{g O}_2 \text{ g}^{-1} \text{ dry soil h}^{-1}$	Natural moisture
(Szafranek-Nakoneczna & Stêpniewska, 2014)	Wetland (moor)	10	18.25	$\mu\text{g O}_2 \text{ g}^{-1} \text{ dry soil h}^{-1}$	Natural moisture
(Szafranek-Nakoneczna & Stêpniewska, 2014)	Wetland (moor)	10	1.52	$\mu\text{g O}_2 \text{ g}^{-1} \text{ dry soil h}^{-1}$	Natural moisture
(Szafranek-Nakoneczna & Stêpniewska, 2014)	Wetland (moor)	10	0.91	$\mu\text{g O}_2 \text{ g}^{-1} \text{ dry soil h}^{-1}$	Natural moisture
(Szafranek-Nakoneczna & Stêpniewska, 2014)	Wetland (moor)	10	1.52	$\mu\text{g O}_2 \text{ g}^{-1} \text{ dry soil h}^{-1}$	Natural moisture
(Szafranek-Nakoneczna & Stêpniewska, 2014)	Wetland (moor)	10	1.22	$\mu\text{g O}_2 \text{ g}^{-1} \text{ dry soil h}^{-1}$	Natural moisture
(Szafranek-Nakoneczna & Stêpniewska, 2014)	Wetland (moor)	10	0.91	$\mu\text{g O}_2 \text{ g}^{-1} \text{ dry soil h}^{-1}$	Natural moisture
(Szafranek-Nakoneczna & Stêpniewska, 2014)	Wetland (moor)	10	0.91	$\mu\text{g O}_2 \text{ g}^{-1} \text{ dry soil h}^{-1}$	Natural moisture
(Szafranek-Nakoneczna & Stêpniewska, 2014)	Wetland (moor)	20	14.90	$\mu\text{g O}_2 \text{ g}^{-1} \text{ dry soil h}^{-1}$	Natural moisture
(Szafranek-Nakoneczna & Stêpniewska, 2014)	Wetland (moor)	20	12.78	$\mu\text{g O}_2 \text{ g}^{-1} \text{ dry soil h}^{-1}$	Natural moisture
(Szafranek-Nakoneczna & Stêpniewska, 2014)	Wetland (moor)	20	6.69	$\mu\text{g O}_2 \text{ g}^{-1} \text{ dry soil h}^{-1}$	Natural moisture
(Szafranek-Nakoneczna & Stêpniewska, 2014)	Wetland (moor)	20	5.17	$\mu\text{g O}_2 \text{ g}^{-1} \text{ dry soil h}^{-1}$	Natural moisture
(Szafranek-Nakoneczna & Stêpniewska, 2014)	Wetland (moor)	20	13.38	$\mu\text{g O}_2 \text{ g}^{-1} \text{ dry soil h}^{-1}$	Natural moisture

(Szafranek-Nakoniczna & Stêpniewska, 2014)	Wetland (moor)	20	9.43	$\mu\text{g O}_2 \text{ g}^{-1} \text{ dry soil h}^{-1}$	Natural moisture
(Szafranek-Nakoniczna & Stêpniewska, 2014)	Wetland (moor)	20	6.39	$\mu\text{g O}_2 \text{ g}^{-1} \text{ dry soil h}^{-1}$	Natural moisture
(Szafranek-Nakoniczna & Stêpniewska, 2014)	Wetland (moor)	20	6.69	$\mu\text{g O}_2 \text{ g}^{-1} \text{ dry soil h}^{-1}$	Natural moisture
(Szafranek-Nakoniczna & Stêpniewska, 2014)	Wetland (moor)	20	7.00	$\mu\text{g O}_2 \text{ g}^{-1} \text{ dry soil h}^{-1}$	Natural moisture
(Szafranek-Nakoniczna & Stêpniewska, 2014)	Wetland (moor)	20	7.60	$\mu\text{g O}_2 \text{ g}^{-1} \text{ dry soil h}^{-1}$	Natural moisture
(Szafranek-Nakoniczna & Stêpniewska, 2014)	Wetland (moor)	20	7.30	$\mu\text{g O}_2 \text{ g}^{-1} \text{ dry soil h}^{-1}$	Natural moisture
(Szafranek-Nakoniczna & Stêpniewska, 2014)	Wetland (moor)	20	4.56	$\mu\text{g O}_2 \text{ g}^{-1} \text{ dry soil h}^{-1}$	Natural moisture
(Szafranek-Nakoniczna & Stêpniewska, 2014)	Wetland (moor)	5	0.91	$\mu\text{g O}_2 \text{ g}^{-1} \text{ dry soil h}^{-1}$	Flooded
(Szafranek-Nakoniczna & Stêpniewska, 2014)	Wetland (moor)	5	0.91	$\mu\text{g O}_2 \text{ g}^{-1} \text{ dry soil h}^{-1}$	Flooded
(Szafranek-Nakoniczna & Stêpniewska, 2014)	Wetland (moor)	5	0.91	$\mu\text{g O}_2 \text{ g}^{-1} \text{ dry soil h}^{-1}$	Flooded
(Szafranek-Nakoniczna & Stêpniewska, 2014)	Wetland (moor)	5	0.61	$\mu\text{g O}_2 \text{ g}^{-1} \text{ dry soil h}^{-1}$	Flooded
(Szafranek-Nakoniczna & Stêpniewska, 2014)	Wetland (moor)	5	0.91	$\mu\text{g O}_2 \text{ g}^{-1} \text{ dry soil h}^{-1}$	Flooded
(Szafranek-Nakoniczna & Stêpniewska, 2014)	Wetland (moor)	5	0.61	$\mu\text{g O}_2 \text{ g}^{-1} \text{ dry soil h}^{-1}$	Flooded
(Szafranek-Nakoniczna & Stêpniewska, 2014)	Wetland (moor)	5	0.61	$\mu\text{g O}_2 \text{ g}^{-1} \text{ dry soil h}^{-1}$	Flooded
(Szafranek-Nakoniczna & Stêpniewska, 2014)	Wetland (moor)	5	0.30	$\mu\text{g O}_2 \text{ g}^{-1} \text{ dry soil h}^{-1}$	Flooded

(Szafranek-Nakoneczna & Stêpniewska, 2014)	Wetland (moor)	5	0.61	$\mu\text{g O}_2 \text{ g}^{-1} \text{ dry soil h}^{-1}$	Flooded
(Szafranek-Nakoneczna & Stêpniewska, 2014)	Wetland (moor)	5	0.61	$\mu\text{g O}_2 \text{ g}^{-1} \text{ dry soil h}^{-1}$	Flooded
(Szafranek-Nakoneczna & Stêpniewska, 2014)	Wetland (moor)	5	1.22	$\mu\text{g O}_2 \text{ g}^{-1} \text{ dry soil h}^{-1}$	Flooded
(Szafranek-Nakoneczna & Stêpniewska, 2014)	Wetland (moor)	5	1.22	$\mu\text{g O}_2 \text{ g}^{-1} \text{ dry soil h}^{-1}$	Flooded
(Szafranek-Nakoneczna & Stêpniewska, 2014)	Wetland (moor)	10	1.52	$\mu\text{g O}_2 \text{ g}^{-1} \text{ dry soil h}^{-1}$	Flooded
(Szafranek-Nakoneczna & Stêpniewska, 2014)	Wetland (moor)	10	1.83	$\mu\text{g O}_2 \text{ g}^{-1} \text{ dry soil h}^{-1}$	Flooded
(Szafranek-Nakoneczna & Stêpniewska, 2014)	Wetland (moor)	10	0.91	$\mu\text{g O}_2 \text{ g}^{-1} \text{ dry soil h}^{-1}$	Flooded
(Szafranek-Nakoneczna & Stêpniewska, 2014)	Wetland (moor)	10	0.30	$\mu\text{g O}_2 \text{ g}^{-1} \text{ dry soil h}^{-1}$	Flooded
(Szafranek-Nakoneczna & Stêpniewska, 2014)	Wetland (moor)	10	0.91	$\mu\text{g O}_2 \text{ g}^{-1} \text{ dry soil h}^{-1}$	Flooded
(Szafranek-Nakoneczna & Stêpniewska, 2014)	Wetland (moor)	10	0.91	$\mu\text{g O}_2 \text{ g}^{-1} \text{ dry soil h}^{-1}$	Flooded
(Szafranek-Nakoneczna & Stêpniewska, 2014)	Wetland (moor)	10	1.22	$\mu\text{g O}_2 \text{ g}^{-1} \text{ dry soil h}^{-1}$	Flooded
(Szafranek-Nakoneczna & Stêpniewska, 2014)	Wetland (moor)	10	1.22	$\mu\text{g O}_2 \text{ g}^{-1} \text{ dry soil h}^{-1}$	Flooded
(Szafranek-Nakoneczna & Stêpniewska, 2014)	Wetland (moor)	10	1.22	$\mu\text{g O}_2 \text{ g}^{-1} \text{ dry soil h}^{-1}$	Flooded
(Szafranek-Nakoneczna & Stêpniewska, 2014)	Wetland (moor)	10	0.30	$\mu\text{g O}_2 \text{ g}^{-1} \text{ dry soil h}^{-1}$	Flooded
(Szafranek-Nakoneczna & Stêpniewska, 2014)	Wetland (moor)	10	0.30	$\mu\text{g O}_2 \text{ g}^{-1} \text{ dry soil h}^{-1}$	Flooded

(Szafranek-Nakoneczna & Stêpniewska, 2014)	Wetland (moor)	10	0.30	$\mu\text{g O}_2 \text{ g}^{-1} \text{ dry soil h}^{-1}$	Flooded
(Szafranek-Nakoneczna & Stêpniewska, 2014)	Wetland (moor)	20	3.65	$\mu\text{g O}_2 \text{ g}^{-1} \text{ dry soil h}^{-1}$	Flooded
(Szafranek-Nakoneczna & Stêpniewska, 2014)	Wetland (moor)	20	3.04	$\mu\text{g O}_2 \text{ g}^{-1} \text{ dry soil h}^{-1}$	Flooded
(Szafranek-Nakoneczna & Stêpniewska, 2014)	Wetland (moor)	20	1.52	$\mu\text{g O}_2 \text{ g}^{-1} \text{ dry soil h}^{-1}$	Flooded
(Szafranek-Nakoneczna & Stêpniewska, 2014)	Wetland (moor)	20	1.52	$\mu\text{g O}_2 \text{ g}^{-1} \text{ dry soil h}^{-1}$	Flooded
(Szafranek-Nakoneczna & Stêpniewska, 2014)	Wetland (moor)	20	4.26	$\mu\text{g O}_2 \text{ g}^{-1} \text{ dry soil h}^{-1}$	Flooded
(Szafranek-Nakoneczna & Stêpniewska, 2014)	Wetland (moor)	20	3.35	$\mu\text{g O}_2 \text{ g}^{-1} \text{ dry soil h}^{-1}$	Flooded
(Szafranek-Nakoneczna & Stêpniewska, 2014)	Wetland (moor)	20	2.13	$\mu\text{g O}_2 \text{ g}^{-1} \text{ dry soil h}^{-1}$	Flooded
(Szafranek-Nakoneczna & Stêpniewska, 2014)	Wetland (moor)	20	1.22	$\mu\text{g O}_2 \text{ g}^{-1} \text{ dry soil h}^{-1}$	Flooded
(Szafranek-Nakoneczna & Stêpniewska, 2014)	Wetland (moor)	20	6.69	$\mu\text{g O}_2 \text{ g}^{-1} \text{ dry soil h}^{-1}$	Flooded
(Szafranek-Nakoneczna & Stêpniewska, 2014)	Wetland (moor)	20	3.65	$\mu\text{g O}_2 \text{ g}^{-1} \text{ dry soil h}^{-1}$	Flooded
(Szafranek-Nakoneczna & Stêpniewska, 2014)	Wetland (moor)	20	3.35	$\mu\text{g O}_2 \text{ g}^{-1} \text{ dry soil h}^{-1}$	Flooded
(Szafranek-Nakoneczna & Stêpniewska, 2014)	Wetland (moor)	20	1.83	$\mu\text{g O}_2 \text{ g}^{-1} \text{ dry soil h}^{-1}$	Flooded
(Brouns et al., 2014)	Wetland (bog)	20	28.16	$\mu\text{g O}_2 \text{ g}^{-1} \text{ dry soil h}^{-1}$	
(Inglett et al., 2012)	Wetland	10	2.37	$\mu\text{g O}_2 \text{ g}^{-1} \text{ dry soil h}^{-1}$	

(Inglett et al., 2012)	Tropical Wetland	10	3.19	$\mu\text{g O}_2 \text{ g}^{-1} \text{ dry soil h}^{-1}$
(Inglett et al., 2012)	Tropical Wetland	10	3.61	$\mu\text{g O}_2 \text{ g}^{-1} \text{ dry soil h}^{-1}$
(Inglett et al., 2012)	Wetland	10	3.29	$\mu\text{g O}_2 \text{ g}^{-1} \text{ dry soil h}^{-1}$
(Inglett et al., 2012)	Wetland	10	2.37	$\mu\text{g O}_2 \text{ g}^{-1} \text{ dry soil h}^{-1}$
(Inglett et al., 2012)	Wetland	20	4.02	$\mu\text{g O}_2 \text{ g}^{-1} \text{ dry soil h}^{-1}$
(Inglett et al., 2012)	Wetland	20	5.53	$\mu\text{g O}_2 \text{ g}^{-1} \text{ dry soil h}^{-1}$
(Inglett et al., 2012)	Wetland	20	5.20	$\mu\text{g O}_2 \text{ g}^{-1} \text{ dry soil h}^{-1}$
(Inglett et al., 2012)	Wetland	20	5.08	$\mu\text{g O}_2 \text{ g}^{-1} \text{ dry soil h}^{-1}$
(Inglett et al., 2012)	Wetland	20	3.31	$\mu\text{g O}_2 \text{ g}^{-1} \text{ dry soil h}^{-1}$
(Inglett et al., 2012)	Wetland	30	7.23	$\mu\text{g O}_2 \text{ g}^{-1} \text{ dry soil h}^{-1}$
(Inglett et al., 2012)	Wetland	30	8.18	$\mu\text{g O}_2 \text{ g}^{-1} \text{ dry soil h}^{-1}$
(Inglett et al., 2012)	Wetland	30	8.67	$\mu\text{g O}_2 \text{ g}^{-1} \text{ dry soil h}^{-1}$
(Inglett et al., 2012)	Wetland	30	7.39	$\mu\text{g O}_2 \text{ g}^{-1} \text{ dry soil h}^{-1}$
(Inglett et al., 2012)	Wetland	30	10.00	$\mu\text{g O}_2 \text{ g}^{-1} \text{ dry soil h}^{-1}$
(Duval & Radu, 2018)	Wetland (fen)	25	2.00	$\mu\text{g O}_2 \text{ g}^{-1} \text{ dry soil h}^{-1}$

(Duval & Radu, 2018)	Wetland (fen)	25	3.84	$\mu\text{g O}_2 \text{ g}^{-1} \text{ dry soil h}^{-1}$
(Duval & Radu, 2018)	Wetland (fen)	25	6.96	$\mu\text{g O}_2 \text{ g}^{-1} \text{ dry soil h}^{-1}$
(Duval & Radu, 2018)	Wetland (fen)	25	5.60	$\mu\text{g O}_2 \text{ g}^{-1} \text{ dry soil h}^{-1}$
(Duval & Radu, 2018)	Wetland (fen)	25	7.28	$\mu\text{g O}_2 \text{ g}^{-1} \text{ dry soil h}^{-1}$
(Duval & Radu, 2018)	Wetland (fen)	25	4.88	$\mu\text{g O}_2 \text{ g}^{-1} \text{ dry soil h}^{-1}$
(Duval & Radu, 2018)	Wetland (fen)	15	1.58	$\mu\text{g O}_2 \text{ g}^{-1} \text{ dry soil h}^{-1}$
(Duval & Radu, 2018)	Wetland (fen)	15	3.09	$\mu\text{g O}_2 \text{ g}^{-1} \text{ dry soil h}^{-1}$
(Duval & Radu, 2018)	Wetland (fen)	15	3.25	$\mu\text{g O}_2 \text{ g}^{-1} \text{ dry soil h}^{-1}$
(Duval & Radu, 2018)	Wetland (fen)	15	3.56	$\mu\text{g O}_2 \text{ g}^{-1} \text{ dry soil h}^{-1}$
(Duval & Radu, 2018)	Wetland (fen)	15	5.70	$\mu\text{g O}_2 \text{ g}^{-1} \text{ dry soil h}^{-1}$
(Duval & Radu, 2018)	Wetland (fen)	15	3.41	$\mu\text{g O}_2 \text{ g}^{-1} \text{ dry soil h}^{-1}$
(Duval & Radu, 2018)	Wetland (fen)	5	1.28	$\mu\text{g O}_2 \text{ g}^{-1} \text{ dry soil h}^{-1}$
(Duval & Radu, 2018)	Wetland (fen)	5	3.20	$\mu\text{g O}_2 \text{ g}^{-1} \text{ dry soil h}^{-1}$
(Duval & Radu, 2018)	Wetland (fen)	5	2.72	$\mu\text{g O}_2 \text{ g}^{-1} \text{ dry soil h}^{-1}$
(Duval & Radu, 2018)	Wetland (fen)	5	1.52	$\mu\text{g O}_2 \text{ g}^{-1} \text{ dry soil h}^{-1}$

(Duval & Radu, 2018)	Wetland (fen)	5	2.80	$\mu\text{g O}_2 \text{ g}^{-1} \text{ dry soil h}^{-1}$
(Turetsky & Ripley, 2005)	Wetland (fen)	NM	2.32	$\mu\text{g O}_2 \text{ g}^{-1} \text{ dry soil h}^{-1}$
(Glatzel et al., 2004)	Wetland	NM	3.65	$\mu\text{g O}_2 \text{ g}^{-1} \text{ dry sed h}^{-1}$
(Glatzel et al., 2004)	Wetland	NM	4.23	$\mu\text{g O}_2 \text{ g}^{-1} \text{ dry sed h}^{-1}$

Table S.4.7 Respiration rate of bulk sediment OM (mean \pm SE, range: 1.43 ± 0.31 , 0–11.39 $\mu\text{g O}_2 \text{ g}^{-1} \text{ dry sediment h}^{-1}$) in dry sediments of perennial and intermittent rivers and ephemeral streams (IRES).

Reference	System	Location	Mean	Unit	Comment
(Harvey et al., 2011)	Perennial stream	Northern California	5.92	$\mu\text{g O}_2 \text{ g}^{-1} \text{ dry sed h}^{-1}$	Gravel
(Harvey et al., 2011)	Perennial stream	Northern California	1.48	$\mu\text{g O}_2 \text{ g}^{-1} \text{ dry sed h}^{-1}$	Sand
(Martin Pusch, 1996)	Perennial stream	Southern Germany, mountain stream	0.06	$\mu\text{g O}_2 \text{ g}^{-1} \text{ dry sed h}^{-1}$	Sand-gravel
(Martin Pusch, 1996)	Perennial stream	Austria and Pyrenees	1.5	$\mu\text{g O}_2 \text{ g}^{-1} \text{ dry sed h}^{-1}$	Sand-gravel
(Battin et al., 1999)	Perennial stream	Austria and Pyrenees	0.16	$\mu\text{g O}_2 \text{ g}^{-1} \text{ dry sed h}^{-1}$	Sand
(Battin et al., 1999)	Perennial stream	Austria and Pyrenees	1.06	$\mu\text{g O}_2 \text{ g}^{-1} \text{ dry sed h}^{-1}$	Sand
(Battin et al., 1999)	Perennial stream	Austria and Pyrenees	1.06	$\mu\text{g O}_2 \text{ g}^{-1} \text{ dry sed h}^{-1}$	Sand

(Battin et al., 1999)	Perennial stream	Austria and Pyrenees	0.89	$\mu\text{g O}_2 \text{ g}^{-1} \text{ dry sed h}^{-1}$	Sand
(Battin et al., 1999)	Perennial stream	Austria and Pyrenees	1.64	$\mu\text{g O}_2 \text{ g}^{-1} \text{ dry sed h}^{-1}$	Sand
(Battin et al., 1999)	Perennial stream	Austria and Pyrenees	2.62	$\mu\text{g O}_2 \text{ g}^{-1} \text{ dry sed h}^{-1}$	Sand
(Battin et al., 1999)	Perennial stream	Austria and Pyrenees	0.5	$\mu\text{g O}_2 \text{ g}^{-1} \text{ dry sed h}^{-1}$	Sand
(Battin et al., 1999)	Perennial stream	Austria and Pyrenees	1.04	$\mu\text{g O}_2 \text{ g}^{-1} \text{ dry sed h}^{-1}$	Sand
(Craft et al., 2002)	Perennial stream	North-western Montana	0.01	$\mu\text{g O}_2 \text{ g}^{-1} \text{ dry sed h}^{-1}$	Gravel
(Craft et al., 2002)	Perennial stream	North-western Montana	0.43	$\mu\text{g O}_2 \text{ g}^{-1} \text{ dry sed h}^{-1}$	Gravel
(Crenshaw et al., 2002)	Perennial stream	North Carolina	0.03	$\mu\text{g O}_2 \text{ g}^{-1} \text{ dry sed h}^{-1}$	Gravel
(Crenshaw et al., 2002)	Perennial stream	North Carolina	0.04	$\mu\text{g O}_2 \text{ g}^{-1} \text{ dry sed h}^{-1}$	Gravel
(Findlay & Sinsabaugh, 2003)	Perennial stream	NM	0.02	$\mu\text{g O}_2 \text{ g}^{-1} \text{ dry sed h}^{-1}$	
(Findlay & Sinsabaugh, 2003)	Perennial stream	NM	0.03	$\mu\text{g O}_2 \text{ g}^{-1} \text{ dry sed h}^{-1}$	
(Findlay & Sinsabaugh, 2003)	Perennial stream	NM	0.04	$\mu\text{g O}_2 \text{ g}^{-1} \text{ dry sed h}^{-1}$	
(Jones, 1995)	Perennial stream	Sonoran desert, Arizona	0	$\mu\text{g O}_2 \text{ g}^{-1} \text{ dry sed h}^{-1}$	
(Logue et al., 2004)	Perennial stream	Switzerland	0.6	$\mu\text{g O}_2 \text{ g}^{-1} \text{ dry sed h}^{-1}$	
(Logue et al., 2004)	Perennial stream	Switzerland	0.8	$\mu\text{g O}_2 \text{ g}^{-1} \text{ dry sed h}^{-1}$	
(Logue et al., 2004)	Perennial stream	Switzerland	0.56	$\mu\text{g O}_2 \text{ g}^{-1} \text{ dry sed h}^{-1}$	

(Logue et al., 2004)	Perennial stream	Switzerland	0.96	$\mu\text{g O}_2 \text{ g}^{-1} \text{ dry sed h}^{-1}$	
(Mermillod-Blondin et al., 2005)	Perennial stream	NM	0	$\mu\text{g O}_2 \text{ g}^{-1} \text{ dry sed h}^{-1}$	Sand
(Pusch & Schwoerbel, 1994)	Perennial stream	Germany	0.08	$\mu\text{g O}_2 \text{ g}^{-1} \text{ dry sed h}^{-1}$	Gravel
(Pusch & Schwoerbel, 1994)	Perennial stream	Germany	1.26	$\mu\text{g O}_2 \text{ g}^{-1} \text{ dry sed h}^{-1}$	Gravel
Uehlinger et al. (2002)	Perennial stream	Sonoran desert, Arizona	0	$\mu\text{g O}_2 \text{ g}^{-1} \text{ dry sed h}^{-1}$	Sand
(Uehlinger et al., 2002)	Perennial stream	Sonoran desert, Arizona	0	$\mu\text{g O}_2 \text{ g}^{-1} \text{ dry sed h}^{-1}$	Sand
(Uehlinger et al., 2002)	Perennial stream	Sonoran desert, Arizona	0	$\mu\text{g O}_2 \text{ g}^{-1} \text{ dry sed h}^{-1}$	Sand
(Uehlinger et al., 2002)	Perennial stream	Sonoran desert, Arizona	0	$\mu\text{g O}_2 \text{ g}^{-1} \text{ dry sed h}^{-1}$	Sand
(Wilczek et al., 2004)	Perennial stream	Germany	1	$\mu\text{g O}_2 \text{ g}^{-1} \text{ dry sed h}^{-1}$	Gravel
(Wilczek et al., 2004)	Perennial stream	Germany	3.81	$\mu\text{g O}_2 \text{ g}^{-1} \text{ dry sed h}^{-1}$	Gravel
(Mendoza-Lera & Mutz, 2013)	Perennial stream	NM	2.28	$\mu\text{g O}_2 \text{ g}^{-1} \text{ dry sed h}^{-1}$	Sand
(Mendoza-Lera & Mutz, 2013)	Perennial stream	NM	1	$\mu\text{g O}_2 \text{ g}^{-1} \text{ dry sed h}^{-1}$	Sand
(Gerull et al., 2011)	Perennial stream	Germany	0.6	$\mu\text{g O}_2 \text{ g}^{-1} \text{ dry sed h}^{-1}$	Sand
(Gerull et al., 2011)	Perennial stream	Germany	5.89	$\mu\text{g O}_2 \text{ g}^{-1} \text{ dry sed h}^{-1}$	Sand
(Ingendahl et al., 2009)	Perennial stream	Germany	0	$\mu\text{g O}_2 \text{ g}^{-1} \text{ dry sed h}^{-1}$	Sandy loam
(Ingendahl et al., 2009)	Perennial stream	Germany	5.37	$\mu\text{g O}_2 \text{ g}^{-1} \text{ dry sed h}^{-1}$	Sandy loam

(Foulquier et al., 2010)	Perennial stream	France (aquifer)	0	$\mu\text{g O}_2 \text{ g}^{-1} \text{ dry sed h}^{-1}$	Gravel
(Foulquier et al., 2010)	Perennial stream	France (aquifer)	0.36	$\mu\text{g O}_2 \text{ g}^{-1} \text{ dry sed h}^{-1}$	Gravel
(Mendoza-Lera & Mutz, 2013)	Perennial stream	NM	1	$\mu\text{g O}_2 \text{ g}^{-1} \text{ dry sed h}^{-1}$	Gravel/sand and gravel+ sand
(Mendoza-Lera & Mutz, 2013)	Perennial stream	NM	4.99	$\mu\text{g O}_2 \text{ g}^{-1} \text{ dry sed h}^{-1}$	Gravel/sand and gravel+ sand
(Gerull et al., 2012)	Perennial stream	NM	0.49	$\mu\text{g O}_2 \text{ g}^{-1} \text{ dry sed h}^{-1}$	Sandy loam
(Gerull et al., 2012)	Perennial stream	NM	2.99	$\mu\text{g O}_2 \text{ g}^{-1} \text{ dry sed h}^{-1}$	Sandy loam
(Mendoza-Lera et al., 2017)	Perennial stream	Germany	2.4	$\mu\text{g O}_2 \text{ g}^{-1} \text{ dry sed h}^{-1}$	Sand
(Mendoza-Lera et al., 2017)	Perennial stream	Germany	11.39	$\mu\text{g O}_2 \text{ g}^{-1} \text{ dry sed h}^{-1}$	Sand
(von Schiller et al., 2019)	IRES	Global	2.3	$\mu\text{g O}_2 \text{ g}^{-1} \text{ dry sed h}^{-1}$	

9. 3. Supplemental information Chapter 5

Table S.5.1 Description and properties of the different sampled environments, with the sampling sites selected for vegetation sampling, elevation (m), time since the last inundation day (days), vegetated (V), bare (B) sediment area, percent area (%) for bare and vegetated sediment, and total area (m²) for each environment. Underlined sites were used to sample CO₂ fluxes and vegetation biomass in the chamber.

Environment	Description	Site	Species	Elevation	Time	B area (%)	V area (%)	T Area
Tail	Flat, organic-rich areas at the tail of the reservoir, exposed in spring 2018	7, 12, 15, 16, <u>23</u>	Persicaria sp, Juncus sp, Gnaphalium type	343.4	396	4,493.87 (21.92)	16,011.66 (78.08)	20,505
Old slope		33, 91, 103, 202, <u>203</u>	Persicaria sp, Juncus sp	340.6	338	18,042.27 (60.03)	12,013.50 (39.97)	30,056
Young slope	Sloppy areas with limes, exposed in winter 2019	65, 66, <u>75</u> , 81, 97	Persicaria sp, Juncus sp, Gnaphalium type	336.6	215	35,594.44 (94.71)	1,986.30 (5.29)	37,581

Plain	Flat areas with limes, exposed in winter 2019	<u>63</u> , 77, 80, 200, 204	Persicaria sp, Juncus sp, Gnaphalium type	332.4	143	27,113.81 (67.28)	13,187.59 (32.72)	40,301
Dam	Flat areas close to the dam zone, exposed in winter 2019	<u>108</u> , 112, 122, 205, 206	Persicaria sp, Juncus sp, Gnaphalium type	325.7	131	12,639.57 (97.84)	278.96 (2.16)	12,919








Table S.5.2 All plant taxa (23) and 31 identified plant species

Plant taxa	Species
1. Juncus sp	<i>J. effusus, J. hybridus, J. articulatus, J. glomeratus</i>
2. Persicaria sp	<i>P. maculosa, P. lapathifolia</i>
3. Gnaphalium type	<i>Gnaphalium luteo-album, Gamochaeta coarctata</i>
4. Salix atrocinerea	<i>Salix atrocinerea</i>
5. Unidentified dicotyledon	<i>Unidentified seedlings</i>
6. Urtica dioica	<i>Urtica dioica</i>
7. Trifolium repens	<i>Trifolium repens</i>
8. Carex sp	<i>Carex remota</i>
9. Lythrum portula	<i>Lythrum portula</i>
10. Digitalis purpurea	<i>Digitalis purpurea</i>
11. Digitaria sp	<i>Digitaria sp</i>
12. Scirpus setaceus	<i>Scirpus setaceus</i>
13. Cardamine sp	<i>Cardamine sp</i>
14. Unidentified graminea	<i>Unidentified graminea</i>
15. Poa annua	<i>Poa annua</i>
16. Veronica sp	<i>Veronica sp</i>
17. Stellaria alsine	<i>Stellaria alsine</i>
18. Prunella sp	<i>Prunella sp</i>
19. Taraxacum officinale	<i>Taraxacum officinale</i>
20. Luzula c. f sylvatica	<i>Luzula c. f sylvatica</i>
21. Callistriche palustris	<i>Callistriche palustris</i>
22. Pinus sp	<i>Seedlings of pinus</i>
23. Illecebrum verticillatum	<i>Illecebrum verticillatum</i>

Table S.5.3 Hourly areal CO₂ fluxes (mmol CO₂ m⁻² h⁻¹) in dark and light conditions for bare sediments and sediments covered by vegetation, vegetation cover (%), biomass density (g m⁻²), plant diversity (number of plant taxa), and biomass (kg) for the five environments. The figures are mean ± SE of the CO₂ three replicates realized for bare sediments and each plant species.

Colonization	Fluxes	Condition	Tail	Old slope	Young slope	Plain	Dam
Bare	FCO ₂	Dark	45.2±15.1	8.16±1.61	8.26±0.14	21.1±4.41	13.7±0.70
		Light	51.9±3.24	6.54±1.76	7.27±0.78	17.1±1.59	12.9±1.76
Gnaphalium spp	FCO ₂	Dark	66.3±1.86	NA	21.3±0.49	31±2.97	21±2.02
		Light	41±3.19	NA	-1.07±0.8	16.8±4.75	13.5±1.74
Juncus spp	FCO ₂	Dark	91.4±21.2	8.95±0.9	17±2.46	25±6.6	18±1.9
		Light	15.4±12.3	1.6±2.7	-1.9±6.2	14.2±4.9	10.3±2.7
Persicaria spp	FCO ₂	Dark	94±24	8±0.02	16.4±3.5	31.3±18	31.8±4.2
		Light	0.5±22	5±1.4	-10.4±5.2	-21±11	4.3±7.5
		B density	1,000	<300	<50	<300	<50
Vegetation	FCO ₂	Diversity	15	10	6	11	5
		Biomass	5,458±1,859	1,587±7.28	321±85.4	2,899±86	117±11.5

The drawdown phase of dam decommissioning is a hot moment of gaseous carbon emissions from a temperate reservoir

Mabano Amani ^{a,b}, Daniel von Schiller ^{a,c}, Isabel Suárez^a, Miren Atristain ^d, Arturo Elosegi ^d, Rafael Marcé ^{e,f}, Gonzalo García-Baquero ^{g,h} and Biel Obrador ^{a,b}

^aDepartament de Biologia Evolutiva, Ecologia i Ciències Ambientals (BEECA), Universitat de Barcelona (UB), Barcelona, Spain; ^bInstitut de Recerca de la Biodiversitat (IRBio), Universitat de Barcelona (UB), Barcelona, Spain; ^cInstitut de Recerca de l'Aigua (IdRA), Universitat de Barcelona (UB), Barcelona, Spain; ^dDepartment of Plant Biology and Ecology, University of the Basque Country (UPV/EHU), Bilbao, Spain; ^eCatalan Institute for Water Research (ICRA), Girona, Spain; ^fUniversity of Girona, Girona, Spain; ^gBiodonostia Health Research Institute, San Sebastian, Spain; ^hSpanish Consortium for Research on Epidemiology and Public Health, Instituto de Salud Carlos III, Madrid, Spain

ABSTRACT

Dam decommissioning (DD) is a viable management option for thousands of ageing dams. Reservoirs are large carbon sinks, and reservoir drawdown results in important carbon dioxide (CO₂) and methane (CH₄) emissions. We studied the effects of DD on CO₂ and CH₄ fluxes from impounded water, exposed sediment, and lotic water before, during, and 3–10 months after drawdown of the Enobietà Reservoir, north Iberian Peninsula. During the study period, impounded water covered 0–100%, exposed sediment 0–96%, and lotic water 0–4% of the total reservoir area (0.14 km²). Areal CO₂ fluxes in exposed sediment (mean [SE]: 295.65 [74.90] mmol m⁻² d⁻¹) and lotic water (188.11 [86.09] mmol m⁻² d⁻¹) decreased over time but remained higher than in impounded water (–36.65 [83.40] mmol m⁻² d⁻¹). Areal CH₄ fluxes did not change over time and were noteworthy only in impounded water (1.82 [1.11] mmol m⁻² d⁻¹). Total ecosystem carbon (CO₂ + CH₄) fluxes (kg CO₂-eq d⁻¹) were higher during and after than before reservoir drawdown because of higher CO₂ fluxes from exposed sediment. The reservoir was a net sink of carbon before reservoir drawdown and became an important emitter of carbon during the first 10 months after reservoir drawdown. Future studies should examine mid- and long-term effects of DD on carbon fluxes, identify the drivers of areal CO₂ fluxes from exposed sediment, and incorporate DD in the carbon footprint of reservoirs.

ARTICLE HISTORY

Received 27 January 2022
Accepted 28 June 2022

KEYWORDS



ageing dams; carbon dioxide fluxes; dam removal; exposed sediment; reservoir drawdown; water reservoirs

Introduction

Reservoirs influence the global carbon (C) cycle and climate system because they are large sinks of organic C and great emitters of carbon dioxide (CO₂) and methane (CH₄) greenhouse gases (GHGs; Downing et al. 2008, Deemer et al. 2016, Mendonça et al. 2017). Emissions of GHGs during the operational phase of reservoirs, ~0.8 Pg CO₂ equivalents (CO₂-eq) yr⁻¹ (Deemer et al. 2016), have been included in the global inventories of anthropogenic GHGs (IPCC 2019) because they play a significant role in global warming. The global C emissions from reservoirs are lower than the organic C burial in their sediments (Deemer et al. 2016, Mendonça et al. 2017), although this finding has been recently challenged (Keller et al. 2021). In addition, during the removal of a dam and its ancillary facilities, (i.e., dam decommissioning), the large stocks of organic C in the

sediments of the reservoir may decompose and emit more CO₂ and CH₄ (Pacca 2007, Perera et al. 2021).

Dam decommissioning (DD) is becoming a credible management solution for tens of thousands of dams that have reached or exceeded their engineered life expectancies of 50–100 years (Doyle et al. 2003, Stanley and Doyle 2003, Perera et al. 2021). Dams are removed for several reasons, including environmental restoration, increasing maintenance costs, gradual reservoir sedimentation, and public safety (Perera et al. 2021). The process of DD has gained high research interest, which has focused mostly on the effects of river connectivity on ecological processes such as migration and dispersal of living organisms (Bednarek 2001, Marks et al. 2010, Bellmore et al. 2019). Although reservoir sediments are important repositories of organic C, previous studies have not examined the fate of that sediment

CONTACT Mabano Amani  amanigama@gmail.com  Departament de Biologia Evolutiva, Ecologia i Ciències Ambientals (BEECA), Universitat de Barcelona (UB), Av. Diagonal 643, 08028 Barcelona, Spain

 Supplemental data for this article can be accessed online here: <https://doi.org/10.1080/20442041.2022.2096977>.

© 2022 The Author(s). Published by Informa UK Limited, trading as Taylor & Francis Group

This is an Open Access article distributed under the terms of the Creative Commons Attribution-NonCommercial-NoDerivatives License (<http://creativecommons.org/licenses/by-nc-nd/4.0/>), which permits non-commercial re-use, distribution, and reproduction in any medium, provided the original work is properly cited, and is not altered, transformed, or built upon in any way.

organic C following DD (Pacca 2007). Dam decommissioning may be a relevant component of the C balance in a reservoir because reservoir drawdown is hot moment for the decomposition of sediment organic C to CO₂ and CH₄ (Deshmukh et al. 2018, Keller et al. 2021, Paranaíba et al. 2021).

The reservoir drawdown phase of DD is likely to first increase CO₂ and CH₄ fluxes from a reservoir through the formation of shallow waters (Harrison et al. 2017, Deshmukh et al. 2018, Li et al. 2020). Small patches of shallow waters can emit, for instance, 75% and 90% of, respectively, the annual CO₂ and CH₄ fluxes from reservoirs (Harrison et al. 2017, Deshmukh et al. 2018). Approximately 35% of total CH₄ fluxes from the surface waters of reservoirs is emitted via diffusion while 65% is emitted via ebullition (Deemer et al. 2016), which is higher in shallow waters (Baulch et al. 2011). Shallow waters emit higher areal C fluxes due to conditions such as increased aeration and temperature that facilitate gas production in sediments, and shallow depth that results in low hydrostatic pressure and readily allows gases to be transported to the overlying water layer and the water–atmosphere interface (Harrison et al. 2017, Li et al. 2020). Dam decommissioning may promote C emissions to the atmosphere because of the increased areal extension in shallow waters resulting from reservoir drawdown.

Reservoir drawdown can furthermore produce high C fluxes when it exposes sediments to the atmosphere. Exposed sediment is a hotspot for CO₂ emissions, whose areal fluxes in reservoirs (4–1533 mmol m⁻² d⁻¹; Gómez-Gener et al. 2016, Jin et al. 2016, Obrador et al. 2018) are higher than CO₂ fluxes from surface waters of lentic waters (18–55 mmol m⁻² d⁻¹; Raymond et al. 2013, Deemer et al. 2016, Holgerson and Raymond 2016), and even comparable to areal CO₂ fluxes from lotic water (120–633 mmol m⁻² d⁻¹; Raymond et al. 2013, Borges et al. 2015, Gómez-Gener et al. 2015). Lotic waters emit higher C fluxes than impounded water because of their highly turbulent water columns and, hence, higher gas exchange coefficients (Gómez-Gener et al. 2015). Furthermore, the higher CO₂ emissions from exposed sediment are related to a closer coupling of CO₂ production and fluxes and increased CO₂ production due to high oxygen availability (Fromin et al. 2010, Keller et al. 2020).

Increased redox potentials in exposed sediment reduce CH₄ production and increase CH₄ oxidation, which results in lower CH₄ fluxes. Thus, CH₄ fluxes from exposed sediment (0.1–1 mmol m⁻² d⁻¹; Yang et al. 2014, Gómez-Gener et al. 2015, Deshmukh et al. 2018) are lower than CH₄ fluxes from lotic waters

(4.2 [8.4] mmol m⁻² d⁻¹; Stanley et al. 2016) and surface waters of lakes and reservoirs (3–10 mmol m⁻² d⁻¹; Deemer et al. 2016). Fluxes of CH₄ from a flooded site may even be 3 orders of magnitude higher than CH₄ fluxes from a nonflooded site of the same reservoir (Yang et al. 2014). Although areal CO₂ fluxes are higher than CH₄ fluxes from reservoirs, CH₄ has a global warming potential 25 times higher than that of CO₂ over a span of 100 years (IPCC 2013); thus, 79% of the annual CO₂-eq emissions from reservoirs occurs as CH₄ (Deemer et al. 2016). In summary, when exposed sediment replaces impounded water during DD, CO₂ emissions may increase, whereas CH₄ emissions may decrease. However, to our knowledge, no empirical evidence exists on the effects of DD on C fluxes in reservoirs. This knowledge would help inform regional and global scale estimates of the C footprint of reservoirs and their perception as a C-neutral source of energy (Barros et al. 2011).

Here, we assessed short-term effects of DD on CO₂ and CH₄ fluxes before, during, and after drawdown of a temperate reservoir. We measured CO₂ and CH₄ fluxes in exposed sediment, deep and shallow zones of impounded water, and lotic water. We hypothesized a temporal change in CO₂ and CH₄ fluxes for the 3 environments along reservoir drawdown, CO₂ fluxes highest in exposed sediment, CH₄ fluxes highest in impounded water, higher CO₂ and CH₄ fluxes from the shallow zone than the deep zone of impounded water, and higher ecosystem C fluxes due to higher areal C fluxes from exposed sediment and lotic water after reservoir drawdown.

Materials and methods

Study site

The Enobieta Reservoir is in the valley of Artikutza (Navarre, northern Iberian Peninsula), where human activities have been restricted since 1919, when the municipality of Donostia-San Sebastián bought the land to ensure the supply of high-quality drinking water. The mean annual air temperature is 12.2 °C with an average rainfall of 2064 mm yr⁻¹ (average 1954–2019; Gobierno de Navarra 2019). The dam was constructed between 1947 and 1953 on the Enobieta Stream. The reservoir had an initial storage capacity of 2.66 hm³, length of 1.1 km, maximum depth of 25.5 m, a concrete dam height of 42 m, and an area of 0.14 km². Geotechnical problems appeared during its construction, forcing a reduction in its storage capacity to 1.40 hm³, and the construction of a larger reservoir (Añarbe Reservoir, 43.8 hm³) downstream in 1976,

after which Enobieta Reservoir was no longer used as a water supply facility (Larrañaga et al. 2019). In addition, Artikutza is part of the Natura 2000 Network and, since 2014, is a special conservation zone. The high conservation status of the valley and the structural instability of the dam led to a DD plan of the Enobieta Reservoir, a process that began in 2017 and extended through and 2019 (Supplemental Fig. S1). To date, the decommissioning has been partial; the reservoir has been completely emptied of water and the river runs freely through a hole in the dam, but the concrete structure of the dam (the physical structure retaining the water) is still standing.

Sampling design

We measured CO₂ and CH₄ fluxes in 3 environments—impounded water, exposed sediment, and lotic water—before, during, and after reservoir drawdown. We conducted 8 sampling campaigns on 16 June 2016, 7 July 2018, 10 September 2018, 22 October 2018, 21 January 2019, 9 April 2019, 2 July 2019, and 18 February 2020 (Table 1, Supplemental Fig. S1). Exposed sediment and lotic water completely replaced impounded water on 25 February 2019. The campaigns conducted before 25 February 2019 correspond to the periods Before and During reservoir drawdown, while the campaigns after this date correspond to the period After reservoir drawdown. Thus, we sampled 2 times prior to drawdown (day -984 and -233), 3 times during drawdown (days -168, -126, and -35), and 3 times after drawdown was complete (day 43, 127, and 358). We identified these days by taking the sampling date minus 25 February 2019 (for instance, 16 June 2016–25 February 2019 = -984 days; Table 1).

Impounded water was sampled from day -984 to day -35 (i.e., when it was present) in 2 zones: deep water (>4 m) and shallow water (<4 m; Harrison et al. 2017; Fig. 1, Table 1, Supplemental Fig. S1). The location of the shallow water zone changed over time as the water level decreased along drawdown. Before exposed sediment and lotic water completely replaced impounded water (day -233 to -35), we measured CO₂ and CH₄ fluxes in lotic water at the stream–reservoir transition inlet (1 site). After complete reservoir drawdown (day 43–358), we measured the fluxes in lotic water at 2 sites across the reservoir. For both impounded water and lotic water, we measured CO₂ and CH₄ fluxes in triplicate (3 samples at each site).

We sampled CO₂ and CH₄ fluxes in exposed sediment from day -233 to day 358 (when it was present; Table 1). To measure CO₂ and CH₄ fluxes in exposed sediment, we used 4 cross-sectional transects (A, B, C,

and D; Fig. 1) comprising between 1 and 5 sites (Supplemental Table S1). We measured 3 CO₂ fluxes and 1 CH₄ flux at each site. The number of transects and the number of sites for some transects increased with time as water retracted from the edge to the center and toward the dam of the reservoir. For instance, because impounded water covered most of the reservoir on day -233, we had only transect A with 1 site (thus, the sample size [*n*] in this campaign was 3 for CO₂ and 1 for CH₄). Moreover, the number of sites among transects varied because the distance from the center to the edge of the reservoir differed across the reservoir. Consequently, the number and length of transects changed with reservoir drawdown (Table 1). During reservoir drawdown (day -168 to -35), we used 3 transects (A, B, and C) with 3 sites each (*n* = 27 for CO₂ and *n* = 9 for CH₄). After reservoir drawdown (from day 43 onward), we used 4 transects, with 3 (A and D), 4 (B), and 5 (C) sites each (*n* = 45 for CO₂ and *n* = 15 for CH₄; Fig. 1, Supplemental Table S1).

Determination of CO₂ fluxes

We determined CO₂ fluxes from exposed sediment and impounded water using the chamber method (Frankignoulle 1988). We measured CO₂ fluxes from exposed sediment with an enclosed opaque soil respiration chamber (SRC-1, PP-Systems, Amesbury, MA, USA). For impounded water, we estimated CO₂ fluxes across the water–air interface with a custom-made floating enclosed opaque chamber. We monitored the partial pressure of CO₂ (*p*CO₂) in the chambers every second with an infrared gas analyser (IRGA-EGM-5, PP-Systems, 1% accuracy). We waited for *p*CO₂ in chambers to change by at least 10 μatm, which took 120–300 s in exposed sediment and 300–600 s in impounded water. We calculated CO₂ fluxes from exposed sediment and impounded water by a linear regression of *p*CO₂ in the chambers over time corrected for temperature and pressure as:

$$FCO_2 = \left(\frac{dpCO_2}{dt} \right) \left(\frac{V}{RTS} \right), \quad (1)$$

where *FCO₂* is CO₂ flux (mol m⁻² d⁻¹), *dpCO₂/dt* is the slope of the regression of *p*CO₂ in the chamber over time (atm d⁻¹), *V* is the volume of the chamber (1.171 × 10⁻³ m³ for exposed sediment, 0.027 m³ for impounded water), *S* is the area of the chamber (7.8 × 10⁻³ m² for exposed sediment and 0.194 m² for impounded water), *T* is temperature (K), and *R* is the ideal gas constant (m³ atm K⁻¹ mol⁻¹). All fluxes reported here follow the convention that efflux to the

Table 1. Sampling campaigns, sampling date (day/month/year), time (d) before or after exposed sediment completely replaced impounded water, phase of DD (pre = before, peri = during, post = after), average reservoir water depth (RWD), surface area and percentage (%) area of each environment, and zone (DS = deep and shallow, S = only shallow) sampled within impounded water, transects (A, B, C, and D) sampled for exposed sediment, (n is the sample size of CO_2 fluxes in exposed sediment while the sample size for CH_4 fluxes is 3 times less than that of CO_2 for each sampling), NA = not applicable.

Sampling date	Time	Phase	RWD (m)	Impounded water			Exposed sediment			Running water	
				Area (m^2)	% area	Depth	Area (m^2)	% area	Transect (n)	Area (m^2)	% area
16/06/16	-984	pre	20	141 400	100	DS	0	0	NA	0	0
07/07/18	-233	pre	19.8	140 800	99.6	DS	526	0.4	A (3)	74	0.1
10/9/18	-168	peri	14.8	101 200	71.5	DS	39 385	28	ABC (27)	815	0.5
22/10/18	-126	peri	9.8	71 500	50.6	DS	69 400	48.4	ABC (27)	1500	1
21/01/19	-35	peri	4.8	15 000	10.6	S	122 500	86.6	ABC (27)	3900	2.8
09/04/19	43	post	0	0	0	NA	135 800	96	ABCD (45)	5600	4
02/07/19	127	post	0	0	0	NA	135 800	96	ABCD (45)	5600	4
18/02/20	358	post	0	0	0	NA	135 800	96	ABCD (45)	5600	4

atmosphere corresponds to a positive flux, and uptake or influx corresponds to a negative flux.

We determined the direction and magnitude of CO_2 fluxes from lotic water by applying Fick's first law of gas diffusion:

$$FCO_{2stream} = kCO_2 \times \beta \times (pCO_{2w} - pCO_{2a}), \quad (2)$$

where $FCO_{2stream}$ is the CO_2 flux from lotic water ($\text{mol m}^{-2} \text{d}^{-1}$), kCO_2 is the transfer velocity of CO_2 (m d^{-1}), β is the solubility coefficient of CO_2 ($\text{mol m}^{-3} \text{atm}^{-1}$), and pCO_{2w} and pCO_{2a} are, respectively, the partial pressures of CO_2 (atm) in surface water and air.

We determined pCO_{2w} and pCO_{2a} in triplicate at each sampling site. The pCO_{2w} was determined by means of a membrane gas exchanger (MiniModule, Liqui-Cel, 3M, Maplewood, MN, USA) coupled to an IRGA. We circulated sampled water via gravity through the membrane contactor at a rate of 300 mL min^{-1}

while recirculating an enclosed volume of gas between the membrane and the IRGA. We determined the solubility of CO_2 , for the temperature and salinity of each sample (Bastviken et al. 2004). We estimated kCO_2 (m d^{-1}) in the lotic water as:

$$kCO_2 = k_{600} \left(\frac{ScCO_2}{600} \right)^{-\frac{2}{3}}, \quad (3)$$

where $ScCO_2$ is the Schmidt number of CO_2 (dimensionless) and k_{600} (m d^{-1}) is k of CO_2 at a Schmidt number (Sc) of 600,

$$k_{600} = 5.14 \times d \times \frac{Vel}{d^{1.33}} \left(\frac{600}{ScCO_2} \right)^{-\frac{2}{3}}, \quad (4)$$

d is depth of the water column (m) and Vel denotes the water velocity (m s^{-1}), noting that this equation is an empirical adjustment for k_{600} in lotic water.

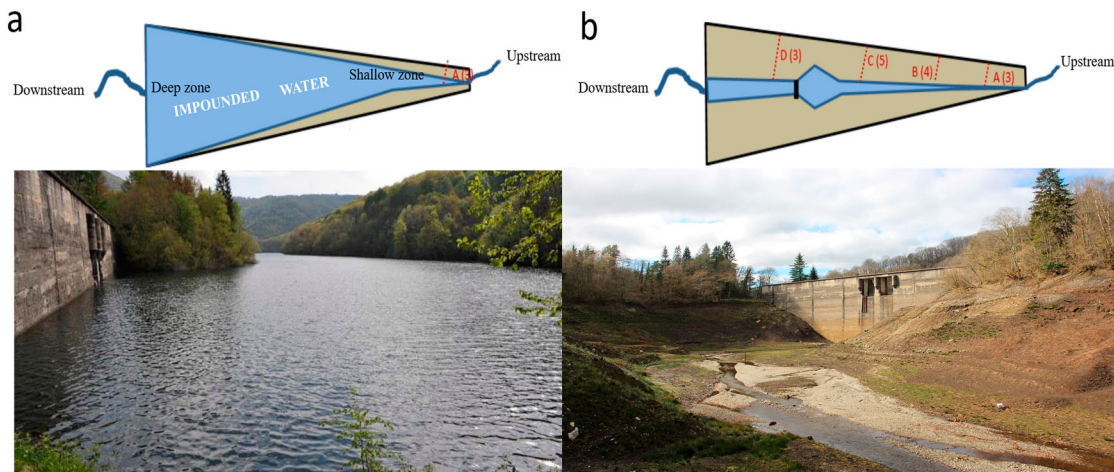


Figure 1. Simplified schematic and photographic view of the sampling design showing the state of Enobietta Reservoir when (a) it was full: photo taken on day -233, July 2018; and (b) when it was empty: photo taken on day 358, February 2020. The scheme shows the 3 sampled environments: exposed sediment, impounded water, and running water. The red dashed lines are the cross-sectional transects used to measure CO_2 and CH_4 fluxes from exposed sediment. The numbers in brackets are the number of sites sampled for each transect of exposed sediment on each day. Photos taken by M. Amani and B. Obrador.

We estimated the velocity of lotic water by the time-conductivity curve that we obtained in instantaneous additions of a tracer (NaCl) at a turbulent point in the channel, 200 m downstream of the point of addition, using a field conductivity meter (WTW 340i, Germany). We recorded changes in electrical conductivity generated by the tracer pulse then used the changes to calculate the speed by dividing the distance by time that electrical conductivity takes to reach the maximum peak (Gordon et al. 2004).

Determination of CH₄ fluxes

Determination of diffusive CH₄ fluxes in water

We determined diffusive CH₄ fluxes from impounded water and lotic water using the gradient of $p\text{CH}_4$ between water and air. We collected 3 samples of $p\text{CH}_4$ in surface water at each sampling site using the headspace technique equilibrated in situ with air (Bastviken et al. 2004). Briefly, we collected 30 mL of water with a 60 mL plastic syringe, which created a headspace with ambient air at 1:1 ratio (collected water:ambient air). We manually shook the syringe for 1 min and then submerged it at each sampling site for 5 min to maintain constant equilibration temperature. Thereafter, we transferred 20 mL of the gas mixture from the plastic syringe to a pre-evacuated vial (Exetainer, Labco Ltd., Lampeter, UK). We took ambient air samples to correct for CH₄ concentration in the headspace.

In the laboratory, we determined $p\text{CH}_4$ in the gaseous mixture using a gas chromatograph equipped with a Flame Ionising Detector (FID; 7820A GC, Agilent, Santa Clara, CA, USA), with an accuracy of 4%. We routinely ran 6 point standard curves obtained from a standard of 15 ppm CH₄ (Crystal, Air Liquide SA, Paris, France).

We determined diffusive CH₄ fluxes as for CO₂ (equation 2). In impounded water, the CH₄ transfer coefficient ($k\text{CH}_4$, in m d^{-1}) was obtained as:

$$k\text{CH}_4 = k_{600} \left(\frac{\text{ScCH}_4}{600} \right)^{-0.5}, \quad (5)$$

with

$$k_{600} = 0.228 \times U_{10}^{2.2} + 0.168, \quad (6)$$

where ScCH_4 is the Schmidt number for CH₄ and U_{10} corresponds to the wind speed (m s^{-1}) at a height of 10 m above impounded water. To find U_{10} we measured the wind speed in situ at 1 m with a portable anemometer (Kestrel 4000, Boothwyn, PA, USA) and converted it to U_{10} following Crusius and Wanninkhof (2003). We determined ScCH_4 in impounded water and lotic water

at the measured water temperature (Howard and Howard 1993, Gómez-Gener et al. 2015). We calculated CH₄ fluxes from lotic water the same way we calculated CO₂ fluxes, using ScCH_4 instead of ScCO_2 in equation 3 to estimate $k\text{CH}_4$.

Determination of ebullitive CH₄ fluxes from impounded water

We measured ebullitive CH₄ fluxes from impounded water with 8 inverted funnel collectors: 4 in deep water and 4 in shallow water. We maintained the funnels for 6–23 h (DelSontro et al. 2010) to get a measurable flux (i.e., a detectable signal). The funnels (collection area of 0.44 m²) had a collector bottle where the gas accumulated during the entire sampling period. We closed the collectors of each funnel underwater and weighed them on the shore to determine the volume of gas, defined as the difference in weight between the collector after collection and the same collector filled with water. We estimated that the detection limit was ~10 mL for the gas collected using the gravimetric method. The collected gas was sampled and stored in pre-evacuated vials. We analysed $p\text{CH}_4$ in the gas samples with a gas chromatograph as detailed earlier for the diffusive CH₄ fluxes. We determined ebullitive CH₄ fluxes based on $p\text{CH}_4$ in the gas mixture, the volume of collected gas, collection time of the funnel, and surface area of the funnel.

Determination of diffusive CH₄ fluxes from exposed sediment

We determined diffusive CH₄ fluxes in exposed sediment with enclosed opaque chambers equipped with gas inlet and outlet valves in a closed mode (no open vent). We installed the chambers (verifying a correct seal between sediments and the atmosphere) in fixed sampling sites within the transects where we installed fixed collar rings (Fig. 1). We sampled the chamber 3 times during each measure: at time 0 (T0), time 1 (T1 ≥ 55 min), and time 2 (T2 ≤ 654 min). We determined $p\text{CH}_4$ in the gas samples using a gas chromatograph as detailed earlier. We determined areal CH₄ fluxes ($\text{mmol m}^{-2} \text{d}^{-1}$) based on the variation of $[\text{CH}_4]$ using the linear regression slope of the $p\text{CH}_4$ -time relationship, the area (0.0168 m²), and the volume ($1.388 \times 10^{-3} \text{ m}^3$) of the chamber (equation 1). For this calculation, we included only the variations in $p\text{CH}_4$ above the detection limit (>0.05 ppmv: parts per million by volume).

Upscaling carbon fluxes to the ecosystem level

We multiplied the mean areal C flux ($\text{mmol m}^{-2} \text{d}^{-1}$) of each environment by the surface area (m²) it occupied

during each sampling campaign (Table 1) to quantify ecosystem C fluxes (mol d^{-1}). We obtained surface areas of impounded water and exposed sediment using satellite Sentinel images (Miranda et al. 2018) taken during the period closest to each sampling campaign, mostly 2–3 days, maximum 1 week. We extracted the surface areas of the reservoir and lotic water, respectively, using pixel-based classification and a digital elevation model using Erdas Image 2020 and ArcMap 10.8 (Maathuis and Wang 2006, Rathore et al. 2018). Finally, we multiplied ecosystem C fluxes by the molar mass of each GHG (16 g for CH_4 and 44 g for CO_2) by the global warming potential of each GHG (25 for CH_4 and 1 for CO_2 considering a span of 100 years) to find $\text{CO}_2\text{-eq}$ in $\text{kg CO}_2\text{-eq d}^{-1}$ (IPCC 2013).

Statistical analyses

We assessed the effect of environment type and time on CO_2 and CH_4 flux rates using mixed effects models (Pinheiro and Bates 2000, Madsen and Thyregod 2010) with the R package *nlme* (Pinheiro and Bates 2018) in R 4.0.5 (R Core Team 2021). Environment, a categorical factor with 3 levels (exposed sediment, impounded water, and lotic water) and time, a numerical variable, were fixed factors. We explored the potential presence of spatial structure, such as differences in C fluxes among transects and sites of exposed sediment via spatial correlograms, but we found no significant spatial pattern. Thus, we applied spatially explicit methods of analysis by using a random factor “Site” within the framework of mixed modeling to account for spatial variability; therefore, site was the random effect. To consider the temporal autocorrelation present in the data and avoid wrong inference, temporal autocorrelation within each site was accounted for by means of a correlation structure with homogeneous variances (compound symmetry). We included a variance function that allowed different standard deviations per environment level to control for heteroscedasticity.

Results

Spatial extent of the environments and areal CO_2 and CH_4 fluxes

Before reservoir drawdown, impounded water occupied almost 100% of the surface area of the reservoir (Table 1). During reservoir drawdown, exposed sediment covered 28–87% of the reservoir. After reservoir drawdown, exposed sediment covered 96% and lotic water 4% of the surface area of the Enobieta Reservoir.

Environment ($p < 0.001$), time ($p = 0.006$), and their interaction ($p < 0.001$) influenced areal CO_2 fluxes (Table 2, Fig. 2a, Supplemental Fig. S2a). Areal CO_2 fluxes (mean [SE]) from exposed sediment ($295.65 [74.90] \text{ mmol m}^{-2} \text{ d}^{-1}$) and lotic water ($188.11 [86.09] \text{ mmol m}^{-2} \text{ d}^{-1}$) decreased over time but remained higher than areal CO_2 fluxes from impounded water ($-36.65 [83.40] \text{ mmol m}^{-2} \text{ d}^{-1}$; Fig. 2a; Supplemental Table S2, Supplemental Fig. S2a). Areal CO_2 fluxes in impounded water increased slightly from negative to positive values over time (Fig. 2a; Supplemental Table S2, Supplemental Fig. S2a).

Environment ($p < 0.001$) but not time ($p = 0.531$) influenced the areal CH_4 fluxes (Table 2, Fig. 2b, Supplemental Fig. S2b). The sum of areal diffusive and ebullitive CH_4 fluxes from impounded water ($1.82 [1.11] \text{ mmol m}^{-2} \text{ d}^{-1}$) were higher than areal diffusive CH_4 fluxes from exposed sediment ($0.06 [0.10] \text{ mmol m}^{-2} \text{ d}^{-1}$) and lotic water ($-0.96 [1.72] \text{ mmol m}^{-2} \text{ d}^{-1}$; Supplemental Table S3). Ebullition was the dominant pathway of areal CH_4 fluxes (i.e., 63% of areal diffusive + ebullitive CH_4 fluxes), whereas the shallow zone emitted 93% of areal CH_4 fluxes from impounded water (Supplemental Fig. S3).

Ecosystem CO_2 and CH_4 fluxes

The total ecosystem C flux was slightly positive (74 mol d^{-1} ; day -984) or even negative (-5904 mol d^{-1} ; day -233) before drawdown (i.e., when the reservoir was almost fully covered by impounded water; Fig. 3a). During reservoir drawdown, total ecosystem C fluxes were $18\,718 \text{ mol d}^{-1}$ (day -168), $12\,540 \text{ mol d}^{-1}$ (day -126), and $12\,393 \text{ mol d}^{-1}$ (day -35 ; Fig. 3a). After reservoir drawdown, total ecosystem C fluxes were, respectively, $23\,669 \text{ mol d}^{-1}$ (day 43), $38\,713 \text{ mol d}^{-1}$ (day 127), and $18\,568 \text{ mol d}^{-1}$ (day 358; Fig. 3a). On average, the total ecosystem C fluxes were -2915 mol d^{-1} before, $14\,550 \text{ mol d}^{-1}$ during, and $26\,983 \text{ mol d}^{-1}$ after reservoir drawdown. Thus, ecosystem C fluxes from the reservoir were 2 and 10 times higher after than, respectively, during and before reservoir drawdown.

Exposed sediment contributed most of total ecosystem C fluxes, and its contribution over time followed the same temporal pattern as total ecosystem C fluxes. The mean of total ecosystem C fluxes from exposed sediment, impounded water, and lotic water was, respectively, $16\,047 \text{ mol d}^{-1}$ (93% of total C flux), 1071 mol d^{-1} (6%), and 154 mol d^{-1} (1%). Thus, exposed sediment contributed most to total ecosystem C fluxes because of its high areal CO_2 fluxes and surface area, whereas lotic water had the lowest contribution to

Table 2. Mixed modeling results for areal CO₂ and areal CH₄ (diffusion + ebullition) fluxes (mmol m⁻² d⁻¹): hypothesis testing for fixed factors (environment and time). df (num) is the numerator degrees of freedom for the *F* test for the fixed variables, df (den) displays the denominator degrees of freedom for the *F* test for the fixed variables, and EnvXTime represents the interaction between environment and time. Significant *p*-values are shown in bold.

Source	df (num)	CO ₂ df (den)	<i>F</i> -value	<i>p</i> -value	df (num)	CH ₄ df (den)	<i>F</i> -value	<i>p</i> -value
Intercept	1	255	37.71	<0.001	1	35	164.76	<0.001
Env	2	255	13.91	<0.001	2	35	316.78	<0.001
Time	1	255	7.82	0.006	1	35	0.40	0.531
EnvXTime	2	255	8.70	<0.001	2	35	0.40	0.676

the total ecosystem C fluxes because of its small surface area.

Ecosystem CO₂ and CH₄ fluxes contributed, respectively, 99% and 1% of total ecosystem C fluxes. Ecosystem CO₂ and ecosystem CO₂-eq fluxes followed the

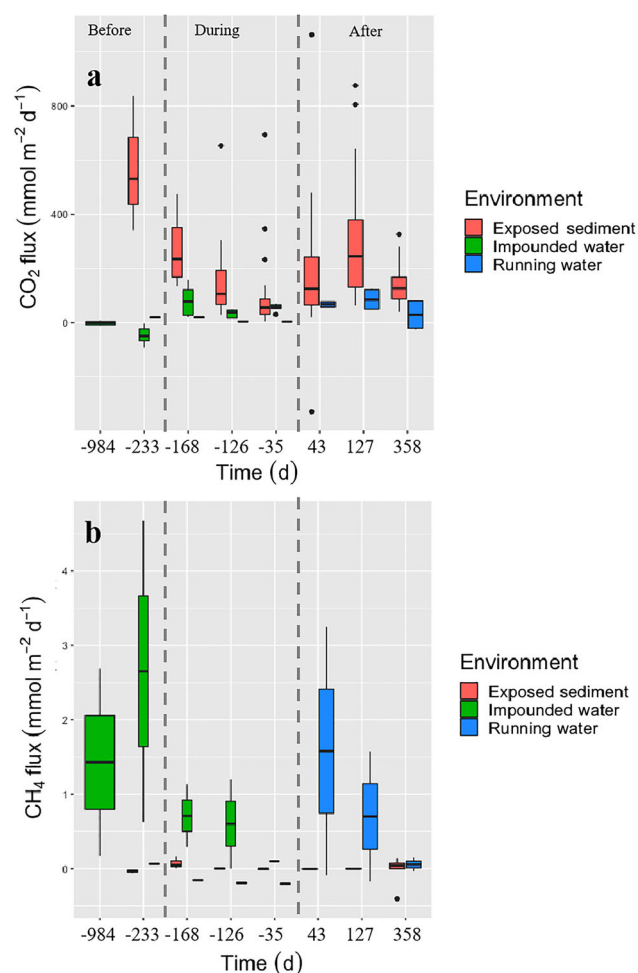


Figure 2. (a) Areal CO₂ and (b) CH₄ fluxes from impounded water (green), exposed sediment (red), and running water (blue). Boxplots display 25th, 50th, and 75th percentiles; whiskers show minimum and maximum values; and points beyond the minimum and maximum whiskers are outliers. The x-axis describes the 8 sampling campaigns, which are divided into 3 categories: Before (days -984 and -233), During (days -168, -126, and -35), and After (days 43, 127, and 358) reservoir drawdown.

temporal pattern of total ecosystem C fluxes in exposed sediment because this environment contributed most of total ecosystem C fluxes, and ecosystem CO₂ fluxes predominated over ecosystem CH₄ fluxes (Fig. 3b–d). By contrast, impounded water emitted 98% of ecosystem CH₄ fluxes (Fig. 3d). Thus, ecosystem CH₄ fluxes from impounded water were higher before reservoir drawdown and then decreased along DD as impounded water was replaced by exposed sediment and lotic water. Exposed sediment contributed 87%, impounded water 12%, and lotic water 1% of total C fluxes expressed in CO₂-eq (814 kg CO₂-eq d⁻¹) over a span of 100 years. The average of C flux after reservoir drawdown was 8 g CO₂-eq m⁻² d⁻¹.

Discussion

As we hypothesized, the drawdown phase of DD increased total ecosystem C (CO₂ + CH₄) fluxes from the reservoir because of higher fluxes from exposed sediment. Exposed sediment emitted, on average, 93% of the CO₂ flux and 87% of the flux expressed in CO₂-eq. At the ecosystem scale, CO₂ fluxes contributed 99% of total C fluxes while the remaining 1% was contributed by CH₄ fluxes. Most of the CH₄ fluxes (98% on average) arose from impounded water and mostly emitted via ebullition. The rates of CO₂ and CH₄ emissions from shallow impounded water were higher than from deep impounded water.

The drawdown phase of DD increased CO₂ and CH₄ fluxes from the reservoir

Before drawdown (days -984 and -233), the reservoir was a net sink of atmospheric CO₂ but a net source of CH₄. Because impounded water took more CO₂ than the CH₄ it emitted, the Enobietta Reservoir was a net sink of C before reservoir drawdown. Note that we conducted these samplings during summer, a season of high primary production in the Northern Hemisphere and

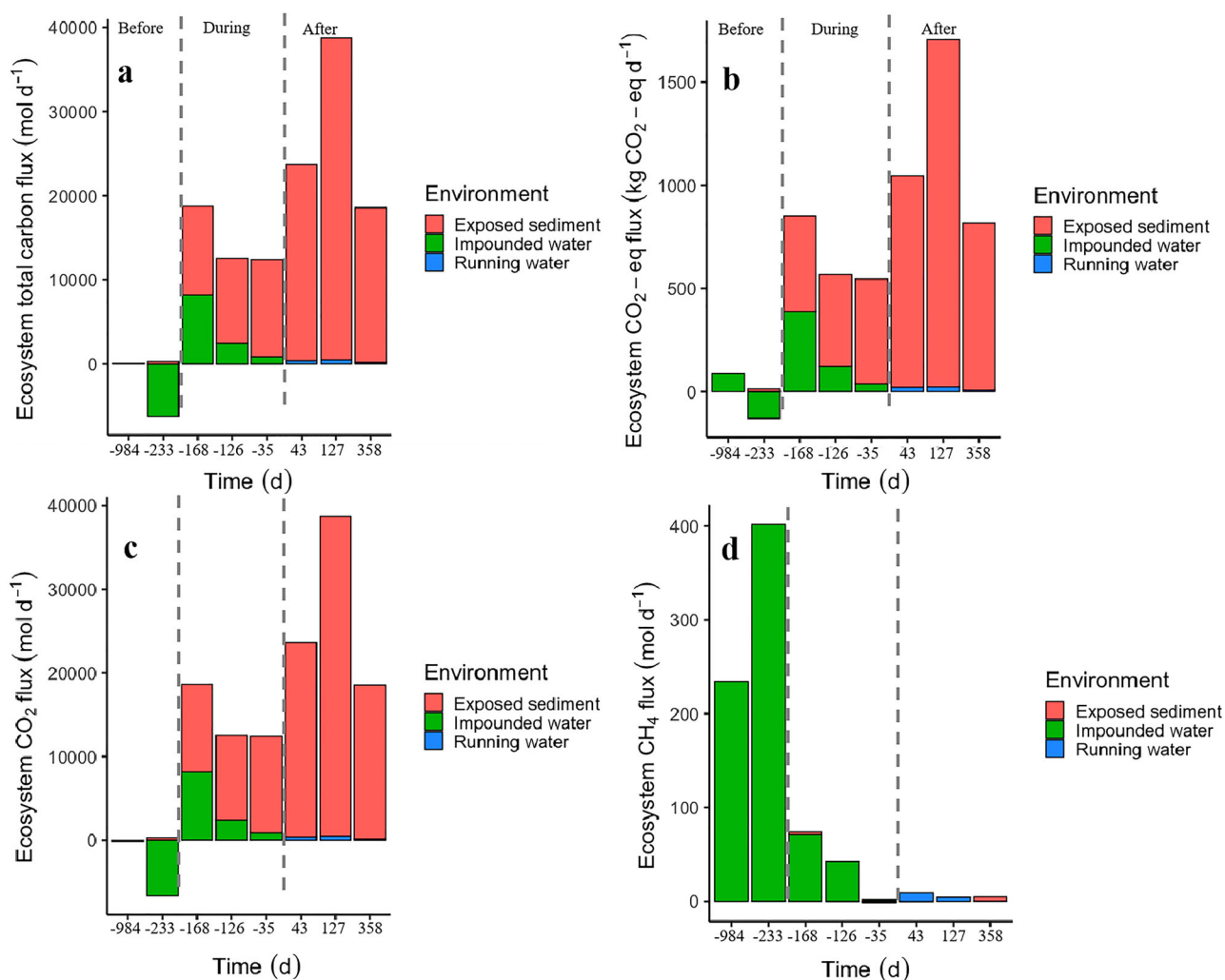


Figure 3. (a) Ecosystem total carbon flux, (b) carbon CO₂-eq flux, (c) ecosystem CO₂ flux, and (d) ecosystem CH₄ flux in exposed sediment, impounded water, and running water. Ecosystem CH₄ fluxes in impounded water are a sum of diffusion and ebullition but are only emitted via diffusion for exposed sediment and running water. The values below $y = 0$ indicate negative carbon fluxes or carbon uptake by the reservoir. Each vertical bar corresponds to a sampling campaign. The x-axis describes the 8 sampling campaigns, which are divided into 3 categories: Before (days -984 and -233), During (days -168, -126, and -35), and After (days 43, 127, and 358) reservoir drawdown.

therefore high CO₂ fixation via photosynthesis (Teodoru et al. 2011).

During reservoir drawdown (days -168, -126, and -35) the reservoir became a net source of C to the atmosphere, especially as CO₂. Areal CO₂ fluxes from impounded water were comparable to areal CO₂ fluxes measured elsewhere in lakes, ponds, and reservoirs (Raymond et al. 2013, Deemer et al. 2016, Holgerson and Raymond 2016). They were, however, lower than fluxes from exposed sediment and lotic water, in agreement with previous studies (Raymond et al. 2013, Kosten et al. 2018, Keller et al. 2020). Impounded waters typically emit lower areal CO₂ fluxes than lotic waters and exposed sediments because of higher CO₂ uptake by primary producers (Howard and Howard 1993, Gómez-Gener et al. 2015). C emissions from reservoirs

are typically highest during their first 10–20 years, when flooded labile C is still available for microbial respiration (St. Louis et al. 2000, Barros et al. 2011). Thus, low areal CO₂ fluxes from impounded water were expected in this oligotrophic reservoir of more than 60 years of existence.

As we expected, areal CH₄ fluxes were lower in exposed sediment and lotic water than in impounded water and higher in shallow than in deep impounded water. Impounded waters are important emitters of CH₄ because of their increased anaerobic microbial functioning (Deemer et al. 2016). Methane is produced in anoxic conditions by anaerobic archaea and bacteria and emitted mainly via ebullition (Bastviken et al. 2004, Baulch et al. 2011, Deemer et al. 2016). Ebullition was the dominant pathway of CH₄ fluxes from impounded

water in this study, consistent with other findings (Del-Sontro et al. 2016, West et al. 2016), mainly in shallow impounded water. Shallow impounded waters are hot-spots for CH₄ emissions because they have a lower capacity to dissolve, trap, and oxidize CH₄. Ebullition might, however, have been underestimated because of its high spatial and temporal heterogeneity (Wik et al. 2016). Impounded water in this study emitted most of CH₄ fluxes; thus, the contribution of CH₄ to total ecosystem C fluxes decreased along reservoir drawdown as impounded water was replaced by exposed sediment.

Exposed sediments emit areal CO₂ fluxes to the atmosphere at higher rates than emissions from the water surface during the flooded periods (Catalán et al. 2014, Gómez-Gener et al. 2016, Obrador et al. 2018). Areal CO₂ fluxes from exposed sediments are higher because of their increased CO₂ diffusivity, higher microbial respiration due to higher oxic conditions, and lower CO₂ uptake by primary producers compared with inundated environments (Howard and Howard 1993, Gómez-Gener et al. 2015, Marcé et al. 2019). In this study, exposed sediment emitted most of the CO₂ fluxes within the reservoir. During the drawdown phase, these CO₂ emissions declined between days -168 and -35, likely reflecting seasonal variations in temperature and humidity. The sampling days were in October (day -126) and January (day -35), the coldest and wettest period in the study area. Lower temperature and higher humidity might have limited oxygen diffusivity, and thus microbial respiration and CO₂ production in exposed sediment, during reservoir drawdown on days -126 and -35.

After reservoir drawdown, total C fluxes at the scale of the reservoir increased and peaked on day 127, following the trend in ecosystem CO₂ fluxes. Microbial respiration, and thus CO₂ production, are higher in exposed sediments with higher content and quality of organic matter (Almeida et al. 2019, von Schiller et al. 2019, Keller et al. 2020). The areal CO₂ fluxes from exposed sediment decreased with time in this study, probably due to the reduction in quantity and quality of sediment organic C. Unfortunately, we did not assess temporal changes in the content and chemical composition of sediment organic C to support this. While the underlying mechanisms for this temporal pattern remain unclear at this stage, they provide evidence for areal emissions to be higher after than before DD.

As we assumed, areal CO₂ fluxes were lower in impounded water than areal CO₂ fluxes from exposed sediment and lotic water. However, we did not expect areal CO₂ fluxes from exposed sediment to be equal to areal CO₂ fluxes from lotic water. Lotic water, because of its high turbulence, should emit higher areal CO₂

fluxes than exposed sediment (Raymond et al. 2013, Borges et al. 2015, Gómez-Gener et al. 2015). The low *p*CO₂ and gas transfer velocity measured in this study might have limited emissions of CO₂ from the lotic water. We reported an average *p*CO₂ in lotic water of 791 µatm, nearly 4 times lower than the average *p*CO₂ = 3100 µatm reported from 6798 streams on a global scale (Raymond et al. 2013). In addition, the average gas transfer velocity (*k*₆₀₀) of 2.6 m d⁻¹ in the lotic water of this study is lower than the mean of *k*₆₀₀ values = 45.0 m d⁻¹ reported in a review on gas exchanges in streams (Ulseth et al. 2019).

Carbon dioxide and CH₄ contributed on average 99% and 1% of total ecosystem C fluxes, respectively. Expressed in CO₂-eq, the contribution of CH₄ rose to 6% of total ecosystem C fluxes because of the higher global warming potential of CH₄ compared to CO₂ (IPCC 2013). Ecosystem CH₄ fluxes are responsible for ~60%–79% of CO₂-eq from surface waters of lakes, ponds, and reservoirs (Deemer et al. 2016, Del-Sontro et al. 2016, van Bergen et al. 2019), whereas exposed sediments are poor emitters of CH₄ because of their increased aerobic conditions (Obrador et al. 2018, Marcé et al. 2019, Arce et al. 2021, Paranaíba et al. 2021). Impounded water emitted 98% of CH₄ fluxes while the remaining 2% was contributed by the combined exposed sediment and lotic water. Although exposed sediment occupied a large surface area, its contribution to ecosystem CH₄ fluxes was low because of its low areal CH₄ fluxes. The contribution of lotic water to ecosystem CH₄ fluxes was low because it occupied a negligible surface area.

Conclusion: implication of DD for the carbon footprint of the reservoir and future perspectives

The average ecosystem flux in CO₂-eq after reservoir drawdown was 8 g CO₂-eq m⁻² d⁻¹, slightly higher than the flux reported on a global scale in surface waters of reservoirs between 4.25 g CO₂-eq m⁻² d⁻¹ (St. Louis et al. 2000) and 6.64 g CO₂-eq m⁻² d⁻¹ (Deemer et al. 2016). The flux reported in this study is also higher than the flux from hydroelectric reservoirs worldwide; 2.55–7.64 g CO₂-eq m⁻² d⁻¹ (Deemer et al. 2016). Hydropower was considered a green source of energy, but GHG emissions from reservoirs contribute to the global C budgets (Deemer et al. 2016, St. Louis et al. 2000, Barros et al. 2011) even before considering their C emissions during and after DD. The high CO₂ fluxes from exposed sediment reported in this study indicate the importance of the drawdown phase of DD as a hot moment for CO₂ and CH₄ emissions from a

reservoir. Thus, the exclusion of GHGs related to the end-of-life of dams may result in an underestimation of the C footprint of reservoirs.

The decrease in CO₂ fluxes in exposed sediment may be a seasonally specific feature that warrants further investigation beyond the short-term duration of this study. Furthermore, exposed sediments are amenable environments for vegetation growth, which may overturn the effects of DD on the C emissions of a reservoir by fixing atmospheric CO₂. However, we lack empirical evidence to clarify the role of plant regrowth in the C dynamics in reservoirs following DD. Thus, we emphasize a need to know the drivers of CO₂ fluxes from exposed sediments and mid- and long-term effects of DD on C emissions in reservoirs, including the role of plant recolonization, and to include DD in the C footprint of reservoirs. To conclude, this study sets a baseline for promising future studies to improve our understanding of how the C dynamics of reservoirs are affected by dam decommissioning.

Acknowledgements

We acknowledge M. Koschorreck and M. Badia who helped in sampling activities.

Disclosure statement

No potential conflict of interest was reported by the author(s).

Funding

This study was funded by the projects Alteration of carbon sinks and sources in shrinking inland waters (Alter-C), the Spanish Ministry of Science, Innovation and Universities (refs: PID2020-114024GB-C31 funded by MCIN/AEI/10.13039/501100011033/) and Effects of the drawdown of Enobieta Reservoir (Navarre) on the biodiversity and functioning of river ecosystems (DESEMBALSE), Foundation BBVA (ref: PI064-17). AM was supported by an FI grant from the Agència de Gestió d'Ajuts Universitaris i de Recerca (AGAUR) of the Generalitat de Catalunya. DvS and BO acknowledge support through the Consolidated Research Group 2017SGR0976. RM acknowledges support by the Generalitat de Catalunya through the Consolidated Research Group 2017SGR1124, and by the CERCA program. AE and MA support of the Basque Government through the Consolidated Research Group IT951-16. AM got a predoctoral grant by the University of the Basque Country (UPV/EHU). DvS is a Serra Hünter Fellow.

ORCID

Mabano Amani  <http://orcid.org/0000-0003-4273-2608>
 Daniel von Schiller  <http://orcid.org/0000-0002-9493-3244>
 Miren Atristain  <http://orcid.org/0000-0002-8515-4150>
 Arturo Elosegui  <http://orcid.org/0000-0001-8809-8484>
 Rafael Marcé  <http://orcid.org/0000-0002-7416-4652>

Gonzalo García-Baquero  <http://orcid.org/0000-0001-6550-1584>

Biel Obrador  <http://orcid.org/0000-0003-4050-0491>

References

- Almeida RM, Paranaíba JR, Barbosa Í, Sobek S, Kosten S, Linkhorst A, Mendonça R, Quadra G, Roland F, Barros N. 2019. Carbon dioxide emission from drawdown areas of a Brazilian reservoir is linked to surrounding land cover. *Aquat Sci.* 81:1–9.
- Arce MI, Bengtsson MM, von Schiller D, Zak D, Täumer J, Urich T, Singer G. 2021. Desiccation time and rainfall control gaseous carbon fluxes in an intermittent stream. *Biogeochemistry.* 155:381–400.
- Barros N, Cole JJ, Tranvik LJ, Prairie YT, Bastviken D, Huszar VLM, del Gioglio P, Roland F. 2011. Carbon emission from hydroelectric reservoirs linked to reservoir age and latitude. *Nat Geosci.* 4:593–596.
- Bastviken D, Cole J, Pace M, Tranvik L. 2004. Methane emissions from lakes: dependence of lake characteristics, two regional assessments, and a global estimate. *Global Biogeochem Cy.* 18:1–12.
- Baulch HM, Dillon PJ, Maranger R, Schiff SL. 2011. Diffusive and ebullitive transport of methane and nitrous oxide from streams: Are bubble-mediated fluxes important? *J Geophys Res.* 116:G04028.
- Bednarek AT. 2001. Undamming rivers: a review of the ecological impacts of dam removal. *Environ Manage.* 27:803–814.
- Bellmore JR, States U, Pess GR, Duda JJ, O'Connor JE, East AE, Foley MM, Wilcox AC, Major JJ, Shafroth PB, et al. 2019. Conceptualizing ecological responses to dam removal: if you remove it, what's to come? *Bioscience.* 69:26–39.
- Borges AV, Darchambeau F, Teodoru CR, Marwick TR, Tamoooh F, Geeraert N, Omengo FO, Guérin F, Lambert T, Morana C, et al. 2015. Globally significant greenhouse-gas emissions from African inland waters. *Nat Geosci.* 8:637–642.
- Catalán N, von Schiller D, Marcé R, Koschorreck M, Gomez-Gener L, Obrador B. 2014. Carbon dioxide efflux during the flooding phase of temporary ponds. *Limnetica.* 33:349–360.
- Crusius J, Wanninkhof R. 2003. Gas transfer velocities measured at low wind speed over a lake. *Limnol Oceanogr.* 48:1010–1017.
- Deemer BR, Harrison JA, Li S, Beaulieu JJ, DelSopntro T, Barros N, Bezerra-Neto JF, Powers SM, Dos Santos MA, Arie Vonk J. 2016. Greenhouse gas emissions from reservoir water surfaces: a new global synthesis. *Bioscience.* 66:949–964.
- DelSontro T, Boutet L, St-Pierre A, del Giorgio PA, Prairie YT. 2016. Methane ebullition and diffusion from northern ponds and lakes regulated by the interaction between temperature and system productivity. *Limnol Oceanogr.* 61: S62–S77.
- DelSontro T, McGinnis DF, Sobek S, Ostrovsky I, Wehrli B. 2010. Extreme methane emissions from a Swiss hydropower reservoir: contribution from bubbling sediments. *Environ Sci Technol.* 44:2419–2425.

- Deshmukh C, Guérin F, Vongkhamso A, Pighini S, Oudone P, Sopraseuth S, Godon A, Rode W, Guédant P, Oliva P, et al. 2018. Carbon dioxide emissions from the flat bottom and shallow Nam Theun 2 Reservoir: drawdown area as a neglected pathway to the atmosphere. *Biogeosciences*. 15:1775–1794.
- Downing JA, Cole JJ, Middelburg JJ, Striegl RG, Duarte CM, Kortelainen P, Prairie YT, Laube KA. 2008. Sediment organic carbon burial in agriculturally eutrophic impoundments over the last century. *Global Biogeochem Cy*. 22:1–10.
- Doyle MW, Stanley EH, Harbor JM, Grant GS. 2003. Dam removal in the United States: emerging needs for science and policy. *EOS*. 84:29–36.
- Frankignoulle M. 1988. Field measurements of air-sea CO₂ exchange. *Limnol Oceanogr*. 33:313–322.
- Fromin N, Pinay G, Montuelle B, Landais D, Ourcival JM, Joffre R, Lensi R. 2010. Impact of seasonal sediment desiccation and rewetting on microbial processes involved in greenhouse gas emissions. *Ecohydrology*. 3:339–348.
- Gobierno de Navarra. 2019. Ficha climática de la estación—Meteo Navarra.es [Climatic data of the meteo-station Navarra]. http://meteo.navarra.es/climatologia/fichasclimaticas_estacion.cfm?IDestacion=74. Spanish.
- Gómez-Gener L, Obrador B, von Schiller D, Marcé R, Casas-Ruiz JP, Proia L, Acuña V, Catalán N, Muñoz I, Koschorreck M. 2015. Hot spots for carbon emissions from Mediterranean fluvial networks during summer drought. *Biogeochemistry*. 125:409–426.
- Gómez-Gener L, Obrador B, Marcé R, Acuña V, Catalán N, Casas-Ruiz JP, Sabater S, Muñoz I, von Schiller D. 2016. When water vanishes: magnitude and regulation of carbon dioxide emissions from dry temporary streams. *Ecosystems*. 19:710–723.
- Gordon ND, McMahon TA, Finlayson BL, Gippel CJ, Nathan RJ, Knight S, editors. 2004. *Stream hydrology. An introduction for the ecologists*. 2nd ed. Chichester (UK): Wiley and Sons Ltd.
- Harrison JA, Deemer BR, Birch MK, Malley MTO. 2017. Reservoir water-level drawdowns accelerate and amplify methane emission. *Environ Sci Technol*. 51:1267–1277.
- Holgerson MA, Raymond PA. 2016. Large contribution to inland water CO₂ and CH₄ emissions from very small ponds. *Nat Geosci*. 9:222–226.
- Howard DM, Howard PJA. 1993. Relationships between CO₂ revolution, moisture content, and temperature for a range of soil types. *Soil Biol Biochem*. 25:1537–1546.
- [IPCC] Intergovernmental Panel on Climate Change. 2013. Summary for policymakers. In: Stocker TF, Qin G–K, Plattner M, Tignor SK, Allen J, editors. *Climate change 2013: the physical science basis. Contribution of work group I to the fifth assessment report on the Intergovernmental Panel on Climate Change*.
- [IPCC] Intergovernmental Panel on Climate Change. 2019. Refinement to the 2006 IPCC guidelines for national greenhouse gas inventories. Volume 4 [accessed 2019 December 24]. <https://www.ipcc-nggip.iges.or.jp/public/2019rf/index.html>
- Jin H, Yoon TK, Lee SH, Im J, Park JH. 2016. Enhanced greenhouse gas emission from exposed sediments along a hydroelectric reservoir during an extreme drought event. *Environ Res Lett*. 11:124003.
- Keller PS, Catalán N, von Schiller D, Grossart HP, Koschorreck M, Obrador B, Frassl MA, Karakaya N, Barros N, Howitt JA, et al. 2020. Global CO₂ emissions from dry inland waters share common drivers across ecosystems. *Nat Commun*. 11:1–8.
- Keller PS, Marcé R, Obrador B, Koschorreck M. 2021. Global carbon budget of reservoirs is overturned by the quantification of drawdown areas. *Nat Geosci*. 14:402–408.
- Kosten S, van den Berg S, Mendonça R, Paranaíba JR, Roland F, Sobek S, Van Den Hoek J, Barros N. 2018. Extreme drought boosts CO₂ and CH₄ emissions from reservoir drawdown areas. *Inland Waters*. 8(3):329–340.
- Larrañaga A, Atristain M, von Schiller D, Elosegi A. 2019. Environmental diagnosis of the river network prior to the dismantling of a dam and preliminary results of the emptying effects of Enobieta. *Navarre Ingeniería Civil*. 193:1–12.
- Li M, Peng C, Zhu Q, Zhou X, Yang G, Song X, Zhang K. 2020. The significant contribution of lake depth in regulating global lake diffusive methane emissions. *Water Res*. 590:115465.
- Maathuis BHP, Wang L. 2006. Digital elevation model based hydro-processing. Hong Kong: Geocarto International Center. 1.
- Madsen H, Thyregod P. 2010. *Introduction to general and generalized linear models*. Boca Raton (FL): CRC Press.
- Marcé R, Obrador B, Gómez-Gener L, Catalán N, Koschorreck M, Arce MI, Singer G, von Schiller D. 2019. Emissions from dry inland waters are a blind spot in the global carbon cycle. *Earth-Sci Rev*. 188:240–248.
- Marks JC, Haden GA, O'Neill M, Pace C. 2010. Effects of flow restoration and exotic species removal on recovery of native fish: lessons from a dam decommissioning. *Restor Ecol*. 18:934–943.
- Mendonça R, Müller RA, Clow D, Verpoorter C, Raymond P, Tranvik L, Sobek S. 2017. Organic carbon burial in global lakes and reservoirs. *Nat Commun*. 8:1694.
- Miranda E, Mutiara AB, Wibowo WC. 2018. Classification of land cover from Sentinel-2 imagery using supervised classification technique (preliminary study). 2018 international conference on information management and technology (ICIMTech). IEEE; p. 69–74.
- Obrador B, von Schiller D, Marcé R, Gómez-Gener L, Koschorreck M, Borrego C, Catalán N. 2018. Dry habitats sustain high CO₂ emissions from temporary ponds across seasons. *Sci Rep*. 8:3015.
- Pacca S. 2007. Impacts from decommissioning of hydroelectric dams: a life cycle perspective. *Climate Change*. 84:281–294.
- Paranaíba JR, Aben R, Barros N, Quadra G, Linkhorst A, Amado AM, Brothers S, Catalán N, Condon J, Finlayson CM, et al. 2021. Cross-continental importance of CH₄ emissions from dry inland-waters. *Sci Total Environ*. 814:151925.
- Perera D, Smakhtin V, Williams S, North T, Curry A. 2021. Ageing water storage infrastructure: an emerging global risk. In: *UNU-INWEH Report Series; Hamilton (ON): United Nations University-Institute for Water, Environment and Health (UNU-INWEH)*. ISBN:978-92-808-6105-1.
- Pinheiro J, Bates D. 2018. nlme: linear and nonlinear mixed effects models, R package version 3.1–137.
- Pinheiro JC, Bates DM. 2000. *Mixed effects models in S and S-Plus*, 3rd ed. New York (NY): Springer.

- R Core Team. 2021. R: a language and environment for statistical computing. R Foundation for statistical computing, Vienna. <http://www.R-project.org/>
- Rathore R, Kumar V, Ranjan A, Tiwari S, Goswami A, Agwan M. 2018. Extraction of watershed characteristics using GIS and digital elevation model. *Int J Res Eng.* 1:62–65.
- Raymond PA, Hartmann J, Lauerwald R, Sobek S, McDonald C, Hoover M, Butman D, Striegl R, Mayorga E, Humborg C, et al. 2013. Global carbon dioxide emissions from inland waters. *Nature.* 503:355–359.
- St. Louis VL, Kelly CA, Duchemin E, Rudd JWM, Rosenberg DM. 2000. Measuring fluxes of greenhouse gases from reservoir surfaces. *Bioscience.* 50:766–775.
- Stanley EH, Casson NJ, Crawford JT, Loken LC, Oliver SK. 2016. The ecology of methane in streams and rivers: patterns, controls and global significance. *Ecol Monogr.* 86:146–171.
- Stanley EH, Doyle MW. 2003. Trading off: the ecological effects of dam removal. *Front Ecol Environ.* 3220:15–22.
- Teodoru CR, Prairie YT, del Giorgio PA. 2011. Spatial heterogeneity of surface CO₂ fluxes in a newly created Eastmain-1 reservoir in northern Quebec, Canada. *Ecosystems.* 14:28–46.
- Ulseth AJ, Hall RO, Boix Canadell M, Madinger HL, Niayifar A, Battin TJ. 2019. Distinct air–water gas exchange regimes in low- and high-energy streams. *Nat Geosci.* 12:259–263.
- van Bergen TJHM, Barros N, Mendonça R, Aben RCH, Althuizen IHJ, Huszar V, Lamers LPM, Lürding M, Roland F, Kosten S. 2019. Seasonal and diel variation in greenhouse gas emissions from an urban pond and its major drivers. *Limnol Oceanogr.* 64:2129–2139.
- von Schiller D, Datry T, Corti R, Foulquier A, Tockner K, Marcé R, García-Baquero OI, Obrador B, Elosegí R, et al. 2019. Sediment respiration pulses in intermittent rivers and ephemeral streams. *Global Biogeochem Cy.* 33:1251–1263.
- West WE, Creamer KP, Jones SE. 2016. Productivity and depth regulate lake contributions to atmospheric methane. *Limnol Oceanogr.* 61:S51–S61.
- Wik M, Thornton BF, Bastviken D, Uhlbäck J, Crill PM. 2016. Biased sampling methane release from northern lakes: a problem of extrapolation. *Geophys Res Lett.* 43:1256–1262.
- Yang M, Geng X, Grace J, Lu C, Zhu Y, Zhou Y, Lei G. 2014. Spatial and seasonal CH₄ flux in the littoral zone of Miyun Reservoir near Beijing: the effects of water level and fluctuation. *PLoS One.* 9:e94275.

Exposed sediments in a temperate-climate reservoir under dam decommissioning contain large stocks of highly bioreactive organic matter

Mabano Amani^{1,2,*} , Biel Obrador^{1,2} , David Fandos¹, Andrea Butturini¹  and Daniel von Schiller^{1,3} 

¹ Departament de Biologia Evolutiva, Ecologia i Ciències Ambientals (BEECA), Universitat de Barcelona (UB), Av. Diagonal 643, 08028 Barcelona, Spain.

² Institut de Recerca de la Biodiversitat (IRBio), Universitat de Barcelona (UB), Av. Diagonal 643, 08028 Barcelona, Spain.

³ Institut de Recerca de l'Aigua (IdRA), Universitat de Barcelona (UB), Montalegre 6, 08001 Barcelona, Spain.

* Corresponding author: amanigama@gmail.com

Received: 06/03/23

Accepted: 26/04/23

ABSTRACT

Exposed sediments in a temperate-climate reservoir under dam decommissioning contain large stocks of highly bioreactive organic matter

Dam decommissioning (DD) is used to solve economic and social problems posed by old dams. However, we ignore the effect of DD on the content and reactivity of large stocks of organic matter (OM) buried in reservoir sediments. We explored temporal changes in the content and reactivity of sediment OM during the first 580 days after the drawdown phase of DD of a large reservoir in the N Iberian Peninsula. We determined the content of sediment OM as organic carbon (OC) in bulk sediment OM and water-extractable OM (WEOM). We estimated the reactivity of bulk sediment OM as its respiration rate and carbon-to-nitrogen ratio, and that of sediment WEOM as its respiration rate, percent biodegradable dissolved OC (%BDOC), and SUVA₂₅₄. The content of bulk sediment OM was 84 ± 5.1 (mean \pm SE) mg OC/ g dry sediment, comparable to the values in the literature on sediment OM in dry sediments from lentic, but higher than in lotic ecosystems. The content of sediment WEOM was 0.81 ± 0.05 mg DOC/g dry sediment, higher than the values in the literature on sediment WEOM from lakes, soils, and rivers. On average, 41 % of WEOM was consumed by microorganisms in two days of incubation, showing the great reactivity of this OM fraction. The content of bulk sediment OM and the respiration rate of WEOM showed a nonlinear temporal trend, while %BDOC increased linearly with sediment exposure time. The labile OM produced by the vegetation that rapidly recolonized the reservoir and photoreactions may explain the temporal increase in %BDOC. Our results suggest that exposed sediments can be a source of labile OM and high C emissions in the river reach downstream of the reservoir after DD.

Key words: ageing dams, dam removal, exposed sediments, sediment organic matter, water reservoirs

RESUMEN

Los sedimentos expuestos tras el desmantelamiento de un embalse de clima templado contienen cantidades elevadas de materia orgánica altamente reactiva

El desmantelamiento de presas (DD) resuelve los problemas económicos y sociales que suponen las presas antiguas. Sin embargo, ignoramos el efecto del DD en la materia orgánica (OM) enterrada en los sedimentos del embalse, sobre todo su contenido y reactividad. En un experimento de incubación, exploramos cambios temporales en el contenido y reactividad de la OM del sedimento durante los primeros 580 días posteriores a la fase de vaciado de un gran embalse en el Norte de la Península Ibérica. Determinamos el contenido de OM del sedimento como carbono orgánico (OC) en sedimento y en materia orgánica extraíble en agua (WEOM) del sedimento. Determinamos la reactividad de la OM en el sedimento como su tasa de respiración y la ratio C:N, y la reactividad de la WEOM del sedimento como su tasa de respiración, el porcentaje de OC disuelto biode-

gradable (%BDOC), y $SUVA_{254}$. El contenido de OC en la OM en peso seco de sedimento fue de 84 ± 5.1 (promedio \pm error estándar) mg OC/g de sedimento seco, comparable a los valores de la literatura de materia orgánica presente en el sedimento en lagos, estanques y presas, pero mayor que en los ríos. El contenido de WEOM del sedimento fue de 0.81 ± 0.05 mg DOC/g sedimento seco, superior a los valores de la literatura de WEOM del sedimento de lagos, suelos y ríos. En promedio, el ~41 % de la WEOM fue consumida por microorganismos en dos días, lo que demuestra la gran reactividad de esta fracción de OM. El contenido de OM del sedimento seco y la tasa de respiración de la WEOM mostraron una tendencia temporal no lineal, mientras que el %BDOC aumentó linealmente con el tiempo de exposición del sedimento. La OM lábil producida por la vegetación que rápidamente recolonizó el embalse y las fotoreacciones pueden explicar el incremento temporal de %BDOC. Nuestros resultados sugieren que los sedimentos expuestos pueden ser una fuente de OM lábil, que puede alterar las emisiones de C en tramos de río aguas abajo de las presas sujetas a desmantelamiento.

Palabras clave: presas en envejecimiento, desmantelamiento de presas, sedimentos expuestos, materia orgánica del sedimento, embalses de agua

This is an open-access article distributed under the terms of the Creative Commons Attribution-NonCommercial 4.0 International (CC BY-NC 4.0) License.

INTRODUCTION

Ageing dams and the growing interest in river restoration have increased the practice of dam decommissioning (DD). Dam decommissioning is a widely hailed option to restore riverine connectivity, biodiversity, and ecosystem function (Allen *et al.*, 2016; Bednarek, 2001; Magilligan *et al.*, 2016). However, DD can also allow the downstream export and decomposition of organic matter (OM) buried in reservoir sediments (i.e., sediment OM) into greenhouse gases (GHGs) (Amani *et al.*, 2022; Pacca, 2007). The decomposition rate of sediment OM depends on extrinsic environmental factors and the content and reactivity of sediment OM (Keller *et al.*, 2020; Obrador *et al.*, 2018; Paranaíba *et al.*, 2021). Thus, DD can affect extrinsic factors of the decomposition of OM in sediments, and hence the content and reactivity of sediment OM by exposing the anoxic sediments to the atmosphere. For instance, exposed sediments in a large temperate reservoir under DD were reported to be a hotspot for carbon dioxide (CO₂) emissions (Amani *et al.*, 2022). These CO₂ emissions decreased with sediment exposure time, hypothetically, due to a decrease in the content and reactivity of sediment OM. However, we lack empirical evidence of the effect of DD on the content and reactivity of the large stocks of OM buried in sediments of reservoirs during their life cycle (Downing *et al.*, 2008; Maavara *et al.*, 2017; Mendonça *et al.*, 2012). The reactivity of sediment OM can affect its fate and

shape the role of reservoirs in regional and global carbon (C) budgets (Kothawala *et al.*, 2021). Reactive sediment OM can decompose into CO₂ in the reservoir or in the river reach downstream of the reservoir and, thus, remain in the short-term atmosphere-biosphere C loop. However, recalcitrant sediment OM may remain buried in the reservoir after terrestrialization (i.e., the transition from an aquatic to a terrestrial system) and/or reach coastal marine sediments and, thus, enter the long-term geological C pool. To include DD in the C footprint of reservoirs on a regional and global scale, it is necessary to test how the content and reactivity of sediment OM in reservoirs change over time after DD.

Reservoir sediments are hotspots for OM burial because, relative to lakes, they receive higher loads of sediment, OM, and nutrients from their relatively larger catchment area (Downing *et al.*, 2008; Mendonça *et al.*, 2017; Thornton *et al.*, 1990). The catchment area to the waterbody area ratio is higher for reservoirs than lakes, implying higher inputs of terrestrial materials and a higher sedimentation rate in reservoirs (Thornton *et al.*, 1990). The higher sedimentation rate in reservoirs creates better conditions for OM preservation because it potentially implies, compared to lakes, a shorter exposure time of sediment OM to oxygen (O₂) (Clow *et al.*, 2015; Sobek *et al.*, 2009, 2012). The shorter exposure time of sediment OM to O₂ and a large portion of allochthonous OM increase the burial efficiency of OM (i.e., the ratio of OM burial to OM deposition) and the areal burial

Sediment organic matter in a decommissioned reservoir

rate of OM in reservoir sediments (Sobek et al., 2009, 2012). The global areal burial rate of OM is six times higher in reservoirs than in lakes (Mendonça et al., 2017). The global burial rate of OM in reservoir sediments is estimated at 35.43 Tg C/yr, of which 75 % is contributed by allochthonous OM (Maavara et al., 2017). However, when this occlusion of OM in sediments is removed due to, for instance, DD, this sediment OM can become highly bioreactive (Bastviken et al., 2004; Freeman et al., 2001; Kothawala et al., 2021).

The bioreactivity of OM depends on its content and molecular composition and extrinsic environmental factors (Amani et al., 2019; Catalán et al., 2013; Webster & Benfield, 1986). The content of organic carbon (OC) is an important factor in the decomposition of OM because low concentrations of some molecules can be below the threshold of energetic requirements of decomposers and, thus, limit some catabolic reactions (Arrieta et al., 2015; Kothawala et al., 2021). The molecular composition of OM affects its decomposition by providing the energy and chemical elements required for the growth and reproduction of decomposers. Organic matter is a complex mixture of several molecules of different molecular size, structure, oxidation degree, hydrolysis degree, and aromaticity (Kellerman et al., 2014; Stubbins et al., 2014) and often characterized using optical techniques (Miller & McKnight, 2010; Stubbins et al., 2014; Weishaar et al., 2003). More bioreactive or labile OM contains molecules with low aromaticity, low carbon-to-nitrogen (C:N) ratio, and low molecular weight (Miller & McKnight 2010; Koehler et al., 2012; Gudasz et al., 2015). Water-extractable OM (WEOM: OM obtained by extracting a given mass of soil/sediment with an aqueous solution (Zsolnay, 1996)) represents only a small fraction of sediment OM, but it is often the most mobile, leachable, and biodegradable fraction (Bolan et al., 2011; Boyer & Groffman, 1996; Chantigny, 2003). Extrinsic environmental factors that affect the decomposition of sediment OM include temperature, O₂, the structure and function of microbial communities, the texture and moisture of the sediment, and exposure to solar radiation (Baumann et al., 2013; Keller et al., 2020; von Schiller et al., 2019; Walz et al., 2017). Dam decommissioning can alter some of

these extrinsic environmental factors, and thus the content and reactivity of sediment OM during sediment exposure to the atmosphere.

Sediment exposure can affect the content and reactivity of sediment OM by mainly reducing sediment moisture, increasing sediment texture, increasing exposure to solar radiation, and promoting plant recolonization of exposed sediments. Low sediment moisture increases O₂ concentration in deeper layers of exposed sediments and the decomposition rate of sediment OM (Gómez-Gener et al., 2015; Kosten et al., 2018; Marcé et al., 2019). However, since extreme desiccation can reduce the decomposition rate of OM through a limited supply of OM to microorganisms (Schimel, 2018), the availability of C substrates, the activity of extracellular enzymes, and, thus, the decomposition rate of OM increase with sediment and soil moisture (Coulson et al., 2022; Manzoni et al., 2016; Manzoni & Katul, 2014). Since DD is a hot moment for the erosion of reservoir sediments (Duda & Bellmore, 2022; Ritchie et al., 2018), sediment texture may increase during sediment exposure due to the loss of fine-sized sediments, which are more susceptible to the erosion and transport downstream (Duda et al., 2022; Warrick et al., 2012). Furthermore, solar radiation (Granéli et al., 1996; Lindell et al., 1995; Wetzel et al., 1995) and plant recolonization can alter the content and reactivity of sediment OM by providing labile OM (Shaver et al., 1992; Shaver & Chapin III, 1986). Therefore, temporal changes in the content and reactivity of sediment OM can depend on the balance between the decomposition of OM and factors such as exposure to solar radiation and vegetation growth after DD. However, there is no clear characterization of how these factors affect the content and reactivity of sediment OM after DD in decommissioned reservoirs.

Here, we assessed whether the content and reactivity of the sediment OM changed during the first 580 days of sediment exposure after the drawdown phase of DD of the Enobieta Reservoir, a large (42 m high) temperate-climate reservoir in the North Iberian Peninsula. We collected sediment samples during six sampling campaigns between 2018 and 2020. We predicted that (1) the content of sediment OM would be high and high

-ly bioreactive, (2) sediment WEOM would be more bioreactive than bulk sediment OM, and (3) the content and reactivity of sediment OM would decrease with sediment exposure time because high precipitation in the region should support OM decomposition in exposed sediments after reservoir drawdown. To contextualize our results in a wider framework of environments, we compared the content and reactivity of sediment OM in the Enobieta Reservoir with literature data about dry soils and dry sediments of lentic and lotic inland waters.

METHODS

Study site

The Enobieta Reservoir (coordinates: 43° 13' 03" N 1° 47' 15" W, elevation: 345 m) was constructed in the Artikutza Valley (Navarre, N Iberian Peninsula) between 1947 and 1953 on the Enobieta Stream to regulate water supply to the municipality of Donostia-San Sebastián. The mean annual air temperature is 12.2 °C with an average rainfall of 2604 mm/yr (period 1954–2019; Gobierno de Navarra 2019). This rainfall rate makes the Artikutza Valley, perhaps, the most humid region of the Cantabrian cornice. The hydrological network of the Artikutza Valley has a drainage basin of 3683 ha, with a geology dominated by acidic rocks, such as granite and schist (Atristain *et al.*, 2022). The Artikutza Valley is mainly covered by mature forests dominated by beech (*Fagus sylvatica* L.) and oak (*Quercus robur* L.) stands, dense autochthonous riparian vegetation with alder (*Alnus glutinosa* (L.) Gaertner) and ash (*Fraxinus excelsior* L.), some old exotic plantations of conifers and red oaks (*Quercus rubra* L.), and pasturelands on the highest terrain (Lozano & Latasa 2019). The reservoir had an initial storage capacity of 2.66 hm³ and an area of ~0.14 km². Geotechnic problems noticed during dam construction required the reduction of storage capacity to 1.63 hm³ and the construction, downstream in the same catchment, of the Añarbe Reservoir in 1976. Subsequently, the Enobieta Reservoir was not used to provide water (Larrañaga *et al.*, 2019) and was not maintained properly to the point that it became a safety prob-

lem. Due to the early structural instability and the conservation status of the Artikutza Valley (it is part of the Natura 2000 Network and a special conservation zone), the decommissioning of the Enobieta Reservoir began in 2017 and continued throughout 2018 and 2019 (Amani *et al.*, 2022). The phase of reservoir drawdown of the Enobieta Reservoir ended on 25 February 2019.

Sampling strategy and treatment of sediment samples

We collected sediment samples during and after the drawdown of the Enobieta Reservoir during six sampling campaigns (C₁–C₆): on 10 September 2018, 22 October 2018, 21 January 2019, 09 April 2019, 02 July 2019, and 18 February 2020 (Table S1, available at <https://www.limnetica.net/en/limnetica>). To assess whether the content and reactivity of sediment OM changed over time, we used the sampling date minus the last inundation date of each site to find sediment exposure time (in days) for each site (Table S1). We determined the last inundation date for each site from the site elevation (Table S2, available at <https://www.limnetica.net/en/limnetica>), the reservoir bathymetry, and the daily evolution of water level in the reservoir (available in Amani *et al.* (2022)). The range of sediment exposure time was 9–580 days (Table S1). We collected sediment samples using six sites (A, B, C, D, E, and F), which were close to the tail of the reservoir, in the section exposed to the atmosphere for longer time (see Table S2 for coordinates). We collected three samples in a 1 × 1 m plot in each site when sediments were still bare and during the early recolonization of the bare sediments by vegetation. Thus, we collected 108 sediment samples: 6 sites × 3 replicate plots per site × 6 sampling campaigns. We lost one sample and, thus, we performed the incubation experiment and other analyses with 107 sediment samples.

In the field, we stored sediment samples in clean polyethylene falcon tubes that we transported in dark portable refrigerators to the laboratory. In the laboratory, we froze the sediment samples at -18 °C. Before all analyses and the incubation experiment performed in this study (Fig. 1), we freeze-dried all sediment samples for 48

Sediment organic matter in a decommissioned reservoir

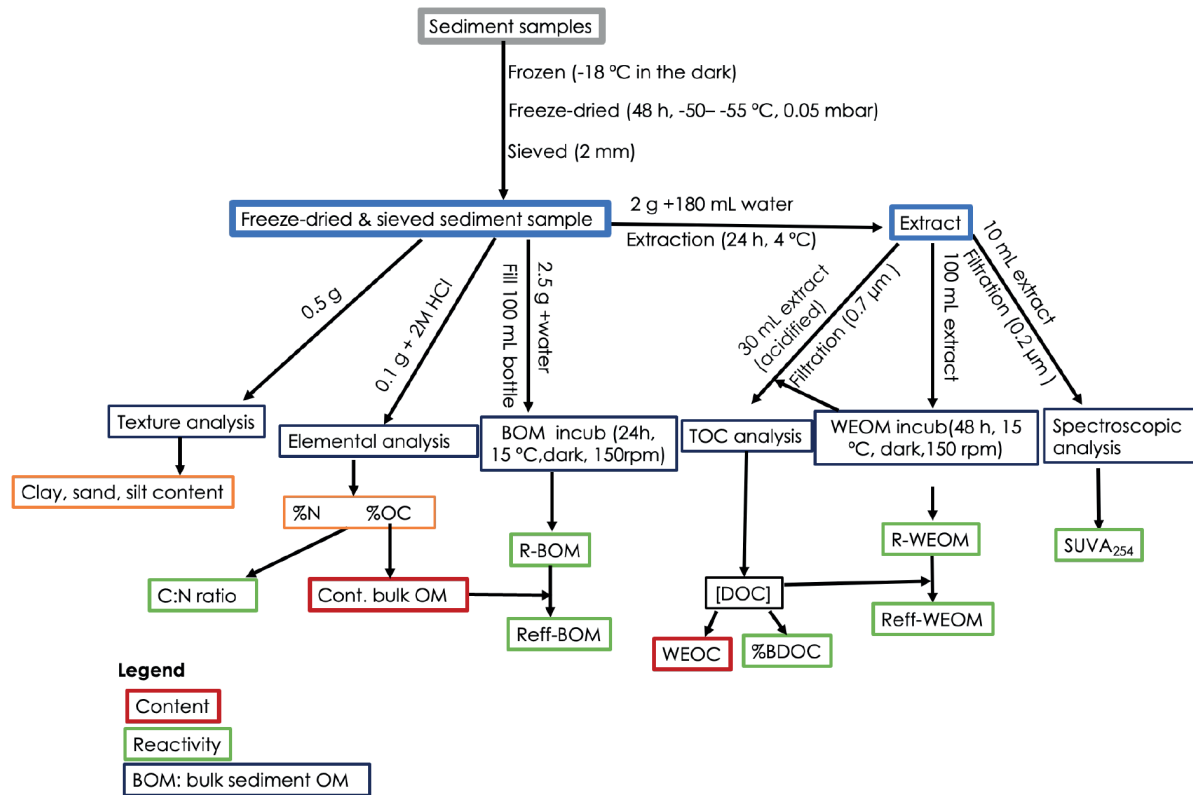


Figure 1. Schematic representation of the experiments conducted in this study. *Representación esquemática de los experimentos realizados en este estudio.*

h in a Telstar LyoQuest at a vacuum pressure of 0.05 mbar and a temperature between -50 and -55 °C. We sieved the freeze-dried sediment samples with a steel sieve of a 2-mm mesh to retain the fine fraction of the sediments. We cleaned the steel sieve between samples with a plastic brush, taking maximum care to avoid contamination. We kept the sieved, freeze-dried sediment samples in clean polyethylene falcon tubes in the laboratory at -18 °C until the incubation experiment and other analyses.

Sediment texture

We assessed the mean sediment size with 0.5 g of freeze-dried, sieved sediment using a laser light diffraction instrument (Coulter LS, 230, Beckman-Coulter, USA) after removing organic C (OC) with H₂O₂ (Arriaga et al., 2006).

Content of bulk sediment OM and sediment WEOM

We determined the content of bulk sediment OM as the amount of OC in the sediments. We determined the percentage of OC content (%OC) and the percentage of total nitrogen content (%N) on a 0.1 g dry sediment sample with an Elemental Analyzer (Model 1108, Carlo-Erba, Italy) after sediment acidification with 2M HCl to remove inorganic C and preserve OM. We reported the content of bulk sediment OM in mg OC/g dry sediment.

We determined the content of sediment WEOM as sediment water-extractable OC (WEOC: mg DOC/g dry sediment). We obtained WEOM by shaking a dry sediment aliquot of 2 g with 180 mL of mineral water (Font Vella) in 250-mL plastic bottles, in a dark incubator for 24 h at 4 °C and 150 rpm. We filtered the sediment-water mixture

through glass fibre filters (0.7 μm pore size; Whatman GF/F, GE Healthcare, UK), pre-ashed for 4 h at 450 $^{\circ}\text{C}$, into clean polyethylene falcons of 50 mL. We used a different filter for each sample. We acidified the filtered samples to pH 2–3 with HCl 10 % to remove dissolved inorganic C and preserve OM. We used the high-temperature catalytic oxidation method to determine the concentration of DOC in a Shimadzu instrument (TOC-VCSH, Tokyo, Japan). We calculated WEOC as the product of [DOC] (mg/L) and the volume of water (L) used to extract WEOM divided by the mass (g) of each dry sediment sample:

$$\text{WEOC} = \frac{[\text{DOC}] \left(\frac{\text{mg}}{\text{L}}\right) \times \text{water volume (L)}}{\text{mass dry sediment (g)}} \quad (1)$$

Reactivity of bulk sediment OM and sediment WEOM

We assessed the reactivity of bulk sediment OM using three parameters: (1) respiration rate of bulk sediment OM, (2) respiration efficiency of bulk sediment OM, and (3) the mass ratio of %OC to %N (i.e., %OC/%N = C:N ratio, which was used as a proxy for reactivity). We determined the respiration rate of bulk sediment OM from the rate of dissolved O_2 consumption during incubation (von Schiller *et al.*, 2019). We introduced 2.5 g of sediment samples into pre-washed 100 mL incubation glass bottles. We sealed the glass bottles with hexagonal glass stoppers (M-29/32, Scharlau, Spain) to avoid contamination of the samples. We left the sealed bottles on a laboratory benchtop for 24 h for the samples to acclimate to laboratory conditions. We aerated the water we used for incubation, Font Vella mineral water (spring: Sant Hilari Sacalm-Girona, Spain, $[\text{HCO}_3^{1-}]$: 143 mg/L, $[\text{Ca}]$: 42 mg/L, $[\text{Mg}]$: 11.3 mg/L, $[\text{Na}]$: 12.5 mg/L, and conductivity: 286 $\mu\text{S}/\text{cm}$), overnight in an open plastic jerrycan placed in a benchtop incubator (Optic Ivy-men System, Spain) at 15 $^{\circ}\text{C}$ and a rotation speed of 150 rpm. We used the air-saturated water to fill the bottles containing sediments and four control bottles without sediments (i.e., with mineral water only). We ensured that no air bubbles formed or stayed in the incubation bottles, which we sealed

with the stoppers throughout the incubations.

We incubated the samples and controls for 24 h at 15 $^{\circ}\text{C}$ in the dark benchtop incubator at 150 rpm. The temperature of 15 $^{\circ}\text{C}$ was close to the mean annual temperature of 12.2 $^{\circ}\text{C}$ in the Artikutza Valley (Gobierno de Navarra, 2019). We conducted the incubation of bulk sediment OM for 24 h because preliminary experiments had shown that more time could result in anoxia. We measured the O_2 concentration four times during the incubations (at 2, 4, 8, and 24 h) with O_2 optode spots (model PSt3, PreSens) attached to the interior of each bottle using a standalone, portable, fiberoptic O_2 meter (Microx 4 trace, PreSens, Regensburg, Germany). We vigorously shook each incubation bottle before each measurement to ensure homogeneous O_2 concentrations inside the bottles. We calculated the respiration rate of the bulk sediment OM (R-BOM; $\mu\text{g O}_2 \text{ g}^{-1}$ dry sediment h^{-1}) as:

$$R - \text{BOM} = \frac{(\text{O}_2^{\text{2h sample}} - \text{O}_2^{\text{24h sample}}) - (\text{O}_2^{\text{2h control}} - \text{O}_2^{\text{24h control}})}{\text{incubation time (h)}} \times \text{volume resp. bottle (L)} \quad (2)$$

where O_2 is $[\text{O}_2]$ (mg/L), subscripts sample and control refer to each analytical replicate and the mean $[\text{O}_2]$ in the four control bottles, and superscripts 2h and 24h correspond to the measurement times (respectively, 2 h and 24 h). The volume of the bottle was 100 mL, the incubation time was 22 h, the sediment mass was 2.5 g. To estimate the respiration efficiency of the bulk sediment OM (Reff-BOM; $\mu\text{g O}_2 \text{ g}^{-1} \text{ OC h}^{-1}$), we replaced mass of dry sediment in the equation (2) by the mass of OC in each sediment sample. The consumption rate of O_2 over incubation time was linear and, thus, we used the initial (2 h) and final (24 h) values, to estimate the decomposition rate of sediment OM.

We determined the reactivity of sediment WEOM using four variables: (1) respiration rate of sediment WEOM, (2) respiration efficiency of sediment WEOM, (3) biodegradable DOC (BDOC), and (4) a chromophoric index; SUVA_{254} . We determined the respiration rate of sediment WEOM by incubating the WEOM extract, which was not filtered. We used a syringe to carefully collect the supernatant, avoiding the

Sediment organic matter in a decommissioned reservoir

intake of the sediment and other particles. We conducted the incubation experiment for 48 h (the time it took to consume at least 1 mg O₂/L in our preliminary experiments) under the same conditions as for the bulk sediment OM; dark conditions, at 15 °C and 150 rpm. We measured [O₂] at 2 h, 24 h, and 48 h using the same PreSens O₂ optodes. We calculated the respiration rate of sediment WEOM (R-WEOM; μg O₂ g⁻¹ dry sediment h⁻¹) as:

$$R - WEOM = \frac{(O_{2sample}^{2h} - O_{2sample}^{48h}) - (O_{2control}^{2h} - O_{2control}^{48h})}{\text{incubation time (h)}} \times \text{resp. bottle volume (L)} \quad (3)$$

mass of dry sediment (g)

We estimated the respiration efficiency of sediment WEOM (Reff-WEOM; μg O₂ g⁻¹ of DOC h⁻¹) by replacing, in the equation (3), mass of dry sediment with the mass of DOC (g) in each WEOM extract. To determine the fraction of biodegradable DOC (BDOC), we measured [DOC] in the samples before and after incubation, and we filtered each WEOM extract using a different filter with a pore size of 0.7 μm before determining [DOC]. We then calculated BDOC as the difference in [DOC] before ([DOC]_i) and after incubation ([DOC]_f) and expressed it as % of [DOC]_i, i.e., %BDOC as:

$$\%BDOC = \left(\frac{[DOC]_i - [DOC]_f}{[DOC]_i} \right) \times 100 \quad (4)$$

We analyzed the optical property of WEOM by filtering 10 mL of the WEOM extract with a 0.2 μm filter (Whatman GF/F, GE Healthcare, UK). We used a PharmaSpec UV-1700 spectrophotometer (Shimadzu, Tokyo, Japan) to obtain ultraviolet-visible (UV-Vis) spectroscopy (200–600 nm) using a 1 cm quartz cuvette (Obrador et al., 2018). We determined a qualitative property of WEOM: the specific ultraviolet absorbance at 254 nm (SUVA₂₅₄; L mg C⁻¹ m⁻¹). We determined SUVA₂₅₄, which is a descriptor of DOC aromaticity (Shao et al., 2009), as in Weishaar et al. (2003):

$$SUVA_{254} = \frac{abs_{254} \times \ln(10)}{[DOC] \times l} \quad (5)$$

where *abs*₂₅₄ is the absorbance at 254 nm, [DOC] is in mg C/L, and *l* is the path length of the cuvette in m.

Meteorological and vegetation data

We evaluated how the accumulated precipitation (a proxy for sediment moisture) and temperature in the Artikutza Valley, and the vegetation growth in the Enobieta Reservoir after drawdown changed with time during our sampling period. We obtained daily precipitation and temperature data from the nearest meteorological station (Artikutza Station of Meteorology and Climate of Navarre). We assessed how the temperature changed during the sampling period using the mean daily temperature (°C) that was recorded on our sampling dates. We used the sum of daily precipitation for seven days (six days preceding the sampling date plus the precipitation on our sampling date) to obtain the accumulated weekly precipitation (mm). We used the sampling date to assess the temporal changes in precipitation during the sampling period. We assessed the temporal change in vegetation recolonization of the exposed sediments using Sentinel 2-Multipectral Instrument (MSI) imaging data taken on the 15th of each sampling month, which was mostly 3–7 days before or after the sampling date, a maximum of 13 days. The Sentinel 2-MSI data were preprocessed using Google Earth Engine. We used these satellite images of the whole reservoir to obtain the normalized difference vegetation index (NDVI, dimensionless). We did not have NDVI values for the first and third sampling campaigns because we could not find satellite images for the two sampling campaigns. We determined sediment exposure time for NDVI, precipitation, and temperature using the sampling date for each variable minus the earliest last inundation date.

Statistical analyses

We determined temporal changes in the content and reactive of sediment OM during the first 9–580 days of sediment exposure after the drawdown phase of DD of the Enobieta Reservoir using generalized additive mixed models (GAMMs), with the R package mgcv (mixed GAM computational

vehicle) in R version 4.0.5 (R Core Team, 2021). We considered as response variable the content and reactivity of sediment OM, and as explanatory variable time as a fixed factor. We used site as a random factor. We visually explored temporal trends of precipitation, temperature, and NDVI during sediment exposure time. We additionally

ran a correlation analysis to explore the direction and significance of the temporal trend in NDVI. We used the paired samples t-test to test the difference between the means of the respiration rates for bulk sediment OM and sediment WEOM and their respiration efficiency. Statistical tests were considered significant when the p -value was ≤ 0.05 .

Table 1. Descriptive statistics of sediment texture and the content and reactivity of sediment OM in the Enobieta Reservoir. Bulk OM content is the content of bulk sediment OM and SE is the standard error of the mean. *Estadística descriptiva de la textura del sedimento y del contenido y reactividad de la materia orgánica del sedimento en el embalse de Enobieta. "Bulk OM content" es el contenido de OM en peso seco de sedimento y SE es el error estándar de la media.*

Factor	Variable	Mean	SE	Range
Sed. texture	Mean sediment size (μm)	33.7	1.0	21.0–43.3
Content	Bulk OM content (mg OC/g dry sediment)	84	5.1	20–143
	Sediment WEOC (mg DOC/g dry sediment)	0.81	0.1	0.29–1.6
Reactivity	R-BOM ($\mu\text{g O}_2 \text{ g}^{-1} \text{ dry sediment h}^{-1}$)	2.8	0.2	0.5–5.1
	Reff-BOM ($\mu\text{g O}_2 \text{ g}^{-1} \text{ OC h}^{-1}$)	32.1	2.4	9.5–78.4
	R-WEOM ($\mu\text{g O}_2 \text{ g}^{-1} \text{ dry sediment h}^{-1}$)	2.4	0.1	0.6–8.1
	Reff-WEOM ($\mu\text{g O}_2 \text{ g}^{-1} \text{ DOC h}^{-1}$)	1103	63	566–1860
	BDOC (%)	41.4	2.0	17.5–64.8
	SUVA ₂₅₄ ($\text{L mg C}^{-1} \text{ m}^{-1}$)	2.91	0.17	1.23–5.7
	C:N ratio (dimensionless)	16.2	1.0	5.1–28.6

RESULTS

Sediment texture

The mean sediment size in the Enobieta Reservoir (Table 1) changed with sediment exposure time. The mean sediment size decreased between the beginning of our sampling campaign and ~ 200 days of sediment exposure, then increased from ~ 200 days to ~ 400 days before slightly decreasing and increasing again (Fig. S1, available at <https://www.limnetica.net/en/limnetica>).

Content of bulk sediment OM and sediment WEOM

The content of bulk sediment OM (Table 1) changed with sediment exposure time (Fig. 2a). The content of bulk sediment OM decreased between the beginning of our sampling period and ~ 200

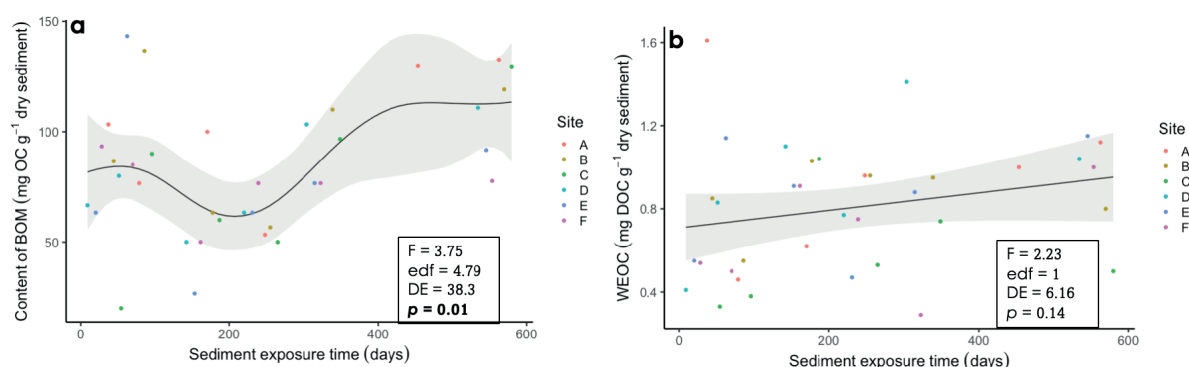


Figure 2. Temporal changes in the content of bulk sediment OM (a) and sediment WEOM (b) along sediment exposure time. The lines and shaded areas represent, respectively, the mean and 95 % confidence interval of GAMMs; each point represents the average of three sediment samples collected at each site for each sampling date; edf is effective degrees of freedom; DE is deviance explained (%); significant p -values are shown in bold. *Cambios temporales en el contenido de materia orgánica presente en el sedimento seco (a) y de la materia orgánica extraíble en agua (WEOM) del sedimento (B) durante el tiempo de exposición. Las líneas y espacios sombreados representan, respectivamente, la media y un intervalo de confianza del 95 % de los modelos aditivos generalizados mixtos; cada punto representa la media de tres muestras de sedimentos, recogidas en cada punto para cada día; edf hace referencia a los grados de libertad efectivos; DE a la desviación explicada (%); en negrita se muestran los p -valores significativos.*

Sediment organic matter in a decommissioned reservoir

days, increased between ~200 and 400 days, and then, between ~400 and 580 days of sediment exposure, it reached a plateau. Sediment WEOC (Table 1) did not change with sediment exposure time (Fig. 2b).

Reactivity of bulk sediment OM and WEOM

R-BOM and R-WEOM were not different ($t(35.0) = 0.85$, $p = 0.40$), while Reff-WEOM was 34.4 times higher than Reff-BOM ($t(35.0) = 16.9$, $p < 0.01$). Reff-WEOM, and %BDOC changed with sediment exposure time, while other parameters for the reactivity of sediment OM did not (Fig. 3 and 4). R-WEOM decreased between the

beginning of our sampling and ~200 days, it also increased between ~400 days and 580 days of sediment exposure to form a nearly U-shaped curve (Fig. 3b). Reff-WEOM showed almost the same temporal trend as R-WEOM, but its increase between ~400 and 580 days was not as strong as for R-WEOM (Fig. 3d). Furthermore, %BDOC increased linearly with sediment exposure time (Fig. 4a).

Meteorological and vegetation data

The accumulated weekly precipitation was 73 ± 11 (0.0–170) mm [mean \pm SE (range)], the temperature was 11.7 ± 0.9 (5.5–18.5) °C during the

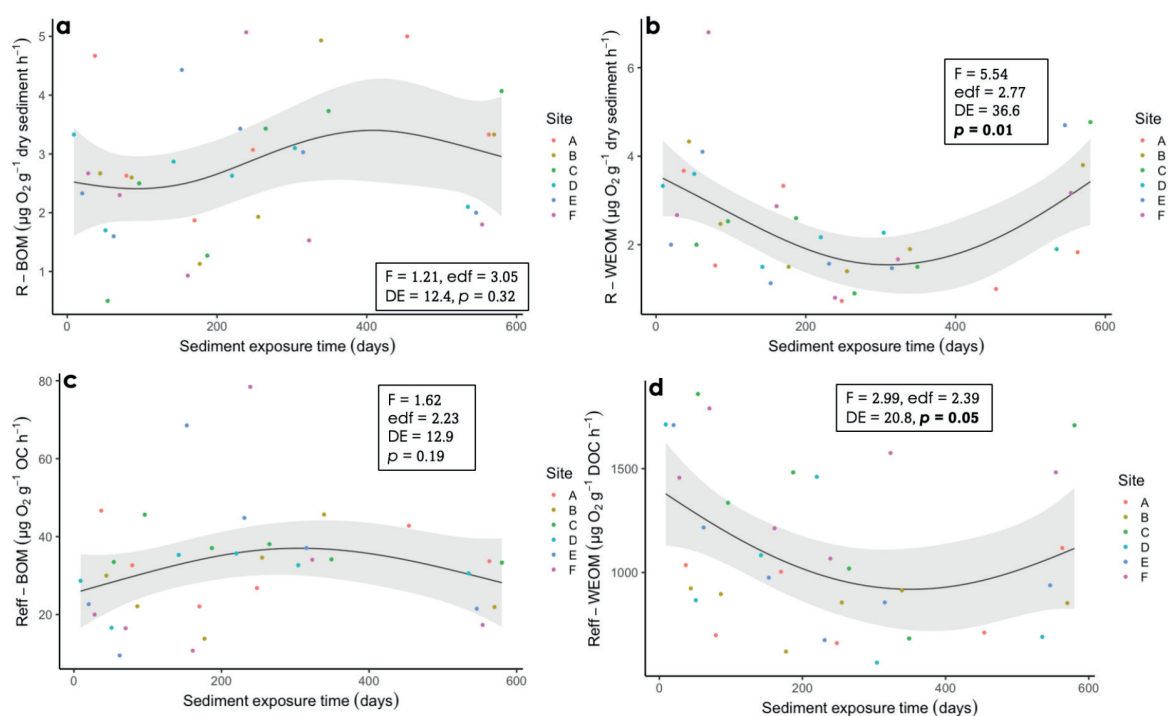


Figure 3. Temporal changes in the respiration rate for bulk sediment OM (R-BOM, a), the rate of microbial respiration for sediment WEOM (R-WEOM, b), respiration efficiency for bulk sediment OM (Reff-BOM, c), and respiration efficiency for sediment WEOM (Reff-WEOM, d) along sediment exposure time. The lines and shaded areas represent, respectively, the mean and 95 % confidence interval of the GAMMs; each point represents the average of three sediment samples collected for each sampling date at each site; edf is effective degrees of freedom; DE is deviance explained (%); significant p -values are shown in bold. *Cambios temporales en la tasa de respiración para la materia orgánica en el sedimento seco (R-BOM, a), tasa de respiración para la WEOM del sedimento (R-WEOM, b), eficiencia de la respiración para la materia orgánica en el sedimento seco (Reff-BOM, c), eficiencia de la respiración para la WEOM del sedimento (Reff-WEOM, d) durante el tiempo de exposición del sedimento. Las líneas y espacios sombreados representan, respectivamente, la media y un intervalo de confianza del 95 % de los modelos aditivos generalizados mixtos; cada punto representa la media de tres muestras de sedimentos, recogidas en cada punto para cada día; edf hace referencia a los grados de libertad efectivos; DE a la desviación explicada (%); en negrita se muestran los p -valores significativos.*

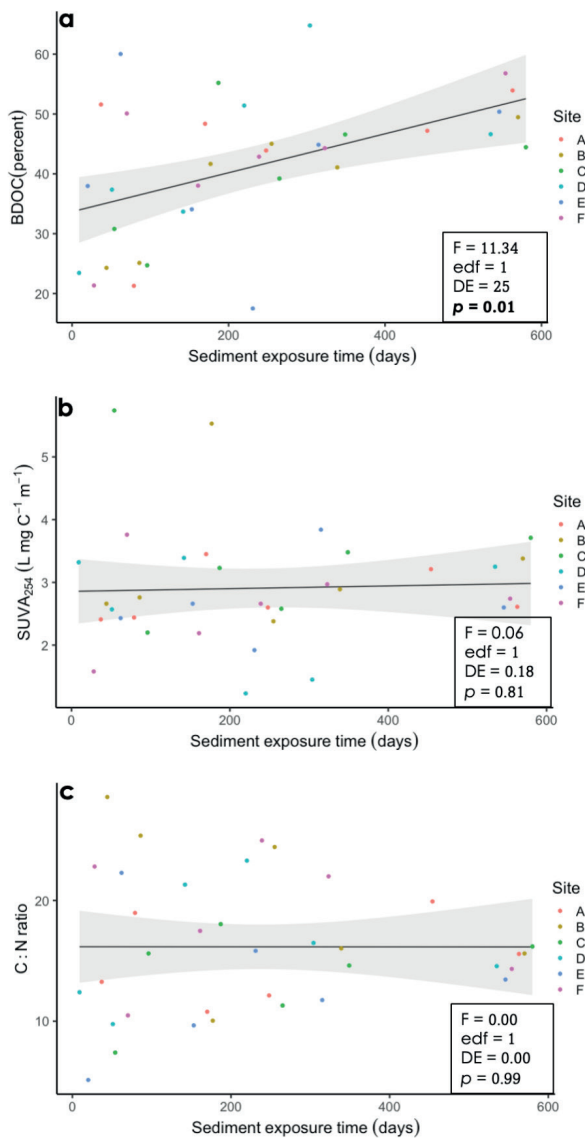


Figure 4. Temporal changes of BDOC (a), $SUVA_{254}$ (b), and C: N ratio (c) during sediment exposure time. The lines and shaded areas represent the mean and 95 % confidence interval of the GAMMs; each point represents the average of three sediment samples collected for each sampling date at each site; edf is effective degrees of freedom; DE is deviance explained (%); significant *p*-values are shown in bold. *Cambios temporales del carbono orgánico disuelto biodegradable (BDOC, a), $SUVA_{254}$ (b), y ratio C:N (c) durante el tiempo de exposición del sedimento. Las líneas y espacios sombreados representan, respectivamente, la media y un intervalo de confianza del 95 % de los modelos aditivos generalizados mixtos; cada punto representa la media de tres muestras de sedimentos, recogidas en cada punto para cada día; edf hace referencia a los grados de libertad efectivos; DE a la desviación explicada (%); en negrita se muestran los *p*-valores significativos.*

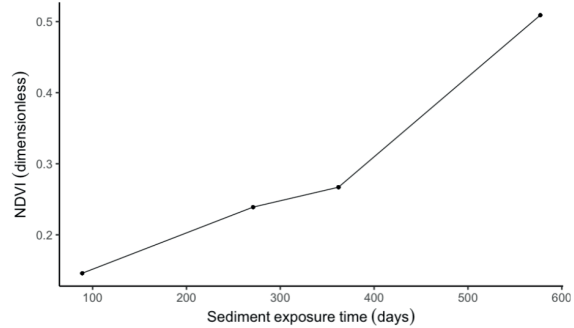


Figure 5. Temporal changes in NDVI (dimensionless) with sediment exposure time. *Gráfico de líneas de los cambios temporales en el índice de diferencia normalizada de vegetación (adimensional) durante el tiempo de exposición del sedimento.*

study period. Precipitation decreased from 18.8 to 0.0 mm between 54 and 96 days, increased from 0.0 to 148 mm between 96 and 265 days, decreased from 148 to 20.9 mm between 265 and 349 days, and increased from 20.9 to 170 mm between 349 and 580 days of sediment exposure (Fig. S2a, available at <https://www.limnetica.net/en/limnetica>). Temperature decreased from 18.5 to 5.5 °C between 54 and 187 days, increased from 5.5 to 8.7 °C between 187 and 265 days, between 256 and 349 days it increased from 8.7 to 18.2 °C, and then decreased from 18.2 to 7.0 °C between 349 and 580 days of sediment exposure (Fig. S2b, available at <https://www.limnetica.net/en/limnetica>). Correlation analysis showed that NDVI increased with sediment exposure time ($r = 0.9$, $p < 0.01$). Vegetation continuously increased during sediment exposure, but the growth rate was greater between 362 and 577 days of sediment exposure (Fig. 5).

DISCUSSION

As expected, we report a high content of highly bioreactive bulk sediment OM and sediment WEOM in the Enobieta Reservoir. However, in contrast to what we expected, the content and reactivity of sediment OM did not decrease with sediment exposure time. For instance, %BDOC increased linearly with sediment exposure time, while the content of bulk sediment OM, R-WEOM, and $Reff$ -WEOM showed complex

Sediment organic matter in a decommissioned reservoir

temporal trends. A common trend for R-WEOM and Reff-WEOM is that they began to increase when vegetation became abundant between 362 and 577 days, while the content of bulk sediment OM reached a plateau at ~400 days of sediment exposure. The linear increase in %BDOC with sediment exposure time and the late increases in R-WEOM and Reff-WEOM may be due to the input of labile OM produced by plants recolonizing the reservoir and the conversion of high molecular, recalcitrant OM to low molecular, labile OM through photodegradation.

The content of bulk sediment OM in the Enobieta Reservoir (84 ± 5.1 mg OC/g dry sediment) was comparable to the global content of sediment OM in ponds (mean \pm SD in mg OC g⁻¹ dry sediment), 180 ± 200 , lakes, 140 ± 170 , and reservoirs, 100 ± 110 , but higher than in streams, 30 ± 40 (Keller et al., 2020). However, sediment WEOC (0.81 ± 0.05 mg DOC/g dry sediment) in the Enobieta Reservoir was higher than WEOC in lakes (mean \pm SE in mg C/g dry sediment), 0.52 ± 0.06 (Table S3, available at <https://www.limnetica.net/en/limnetica>), soils, 0.35 ± 0.03 (Table S4, available at <https://www.limnetica.net/en/limnetica>), and rivers, 0.29 ± 0.02 (Table S5, available at <https://www.limnetica.net/en/limnetica>). The mean content of sediment OM in the Enobieta Reservoir may be comparable to the global mean content of sediment OM in ponds due to a high perimeter-to-area ratio of ponds that may lead to higher input and burial of OM in the sediments of ponds (Keller et al., 2020). Since the areal C burial rate in natural lakes is 4–12 times lower than in reservoirs (Mendonça et al., 2017), the content of bulk sediment OM in the Enobieta Reservoir should be higher than in lakes. However, our findings are consistent with those of Keller et al. (2020) who found no difference between the content of sediment OM in lakes and reservoirs worldwide. Furthermore, as found in this study, a previous study reported a higher content of sediment OM in reservoirs than in streams (Keller et al., 2020). High inputs of sediment and OM from the catchment increases C burial and content in reservoir sediments.

The content of bulk sediment OM decreased between the first sampling campaign and ~200 days of sediment exposure, which may be due to a rapid decomposition of labile OM contained in

sediments that were mostly bare (with almost no vegetation) (Gómez-Gener et al., 2015; Kosten et al., 2018; Marcé et al., 2019). The content of bulk sediment OM increased between ~200 and 400 days of sediment exposure, which may be due to the input of OM produced by plants recolonizing the exposed sediment. However, the content of bulk sediment OM reached a plateau at ~400 days of sediment exposure. At this stage, we do not have a clear explanation of why the content of bulk sediment OM reached this plateau, especially, because vegetation continued to grow. We can speculate that there may have been a developing microbial community associated with root development. These microorganisms could have compensated for the effect of vegetation regrowth, a potential new source of OM, on the content of bulk sediment OM by increasing heterotrophic respiration. The balance between the supply of OM by plants and the loss through respiration could have led to a plateau of bulk sediment OM at ~400 days of sediment exposure. However, the role of vegetation recolonization in C content and microbial structure and function in exposed sediments after DD deserves further research.

Sediment OM in the Enobieta Reservoir was highly bioreactive. The mean O₂ consumption rate for bulk sediment OM (mean \pm SE in $\mu\text{g O}_2 \text{ g}^{-1}$ dry sediment h⁻¹: 2.76 ± 0.20) was lower than the global mean of the O₂ consumption rate of bulk soil OM in dry soils of wetlands, 3.74 ± 0.39 (Table S6, available at <https://www.limnetica.net/en/limnetica>), but was ~2 times higher than the global mean of the O₂ consumption rate in dry sediments of streams, 1.43 ± 0.31 (Table S7, available at <https://www.limnetica.net/en/limnetica>). The mean decomposition rate of OM in dry soils of wetlands may be higher than in dry sediments of reservoirs because wetlands are more likely to bury large stocks of bioreactive OM due to high primary productivity and low O₂ concentration (due to soil water saturation), which inhibits the decomposition of OM in wetlands (Freeman et al., 2001; Mitsch et al., 2013). Carbon buried in wetlands comprises ~33 % of wetland soils (Villa & Bernal, 2018), and the decomposition of OM increases with the content of OM (Keller et al., 2020; Kothawala et al., 2021; Paranaíba et al., 2021). Thus, the lower amount of sediment OM may explain its

lower decomposition rate in streams than in the Enobieta Reservoir. By comparing the C:N ratio, we may also infer that sediment OM in the Enobieta Reservoir (C:N ratio = 16.2 ± 1.0) was more bioreactive than sediment OM in streams, C:N ratio: 26.0 ± 2.2 (von Schiller *et al.*, 2019). The C:N ratio in the Enobieta Reservoir was, however, higher than in lakes (Dean & Gorham, 1998). In addition, we report %BDOC for a two-day incubation, $41.4 \pm 2.0\%$, which is 1.4 times lower than %BDOC in dry sediments of three reservoirs in the Three Gorges Reservoir region in China and dry soils from a wetland in Southeastern China, which were, however, incubated for an average time of 28 days at 28 °C, mean: 58.0 % (Table S3). Since the decomposition of sediment OM increases with temperature (Gudasz *et al.*, 2010, 2015), %BDOC in the Enobieta Reservoir would be comparable or even higher than %BDOC in the three reservoirs and the wetland if the incubation temperature and time were equal. Furthermore, %BDOC in the Enobieta Reservoir was ~2 times higher than the global mean %BDOC in dry soils incubated for an average time of 50 days at 16.9 °C, $22.1 \pm 1.4\%$ (Table S4). Thus, although the experimental approaches adopted to estimate %BDOC differ among studies, our results highlight that reservoir sediments may be hotspots of highly biodegradable OM.

Reff-WEOM was 34.4 times higher than Reff-BOM. This result reinforces that WEOM is the most bioavailable fraction of OM (Boyer & Groffman, 1996; Chantigny, 2003), and that most of the degradation of OM in bulk sediments is based on WEOM. Furthermore, our results suggest that C burial in reservoir sediments is due to conditions not favorable for C decomposition, rather than the inherent C recalcitrance (Catalán *et al.*, 2016; Kellerman *et al.*, 2015; Kothawala *et al.*, 2021). If the OM buried in the sediments of the Enobieta Reservoir was inherently recalcitrant against microbial decomposition, we should have reported low decomposition rates in our incubation experiment. Since we conducted our incubation experiment with the native microbial community under dark conditions, at a temperature close to the temperature in the region of the Enobieta Reservoir and without the addition of nutrients, we may speculate that the key factor

that restricted the decomposition of sediment OM during the operational phase of the Enobieta Reservoir was anoxia. The high sedimentation rate and the limited exposure time of sediment OM to O₂ (Sobek *et al.*, 2009, 2012) can result in the burial of inherently bioreactive OM in reservoir sediments. However, we expected that the content and reactivity of sediment OM would decrease with sediment exposure time, as increased availability of O₂ would increase the microbial decomposition of OM during sediment exposure.

Interestingly, %BDOC increased linearly with sediment exposure time, while the content of bulk sediment OM, R-WEOM and Reff-WEOM exhibited complex temporal trends during the first 9–580 days of sediment exposure. The linear increase in %BDOC with sediment exposure time may be explained by the rapid recolonization of exposed sediments by vegetation and the effect of photodegradation. As shown by the NDVI values, vegetation rapidly recolonized the reservoir after reservoir drawdown. Growing plants may supply an important amount of fresh and labile OM. For instance, depending on plant species, roots release 10–250 mg C/g root produced as root exudates (McNear, 2013; Vranova *et al.*, 2013). Root exudates comprise labile, low molecular weight organic compounds, such as amino acids, peptides, and sugars (Rovira, 1969). These root exudates can also increase microbial biomass (Eisenhauer *et al.*, 2017; Sung *et al.*, 2006; Wang *et al.*, 2012), which can contribute to the labile C pool. However, the labile OM of microbial biomass and plants that recolonize exposed sediments after drawdown can also increase the bioreactivity of old recalcitrant OM buried in sediments, a process called the priming effect (Bianchi *et al.*, 2015; Guenet *et al.*, 2010, 2014). Thus, the priming effect due to labile OM produced by microorganisms and regrowing plants could lead to a decrease in the content and reactivity of sediment OM. Furthermore, high-molecular weight, recalcitrant molecules in sediment OM of exposed sediments may also be converted into low-molecular weight, bioreactive molecules, due to sediment exposure to solar radiation (Granéli *et al.*, 1996; Lindell *et al.*, 1995; Wetzel *et al.*, 1995). Though photoreactions produce mainly inorganic C (CO₂), they also produce

Sediment organic matter in a decommissioned reservoir

organic compounds of low molecular weight and low aromaticity called biologically available photoproducts (Backlund, 1992; Catalán et al., 2013; Kieber et al., 1989; Mopper & Stahovec, 1986). Since sediment exposure is a hot moment of OM decomposition, aromaticity should have increased with sediment exposure time (Hansen et al., 2016). Thus, we expect photodegradation to be one of the reasons sediment exposure time did not affect the aromaticity of sediment OM. However, future studies should assess the specific effect of solar exposure on the molecular weight of sediment OM after DD.

Other parameters of the content and reactivity of sediment OM showed non-linear temporal trends. R-WEOM and Reff-WEOM showed almost the same temporal trend as the content of bulk sediment OM but did not reach a plateau at ~400 days of sediment exposure. The effects of terrestrialization and associated development of the microbial community and solar radiation may explain why R-WEOM and Reff-WEOM continued to increase with sediment exposure time. With current data, we cannot, beyond speculation, explain why other factors, such as the decomposition rate for bulk sediment OM and its respiration efficiency, $SUVA_{254}$, sediment WEOC, and the C:N ratio did not change with time. However, $SUVA_{254}$ in sediment WEOM of the Enobieta Reservoir was in the range of $SUVA_{254}$ of dissolved OM reported from sediments of different types of inland waters (0.2–3.7 L mg C⁻¹ m⁻¹, Chen & Hur (2015)), but lower than $SUVA_{254}$ of dissolved OM in waters collected from a range of aquatic systems, 3.2–10.6 L mg C⁻¹ m⁻¹ (Helms et al. 2008).

The observed temporal trend of the sediment texture was not expected since water withdrawal should result in rapid transport of fine-sized sediment, which would increase the mean size of the sediment during the early sampling campaigns. The late increase in mean sediment size may be explained by a higher transport of fine sediment and the accumulation of coarse sediment in the reservoir. Furthermore, sediment texture did not affect the content and reactivity of sediment OM in the Enobieta Reservoir, and previous studies also reported conflicting results on the role sediment texture in the reactivity of sediment OM (Mendoza-Lera et al., 2017; von Schiller et al., 2019).

Amani et al. (2022) hypothesized that the areal CO₂ fluxes in exposed sediments decreased with the sediment exposure time due to a decrease in the content and reactivity of sediment OM in the Enobieta Reservoir after the drawdown phase of DD. This study rejects the hypothesis that the content and reactivity of sediment OM in the Enobieta Reservoir decreased with sediment exposure time. Decreasing areal CO₂ fluxes in exposed sediments due to reduced C availability and microbial activity due to sediment drying should not be expected in a humid region, such as the Artikutza Valley with a rainfall of 2604 mm/yr (Atristain et al., 2022). However, a decrease in temperature over the last two sampling campaigns shown in this study may explain why areal CO₂ emissions in exposed sediments and running water decreased during the sampling period in Amani et al. (2022).

CONCLUSION

This study explored the content and reactivity of bulk sediment OM and sediment WEOM in a reservoir under DD. We reported a high content of highly bioreactive sediment OM, with the respiration efficiency of sediment WEOM being higher than that of bulk sediment OM. Sediment OM in exposed sediments during and after DD is susceptible to erosion and lateral transport downstream of the reservoir. Our results suggest that exposed sediments may be a great source of labile OM in downstream river reaches. Lateral transport of labile OM from the reservoir can imply higher C respiration and CO₂ fluxes in the river network downstream of the reservoir, therefore, interfering in the final OM delivered to the coastal ocean after DD. It is necessary to know how the lateral transport of C from the reservoir alters C dynamics in the river segments downstream from the removed reservoir. Future studies should also examine the effects of vegetation recolonization on C dynamics in the reservoir and the lateral transport of C downstream of the reservoir after DD.

ACKNOWLEDGMENTS

This study was funded by the project PID2020-114024GB-C31 (*Alteration of carbon sinks and*

sources in shrinking inland waters – Alter-C) funded by MCIN/AEI/10.13039/501100011033/. Additional support was provided by Agència de Gestió d'Ajuts Universitaris i de Recerca (AGAUR), and Institut de Recerca de l'Aigua (IdRA). DvS is a Serra Húnter Fellow. The authors also acknowledge Montse Badia, Miren Atristain, and Arturo Elosegi for their valuable help with field and laboratory activities, and Camille Minaudo for helping with statistics and NDVI data.

CONFLICT OF INTEREST

The authors claim no conflict of interest.

REFERENCES

- Allen, M. B., Engle, R. O., Zendt, J. S., Shrier, F. C., Wilson, J. T., & Connolly, P. J. (2016). Le saumon et la truite arc-en-ciel dans la rivière White Salmon après la destruction du barrage de Condit – résultats des travaux de planification et de la recolonisation. *Fisheries*, 41, 190–203. DOI: 10.1080/03632415.2016.1150839
- Amani, M., Ferreira, V., & Graça, M. A. S. (2019). Effects of elevated atmospheric CO₂ concentration and temperature on litter decomposition in streams : A meta - analysis. *International Revi*, 2019, 1–12. DOI: 10.1002/iroh.201801965
- Amani, M., von Schiller, D., Suárez, I., Atristain, M., Elosegi, A., Marcé, R.,... Obrador, B. (2022). The drawdown phase of dam decommissioning is a hot moment of gaseous carbon emissions from a temperate reservoir. *Inland Waters*, 12, 451–462. DOI: 10.1080/20442041.2022.2096977
- Arriaga, F. J., Lowery, B., & Mays, M. D. (2006). A fast method for determining soil particle size distribution using a laser instrument. *Soil Science*, 171, 663–674. DOI: 10.1097/01.ss.0000228056.92839.88
- Arrieta, J. M., Mayol, E., Hansman, R. L., Herndl, G. J., Dittmar, T., & Duarte, C. M. (2015). Dilution limits dissolved organic carbon utilization in the deep ocean. *Science*, 348, 331–333. DOI: 10.1126/science.1258955
- Atristain, M., von Schiller, D., Larrañaga, A., & Elosegi, A. (2022). Short-term effects of a large dam decommissioning on biofilm structure and functioning. *Restoration Ecology*. DOI: 10.1111/rec.13779
- Backlund, P. (1992). Degradation of aquatic humic material by ultraviolet light. *Chemosphere*, 25, 1869–1878. DOI: 10.1016/0045-6535(92)90026-N
- Bastviken, D., Persson, L., Odham, G., & Tranvik, L. (2004). Degradation of dissolved organic matter in oxic and anoxic lake water. *Limnology and Oceanography*, 49, 109–116. DOI: 10.4319/lo.2004.49.1.0109
- Baumann, K., Dignac, M. F., Rumpel, C., Bardoux, G., Sarr, A., Steffens, M., & Maron, P. A. (2013). Soil microbial diversity affects soil organic matter decomposition in a silty grassland soil. *Biogeochemistry*, 114, 201–212. DOI: 10.1007/s10533-012-9800-6
- Bednarek, A. T. (2001). Undamming rivers: A review of the ecological impacts of dam removal. *Environmental Management*, 27, 803–814. DOI: 10.1007/s002670010189
- Bianchi, T. S., Thornton, D. C. O., Yvon-Lewis, S. A., King, G. M., Eglinton, T. I., Shields, M. R.,... Curtis, J. (2015). Positive priming of terrestrially derived dissolved organic matter in a freshwater microcosm system. *Geophysical Research Letters*, 42, 5460–5467. DOI: 10.1002/2015GL064765
- Bolan, N. S., Adriano, D. C., Kunhikrishnan, A., James, T., McDowell, R., & Senesi, N. (2011). Dissolved organic matter. Biogeochemistry, dynamics, and environmental significance in soils. In *Advances in Agronomy* (Vol. 110, Issue C). DOI: 10.1016/B978-0-12-385531-2.00001-3
- Boyer, J. N., & Groffman, P. M. (1996). Bioavailability of water extractable organic carbon fractions in forest and agricultural soil profiles. *Soil Biol. Biochem*, 28, 783–790. DOI: 10.1016/0038-0717(96)00015-6
- Catalán, N., Marcé, R., Kothawala, D. N., & Tranvik, L. J. (2016). Organic carbon decomposition rates controlled by water retention time across inland waters. *Nature Geoscience*, 9, 501–504. DOI: 10.1038/ngeo2720
- Catalán, N., Obrador, B., Felip, M., & Pretus, J. L. (2013). Higher reactivity of allochthonous

Sediment organic matter in a decommissioned reservoir

- vs. autochthonous DOC sources in a shallow lake. *Aquatic Sciences*, 75, 581–593. DOI: 10.1007/s00027-013-0302-y
- Chantigny, M. H. (2003). Dissolved and water-extractable organic matter in soils: A review on the influence of land use and management practices. *Geoderma*, 113, 357–380. DOI: 10.1016/S0016-7061(02)00370-1
- Chen, M., & Hur, J. (2015). Pre-treatments, characteristics, and biogeochemical dynamics of dissolved organic matter in sediments: A review. *Water Research*, 79, 10–25. DOI: 10.1016/j.watres.2015.04.018
- Clow, D. W., Stackpoole, S. M., Verdin, K. L., Butman, D. E., Zhu, Z., Krabbenhoft, D. P., & Striegl, R. G. (2015). Organic Carbon Burial in Lakes and Reservoirs of the Conterminous United States. *Environmental Science and Technology*, 49, 7614–7622. DOI: 10.1021/acs.est.5b00373
- Coulson, L. E., Weigelhofer, G., Gill, S., Hein, T., Griebler, C., & Schelker, J. (2022). Small rain events during drought alter sediment dissolved organic carbon leaching and respiration in intermittent stream sediments. *Biogeochemistry*, 159, 159–178. DOI: 10.1007/s10533-022-00919-7
- Dean, W. E., & Gorham, W. (1998). Magnitude and significance of carbon burial in lakes, reservoirs, and peatlands. *Geology*, 26, 535–538. DOI: 10.1130/0091-7613(1998)026<0535:MASOCB>2.3.CO;2
- Downing, J. A., Cole, J. J., Middelburg, J. J., Striegl, R. G., Duarte, C. M., Kortelainen, P.,... Laube, K. A. (2008). Sediment organic carbon burial in agriculturally eutrophic impoundments over the last century. *Global Biogeochemical Cycles*, 22, 1–10. DOI: 10.1029/2006GB002854
- Duda, J. J., & Bellmore, J. R. (2022). Dam removal and river restoration. *Encyclopedia of Inland Waters*, 576–585. DOI: 10.1016/b978-0-12-819166-8.00101-8
- Eisenhauer, N., Lanoue, A., Strecker, T., Scheu, S., Steinauer, K., Thakur, M. P., & Mommer, L. (2017). Root biomass and exudates link plant diversity with soil bacterial and fungal biomass. *Scientific Reports*, 7, 44641. DOI: 10.1038/srep44641
- Freeman, C., Ostle, N., & Kang, H. (2001). An enzymatic latch on a global carbon store. *Nature*, 409, 149. DOI: 10.1038/35051650
- Gobierno de Navarra. (2019). *Ficha climática de la estación—Meteo Navarra*. navarra.es. http://meteo.navarra.es/climatologia/fichasclimaticas_estacion.cfm?IDestacion=74.
- Gómez-Gener, L., Obrador, B., von Schiller, D., Marcé, R., Casas-Ruiz, J. P., Proia, L.,... Koschorreck, M. (2015). Hot spots for carbon emissions from Mediterranean fluvial networks during summer drought. *Biogeochemistry*, 125, 409–426. DOI: 10.1007/s10533-015-0139-7
- Granéli, W., Lindell, M., & Tranvik, L. (1996). Photo-oxidative production of dissolved inorganic carbon in lakes of different humic content. *Limnol. Oceanogr*, 41, 698–706. DOI: 10.4319/lo.1996.41.4.0698
- Gudasz, C., Bastviken, D., Steger, K., Premke, K., Sobek, S., & Tranvik, L. J. (2010). Temperature-controlled organic carbon mineralization in lake sediments. *Nature*, 466, 478–481. DOI: 10.1038/nature09186
- Gudasz, C., Sobek, S., Bastviken, D., Koehler, B., & Tranvik, L. J. (2015). Temperature sensitivity of organic carbon mineralization in contrasting lake sediments. *Journal of Geophysical Research G: Biogeosciences*, 120, 1215–1225. DOI: 10.1002/2015JG002928
- Guenet, B., Danger, M., Abbadie, L., Gé, A., & Lacroix, R. (2010). Priming effect: bridging the gap between terrestrial and aquatic ecology. *Ecology*, 91, 2850–2861. DOI: 10.1890/09-1968.1
- Guenet, B., Danger, M., Harrault, L., Allard, B., Jauset-Alcala, M., Bardoux, G.,... Lacroix, G. (2014). Fast mineralization of land-born C in inland waters: First experimental evidences of aquatic priming effect. *Hydrobiologia*, 721, 35–44. DOI: 10.1007/s10750-013-1635-1
- Hansen, A. M., Kraus, T. E. C., Pellerin, B. A., Fleck, J. A., Downing, B. D., & Bergamaschi, B. A. (2016). Optical properties of dissolved organic matter (DOM): Effects of biological and photolytic degradation. *Limnology and Oceanography*, 61, 1015–1032. DOI: 10.1002/lno.10270
- Helms, J. R., Stubbins, A., Ritchie, J. D., Minor, E. C., Kieber, D. J., & Mopper, K. (2008).

- Absorption spectral slopes and slope ratios as indicators of molecular weight, source, and photobleaching of chromophoric dissolved organic matter. *Limnology and Oceanography*, 53, 955–969. DOI: 10.4319/lo.2008.53.3.0955
- Keller, P. S., Catalán, N., von Schiller, D., Grossart, H. P., Koschorreck, M., Obrador, B.,... Marcé, R. (2020). Global CO₂ emissions from dry inland waters share common drivers across ecosystems. *Nature Communications*, 11, 1–8. DOI: 10.1038/s41467-020-15929-y
- Kellerman, A. M., Dittmar, T., Kothawala, D. N., & Tranvik, L. J. (2014). Chemodiversity of dissolved organic matter in lakes driven by climate and hydrology. *Nature Communications*, 5, 3804. DOI: 10.1038/ncomms4804
- Kellerman, A. M., Kothawala, D. N., Dittmar, T., & Tranvik, L. J. (2015). Persistence of dissolved organic matter in lakes related to its molecular characteristics. *Nature Geoscience*, 8, 454–457. DOI: 10.1038/NCEO2440
- Kieber, D. J., McDaniel, J., & Mopper, K. (1989). Photochemical source of biological substrates in sea water: implication for carbon cycling. *Nature*, 341, 637–639. DOI: 10.1038/341637a0
- Koehler, B., Wachenfeldt, E. Von, Kothawala, D., & Tranvik, L. J. (2012). Reactivity continuum of dissolved organic carbon decomposition in lake water. *Journal of Geophysical Research: Biogeosciences*, 117, 1–14. DOI: 10.1029/2011JG001793
- Kosten, S., Berg, S. van den, Mendonça, R., Paranaíba, J. R., Roland, F., Sobek, S.,... Barros, N. (2018). Extreme drought boosts CO₂ and CH₄ emissions from reservoir draw-down areas. *Inland Waters*, 8, 329–340. DOI: 10.1080/20442041.2018.1483126
- Kothawala, D. N., Kellerman, A. M., Catalán, N., & Tranvik, L. J. (2021). Organic matter degradation across ecosystem boundaries: The need for a unified conceptualization. *Trends in Ecology and Evolution*, 36, 113–122. DOI: 10.1016/j.tree.2020.10.006
- Larrañaga, A., Atristain, M., von Schiller, D., & Elosegi, A. (2019). *Artikutza (Navarra): diagnóstico ambiental de la red fluvial previo al desmantelamiento de un embalse y resultados preliminares del efecto del vaciado Artikutza (Navarra): Environmental Diagnosis of the River Network Prior to the Dismantling of a Dam and Preliminary Results of the Emptying Effects*. www.embalses.
- Lindell, M., Granéli, W., & Tranvik, L. (1995). Enhanced bacterial growth in response to photochemical transformation of dissolved organic matter. *Limnology and Oceanography*, 40, 195–199. DOI: 10.4319/lo.1995.40.1.0195
- Lozano P, Latasa I (2019) Vegetación. Pages 334–359. In: *Artikutza, natura eta historia*. Donostiako udaleko Osasun eta Ingurumen Saila. Donostia - San Sebastian.
- Maavara, T., Lauerwald, R., Regnier, P., & van Cappellen, P. (2017). Global perturbation of organic carbon cycling by river damming. *Nature Communications*, 8, 1–10. DOI: 10.1038/ncomms15347
- Magilligan, F. J., Graber, B. E., Nislow, K. H., Chipman, J. W., Sneddon, C. S., & Fox, C. A. (2016). River restoration by dam removal: Enhancing connectivity at watershed scales. *Elementa*, 2016. DOI: 10.12952/journal.elementa.000108
- Manzoni, S., & Katul, G. (2014). Invariant soil water potential at zero microbial respiration explained by hydrological discontinuity in dry soils. *Geophysical Research Letters*, 41, 7151–7158. DOI: 10.1002/2014GL061467
- Manzoni, S., Moyano, F., Kätterer, T., & Schimel, J. (2016). Modeling coupled enzymatic and solute transport controls on decomposition in drying soils. *Soil Biology and Biochemistry*, 95, 275–287. DOI: 10.1016/j.soilbio.2016.01.006
- Marcé, R., Obrador, B., Gómez-Gener, L., Catalán, N., Koschorreck, M., Isabel, M.,... von Schiller, D. (2019). Emissions from dry inland waters are a blind spot in the global carbon cycle. *Earth-Science Reviews*, 188, 240–248. DOI: 10.1016/j.earscirev.2018.11.012
- McNear, D. H. (2013). The rhizosphere-Roots, soil and everything in between. *Nature Education Knowledge*, 1, 1–12. <http://cse.naro.affrc.go.jp>.
- Mendonça, R., Kosten, S., Sobek, S., Barros, N., Cole, J. J., Tranvik, L., & Roland, F. (2012). Hydroelectric carbon sequestration. *Nature Geoscience*, 5, 838–840. DOI: 10.1038/geo1653

Sediment organic matter in a decommissioned reservoir

- Mendonça, R., Müller, R. A., Clow, D., Verpoorter, C., Raymond, P., Tranvik, L. J., & Sobek, S. (2017). Organic carbon burial in global lakes and reservoirs. *Nature Communications*, 8, 1694. DOI: 10.1038/s41467-017-01789-6
- Mendoza-Lera, C., Frossard, A., Knie, M., Federlein, L. L., Gessner, M. O., & Mutz, M. (2017). Importance of advective mass transfer and sediment surface area for streambed microbial communities. *Freshwater Biology*, 62, 133–145. DOI: 10.1111/fwb.12856
- Miller, M. P., & McKnight, D. M. (2010). Comparison of seasonal changes in fluorescent dissolved organic matter among aquatic lake and stream sites in the Green Lakes Valley. *Journal of Geophysical Research*, 115, 1–14. DOI: 10.1029/2009jg000985
- Mitsch, W. J., Bernal, B., Nahlik, A. M., Mander, Ü., Zhang, L., Anderson, C. J.,... Brix, H. (2013). Wetlands, carbon, and climate change. *Landscape Ecology*, 28, 583–597. DOI: 10.1007/s10980-012-9758-8
- Mopper, K., & Stahovec, W. L. (1986). Sources and sinks of low molecular weight organic carbonyl compounds in seawater. *Marine Chemistry*, 19, 305–321. DOI: 10.1016/0304-4203(86)90052-6
- Obrador, B., Schiller, D. von, Marcé, R., Gómez-Gener, L., Koschorreck, M., Borrego, C., & Catalán, N. (2018). Dry habitats sustain high CO₂ emissions from temporary ponds across seasons. *Scientific Reports*, 8, 3015. DOI: 10.1038/s41598-018-20969-y
- Pacca, S. (2007). Impacts from decommissioning of hydroelectric dams : a life cycle perspective. *Climate Change*, 84, 281–294. DOI: 10.1007/s10584-007-9261-4
- Paranaíba, J. R., Aben, R., Barros, N., Quadra, G., Linkhorst, A., Amado, A. M.,... Kosten, S. (2021). Cross-continental importance of CH₄ emissions from dry inland-waters. *Science of The Total Environment*, 151925. DOI: 10.1016/j.scitotenv.2021.151925
- R Core Team. (2021). *R: a language and environment for statistical computing*. R Foundation for statistical computing, Vienna. Retrieved from: <http://www.R-project.org>.
- Ritchie, A. C., Warrick, J. A., East, A. E., Magirl, C. S., Stevens, A. W., Bountry, J. A., ... & Ogs-ton, A. S. (2018). Morphodynamic evolution following sediment release from the world's largest dam removal. *Scientific Reports*, 8, 13279. DOI: 10.1038/s41598-018-30817-8
- Rovira, A. D. (1969). Plant root exudates. *Bot. Rev.*, 35, 35–57. DOI: 10.1007/BF02859887
- Schimel, J. P. (2018). Life in dry soils: Effects of drought on soil microbial communities and processes. *Annu. Rev. Ecol. Evol. Syst.*, 49, 409–432. DOI: 10.1146/annurev-ecolsys-110617
- Shao, Z., He, P., Zhang, D., & Shao, L. (2009). Characterization of water-extractable organic matter during the biostabilization of municipal solid waste. *Journal of Hazardous Materials*, 164, 1191–1197. DOI: 10.1016/j.jhazmat.2008.09.035
- Shaver, G. R., Billings, W. D., Chapin, F. S., Giblin, A. E., Nadelhoffer, K. J., Oechel, W. C., & Rastetter, E. B. (1992). Global change and the carbon balance of arctic ecosystems. Carbon/nutrient interactions should act as major constraints on changes in global terrestrial carbon cycling. *Bioscience*, 42, 433–441. DOI: 10.2307/1311862
- Shaver, G. R., & Chapin III, F. S. (1986). Effect of fertilizer on production and biomass of tussock tundra, Alaska, USA. *Arctic and Alpine Research*, 18, 261–268. DOI: 10.1080/00040851.1986.12004087
- Sobek, S., Delsontro, T., Wongfun, N., & Wehrli, B. (2012). Extreme organic carbon burial fuels intense methane bubbling in a temperate reservoir. *Geophysical Research Letters*, 39, 1–4. DOI: 10.1029/2011GL050144
- Sobek, S., Durisch-Kaiser, E., Zurbrugg, R., Wongfun, N., Wessels, M., Pasche, N., & Wehrli, B. (2009). Organic carbon burial efficiency in lake sediments controlled by oxygen exposure time and sediment source. *Limnology and Oceanography*, 54, 2243–2254. DOI: 10.4319/lo.2009.54.6.2243
- Stubbins, A., Lapierre, J., Berggren, M., Prairie, Y. T., Dittmar, T., & Giorgio, P. A. (2014). What's in an EEM ? Molecular signatures associated with dissolved organic fluorescence in Boreal Canada. *Environmental Science & Technology*, 48, 10598–10606. DOI: 10.1021/es502086e

- Sung, K., Kim, J., Munster, C. L., Corapcioglu, M. Y., Park, S., Drew, M. C., & Chang, Y. Y. (2006). A simple approach to modeling microbial biomass in the rhizosphere. *Ecological Modelling*, 190, 277–286. DOI: 10.1016/j.ecolmodel.2005.04.020
- Thornton, K., Kimmel, B., & Payne, F. (1990). *Reservoir Limnology: Ecological Perspectives*. Wiley.
- Villa, J. A., & Bernal, B. (2018). Carbon sequestration in wetlands, from science to practice: An overview of the biogeochemical process, measurement methods, and policy framework. *Ecological Engineering*, 114, 115–128. DOI: 10.1016/j.ecoleng.2017.06.037
- von Schiller, D., Datry, T., Corti, R., Foulquier, A., Tockner, K., Marcé, R.,... Zoppini, A. (2019). Sediment respiration pulses in intermittent rivers and ephemeral streams. *Global Biogeochemical Cycles*, 33, 1251–1263. DOI: 10.1029/2019GB006276
- Vranova, V., Rejsek, K., Skene, K. R., Janous, D., & Formanek, P. (2013). Methods of collection of plant root exudates in relation to plant metabolism and purpose: A review. In *Journal of Plant Nutrition and Soil Science*, 176, 175–199. DOI: 10.1002/jpln.201000360
- Walz, J., Knoblauch, C., Böhme, L., & Pfeiffer, E. M. (2017). Regulation of soil organic matter decomposition in permafrost-affected Siberian tundra soils - Impact of oxygen availability, freezing and thawing, temperature, and labile organic matter. *Soil Biology and Biochemistry*, 110, 34–43. DOI: 10.1016/j.soilbio.2017.03.001
- Wang, J., Li, X., Zhang, J., Yao, T., Wei, D., Wang, Y., & Wang, J. (2012). Effect of root exudates on beneficial microorganisms-evidence from a continuous soybean monoculture. *Plant Ecology*, 213, 1883–1892. DOI: 10.1007/s11258-012-0088-3
- Warrick, J. A., Duda, J. J., Magirl, C. S., & Curran, C. A. (2012). River turbidity and sediment loads during dam removal. *EOS, Transactions American Geophysical Union*, 93, 425-426. DOI: 10.1029/2012eo430002
- Webster, J. R., & Benfield, E. F. (1986). Vascular plant breakdown in freshwater ecosystems. *Annual Review of Ecology and Systematics*, 17, 567–594. DOI: 10.1146/annurev.es.17.110186.003031
- Weishaar, J. L., Aiken, G. R., Bergamaschi, B. A., Fram, M. S., Fujii, R., & Mopper, K. (2003). Evaluation of specific ultraviolet absorbance as an indicator of the chemical composition and reactivity of dissolved organic carbon. *Environmental Science and Technology*, 37, 4702–4708. DOI: 10.1021/es030360x
- Wetzel, R. G., Hatcher, P. G., & Bianchi, T. S. (1995). Natural photolysis by ultraviolet irradiance of recalcitrant dissolved organic matter to simple substrates for rapid bacterial metabolism. *Limnol. Oceanogr*, 40, 1369–1380. DOI: 10.4319/lo.1995.40.8.1369
- Zsolnay, A. (1996). In “*Humic Substances in Terrestrial Ecosystems*” (A. Piccolo, Ed.), pp. 171–223. Elsevier, Amsterdam. DOI: 10.1016/B978-044481516-3/50005-0